Jacking and suction installation of bucket foundation for offshore wind turbines

Koteras, Aleksandra Katarzyna

Publication date:
2019

Document Version
Publisher's PDF, also known as Version of record

JACKING AND SUCTION INSTALLATION OF BUCKET FOUNDATION FOR OFFSHORE WIND TURBINES

BY
ALEKSANDRA KATARZYNA KOTERAS

DISSERTATION SUBMITTED 2019

AALBORG UNIVERSITY
DENMARK

Jacking and suction installation of bucket foundation for offshore wind turbines

Ph.D. Dissertation

Aleksandra Katarzyna Koteras

Dissertation submitted November 7, 2019

Dissertation submitted: November 7, 2019

PhD supervisor: Prof. Lars Bo Ibsen
Aalborg University

Assistant PhD supervisor: Assoc.Prof. Johan Christian Steffensen Clausen
Aarhus University (former Aalborg University)

PhD committee: Professor Lars Damkilde (chairman)
Aalborg University

Professor, Dr.-Ing. Martin Achmus
University of Hannover

Geo Engineering Director Lindita Kellezi
GEO

PhD Series: Faculty of Engineering and Science, Aalborg University

Department: Department of Civil Engineering

ISSN (online): 2446-1636
ISBN (online): 978-87-7210-536-9

Published by:
Aalborg University Press
Langagervej 2
DK – 9220 Aalborg Ø
Phone: +45 99407140
aauf@forlag.aau.dk
forlag.aau.dk

Printed in Denmark by Rosendahls, 2019

Preface

The thesis "Jacking and suction installation of bucket foundation for offshore wind turbines" has been submitted as a fulfillment of the Doctoral School requirements for the Ph.D. study. The research was carried out at the Department of Civil Engineering in Aalborg University, Denmark. The work presented in the thesis was funded by the European Union via the project "Innwind - Innovative Wind Conversion Systems for Offshore Applications". The work was also supported by the two other projects from the Energy Technology Development and Demonstration Program (EUDP) concerning the industrialized bucket foundation concept. The thesis is intended not only for the experienced engineers, but it was written with a hope of being interesting within a larger audience, that has an interest in the offshore wind energy.

The research work was conducted at Aalborg University under the supervision of Professor Lars Bo Ibsen, whom I would like to thank for the opportunity and the guidance during my research. The guidance and support from the co-supervisor Johan Clausen is also greatly appreciated.

Most of the research work is based on the laboratory tests, performed in the geotechnical laboratory at Aalborg University. The research work would not be finalized without a specialized knowledge of the entire technical staff. I would like to express my appreciation for their help in the set-up arrangement and in solving the unexpected problems I have come across, which were present on a day to day basis as a researcher. Moreover, I would like to thank to my colleagues for a support and interesting discussions.

Finally, I am very grateful to my husband for his love, patience and a huge support in the past few months and to our son Borys for being my biggest life-motivation.

Aleksandra Katarzyna Koteras
Aalborg University, November 7, 2019

Curriculum Vitae

Aleksandra Katarzyna Koteras

Professional Experience

2018	Research assistant at the Department of Civil Engineering, Aalborg University (continuation of PhD project)
2015 - 2018	PhD Fellow at the Department of Civil Engineering, Aalborg University (incl. maternity leave 04.2017-04.2018)
2011 - 2012	Assistant of a Contract Engineer at the Engineering Company NBQ in Szczecin, Poland

Higher Education

2012 - 2014	M.Sc. in Structural and Civil Engineering, Aalborg University, Denmark
2008 - 2012	B.Sc. in Civil Engineering, West Pomeranian University of Technology, Szczecin, Poland

Recent Research Projects

2018 – 2020	EUDP: Offshore wind suction bucket on an industrial scale – Part 2 Trial Installation (Siemens Gamesa, Universal Foundation, AAU, Fred. Olsen)

2016 - 2018 EUDP: Offshore wind suction bucket on an industrial scale (Siemens Gamesa, IB Andersen Industri A/S, AAU, Universal Foundation)

from 2015 Cost-Effective mass production of Universal Foundations for large offshore wind parks (AAU, Universal Foundation, FORCE, LIC, DTU Wind)

from 2015 InnWind – Work Package 1; EU7 (27 international partners)

Teaching Expierience

Master lever Course Geotechnics and Foundations

Supervision of the final projects for MSc Structural and Civil Engineering

Publications

Journal paper Koteras, A.K., and Ibsen, L.B. (2019) Medium-scale Laboratory Model of Mono-bucket Foundation for Installation Tests in Sand. *Canadian Geotechnical Journal*, Vol. 56, No. 8: pp. 1142 – 1153.

Conference papers Koteras, A.K., Sabaliauskas, T., and Ibsen, L. B. (2019) Cyclic CPT Measurements of Disturbed Soil State. *Proceedings of the* 7^{th} *International Symposium on Geotechnical Safety and Risk*. 11-13 December, 2019. Taipei , Taiwan.

Koteras, A.K., and Ibsen, L.B. (2018) Reduction in Soil Penetration Resistance for Suction-assisted Installation of Bucket Foundation. *Proceedings of the* 9^{th} *International Conference on Physical Modeling in Geotechnics*. July 17-20, 2018. London, UK.

Koteras, A.K., Ibsen, L.B., and Clausen, J. (2016) Seepage Study for Suction Installation of Bucket Foundation in Different Soil Combinations. *Proceedings of the* 26^{th} *International Ocean and Polar Engineering Conference*. 25 June-1 July, 2016. Rhodes, Greece.

Technical reports

Koteras, A.K. (2019). Suction and jacking installation of bucket foundation models: laboratory manual. *DCE Technical Memorandum, No. 74*. Aalborg: Department of Civil Engineering, Aalborg University.

Koteras, A.K. (2017). Set-up and Test Procedure for Suction Installation and Uninstallation of Bucket Foundation. *DCE Technical Memorandum, No. 63*. Aalborg: Department of Civil Engineering, Aalborg University.

Koteras, A.K., and Ibsen, L.B. (2015). Investigation of seepage around the bucket skirt during installation in sand: AAU CPT-based method for the installation of suction bucket. *DCE Technical Memorandum, No. 52*. Aalborg: Department of Civil Engineering, Aalborg University.

Contract reports

Koteras, A.K., and Ibsen, L.B. (2017). Medium-scale Laboratory Installation of Suction Bucket Foundation in Sand: Results analysis. *DCE Contract Report, No. 182*. Aalborg: Department of Civil Engineering, Aalborg University.

Ibsen, L.B., and Koteras, A.K. (2016) Deinstallation of Monopile: Technical Documentation for deinstallation tests on a model pile. *DCE Contract Report, No. 181*. Aalborg: Department of Civil Engineering, Aalborg University.

Ibsen, L.B., Vahdatirad, M.J., Koteras, A.K., and Ibsen, M. (2015) Evaluation of kp and kf factors from field trial installations at Dogger Bank, Hornsea and Dudgeon. *DCE Contract Report, No. 169*. Aalborg: Department of Civil Engineering, Aalborg University.

Abstract

The production of renewable energy on the global scale experiences a large growth due to the well-known reasons. Offshore wind power is one of the most promising sources with a high development range. The costs of offshore energy are being rapidly reduced; however, there is still much to be improved. Lowering the costs of offshore wind farms is not only the key to lower energy prices, but primarily is the great contribution to the climate goals for the future.

The installation of foundations is often named as one of the main issues that influences the total costs of the offshore energy. The majority of offshore wind turbines are supported by monopile foundations. However, the demand for increasing size of offshore wind turbines is the reason why a better solution is desired. Therefore, more and more effort is put on the development of a suction bucket foundation that seems to be more cost-effective and environmentally friendly due to the suction installation manner. The concept is commonly used in the oil and gas industry, but as loading conditions for offshore wind turbines are very different, a further research and new design methods are required. The concept is already proven to be feasible, but the suction installation process is still not fully understood and can be optimized.

This thesis focuses on the bucket installation by analyzing the soil-structure response during the suction and the jacking installation. Medium-scale tests of the installation have been performed at Aalborg University laboratory in fine grained sand. The tests prove that the suction installation can be performed and easily controlled even in very dense sand. The suction applied during the installation can be much higher that the proposed suction limits and no failure is observed. Moreover, the tests results indicate a huge difference between the soil resistance against two different installations, as the seepage flow, induced by the applied suction, reduces the soil stresses inside the bucket and below the skirt tip. The cone penetration tests performed before and after each test confirm that the soil trapped inside the bucket is significantly loosened up.

The thesis covers also the numerical analysis of seepage around the skirt for different boundary conditions and with applied changes in the soil perme-

ability of the inside soil plug due to the mentioned loosening. The numerical part is a basis for the analysis of the critical suction which is later on evaluated by laboratory tests results.

Finally, the thesis includes results of the test campaign where two different bucket models are used and compared. An increase in bucket foundation diameter requires an increase in skirt thickness at the same time. Otherwise, too thin structure will lead to a buckling failure during the installation. Obviously, the total cost of steel material increases significantly. However, a modular bucket with the internal stiffeners used for tests has a much lower skirt thickness. The changed shape gives much higher buckling resistance and savings in material costs at the same time. Jacking tests show that the soil resistance for the modular bucket is significantly higher than for the round bucket with a similar diameter, but the suction installation tests show that the reduced soil resistance is almost the same in both cases. These results are very promising, showing that large-diameter mono-buckets with modular shape can be feasible for suction installation.

Resumé

Vedvarende energi bidrager til en progressiv vækst i den globale energiproduktion på grund af velkendte årsager. Vindenergi fra havvindmøller er en af de mest lovende kilder med et højt udviklingspotentiale. Omkostningerne til offshore energi reduceres i øjeblikket hurtigt; der er dog stadig meget, der kan forbedres. Sænkning af omkostningerne ved havvindmølleparker er ikke kun nøglen til lavere energipriser, men primært et stort bidrag til klimamålene for fremtiden.

Installation af fundamentet er ofte et af hovedbidragene til de samlede omkostninger til produktion af energi fra havvindmøller. De fleste havvindmøller er funderet på monopæle, men stigende størrelse på havvindmøller kræver en bedre løsning. Derfor satses der mere og mere på udviklingen af bøttefundamenter, som umiddelbart er mere omkostningseffektive og miljøvenlig på grund af der anvendes undertryk i stedet for ramning som drivmåde ved installationen. Konceptet bruges ofte i olie- og gasindustrien, men da lasterne for havvindmøller er meget anderledes, kræves der en yderligere undersøgelse og nye designmetoder. Konceptets anvendelighed er allerede bevist, men sugeinstallationsprocessen er stadig ikke helt forstået og kan optimeres.

Denne afhandling fokuserer på bøtteinstallation ved at analysere jord/ struktur responsen under suge- og jacking- installation. Medium-scale test af installationen er blevet udført på Aalborg Universitets laboratorium i finkornet sand. Testene viser, at sugeinstallationen kan udføres og let kontrolleres, selv i meget tæt sand. Testene viser, at installationen med sug kan udføres og let kontrolleres, selv i meget komprimeret sand. Undertrykket, der påføres under installationen, kan være meget højere end de grænser der anvendes i dag uden at brud observeres.

Testresultaterne indikerer endvidere en enorm forskel på installationsmodstanden ved de to metoder da strømningen, genereret af det påførte undertryk, reducerer jordspændingerne inde i bøtten og under skørtespidsen. CPT forsøg, udført før og efter hver test, bekræfter, at jorden fanget inde i bøtten er betydeligt løsere end før forsøget.

I afhandlingen foretages der også numeriske analyser af strømningerne

rundt om skørtet. Her anvendes der forskellige randbetingelser og permeabiliteten af den indre jordprop ændres svarende til den målte ædring i lejringstætheden. De numeriske analyser danner grundlag for studie af det kritiske undertryk, som senere sammenlignes med forsøgsresultater.

Afhandlingen indeholder også resultater fra forsøg, hvor to forskellige bøttemodeller installeres og sammenlignes. En forøgelse af bøttefundamentets diameter kræver en forøgelse af tykkelsen af skørtet idet en for tynd struktur vil føre til kollaps på grund af buckling under installationen. Der er udviklet en modulær bøtte hvor den ædrede form giver meget højere bucklingmodstand og besparelser i materialeomkostninger på samme tid. Jacking testene viser, at installationsmodstanden for den modulære bøtte er væsentligt højere end for den runde bøtte med en lignende diameter. Derimod viser installationsforsøgene med undertryk, at den reducerede installationsmodstand næsten er den samme i begge tilfælde. Disse resultater er meget lovende og viser at den modulær formet bøtte har et stort potentiale, idet den vil reducerer stålmaterialet og produktionsprisen, uden at ændre det undertryk og derved diameter der krævet for at installere den.

Contents

Part I

PhD Thesis

Chapter 1

Introduction

The chapter gives a basic introduction into the research work performed for the Ph.D. The itroduction consists of short summary of wind energy market and the newest development in this area, what in deed, is a motivation for the Ph.D. research. Moreover, the chapter presents an outline of history for wind offshore turbines established on the experience gained from the oil and gas sector. Basic offshore foundation concepts are demonstrated, with a focus on the suction bucket foundation. Both, the installation phase and the in-place performance of suction bucket is described.

The concept is still in a developing phase and much research work is devoted to the topic. There is however a visible goal in nearly future for the mono bucket concept to be ready for a commercial use.

1.1 Offshore wind energy

A continuous growth in the energy demand all over the world leads to an improvement of sustainable energy sector. Nevertheless, most of countries still rely on fossil fuels, whose mining contributes substantially to the climate changes and a decreased air quality. The environmental policies push a lot on the development of renewable energy, but the costs of such energy must become smaller in order to satisfy the energy requirements. The main target for the European Environment Agency is not only to increase the share of renewable energy in the total energy consumption (to at least 32% in 2030), but also to improve the energy efficiency (EEA, 2019).

Wind energy is the most cost-effective energy in Europe today, according to WindEurope (2019a). It is the onshore wind power to be claimed as the cheapest solution; however, the offshore wind sector has reduced energy cost significantly in previous years, and starts to be seen as a major energy source in future Europe. The development of offshore wind farms grows due to the

(a) (b)

Fig. 1.1: (a) Installation of the first turbine at Horns Rev 2 (Kanter, 2009); (b) Horns Rev 2 offshore wind farm (Naturstyrelsen, 2014)

countless siting possibilities and the advantage of much better wind resource than in the on-shore conditions. Offshore wind speeds are not necessary higher than onshore winds, but they are more consistent. A high cost of offshore foundation is, however, the key drawback. The support structure of offshore wind turbine consists of up to 35% of the total costs (Byrne and Houlsby, 2003), and even up to 50% for foundations in deep waters (Madsen et al., 2012). The foundation must be sufficient to transfer all environmental loads, mainly from wind, waves and currents, safely to the ground.

The wind energy consists of 14% of the total European Union's electricity and Denmark is the leading country, with the wind share in its total electricity equal to 41% in 2018 (WindEurope, 2019c). The leading position is not only in the operation sector, but also in the research and the manufacturing. Denmark is on the third place in Europe when comparing the energy capacity from the offshore turbines (after United Kingdom and Germany) (WindEurope, 2019b). The North Sea is registered as a location with the largest installed offshore wind capacity.

A world first offshore turbine was installed in Nogersund, the North part of Sweden in 1990, with a rated power of barely 220 kW. First offshore wind farm was raised at Vindeby, the south of Denmark, by a danish power station Elkraft in 1991. The farm consisted of 11 turbines with a total capacity of 5MW founded on concrete gravity based foundations. The water level in this location was relatively small, with 2 - 5 m. A total decommissioning of the farm after 25 years was a big success of Dong Energy in 2017. In 1995 another offshore farm called Tunø Knob was raised in the Bay of Aarhus by Vestas company. The turbines were also based on the concrete foundations. Both farms marked a great start for the offshore wind energy, but due to the complexity of power cables and the increased cost of the foundation, the total cost of energy were almost doubled than the onshore energy prices. (Bilgili et al., 2011)

Moving the farms to the deeper water depth requires the use of steel instead of concrete for the foundation solution to be more cost-effective (Birck and Gormsen, 1999). The first offshore farm founded on drilled monopiles, Bockstigen offshore wind farm, has been commissioned in the south-west of Swedish island Gotland in the Baltic Sea, with a water depth of approximately 6 m (Lange et al., 1999). After many small demonstration projects, the first large offshore wind farm, Horns Rev I, has been built by the danish company Elsam (now Ørsted) in the North Sea in 2002. The offshore farm with a total capacity of 160 MW consists of 80 turbines founded on steel mono piles of 4 m diameter. The extension of this farm came into life a couple years later, consisting of two other parts in a deeper water depth, up to 19m. The Horns Rev II and the Horns Rev III inaugurated in 2008 and 2019 added more than 600 MW rated power. The structure of all turbines consists of a monopile as foundation and a transition piece. The 8-MW model turbines from Vestas executed in Horns Rev III are one of the world's largest turbines in the use. The largest operational offshore wind farm in the world, Walney Extension, is located in the Irish Sea and includes the 7 MW and the 8 MW turbines founded also on the monopiles. (Ørsted, 2019)

The monopiles still remain the most often used offshore foundation structures in 2018, according to WindEurope (2019b). 74.5% of all installed foundations are the monopiles, however this number has decreased from 2017 when the monopiles consisted of 86% of all installed offshore foundations. Next is a jacket foundation which gives 24.5% of all installed foundations.

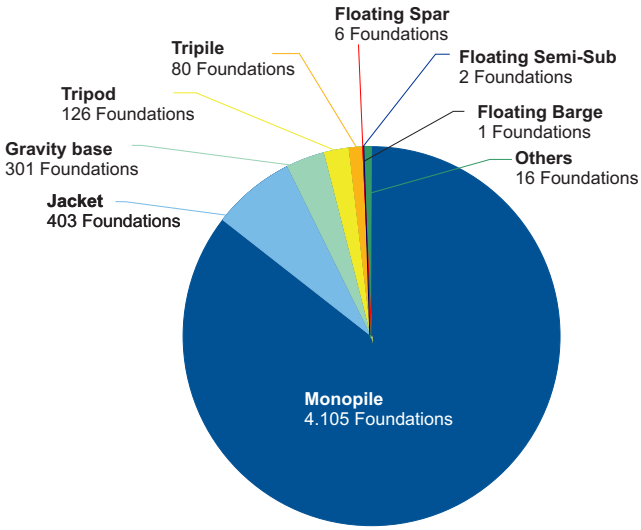

Fig. 1.2: Substructure types used for offshore wind turbines at the end of 2018 (WindEurope, 2019b)

The offshore wind turbines are in a progression stage, Fig. 1.3, and therefore, more cost-effective solutions are under the research. Such a concept must result from minimizing the offshore work and also the manufacturing process.

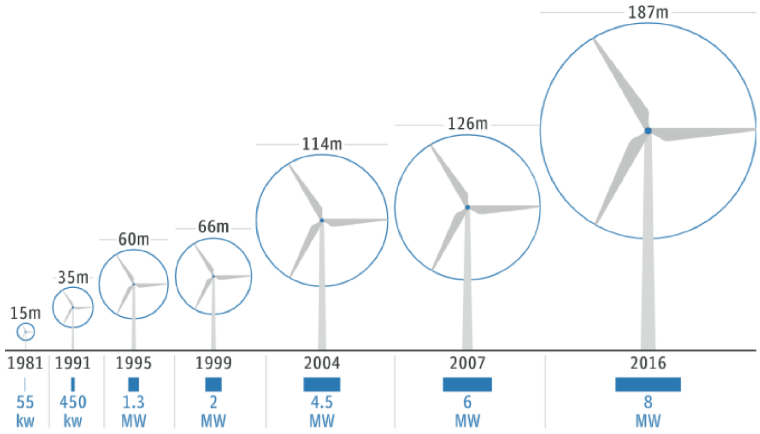

Fig. 1.3: Progression in size of wind turbines with their rated energy output in MW (NorthSEE, 2014)

An example is a suction bucket foundation (Tjelta, 1995; Byrne and Houlsby, 1999). The concept of offshore suction foundation was initiated in 1970's by the testing mooring suction piles. The first real installation of the suction piles took place in the Gorm field in 1981 (Senpere and Auvergne, 1982). Further, the anchors installations began to use the suction technology. The first significant example was a large concrete oil platform, The Gullfaks C, installed in the North Sea for a water depth of 218 m. Two suction anchors connected to the concrete foundation assisted the installation process (Tjelta et al., 1986). Finally, the pile suction foundations started to be replaced by the suction buckets, Draupner E and Sleiper T (Bye et al., 1995). Both located in a dense sand with a high bearing capacity, proved the feasibility of the concept as a shallow foundation. The most interesting experience from the Draupner E platform was captured by the monitoring system. The foundation was exposed to a 'Monster Wave' causing an extreme impact load on the structure. The acceleration measured on the foundation was negligible due to the pore pressure response inside the buckets. The pore pressure was huge during the action, but disappeared quickly when the foundation was unloaded. The experience from oil and gas sector gave high hopes for the presence of the suction bucket concept in the offshore wind industry.

1.2 Offshore foundations

1.2.1 Offshore environment

The experience on which the design of offshore wind turbines relies on comes from the oil and gas offshore sector, where the first oil rig 'Superior' was installed in 1947 in the coast of United States (Randolph and Gourvenec, 2011). The dominant load for the oil and gas platforms is their huge self-weight, leaving them less exposed to the dynamic excitations caused by waves and wind. The offshore turbine is a slender, high structure that is relatively light. The self-weight is much smaller in comparison to the moment at the seabed and the strong cyclic loads induced by waves and wind. The difference in loading between the oil and gas platform and the wind turbine is demonstrated in Fig. 1.4. Susceptibility to the wave and wind load, cyclic in their nature, requires a whole new foundation design, that is not governed by the ultimate bearing capacity, but rather driven by a changeable stiffness of the soil-foundation system due to the cyclic loading and the fatigue limit state (Houlsby et al., 2005).

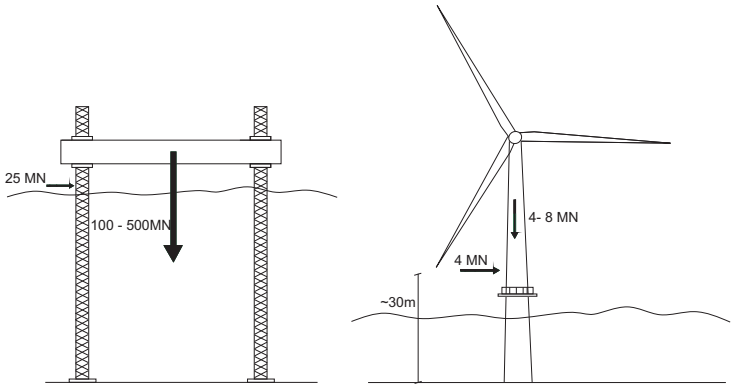

Fig. 1.4: Difference in typical offshore loads for oil and gas platform and wind turbine

1.2.2 Choice of foundation concept

Soil conditions are diverse at the offshore sites with soil particles ranging from clay size to boulders. The site requires a ground investigation before the choice of foundation can be made. The soil properties are heavily affected by the kind of particles met at the site. An offshore site investigation is often based on the soundings, the drillings with further laboratory sample testing and on the cone penetration testing, CPT. The North Sea seabed consists mainly of highly over consolidated soils and often sand deposits in the top layers (Lesny, 2011).

The choice of foundation is also directly related to the water depth, through which it is related to the size of overturning moment on the seabed. Some foundations are more cost-effective in shallow water depths, whereas other are more suitable for transitional or deep water depths. The environmental conditions play an important role in the choice of foundation as well. The specific conditions, where current is dominant, creates more favorable conditions for the development of scour. The protection against scour can be less economical than a choice of different foundation type.

Finally, there could be more demands coming from the country specific requirements, like the noise limitation. For example, the monopiles can be rejected due to their noisy installation method.

1.2.3 Different foundation types

The support structure used for the offshore wind turbine must resist a high overturning moment, safely transferring the load to the seabed. The structure can be a single monopod structure or a multipod with three or four structures interfacing with the soil. The conventional foundation concepts of monopods come from the oil and gas sector experience. This includes a gravity based foundation, a monopile and a bucket foundation, see fig. 1.5. The multipods support structures connect three or four previously mentioned single structure into one foundation. Most often used are a tripod and a jacket structure supported on piles or bucket foundations, see fig. 1.5. A short description on each foundation is given below.

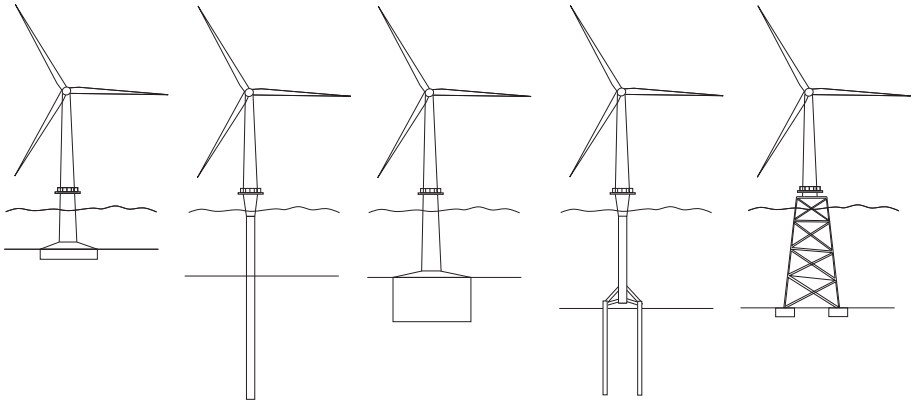

Fig. 1.5: Conventional foundations for offshore wind turbines. From left: Gravity based foundation, Monopile, Mono bucket, Tripod on piles, Jacket structure on mono buckets

Gravity base foundation

The stability of structure founded on a gravity base foundation, GBF, is kept thanks to a huge self-weight of the foundation. This solution is the most suitable for shallow water depths. For the offshore sector this type of foundation has a shape of caisson, made of reinforced concrete, steel or a composite structure. Foundations are mainly prepared on land and transported to the location, which is rather close to the shore. The foundation at the location is sunk by a ballasting made of sand, gravel, concrete or water. The foundation requires a preparation of the seabed as the contact area between soil and base of foundation must be uniform, but on the other hand, the material and the construction costs are low. The installation process is not very time consuming, but requires a calm weather conditions.

The overturning moment is balanced by the self-weight and the load is transferred to the seabed through the foundation's base line. The dead load must as well prevent the foundation from the uplifting, sliding and tilting. Therefore, soft soils deposits in the top layers exclude the use of GBF. (Lesny, 2011)

Monopile foundation

A monopile is a simple structure that consist of welded steel piles with circular cross section of diameter 6-8 m, typically 20-40 m long. The monopile top partextends above the seabed where it is connected to a transition piece. The transition piece is grouted to the monopile. There are no special requirements for the seabed preparation, but there is a demand for a heavy and expensive piling or drilling equipment required for installation. The driving installation process is not very time consuming, but very noisy. However, if drilling must be performed first, time and costs of installation increase significantly. This type of foundation is adequate for shallow water depth, up to 30m. However, an increase in water depth often makes monopiles more cost-effective solution than GBF. Monopiles are suitable for location with soft soils in the top layers, as the long structure transfers the load into deeper soil layers. On the other hand, the cost of material is much higher comparing to the GBF.

The overturning moment is balanced by the horizontal earth pressure on the pile. An increase in water depth, hence in loading, requires larger diameter and embedded depth of the monopile. Pile foundations require a scour protection as the eroded soil directly affects the bearing capacity of piles.

Monopiles are the most often used for both offshore platforms and wind turbines, and therefore associated with rather small risk. Experience from Gulf of Mexico dominated the design for offshore structure in early years, where the soft clays in that area required the use of monopiles. However, moving to the North Sea where sands and strong clays are dominant, the

shallow foundations provide satisfactory bearing capacity and therefore are more cost-effective than monopiles (Byrne and Houlsby, 2003).

Bucket foundation

A bucket foundation for offshore wind turbines in Europe is now developing on the base of the Universal Foundation concept. The company refers to its main advantages (Nielsen, 2016a):

- low self-weight,
- low installation time,
- locally manufactured,
- cost reduction seen in both design and installation,
- suitable for a wide range if soil profiles,
- completely removable.

Fig. 1.6: Universal Foundation bucket concept (Universal Foundation, 2019a)

A bucket foundation is made of a thin shell structure of a cylindrical shape with open bottom and sealed top. The top plate of bucket is called a lid, and the cylindrical part that penetrates the soil is referred as a skirt. The differences between the bucket foundation and monopile, apart of the closed top plate, are larger diameter and smaller length to diameter ratio, L/D, for the former. The bucket foundation has a hybrid design combining main advantages of gravity base foundation and monopile, see fig. 1.7. Additionally, an installation method resembles the suction anchors; the suction pump is attached to the lid. The embedded skirt additionally mitigate the scour effects. DNV (2014) recommends mono buckets for water depths from 0 to 25 m, but Nielsen (2016a) reported that their concept can be used in water depths up to 55 m for 8 MW turbines, closing the gap between the most often used

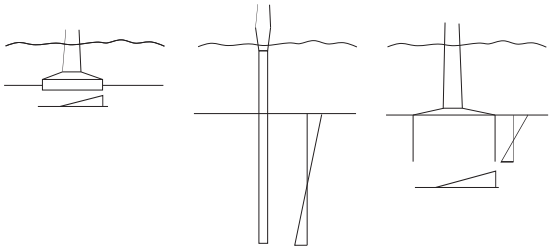

Fig. 1.7: Soil reaction to the overturning moment

monopiles and the jacking structures; and being still a cost effective solution. The preparation of the seabed is not required and the transport to the offshore location of such a light structure is easy, also possible by a self-floating. The experience from Met Mast at Horns Rev II proves the self-floating feature of bucket foundation. The installation is noise-free and does not require expensive equipment what reduces the installation costs. Universal foundation reports a 25% reduction in the required steel compared to the monopile foundation (Nielsen, 2016a), again reducing the costs significantly. Finally, when the turbine exceeds its design life-time, a reverse suction process removes the entire bucket structure from the seabed. The monopiles are only cut above the soil, leaving a substantial part of the structure inside the seabed. The process of decommissioning with a reverse suction has been already succeededat Horn Rev II (offshoreWind, 2015).

The overturning moment can be balanced by the horizontal forces on the skirt, like in case of the monopiles. However, the soil trapped inside the bucket can acts as a self-weight, like in case of GBF, and resist the load on the skirt tip level. This has an advantage over the gravity foundation as the load is transferred into deeper, more resistant soil layers. However, if soil trapped inside the bucket should work together with the skirt as a dead load, soil and skirt must be in a full contact. This area can be grouted if necessary. Moreover, it has been proven than in case of the transient loads, bucket foundation works as a suction anchor. The excess pore pressure accumulates inside the bucket and prevents the foundation from rotating (Nielsen et al., 2017).

An increase in water depth requires a larger bucket diameter for the design. When the diameter to skirt thickness ratio, D/t, increases, the buckling resistance against installation is lower, increasing the risk of buckling instability (Madsen et al., 2012). There are also other aspects that must be taken into consideration while designing the installation phase of suction bucket foundation. Next section describes in details possible installation failures.

Multipods and jackets

Jackets and tripods are installed with a previous preparation of the seabed, so that the installation will keep the wind turbine tower vertically. They are most cost-effective when used in transitional water depths, 30-60 m (Musial and Butterfield, 2006). A jacket is a lattice structure ended with three or four monopods at the seabed. The outer legs are inclined by $5° - 10°$ what improves the vibration behaviour and reduces the reaction forces (Lesny, 2011). A tripod structure consists of a main pipe and three legs. The structure is more spread-out what also reduces the reaction forces.

There is a significant difference in how foundations behave while loaded in case of a mono structure or a multipod. For a multipod structure the overturning moment is transferred as a tension and as a compression forces on the individual mono foundation structures.

Both the monopiles and the suction buckets are used as supporting structures for multipods. The suction buckets are suitable for water depth of 20-50 m according to DNV (2014). Carbon Trust (2019b) reported suitable depth to be in a range of 30-60 m, and SPT Offshore (2019) reported that suction piles can be used in water depths up to 120 m.

Floating foundations

The floating foundations are the most economical solution for deep and ultra-deep water depths. The more deep is the water depth, the higher is the loading and, as a consequence, the mass of fixed structure increases to uneconomical design sizes. Moreover, the dynamic beaviour starts to be more critical. The floating structures are design in a way that the inertia forces are compensated by the buoyancy forces what makes the dynamic behaviour of the structure more favorable. (Lesny, 2011)

Fig. 1.8: Floating offshore turbine from Kincardine Offshore Floating Wind Farms in Scotland (Cobra Group, 2019)

1.3 Suction bucket foundation

1.3.1 Suction installation process

The installation of suction bucket foundation consists of three steps. The first step is to lower the foundation to the seabed. Next, a self-weight installation stage begins. The bucket penetrates soil due to its own weight, ensuring a hydraulic seal between soil and the skirt that is essential for the further installation. The second installation stage is a suction penetration. A start of the pump enables the under pressure inside the bucket causing a downward force that pushes the foundation inside the soil, see fig. 1.9.

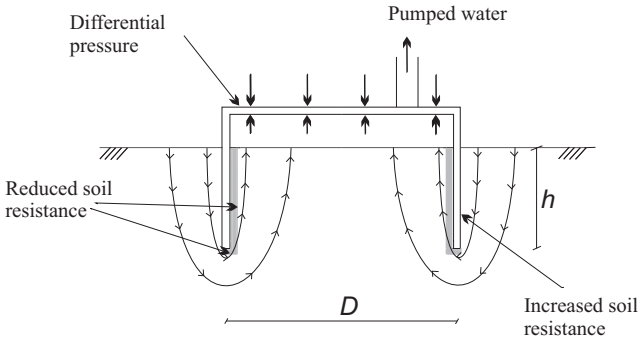

Fig. 1.9: Seepage around the skirt during suction installation in sand (Koteras et al., 2016)

Each of the steps is important for the final target penetration depth of foundation. The self-weight part is highly uncontrolled; therefore the structure must be carefully dropped as close to the seabed as possible, keeping the bucket in a vertical position. This is achieved by keeping an appropriate sinking speed for bucket. The installation of suction bucket is especially easy in soft clays, where the force resulting from applied suction balances the soil penetration resistance. The recent experience proves that in permeable soils like sand, the initially large soil penetration resistance is significantly reduced during suction installation, and therefore, the installation even in dense sand is not a limitation for this concept (Hogevorst, 1980; Tjelta et al., 1986; Bye et al., 1995). When the bucket achieves the final penetration depth, a valve connected to the pump is closed in order to seal the foundation with soil, what gives an extra pull-out capacity (Tjelta, 2015).

The suction applied under the bucket lid induces a flow around the bucket skirt very quickly if soil has a high permeability. The applied pressure induces an excess pore pressure around the bucket skirt, resulting in the drained soil response. The additional excess pore pressure changes the water head and starts the development of water flow in soil from the outside to the inside of the bucket. The upward flow results in a hydraulic gradient

that decreases the vertical effective stress, thus reduces the inside friction on the skirt. A very high gradient around the tip reduces significantly the tip resistance as well. The outside friction on the skirt might be increased due to a downward hydraulic gradient, but research indicates rather no changes in the outside friction (Lian et al., 2014a; Chen et al., 2016). For less permeable soil, the time required for the flow development is often not given during installation process, what results in the undrained response and no excess pore pressure development.

The suction applied during installation is limited by the cavitation pressure which increases with the water depth. The value of the allowable pressure before the cavitation limit is often reduced due to the pump capacity. For the oil and gas sector, the suction anchors were installed at deep waters, allowing a significant head difference. Moreover, those anchors were most often installed in clays, where the penetration resistance is relatively small. The suction bucket foundation for offshore wind turbines designed for both, smaller water depths and in much more resistant dense sand, were therefore initially rejected.

Two more restrains result in even smaller suction allowance, namely the structural and the geotechnical issue. The applied pressure creates a high load difference between the outside and the inside of skirt that might result in a buckling failure. Such failure can happen at the very beginning of suction phase, where there is not much skirt penetrated into the soil acting as a support. Failure takes place often also at the final stage of suction penetration, when the pressure is significantly increased and the soil strength is additionally reduced. A buckled skirt has a negative influence on the further installation and affect the performance of installed foundation. The Geotechnical restriction, described in the following section, are more complex and extended. The installation design is obviously more complex, comparing to other types of foundation, but still feasible and with many advantages.

As mentioned before, the suction bucket has been proven to be installed in many different soil combinations. Nevertheless, hard clays as top layers still are seen as a limitation for the suction bucket concept, especially in shallow waters.

Geotechnical failures during suction installation

The main geotechnical failure is due to piping. The recommendations found in different research work say that there is a critical suction for the installation design that, when exceeded, causes a piping failure. The piping channels develop around the entire skirt and break the hydraulic seal between soil and skirt, preventing from the further penetration. The suction pressure cannot be built up below the lid, so installation stops as the driving force drops significantly. Senders and Randolph (2009) reported that it is the exit hydraulic

gradient adjacent to the inside skirt that controls the piping. The critical suction for piping is often used in the proposals for the design of suction installation when addressing the reduction in soil penetration resistance.

Another challenge is the installation in layered soil, where clay layer is below sand. The seepage can be induced in sand layer, but the water is accumulated below clay layer in a gap, what is referred as a soil plug lift (Sturm, 2017). This has a negative effect on the further performance of foundation. The soil plug can also develop in a uniform soil as a heave, both in clays and sands. The soil plug heave prevents from reaching the final penetration depth.

The soil loosening due to the hydraulic gradient is rather seen as an advantage of the installation method in permeable soil. However, too excessive loosening might prevent from the total penetration depth because the required flow in soil cannot be reached. Sturm (2017) reported that the installation must proceed with a high penetration rate in order to avoid the excessive loosening.

Another problems result from the initial conditions before installation, f.ex. an uneven seabed , boulders on the way of the penetrating skirt, inclined low permeable layers.

Mitigation measures for installation

There are additional techniques that simplify the installation process in the difficult soil conditions, where the penetration resistance is higher than the one that can be overcome by the allowable suction. For example, the bucket skirt tip can be equipped with a nozzle system for water injection during installation. The water-jet alongside the skirt tip cause a liquefaction of seabed in case of sand, or remolding of clay; either way reducing the tip penetration resistance. The water injection at the skirt tip was investigated by Cotter (2010). The tests confirmed that the required suction for installation was reduced as an effect of the tip injection and this reduction was proportional to the pressure of injected water. Moreover, even though the injection pressure was high, it did not cause any piping failure.

Another method is a so-call 'cyclic penetration'. The applied pressure is cyclically stopped and started again, causing the skirt moving up before again penetrating the same location. Over-consolidated clays become remolded due to this process, leaving reduced friction on the skirt. In sands, the soil dilates in location of skirt tip because of the unloading. (Sturm, 2017). Figure 1.10 demonstrates the nozzle system on the skirt tip for water injection.

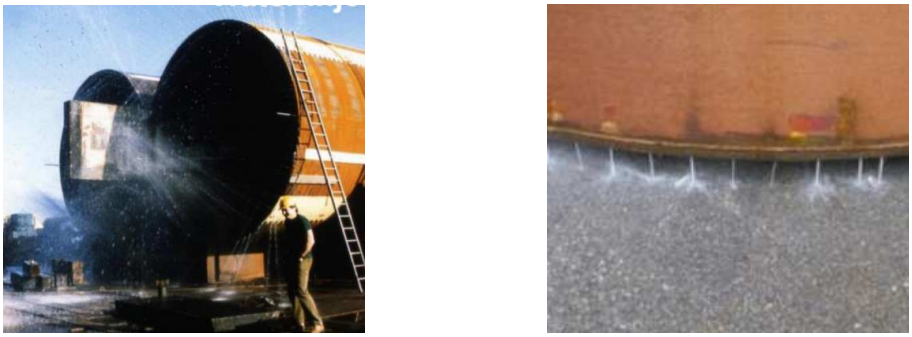

(a) (b)

Fig. 1.10: (a) Nozzle system on bucket skirt tip used for Gullfaks C platform and (b) for OWT Trial Installation tests (Tjelta, 2014)

Both mitigation methods have been first used in the oil and gas sector, when installing the Gullfaks C platform (Tjelta, 2015). Recently, both methods were used in OWA Trial installation tests on the Universal Foundation bucket concept (Universal Foundation, 2019b). In practice, both methods are often combined together in order to limit the effects on the soil state after the installation. Unfortunately, the experience in this area is still very limited.

Finally, structure can be additionally ballasted f.ex. sand bags, to either get a sufficient self-weight installation in very stiff clays, or to avoid a very high suction application that could result in the piping failure.

1.3.2 Suction bucket performance

As mentioned previously, the bucket foundation either transfers the load to the seabed by the tip resistance and the shaft friction as the monopile or, if the plug is formed, the entire base area works together as the base resistance next to the shaft friction. However, when bucket is sealed and loaded with tension, the suction pressure develops inside the soil plug and gives an extra bearing capacity. For high permeable soil this is only a short-time phenomena, which however is still sufficient to resist a force coming from a high wave (Tjelta, 2015).

Generally, foundation for offshore wind turbine must fulfill main requirements:

- the overall stability - ultimate limit state, ULS and accidental limit state, ALS,
- the permanent rotation not exceeding typically 0.5° - serviceability limit state, SLS,
- and appropriate stiffness to reach the requirements for a natural frequency of the structure.

The experience from monitoring of bucket foundations used in the oil and gas sector, the Gullfaks C and the Draupner E, shows a great advantage of the suction buckets installed in sand. For a short-term loading the response is undrained, whereas for long, multiply cyclic loads the soil response is drained (Tjelta, 2015). The pore pressure resulting from the transient load increases the pull-out capacity of the foundation; however, the accumulation of pore pressure reduces the effective stress, hence the strength of soil. The drained response during cyclic long-term loads does not allow the pore pressure accumulation. Too less experience in this area still leaves a limitation to the design with a decision if the tensile capacity in sand should be design as a short or a long-term behaviour.

For cyclic loading a drained bearing capacity is used and a degradation of strength with time is recommended. However, the behaviour of cyclically loaded foundation is still being questionable. Tjelta (2015) suggested that, in case of dense sand, there is an undrained response fur a duration of one cycle load. The pore pressure disappears after the cycle and do not cause the accumulation of rotation, hence do not reduce the strength of soil during storms.

1.3.3 General design basis for suction bucket performance

The design recommendations for offshore structure can be found in the DNV specifications or API recommended practice for fixed offshore platforms. Very recently, Carbon Trust OWA Programme has produced the design guidelines for suction caisson foundations for offshore wind farm (Carbon Trust, 2019b). Still, these are only recommendations and the design requires the assistance of results from the model tests and the full-scale monitoring always when some issues concerning the foundation design are not covered by the regulations.

1.4 Development of the Mono Bucket concept for the offshore wind turbines

The first prototype mono bucket for an offshore wind turbine has been installed with the suction assistance in Frederikshavn, Denmark in 2002 for a 3 MW Vestas turbine (Ibsen, 2008). The bucket has a diameter of 12 m and a skirt length of 6 m. Aalborg University carried out the installation of the bucket, and the behaviour of foundation has been fully monitored. Damgaard et al. (2013) described the dynamic response of the foundation.

Another big success was the choice of suction bucket foundation, the Universal Foundation concept (Universal Foundation, 2019a), as one of the winning concepts for the Offshore Wind Accelerator Programme, OWA. The

Fig. 1.11: Prototype of bucket foundation in Frederikshavn, Denmark (Larsen, 2008)

project was started by The Carbon Trust and other offshore wind developers in 2008 (Carbon Trust, 2019a). Since then, the Universal Foundation concept was used as a foundation for the meteorology masts at Horns Rev II in 2009 and at Dogger Bank in 2011. In 2014, the programme performed a trial installation campaign completing 28 suction bucket installations in only 24 days on the North Sea. The soil conditions were very diverse including soft clays, moraine clays, silts and layered soil profiles (Universal Foundation, 2019b).

The development of the mono bucket concept continues and Northland Deutsche Bucht GmbH announces the Deutsche Bucht Mono Bucket pilot demonstrator project in 2018. Deutsche Bucht is an existing offshore farm located at the German Bright in the North Sea. The project will test the Mono

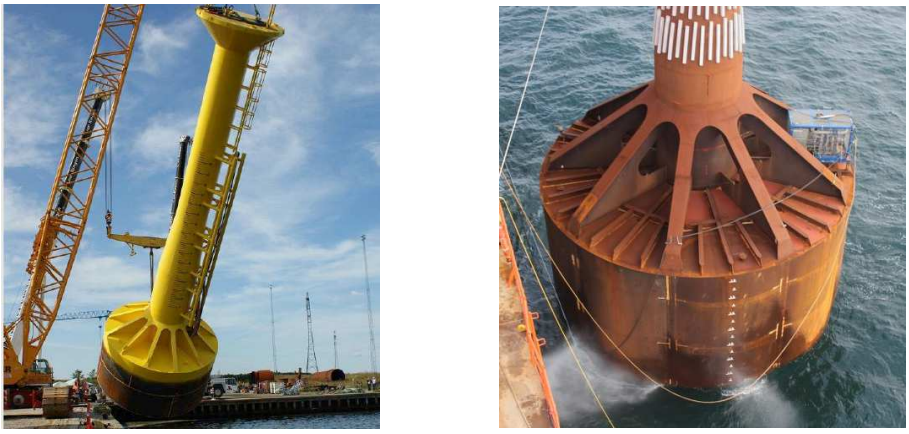

(a) **(b)**

Fig. 1.12: (a) Universal Foundation concept for Met Mast at Horns Rev II and (b) installation of foundation at Dogger Bank. Photo by Universal Foundation A/S

Bucket foundation concept under commercial operating conditions with a MHI Vestas wind turbine of 8.4 MW capacity installed on the top of the bucket foundation. 2 structures will be commissioned at Deutsche Bucht, starting in 2019. The Mono bucket prototype have a diameter of 18.5 m and skirt length of 18.5 m and will be installed in 40 m water depth. The project is funded by DemoWind with Universal Foundation A/S (Denmark) as the coordinator and the originator of the Mono Bucket concept used in this project. (Universal Foundation, 2019a)

The commercial use of the Mono Bucket concept gives the possibility of another great project the "OWA Mono Bucket Monitoring Part-A" (MoMo-A). It is a joint industry project within OWA Program (Carbon Trust) with the main purpose of the improvement of the Mono Bucket design with its risk reduction. The project will be based on the data evaluation from the full-scale demonstration and hopefully, will increase the competitiveness of the bucket foundation in the offshore wind market and the confidence in the industrialization.

The bucket foundation of the offshore wind turbine evolved during previous 18 years. Figure 1.13 demonstrates how the concept has been developing and reaching higher and higher technology readiness level, TRL (European Commission, 2017). The MoMo bucket project will lead to TRL 8 which means that the technology will be qualified for a commercial use.

The structure of bucket foundation has also evolved during that time. The increasing offshore market search for the solutions appropriate for large turbines. However, the cost-effectiveness demand for the offshore foundation

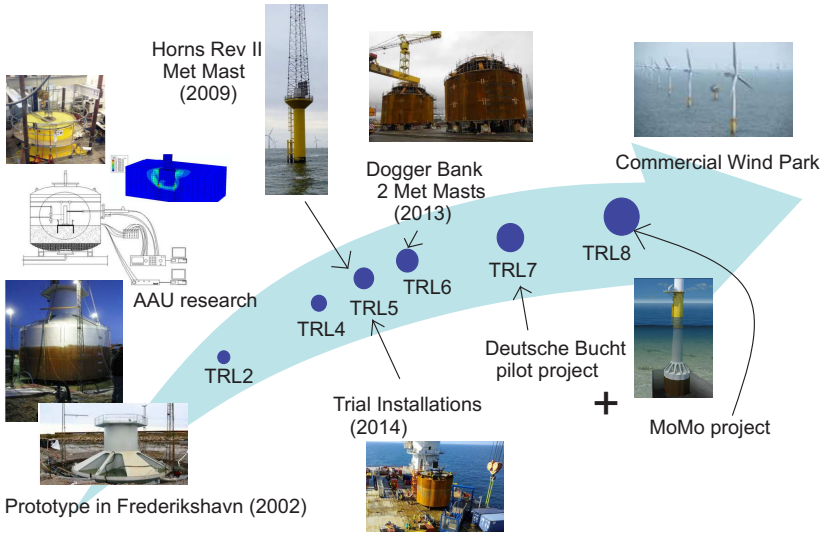

Fig. 1.13: Improvement in the technology readiness level for bucket concept (Ibsen, 2019)

did not allow for a constant increase in the bucket diameter and the skirt thickness. New solutions were tested in order to find an optimal design of a thin bucket skirt, possible for the installation (Madsen and Gerard, 2016). The buckling resistance of the structure was of a high importance. The development of the industrialized bucket foundation is a part of the Energy Technology Development and Demonstration Program (EUDP) with projects "Offshore wind suction bucket on an industrial scale - part 1" that included laboratory tests on a large-scale and "Offshore wind suction bucket on an industrial scale - part 2 Trial installation". EUDP projects have resulted in a modular suction bucket that consists of modulus with trapezoid profiles of skirt thickness only 17 mm with the industry already being prepared for a mass-production. The concept is planned to be used as a supporting structure for the jacket foundation in another project proposed for the Competitive Low-Carbon Energy application made by European Commission. The project proposal title is "Integrated Implementation of Industrial Innovations for Offshore Wind Cost Reduction" (i4offshore). The project assumes the commercial use of the jacking structure for 10 MW turbine with a very low-cost cabling solution in deep water depth. In 2018, Vattenfall installed already the first commercial suction bucket jackets in the North-east Scotland for the Vattenfall's European Offshore Wind Deployment Center (Vattenfall, 2018), with turbines of 8.4 MW and 8.8 MW capacity. The development of the bucket concept through different projects is presented in Fig. 1.14.

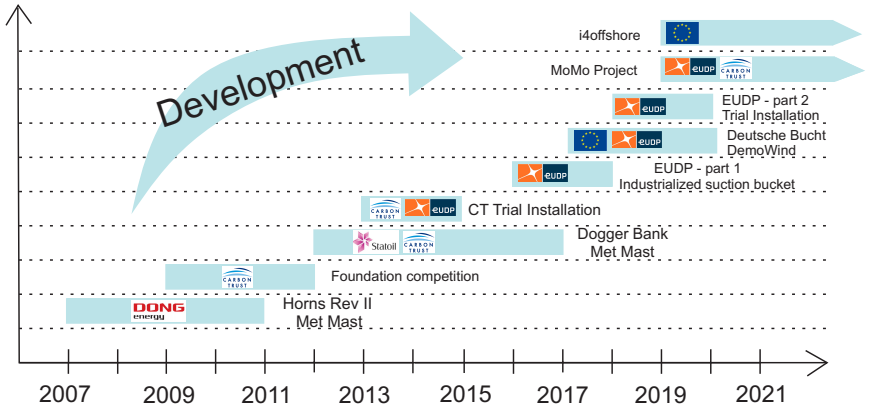

Fig. 1.14: Development of the bucket concept through different projects over years

The Ph.D. research presented in this thesis was finalized by European Union via the project "Innwind - Innovative Wind Conversion Systems for Offshore Applications". The work performed during the Ph.D. study was partially covering the EUDP projects mentioned above. The performance of suction bucket has been already tested at Aalborg University laboratory during Ph.D. researches (Foglia, 2015; Vaitkunaite, 2016; Nielsen, 2016b). The

research presented in this thesis is only based on the analysis of bucket foundation installation. The work includes the analysis of the suction installation for the initial concept with a round skirt structure, that have been used as a prototype in Frederikshavn, Denmark (2002), and also the results of the large-scale tests for the modular bucket.

Chapter 2

Design of suction installation

The chapter includes the reference to the most important scientific research concerning the design methods and the limitations for the suction installation procedure of bucket foundation in sand.

2.1 Calculation methods for suction installation of bucket foundation in sand

The installation process for a suction bucket involves design calculations in order to check the feasibility for the target penetration depth and the suction required for the process. The first step is the calculation of soil penetration resistance. If the resistance is larger than the load applied by the self-weight of the structure, the suction is applied under the lid and it gives the main driving force for the installation. Two methods for skirt penetration resistance are presented in this chapter.

2.1.1 Soil penetration resistance

The penetration resistance, R_{tot}, is a sum of the side shear on the outside and inside skirt, F_{out} and F_{in} respectively, and the bearing capacity of the tip, Q_{tip}, see Eq. (2.1). One analytical method on how to calculate the penetration resistance of skirted structure is to adopt the conventional pile design for the skirt friction and the bearing capacity theory for strip footing that is modified for the skirt tip resistance (API, 2000), see Eq.(2.2).

$$R_{\text{tot}} = F_{\text{out}} + F_{\text{in}} + Q_{\text{tip}} \tag{2.1}$$

$$R_{\text{tot,API}} = (A_{\text{s,o}} + A_{\text{s,i}}) \min \left[K_0 \tan\delta \int_0^h \sigma'_v(z)\, dz, f_{\text{lim}} \right] + A_{\text{tip}} \min \left[\sigma'_v(h) N_q, Q_{\text{lim}} \right] \tag{2.2}$$

where

$$A_{\text{s,o}} = \pi D_o$$
$$A_{\text{s,i}} = \pi D_i$$
$$A_{\text{tip}} = \frac{\pi}{4} \left(D_o^2 - D_i^2 \right)$$

$A_{\text{s,o}}$	outer skirt perimeter
$A_{\text{s,i}}$	inner skirt perimeter
A_{tip}	tip area of skirt
K_0	lateral earth pressure coefficient at rest
δ	interface friction angle
σ'_v	vertical effective stress
f_{lim}	limiting unit friction
N_q	bearing capacity factor (overburden)
N_γ	bearing capacity factor according to API (2000)
Q_{lim}	limiting unit end bearing
D_o	outside diameter
D_i	inside diameter

Recommended values for soil parameters are given in accordance to soil density, see Tab. 2.1. However, it is mentioned that these values are presented as guidelines only and for a detailed design they should be estimated based on soil tests.

Table 2.1: Design parameters for penetration resistance of piles in sand (API, 2000)

Density	δ [°]	f_{lim} [kPa]	N_q [-]	Q_{lim} [MPa]
Very Loose	15	47.8	8	1.9
Loose	20	67	12	2.9
Medium	25	81.3	20	4.8
Dense	30	95.7	40	9.6
Very dense	35	114.8	50	12.0

The vertical effective stress is normally assumed as $\gamma' z$, where γ' is the effective soil unit weight and z is the depth. In case of long skirts with small skirt wall thickness the skirt friction pushes the adjacent soil downward and

this may result in an increase of vertical stress outside the skirt wall. This changes the equilibrium of soil stress both inside and outside of the bucket, and additionally increase the skirt tip resistance. By analyzing the stress state during installation Houlsby and Byrne (2005) suggested the increase in vertical stress and modification of Eq.(2.2) to account for this increase. $\sigma'_{\mathrm{v,o}}$, $\sigma'_{\mathrm{v,i}}$ and σ'_{end} are the effective stress at the outside and inside skirt and at the skirt tip and they are influenced by the additional frictional force working on the skirt;

$$R_{\mathrm{tot,Houlsby\ and\ Byrne}} = A_{\mathrm{s,o}} \left(K_0 \tan\delta\right)_o \int_0^h \sigma'_{\mathrm{v,o}}(z)\, dz + A_{\mathrm{s,i}} \left(K_0 \tan\delta\right)_i \cdot \int_0^h \sigma'_{\mathrm{v,i}}(z)\, dz + A_{\mathrm{tip}} \sigma'_{\mathrm{end}} \tag{2.3}$$

Second recommended method is based on correlation of skirt wall friction and skirt tip resistance with measured cone resistance, q_c, in cone penetration test, CPT, see Eq.(2.4) (DNV, 1992). k_p and k_f are the empirical coefficients for skirt tip resistance and skirt friction respectively. The formulation is recommended for skirted structure foundations, e.g. bucket foundation.

$$R_{\mathrm{tot,DNV}} = Q_{\mathrm{tip}} + \left(F_{\mathrm{in}} + F_{\mathrm{out}}\right) = k_p\left(h\right) A_{\mathrm{tip}} q_c\left(h\right) + \left(A_{\mathrm{s,o}} + A_{\mathrm{s,i}}\right) \cdot \int_0^h k_f\left(z\right) q_c\left(z\right) dz \tag{2.4}$$

DNV (1992) suggested values of k_p and k_f coefficients for dense sand and stiff clay in North Sea conditions that allows for calculation of the most probable soil resistance and the highest expected soil resistance for given soil conditions, see Table 2.2. The correlation between penetration resistance of skirt tip and cone penetration test have been already suggested by Hogevorst (1980) for suction piles. Continuing the trend, Tjelta et al. (1986) proposed a linear correlation between measured cone resistance and both unit skirt friction, $\tau_{\mathrm{skirt,u}} = K_s q_c$, and unit tip resistance, $\sigma_{\mathrm{tip,u}} = K_t q_c$, with K_s equal to 0.001 and K_t ranging between 0.2-0.25 for sand. The solution was proposed for pile foundations. Correlation value for skirt friction is the same as the one proposed by DNV, but it is smaller for unit tip resistance.

Table 2.2: Empirical coefficients recommended by DNV (1992) for North Sea conditions

Type of soil	Most probable		Highest expected	
	k_p	k_f	k_p	k_f
Clay	0.4	0.03	0.6	0.05
Sand	0.3	0.001	0.6	0.003

The CPT-based solution was widely used in the suction bucket research area, but with some variations in the resistance calculation. One of the examples is (Feld, 2001), where the skirt tip resistance of mono bucket is related to

the cone resistance. Feld (2001) reported that the skirt friction should not be related to cone resistance in the same manner, as the empirical coefficient k_f is very uncertain. Instead, the skirt friction is based on the effective stress and a factor that depends on a roughness of the structure and on a friction angle. The roughness should be calibrated from field tests and the friction angle derived from CPT results. Following these observations Houlsby et al. (2005) suggested that the friction on the skirt should be related to sleeve friction measured during CPT, f_s, while leaving the relation between cone resistance and skirt tip resistance. However, Senders and Randolph (2009) reported that the use of sleeve friction from the cone of CPT did not prove its reliability for developing pile design methods and recommended to use cone resistance to relate both, skirt tip resistance and skirt side friction, as proposed by DNV (2014).

Both solutions can be used for the design of penetration resistance of bucket foundation, and both are limited in a way. Total penetration resistance based on the conventional bearing capacity approach requires estimation of many soil parameters, starting with the soil unit weight, the friction angle and fianlly, the lateral earth pressure coefficient. Especially the last mentioned includes many uncertainties. The CPT-based method is more direct as the required CPT captures already all soil variability. However, research shows that the empirical coefficients k_p and k_f are also burdened with some uncertainties. No matter which method is used, the presence of the internal stiffeners on the bucket foundation structure influence the penetration soil resistance, as the area of penetrated skirt is increased. All changes in geometry of bucket foundation that changes the area of penetrated structure must be taken into consideration during calculations.

2.1.2 Reduction due to suction

The installation process in sand relies more on the reduction of soil stress around the skirt than on the downward force coming from the differential pressure on the lid. Therefore, the appropriate seal from the self-weight installation is of a great importance. When the suction process begins, the attention is set on how fast the suction is applied. Too fast application might cause a piping channels occurrence and failure of installation.

Drained loading during installation in sand induces the excess pore pressure and the flow around the skirt. This results in the hydraulic gradient development around the skirt and a change in the vertical soil effective stress. The upward flow decreases the soil stress and the downward flow increases the soil stress, see Eq. (2.5). This must be accounted for in the design of the installation process.

$$\sigma'_v = \gamma' z \pm i \gamma_w z \tag{2.5}$$

i	hydraulic gradient
γ_w	water unit weight

For the conventional approach based on bearing capacity theory, this is captured by changing the effective vertical stress included in the calculations. Houlsby and Byrne (2005), who proposed the use of this method, made an assumption on linear distribution of excess pore pressure around the skirt. For the inside skirt the excess pore pressure drops from the value of applied suction under the bucket lid, p, to the excess pore pressure developed at the tip, u_{tip}. This approach requires an estimation of pore pressure factor, α, which is the ratio between developed excess pore pressure at the tip and the applied suction.

$$\alpha = \frac{u_{\text{tip}}}{p} \tag{2.6}$$

The pore pressure factor is derived from the numerical calculations assuming a fully-developed seepage flow. The formulations for the α values are presented in the following subsection. For the outside skirt the excess pore pressure drops from u_{tip} value to 0 at the soil surface. When the pore pressure factor is known, the effective soil unit weight in Eq. (2.3) is replaced by its changed value due to hydraulic gradient: $\gamma'_{\text{out}} = \gamma' + \frac{\alpha p}{h}$ for the outside soil and $\gamma'_{\text{in}} = \gamma' - \frac{(1-\alpha)p}{h}$ for the inside soil. There are some research study on the distribution of excess pore pressure on the skirt, showing that the distribution is not linear, especially close to the skirt tip. The models are complex and based only on the numerical study, so far not tested in scale or field tests (Harireche et al., 2014; Guo et al., 2016).

When the penetration resistance is designed based on CPT results the approach is slightly different. The parts of soil penetration resistance are changed in relation to the ratio of applied suction to its critical value, p_{crit}. Feld (2001) proposed that calculated parts of soil penetration resistance are multiplied by α-factors:

$$\alpha_t = \left(1 - r_t \frac{p}{p_{\text{crit}}}\right), \tag{2.7}$$

$$\alpha_s = \left(1 - r_i \frac{p}{p_{\text{crit}}}\right), \tag{2.8}$$

$$\alpha_o = \left(1 + r_o \frac{p}{p_{\text{crit}}}\right); \tag{2.9}$$

for the skirt tip resistance, the inside skirt friction and the outside skirt friciton respectively. r_t and r_i are the maximum reduction in the tip resistance and in the inside friction. Feld (2001) reported that the outside friction on the skirt should be increased, but the maximum increase is limited by $r_o = 0.1\,(h/D)^{1/4}$.

The same approach is used by Houlsby et al. (2005), with the difference that the sleeve friction from CPT is used for skirt friction calculations. The following relations for reduced soil penetration resistance are proposed:

$$\begin{aligned} R_{\text{red}} &= K_t(h) A_{\text{tip}} q_c(h) + A_{\text{out}} \int_0^h K_{\text{out}}(z) f_s(z) dz \\ &\quad + A_{\text{in}} \int_0^h K_{\text{in}}(z) f_s(z) dz; \end{aligned} \tag{2.10}$$

where

$$K_t = k_p \left(1 - r_t \frac{p}{p_{\text{crit}}}\right)^{\beta_t},$$

$$K_{\text{out}} = \alpha_{\text{out}} \left(1 + r_{\text{out}} \frac{p}{p_{\text{crit}}}\right)^{\beta_{\text{out}}},$$

$$K_{\text{in}} = \alpha_{\text{in}} \left(1 - r_{\text{in}} \frac{p}{p_{\text{crit}}}\right)^{\beta_{\text{in}}}.$$

α_{out} and α_{in} are the empirical coefficients relating f_s to the skirt friction during self-penetration; r_t, r_{out} and r_{in} are showing the maximum changes in resistance; and β_t, β_{out} and β_{in} are empirical factors. This methodology requires a lot of testing experience in order to establish coefficients and factors, which are neither described by Feld (2001), nor by Houlsby et al. (2005).

The solution for reduced penetration resistance presented by Senders and Randolph (2009) is more simplified and requires only an estimation of critical suction against piping failure, see Eq. (2.11). The reduction in inside friction and tip resistance is linear in accordance to the pressure ratio. Reaching the critical suction reduces the inside friction and the tip resistance to zero. Moreover, the outside friction is left unaffected during the suction installation.

$$R_{\text{red}} = F_{\text{out}} + (F_{\text{in}} + Q_{\text{tip}}) \left(1 - \frac{p}{p_{\text{crit}}}\right) \tag{2.11}$$

Lian et al. (2014a) reported that the critical limit for suction given by Senders and Randolph (2009) is too conservative as the suction applied in medium-scale tests described by them was exceeding the critical value without causing a piping failure. The calculation of total reduced resistance should be then changed according to their results of applied suction that

was in a limit of $1.5p_{\text{crit}}$.

$$R_{\text{red}} = F_{\text{out}} + \left(F_{\text{in}} + Q_{\text{tip}}\right)\beta \tag{2.12}$$
$$\beta = 1 - \frac{p}{p_{\text{crit}}} \quad \text{for } p \leq p_{\text{crit}}$$
$$\beta = 0 \quad \text{for } p_{\text{crit}} \leq p \leq 1.5p_{\text{crit}}$$

2.1.3 Required suction

The suction required for penetration of skirt is based on the calculated soil penetration resistance. The self-weight of the structure, accounted for the buoyancy, works already as a driving force during installation. However, as the soil penetration resistance in sand is high, the self-weight is not sufficient and the suction applied under the bucket lid results in a main driving force. The required suction is calculated as follows:

$$p_{\text{req}} = \frac{R_{\text{red}} - V'}{A_{\text{lid,in}}} \tag{2.13}$$

p_{req}	required suction for the installation
V'	effective vertical load resulting from the self-weight of bucket
$A_{\text{lid,in}}$	inside area of the bucket lid

The penetration resistance included in Eq.(2.13) is calculated for the chosen design method. The unreduced resistance gives a very safe prediction, which is too conservative. The resistance should account for the reduction due to the seepage flow.

2.1.4 Critical suction for installation

A critical suction is a theoretical value for each penetration depth at which the exit hydraulic gradient, i_{exit}, adjacent to the inside skirt is equal to a critical hydraulic gradient, i_{crit}, which is calculated with the following equation.

$$i_{\text{crit}} = \frac{\gamma'}{\gamma_w} \tag{2.14}$$

A safe installation assumes that the critical suction is not exceeded at any of penetration depths. However, a full formation of piping channels takes time, even in drained conditions. The applied suction that exceeds the critical limit only for a short-time does not necessarily prevent further installation (Feld, 2001).

Obviously, the critical gradient during suction installation of bucket foundation is first developed around the bucket tip, where the flow is most abrupt

and changes from downward to upward direction. Nevertheless, the skirt is continuously penetrating into the soil, so the skirt tip is experiencing some of the resistance from the lower soil layers. During installation the critical gradient is extending and might be developed on the entire embedded skirt. When the critical gradient reaches the soil surface inside the bucket compartment, referred to as the exit location, the piping channels occur (Senders and Randolph, 2009). Therefore it is the exit hydraulic gradient that controls the piping failure.

The expression for critical suction is derived as an analytical solution based on the exit hydraulic gradient. From the definition, the hydraulic gradient is the ratio between the change in hydraulic head, ΔH, and the seepage length, s. By performing numerical simulations of seepage flow, the applied change in water head is controlled. The hydraulic gradient can be calculated based on Darcy's law saying that the flow velocity is proportional to the hydraulic gradient through the coefficient of permeability, k.

$$i_{\text{exit}} = \frac{v_{\text{exit}}}{k} \tag{2.15}$$

The flow velocity at the exit, v_{exit} is extracted from numerical simulations. The seepage length can be determined as the change in the water head divided by the hydraulic gradient.

$$s = \frac{\Delta H}{i_{\text{exit}}} = \frac{p}{\gamma_w i_{\text{exit}}} \tag{2.16}$$

The expressions for critical suction is derived by assuming the exit hydraulic gradient to be equal to the critical gradient. The applied pressure in Eq.(2.16) becomes the critical pressure.

$$p_{\text{crit}} = s\gamma_w i_{\text{crit}} = s\gamma' \tag{2.17}$$

The most basic solution for critical suction comes from the analysis of equipotential and flow lines around the sheet pile wall. By derivation of the water head with respect to the distance for the exit location, the formula for critical suction is given as one of the principles of soil mechanics (Scott, 1963).

$$\frac{p_{\text{crit}}}{h\gamma'} = \pi \tag{2.18}$$

First research study for critical suction based on the design of bucket foundation was described by Clausen and Tjelta (1996). Solution for critical suction was derived from axisymetric numerical simulation of steady-stage flow, but only for penetration ratio, $h/D < 0.5$, see Eq.(2.19). Shortly after, the solution was investigated in different numerical programs and with different geometries. Similar normalized expression for critical suction are described

by Guttormsen et al. (1997), Eq.(2.20) for much more extended h/D ratio between 0 to 4, and by Feld (2001), Eq.(2.21).

$$p_{\text{crit}} = \frac{\gamma' h}{1 - 0.68/\left(1.46\left(\frac{h}{D}\right) + 1\right)} \tag{2.19}$$

$$\frac{p_{\text{crit}}}{h\gamma'} = 1.48\left(\frac{h}{D}\right)^{-0.26} \tag{2.20}$$

$$\frac{p_{\text{crit}}}{h\gamma'} = 1.32\left(\frac{h}{D}\right)^{-0.25} \tag{2.21}$$

More recently Senders and Randolph (2009) performed seepage flow analysis in the commercial program PLAXIS. The seepage flow normalized by the skirt embedded length is proposed for a larger extend of h/D. The solution tends to unity for infinitely long caissons, as the hydraulic gradient is essentially lost, and to the theoretical sheet pile solution, π, when h/D ratio is very small.

$$\left(\frac{s}{h}\right)_{\text{exit}} = \pi - \arctan\left[5\left(\frac{h}{D}\right)^{0.85}\right]\left(2 - \frac{2}{\pi}\right) \tag{2.22}$$

A normalized seepage length as a function of penetration ratio is also proposed by Ibsen and Thilsted (2010). The seepage problem during suction installation is solved numerically in program FLAC3D with an axisymmetric model and is valid for $0.1D > h > 1.2D$. This research included 2 cases, where the first case investigates the installation in homogenous soil, Eq.(2.23), and the second case investigates the installation in a sand layer that lies over an impermeable soil, Eq.(2.24). L_Ω is indicating the distance from the soil top to the impermeable layer.

$$\left(\frac{s}{h}\right)_{\text{ref}} = 2.86 - \arctan\left[4.1\left(\frac{h}{D}\right)^{0.8}\right]\left(\frac{\pi}{2.62}\right) \tag{2.23}$$

$$\left(\frac{s}{h}\right) = \left(\frac{s}{h}\right)_{\text{ref}} + 0.1\left(\frac{D}{L_\Omega}\right)\left(\frac{h}{L_\Omega - h}\right)^{0.5} \tag{2.24}$$

With the normalized seepage length, the normalized critical suction can be calculated with Eq. (2.25). Figure 2.1 (a) presents the comparison of normalized critical suction versus penetration ratio for some of the aforementioned solution. Figure 2.1 (b) indicates how the impermeable layer below sand is changing the suction limit according to Ibsen and Thilsted (2010).

$$\frac{p_{\text{crit}}}{\gamma' D} = \left(\frac{h}{D}\right)\left(\frac{s}{h}\right) \tag{2.25}$$

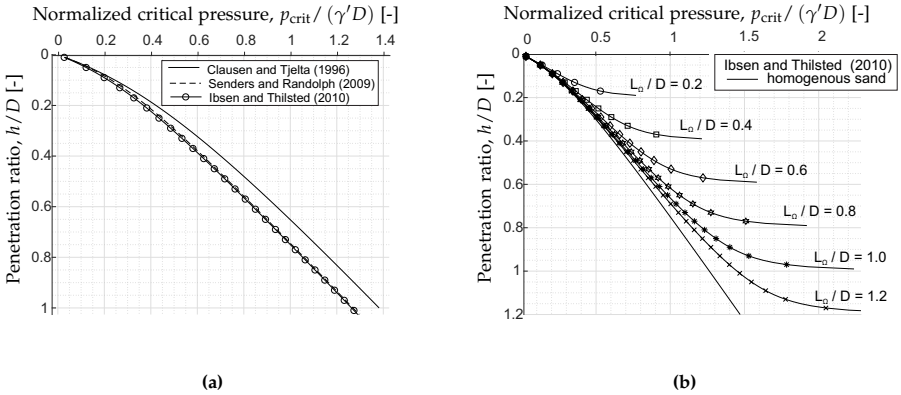

Fig. 2.1: (a) Normalized critical pressure versus penetration ratio of different solutions and (b) an influence of impermeable layer below sand on the suction limits

The comparison between different suggested p_{crit} are very similar and only solution proposed by Clausen and Tjelta (1996) gives a higher suction limit. This difference is increasing with penetration depth, but the solution proposed by Clausen and Tjelta (1996) is valid only for $h/D < 0.5$. Whereas different solutions are similar, there is a great difference when impermeable layer is introduced below the sand. Such a flow boundary increases the allowable suction and this increase is very significant when approaching the impermeable layer.

The mentioned solutions are derived for a uniform soil where permeability is constant. However, when the applied pressure approaches its critical value the soil plugged inside the bucket tends to swell and permeability of soil plug increases. It has been already well-understood that an increase in permeability increases the allowable suction, but it was considered as a safety factor (Clausen and Tjelta, 1996). More recently, when bucket foundation has started to be used in offshore wind energy, the cost-cuts are desired in the foundation design. Overly conservative design should rather be avoided.

The dependency of critical suction on the change in soil plug permeability was already proposed in 1999 by Erbrich and Tjelta. "Suction Number"presented in that research shows what is the limit for the under pressure in relation to the permeability ratio, $k_{\text{fac}} = k_i/k_o$. k_i is the permeability of the inside soil plug and k_o is the permeability of the surrounding soil. Solution is based on the finite element steady state seepage and the results are presented as diagrams where the critical suction number, S_N, is a function of penetration ratio h/D.

$$S_N = \left(\frac{\Delta H}{z}\right)\left(\frac{\gamma_w}{\gamma'}\right) = \frac{p_{\text{crit}}}{h\gamma'} \tag{2.26}$$

Additionally, the critical condition is defined by either the average hydraulic

gradient or the exit hydraulic gradient. What is more Erbrich and Tjelta presented diagrams for two cases: the first, where the entire soil plug is loosened and the second, where only a thin zone adjacent to the inside skirt has a higher permeability. Andersen et al. (2008) presented a diagram where the same approach is used, but only for exit hydraulic gradient and, where the entire soil plug is loosened, see Fig. 2.2.

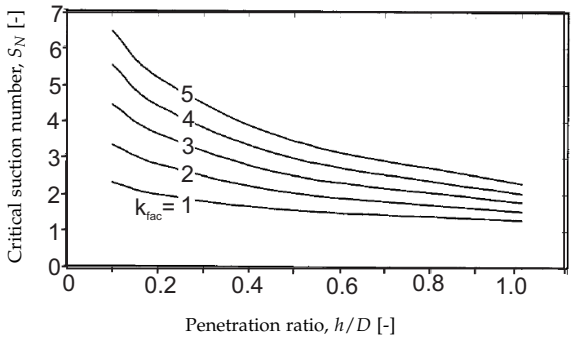

Fig. 2.2: Critical suction number (after (Andersen et al., 2008))

Houlsby and Byrne (2005) proposed that the critical suction should be calculated based on the upward hydraulic gradient that reaches its critical value. This causes the effective stress to be reduced to zero. The critical pressure is therefore calculated as

$$p_{\text{crit}} = \frac{\gamma' h}{1-\alpha}. \tag{2.27}$$

(2.28)

Based on the finite element analysis a formulation for pore pressure factor is proposed in the same paper as

$$\alpha = 0.45 - 0.36\left(1 - \exp\left(\frac{h}{0.48D}\right)\right). \tag{2.29}$$

However, Houlsby and Byrne (2005) reported that the suction applied under the bucket lid might cause a loosening of soil plug. The solution for pore pressure factor that accounts for the permeability ratio is shown in Eq.(2.30). This equation was fitted to the measured data from installation, but details of these installations are not specified in the paper. α used in this equation is the pore pressure factor for uniform permeability, Eq.(2.29). The dependency on k_{fac} on pore pressure factor is automatically included in the calculations of suction pressure, and also in the calculations of reduced soil penetration resistance. Senders and Randolph (2009) calculated that for typical values of

h/D the critical suction increases by 15-25% if k_{fac} increases from 1 to 2 and even by 30-50% if k_{fac} increases to 3. However, they did not include k_{fac} in their CPT-based method.

$$\alpha(k_{\text{fac}}) = \frac{\alpha\ k_{\text{fac}}}{(1-\alpha) + \alpha\ k_{\text{fac}}} \tag{2.30}$$

The change in soil plug permeability is a complex problem. There is an increase in permeability resulting from the increasing depth and the compaction of soil self-weight and there is a reduction caused by the seepage flow. More and more studies show that the permeability changes in the soil plug must be taken into account to make a reasonable design of suction bucket installation (Tran, 2005; Andersen et al., 2008). Increased permeability in soil plug results not only in higher allowable suction, but also changes the extend of reduction in the soil penetration resistance. Moreover, any changes in the soil stress state of the soil plug are important for the in-place performance of the foundation. Figure 2.3 show how the increased permeability in soil plug influences the limit for suction on the example of two aforementioned solutions (Houlsby and Byrne, 2005; Andersen et al., 2008).

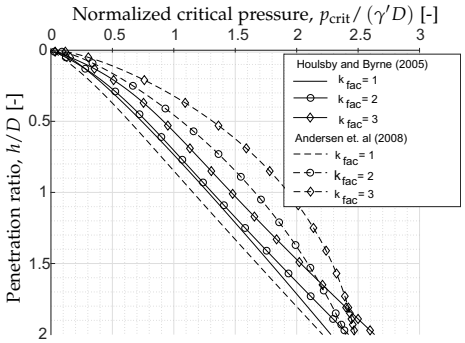

Fig. 2.3: Normalized critical pressure versus penetration ratio with the k_{fac} influence (Houlsby and Byrne, 2005; Andersen et al., 2008)

The increase in soil plug permeability results in much higher values of critical suction. There is also discrepancy between the limit suggested by these two different solution. The solution proposed by Andersen et al. (2008) varies much more when k_{fac} is increasing in comparison with the solution proposed by Houlsby and Byrne (2005).

2.2 Testing and monitoring of installation in sand

Some data from installation of real-scale suction caissons have been published already in 1980 by Hogevorst. Caissons of 3.8 m diameter and 5 to 10 m skirt

length were installed in dense sand at the mud-line of shallow lake. The obstacles in sand were not problematic for installation and, additionally, it was reported that the sand soil plug was loosened up, or even could have become liquefied. These were very important observations for the further research. Later, Tjelta et al. (1986) described exactly the same favorable installation effects for larger caissons. The beneficial effects of additional surcharge on the bucket, e.g. an increased dead weight, for reduction in required suction was reported by Tjelta (1995).

The development of excess pore pressure at the inside skirt of suction caisson installed in sand has been reported by Iskander et al. (2002). Tests were performed in a 1 g equipment with caisson models of 100 mm and 150 mm diameter and with the skirt length to the diameter ratio, L/D, of 2:1. Firstly, the minimum required suction for penetration was applied, and secondly, the maximum available suction was applied. Both tests showed very similar excess pore pressure development at the skirt and also both tests indicated that sand was liquefied during installation leading to excess soil plug heave. A significant reduction in required driving force was reported when compared to the jacking installation. However, it is questionable how such a small scale reflects on the real behaviour of soil plug.

Centrifuge tests on installation of suction caissons in sand were reported by (Allersma, 2003). Described tests showed that the suction application decreased the required force for final penetration in comparison to the jacking installation about 8 times. Moreover, the suction during installation tests were applied in two different manners: as a constant pressure and, as a suction pressure applied in pulses. The latter technique brought some small beneficial effects to the installation process, which was less susceptible to piping. When studying the normalized pressure for cases where the caisson dimensions were different, (Allersma, 2003) reported no significant influence of caissons dimensions on the penetration force. This finding is contradictory with full-scale observations, where additional dead weight (caisson dimensions are directly correlated with its dead load) reduces the required suction for installation (Tjelta, 1995). Again, small-scale of models could not reflect all soil phenomena that happen in real conditions.

Research presented by Tran (2005), which was a part of his Ph.D. study, gave many interesting observation on soil plug behaviour during suction installation. The speed rate of installation has been tested, both in a 1g equipment and in a centrifuge. For the 1g tests the models with following geometry was used: D=70-100 mm, L=100-140 mm and t=0.35-1.6 mm. The models used for centrifuge where even smaller. The developed suction pressure was found to be dependent on the installation rate. Tran (2005) discussed a possible explanation of such a soil behaviour in the seepage flow that is not a steady-state, but rather transient and the excess pore pressure development is very time-dependent. “The faster the installation is, the less time is available

for the pore pressure generation and any subsequent sand loosening to occur " (Tran, 2005). The fast installation did not cause any problems with piping. Moreover, the soil plug loosening was accessed by permeability factor k_{fac} to be equal 1.5 - 2.0.

Tran and Randolph (2008) also described the same tests performed in 1 g equipment and in centrifuge. They found that the initial depth of self-weight penetration has no influence on the final required suction, as long as the self-weight of caisson is kept constant. The applied suction creates the same seepage path with the same reduction effects on soil stress. The increase in self-weight, on the other hand, influences the required suction for further penetration by reducing it. The reduction is, however, much smaller than the increase in the self-weight, but the trend shows that the extra weight does not change the suction behaviour, but only shifts the suction path to the new starting point. Tran and Randolph (2008) also showed the dependency of installation on the skirt thickness. By keeping the same size and self-weight, the installation of bucket with a thinner skirt can stay longer in a self-weight installation stage, as the penetration resistance is much smaller. For suction installation that difference is almost neglected. This shows that the tip resistance is highly reduced due to the seepage flow. Again, the scale of models is very small.

Senders and Randolph (2009) tested their method for penetration resistance on full-scale caissons installations of Draupner E platform (Tjelta, 1995; Clausen and Tjelta, 1996; Bye et al., 1995) and Sleipner platform (Bye et al., 1995), both performed in a very dense sand. Draupner E platform included buckets with a diameter of 12 m, an embedded skirt length of 6 m and a wall thickness of 40 mm (h/D=0.5 and t/D=0.003). Caissons used for Draupner E installation were very well instrumented and gave many interesting data for analysis.

In order to make a comparison the CPT-based method was used with k_p=0.15 and k_f=0.0015. Whereas the coefficient for skirt friction is in a range given by DNV (1992), the other coefficient related to the skirt tip resistance is much lower. Even then the self-weight penetration was still much lower than the predictions. Tjelta et al. (1986) have already reported that for such dense sand lower values of k_p may be more adequate than the values suggested by DNV (1992). In second phase of installation the suction applied was in a close correlation with the prediction of required suction, but in all 4 caissons measured pressure slightly exceeded this prediction and also, the limit for a critical suction, see Fig. 2.4 (a). This could mean that the tip resistance and the inside skirt friction were reduced completely. However, by analyzing the total penetration resistance Clausen and Tjelta (1996) reported that, even with an increased outside skirt friction, the tip resistance and the inside skirt friction could not have been reduced to zero.

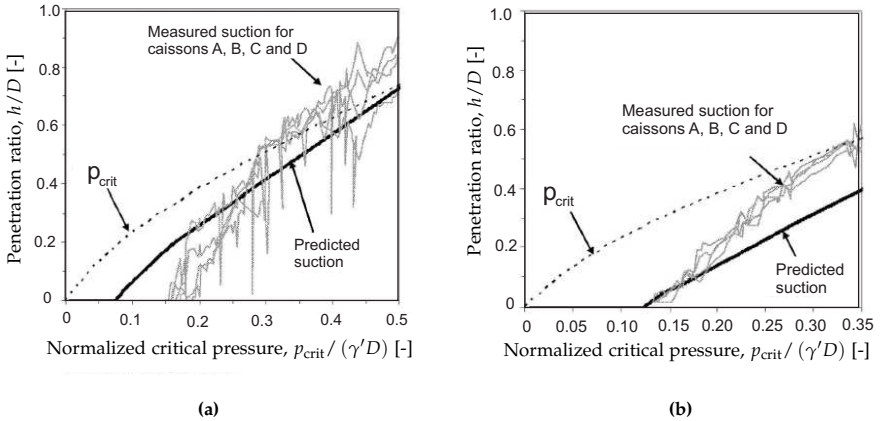

Fig. 2.4: (a) Normalized pressure applied during installation of caissons for Draupner E and (b) for Sleipner (Senders and Randolph, 2009)

Caissons used for Sleipner platform had a diameter of 14 m, an embedded skirt length of 5 m and a wall thickness of 35 mm (h/D=0.36 and t/D=0.0035). The applied suction was close to the predicted suction with CPT-based method at the beginning of suction installation phase, but after a while, the predicted suction is significantly exceeded by the real applied pressure, see Fig. 2.4 (b). The applied suction was at the critical limit in the final installation stage.

Interestingly, the pressure applied for caissons of Draupner platform exceeds the critical limit without experiencing an installation failure. For caissons installed for Slepiner platform, the applied suction lies in a range given by the predicted suction, as a lower limit, and the critical suction, as an upper limit.

Ibsen and Thilsted (2010) compared the values of applied suction with their proposed critical suction during an installation tests in Frederikshavn, Denmark. The tested bucket had a diameter equal to 2m and a skirt length equal to 2m. With this comparison Ibsen and Thilsted (2010) proved that impermeable layers below sand increases the allowable suction for installation. The measured suction was in some cases higher than the critical value predicted for homogenous sand, but not higher than the critical suction predicted for sand with some flow boundaries below.

Larger scale tests on the bucket installation in sand have been also reported by Lian et al. (2014a) and Chen et al. (2016). In the former research a bucket foundation with the following dimensions was used: D=0.5 m, L=0.5 m and t=0.01 m. Medium-dense sand was obtained after the vibration procedure, D_R=0.68. The bucket model was equipped with soil pressure sensors on the inside and outside skirt at different heights. The under pressure for

the suction installation was applied in pulses. A constant value of suction was kept until the bucket penetrated, then the suction was removed and started again with slightly higher value. Soil pressure measured on the outside and inside skirt shows that the soil is compacted during the penetration. The soil compaction is represented by a factor K which is the ratio between the effective pressure measured on the skirt (lateral pressure) and the effective vertical stress calculated based on γ'. K is much higher that the lateral earth pressure coefficient proposed by Jaky (1944) ($K_0 = 1 - \sin\varphi'$, which, in this case, is reported to be 0.38). This is mainly due to sand dilation during compaction that happens when skirt penetrates the soil. The measurements also show that during penetration much more pressure is developed on the inside skirt compared to the pressure on the outside skirt. The calculated value of K starts from around 10 for both inside and outside skirt. After reaching around 0.3 h/D there is a linear increase in K for the inside skirt. K on the outer skirt decreases gradually, but slowly with depth. The pressure inside the skirt is increasing significantly, probably due to the formation of soil plug. The comparison of suction tests with the critical suction indicates that the limit is too conservative. Moreover, the comparison between jacking and suction installation show that the ratio between inner friction and tip resistance measured in both tests is close to zero, whereas the ratio for outer friction is close to 1. Total reduction in resistance is assessed to be 78-94%.

Chen et al. (2016) used even larger bucket model, D=1.5 m, L=0.5 m, t=0.01 m, in the same set-up. Soil relative density was also indicating medium-dense sand, I_D=0.63. Additionally to the pressure sensors at the skirt wall, a micro pressure sensors were embedded in the skirt tip for a direct measurement of skirt tip resistance. Chen et al. (2016) reported the compaction of soil due to skirt penetration into the soil during jacking installation similar as Lian et al. (2014a), but there was no increase in measured pressure on the inside skirt due to the soil plug; both inside and outside pressure at the skirt are comparable. The lateral earth pressure coefficient $K_0 = 0.8 - 1.85$ was proposed by Andersen et al. (2008) based on the back-calculations of field tests. K equal to 1.85 is close to the results reported by Chen et al. (2016). For suction installation tests, where pressure is applied in pulses, the soil pressure at the inside skirt decreases straight after the suction is applied, but come back on its path when suction stops. On the outside skirt, the pressure increases slightly when suction is applied, but this increase is lost after short period of time when suction is still on. The comparison between jacking and suction installation gives the ratio for outer skirt friction close to 1, but it shows a reduction in tip resistance up to 50% at the end of the installation and, even up to 85% reduction for the inner skirt friction. Chen et al. (2016) reported fitting functions for the ratio between jacking and suction resistance

based on their experimental results:

$$\left(\frac{R_j}{R_s}\right)_I = 0.865\left(\frac{p}{p_{\text{crit}}}\right), \tag{2.31}$$

$$\left(\frac{R_j}{R_s}\right)_{\text{tip}} = 0.707\left(\frac{p}{p_{\text{crit}}}\right); \tag{2.32}$$

for the inner friction and the tip resistance respectively. These two equations were fitted to data with p_{crit} proposed by Senders and Randolph (2009). However, the critical suction suggested by Senders and Randolph (2009) was exceeded in tests without any piping failure observed.

2.3 Soil plug heave inside the bucket

A heave development is important for the design, as it prevents the target skirt penetration to be reached. The total length of skirt used for calculation of in-place performance must account for the reduction due to heave.

A soil plug heave was first experienced at Gorm field for caissons installation (Senpere and Auvergne, 1982). The heave prevented from reaching the target penetration depth. The excessive sand had to be first removed by water jetting to finally reach the desired penetration. The jetting might have a reducing influence on caisson capacity what has not been analyzed. Due to the experience with excessive heave, the research on suction foundation concept was pushed a bit out of interest for some years.

Data from installation of bucket foundations for jackets of Europipe platform indicates a very small soil plug heave of 4% of the total penetrated skirt length (Tjelta, 1995). The installation was performed in a very dense sand with I_D=90-100% and the applied suction was within the limit for critical value proposed by Clausen and Tjelta (1996). Iskander et al. (2002) reported that the soil plug heave is developed during suction installation and this does not depends on the amount of suction that is applied. (Allersma, 2003), through centrifuge installation tests, reported 5-10% of heave; however, the soil heave development was found to be strongly related to the skirt thickness. More heave was observed for thicker skirt wall. Slightly lower heave was observed when the suction during installation was applied in pulse instead of a continuous pressure application.

The research by Tran et al. (2007) in centrifuge resulted in the measured heave in a range of 7-9% of the total embedded skirt length. For installation with higher speed rate there was significantly less heave development (Tran, 2005). Additional to the heave a small conical depression was reported around the outside skirt after full penetration, but the volume change was very small compared to the volume change of inside soil heave. Tran (2005)

concluded that there is not much soil flowing into the caisson with seepage, otherwise the depression outside would be more significant. The heave development inside the caisson is rather resulting from the soil plug expansion due to dilation.

2.4 Empirical coefficients k_p and k_f

The approach based on the conventional bearing capacity theory requires estimation of soil parameters that can be based on soil tests or previous experience. However, they are often underestimated, especially the coefficient of lateral earth pressure when sand is very dense. It is more direct to base the design on the results of cone resistance from CPT, which already accounts for the soil properties. The difficulty lies, however, in the appropriate choice of empirical coefficients k_p and k_f, see Eq.(2.4), that rather should imply the geometry change between the cone from CPT and the penetrated skirt.k_p and k_f values are recommended by DNV (1992), see Tab.2.2, and their are based on the experience from oil and gas platforms. The approach is only valid for the unreduced soil penetration resistance where the suction is not applied. The appropriate method for the reduction must be additionally applied.

DNV (1992) states that the recommended value are appropriate for skirt of 20-30 mm thickness and if the tip area is larger or there are some internal stiffeners included in the design, k_f coefficient should be decreased. Generally, (Clausen and Tjelta, 1996) reported that empirical coefficient for very dense sand need to be reduced significantly. This is based on the self-weight penetration of platform for Europipipe, where the predicted penetration of 0.6-1.1 m in reality reached 1.8 m out of targeted 6 m. For the design of pile axial resistance Lehane et al. (2005) proposed a formulation for k_f coefficient, where the variation in coefficient are linked to the skirt thickness.

$$k_f = C\left[1 - \left(\frac{D_i}{D_o}\right)^2\right]^{0.3} tan\delta \tag{2.33}$$

C	coefficient suggested to be 0.021
δ	interface friction angle

The proposal was made based on the installation data. For some typical values for suction bucket foundations this give a range of 0.0033-0.0046, a bit higher than DNV range. In contrast to DNV (1992) recommendations, the increase in skirt thickness results in increased k_f. But that does not necessary mean that the trend of increasing k_f is similar for buckets with significantly larger diameters.

A broad investigation of k_f and k_p has been performed by Andersen et al. (2008). The back-calculations of the self-weight penetration for prototype tests, laboratory tests and field test led to a wide range of both parameters, see tab. 2.3

Table 2.3: Back-calculated k_p and k_f coefficients from different testing cases (Andersen et al., 2008)

Case	D(m)	h(m)	t(m)	k_f	k_p	I_D
Prototype A	5	0.75	0.02	0.13	0.0015	∼100
				0.15	0.0010	
Draupner E	12	1.8	0.04	0.01	0.0015	∼100
				0.03	0.0010	
				0.08	0.0000	
Sleipner T	14	1.95	0.0375	0.05	0.0015	∼100
				0.08	0.0010	
				0.13	0.0000	
16/11 E1	1.5	0.4	0.012	0.12	0.0015	∼100
				0.14	0.0010	
16/11 E2	1.5	0.8	0.012	0.09	0.0015	∼100
				0.12	0.0010	
16/11 E3	1.5	0.2	0.012	0.24	0.0015	∼100
				0.25	0.0010	
Sleipner T1	1.5	0.8	0.012	0.21	0.0015	∼100
				0.23	0.0010	
Sleipner T2	1.5	0.8	0.012	0.21	0.0015	∼100
				0.24	0.0010	
Sleipner T3	1.5	0.4	0.012	0.23	0.0015	∼100
				0.25	0.0010	
Sleipner T4	1.5	0.8	0.012	0.20	0.0015	∼100
				0.22	0.0010	
Sleipner T5	1.5	0.8	0.012	0.21	0.0015	∼100
				0.24	0.0010	
PEN5	0.557	0.04	0.008	1.24	0.0053	84
PEN9	0.557	0.05	0.008	0.95	0.0053	82
PEN12	0.557	0.05	0.008	0.93	0.0053	83
PEN13	0.557	0.02	0.008	1.18	0.0053	81
PEN1-3	0.557	0.45	0.008	1.03-1.19	0.0053	82

The results show that for a full-scale tests k_p coefficient is indeed reduced from values recommended by DNV (1992) and they are ranging between 0.01-0.15. The same holds for field tests (16/11 E1-3 and Sleipner T1-T5), where k_p varies from 0.09 to 0.25. The laboratory tests with small diameter buckets results in much higher values of both k_p and k_f. With k_f equal to 0.0053, k_p oscillates around 1 with its maximum value of 1.24. This confirms the soil plug development in the small scale models, which is much more dominant than in the medium-scale or larger-scale models.

Centrifuge tests presented by Senders and Randolph (2009) show that unreduced soil penetration resistance fits very well with CPT-based approach. Both the skirt friction and the tip resistance estimated with API (2000) theory

was significantly higher than the estimations based on the cone resistance results. k_p equal to 0.2 and k_f equal to 0.0015 was used in the estimations. The installation was performed in a very dense sand of $I_D \sim 90$ %.

For the medium-scale tests in medium dense sand Lian et al. (2014a) reported that for the prediction of tip resistance k_p equal to 0.6 is underestimating the real measurements. For fitting the data k_p equal to 1.2 was chosen. For the outer skirt friction value k_f equal to 0.003 is adequate, but completely underestimates results of the inner friction. By applying the method where the soil plug is formed a good correlation with results was obtained. The ratio between the base resistance of plug and the cone resistance, q_{plug}/q_c was chosen to be equal 0.05.

Chen et al. (2016) made also a comparison of measured tip resistance with the API approach (with N_q =40 according to table 2.1) and the DNV approach (with k_p =0.35) for medium dense sand. The tests were performed on a large bucket with a diameter of 1.5 m. The results are more consistent with the CPT-based method, see Fig. 2.5. The friction was measured almost the same for the inside and the outside skirt. The predicted friction for the CPT-based method uses $k_f = 0.0018$.

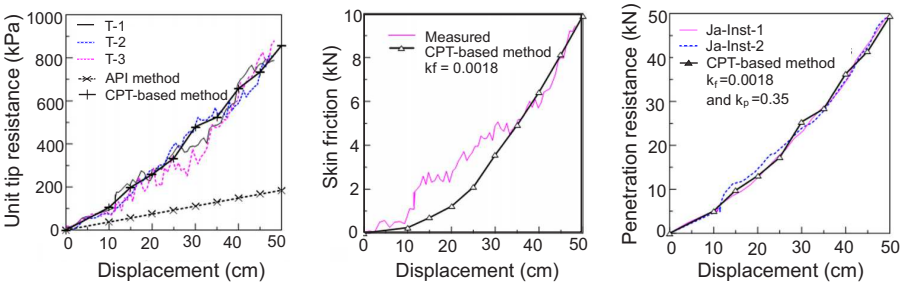

Fig. 2.5: Comparison of: (a) unit tip resistance with prediction from API (2000) and DNV (1992) with k_p=0.35, (b) skirt friction with prediction from DNV (1992) with k_f=0.0018 and (c) total penetration resistance (Chen et al., 2016)

Chapter 3

Scope of the thesis

The chapter gives an outline of the main findings from the state-of-art on the design of the suction bucket installation process and describes what are the main aims and objectives of the research work. The research work has been performed in order to understand the seepage flow effects on the soil adjacent to the bucket during and after installation and to optimize the design of suction buckets.

3.1 The state-of-art main findings

The suction installation of bucket foundation is based on the designing value of required suction for the target penetration depth. The calculation of the required suction depends on the soil penetration resistance. There are two different approaches that can be used in order to calculate the soil penetration resistance. The first approach is based on the classical bearing capacity theory with selected soil parameters, the API approach. The other method relates the resistance of the bucket skirt and the tip of skirt to the cone resistance measured during CPT through the empirical coefficients, the CPT approach. The research proves that the applied suction induces the seepage flow around the bucket skirt and this causes the reduction in the total soil penetration resistance.

The general installation mechanism is well established, but the detailed behaviour of the soil adjacent to the skirt and trapped inside the bucket is poorly accounted for. There are many assumptions that lead to an overly conservative design. The critical suction limit for the installation is described by many researchers; however, often the limit is indicated as underestimated. These aspects are confirmed with the field tests observations.

The seepage flow plays the most important role in the suction installation design. The flow has been analyzed thoroughly, but mainly in the finite

element programs. The seepage flow analyzed during the real installation should be addressed.

The inside soil plug is loosened due to the flow and this affects both the final reduction in the soil penetration resistance and the critical suction limit. The change in the soil plug permeability should be accounted for in the design method to make the design more cost-effective.

The soil plug heave analyzed in larger scale tests is very limited. The small-scale tests and the centrifuge tests indicate the soil plug heave reaching up to 10% of the total penetrated skirt. This needs to be included in the design of the in-place performance of the bucket. However, the scale is having a big influence on these results. As the dimensions of the bucket increases, there is less constrain on the trapped soil inside the bucket.

The research on the suction bucket installation in sand is rather devoted to dense sand state. The information on the empirical coefficients for CPT-based approach, the soil plug heave development and the critical suction limit for loose or medium dense sand are rather scarce.

Finally, there is not much research concentrated on the suction bucket foundations for the large offshore wind turbines. Only a few examples are given, (Lian et al., 2014b; Kim et al., 2013), but none of them show how the new idea should be implemented in the industrial process.

3.2 Research objectives

The main motivation for the thesis was to investigate a foundation concept that can be acceptable and cost-effective for the large wind turbines (e.g. a 10 MW turbine). This was driven by the requirements of the European offshore energy market that still seeks for solutions to make the offshore energy prices more competitive with the onshore market.

The first step in the research is based on the overall understanding of the suction bucket foundation and its behaviour during the installation. The objectives are firstly to optimize the size of the foundation by taking into consideration the critical states for the installation process and to optimize the shape of the bucket foundation by the comparison process between different geometries. This is accomplished by the medium scale laboratory tests at $1g$ for the bucket installation, through the analysis of the seepage flow based on the recordings of the pore pressure transducers around the bucket skirt.

The study is aiming at the verification of the seepage flow during the installation, the limits for the critical suction and the method that allows for the design of the required suction. The tests performed in the laboratory conditions account for the different boundaries, the different sand relative densities and the different bucket geometries. Moreover, the important aspects for the design are analyzed, like the soil plug loosening and the soil

plug heave development in a larger scale.

The general scope is to focus on the improvement in the design of the installation process. This also leads to the investigation of the modular bucket model, which is more adequate as a large foundation concept. Hopefully, the outcome of this research raises the awareness of the possibilities in the reduction of the costs for the offshore foundations located in the shallow and transient water depths.

Chapter 4

The research project

The chapter includes the summary of the research that has been performed during the PhD study. The research results have been published in the conference proceedings and in the journals. This summary is supported by the research papers attached to the thesis as the appendices. The most important findings are outlined with some supporting data and information gathered during the research.

The following articles are covering the research work:

- Paper A: Koteras, A.K., Ibsen, L.B., and Clausen, J. (2016) Seepage Study for Suction Installation of Bucket Foundation in Different Soil Combinations. *Proceedings of the* 26^{th} *International Ocean and Polar Engineering Conference*. 25 June-1 July, 2016. Rhodes, Greece.
- Paper B: Koteras, A.K., and Ibsen, L.B. (2019) Medium-scale Laboratory Model of Mono-bucket Foundation for Installation Tests in Sand. *Canadian Geotechnical Journal*, Vol. 56, No. 8: pp. 1142 – 1153.
- Paper C: Koteras, A.K., and Ibsen, L.B. (2018) Reduction in Soil Penetration Resistance for Suction-assisted Installation of Bucket Foundation. *Proceedings of the* 9^{th} *International Conference on Physical Modeling in Geotechnics*. July 17-20, 2018. London, UK.
- Paper D: Koteras, A.K., and Ibsen, L.B. (2019) Large scale installation testing of modular suction bucket. *Journal Geotechnique*. Submitted: 26-09-2019

Two more appendices are included in reference to the research:

- Appendix E: Manual for laboratory testing
- Appendix F: Laboratory tests results

4.1 Methodology

A relevant part of the design procedure for the bucket foundation is presented in Fig. 4.1, with areas of the research marked in color.

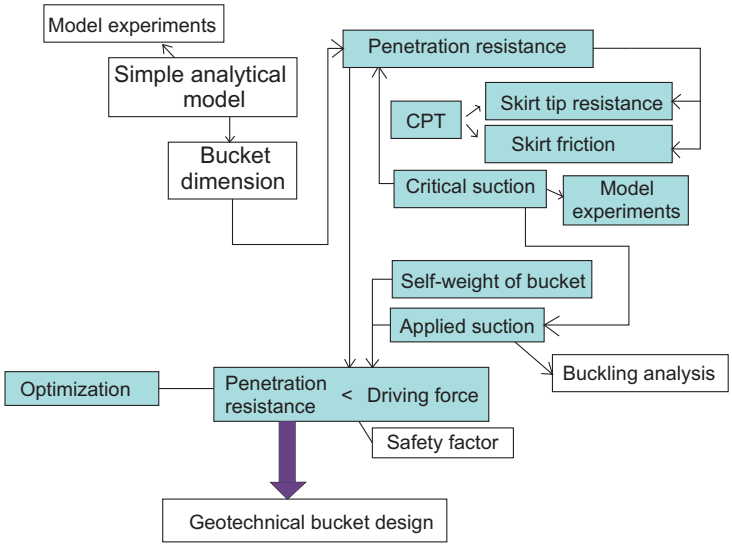

Fig. 4.1: Design basis for the bucket (The coloured boxes represents the research area included in the project) (Ibsen, 2008)

To analyze the installation process of the bucket foundation, the CPT-based method is chosen for the soil penetration resistance calculations. The choice is dictated by the experience gained from the previous research at Aalborg University and the well-prepared small scale CPT procedure that allows for the soil parameters derivation. The CPT cone resistance results consist already of all required soil parameters what moves away many uncertainties from the design.

The CPT-based approach allows for the calculation of the soil penetration resistance in depth intervals allowing for the variation in soil profiles. k_p and k_f are used as the empirical coefficients relating the cone resistance to the skirt penetration resistance (Eq.(2.4)). The reduction due to the seepage flow is accounted for through the β-factors that are applied on the inside skirt friction, the outside skirt friction and the skirt tip resistance. The β-factors, both in their form and their magnitude, are studied during the research work.

The critical suction is investigated through the numerical simulations of the seepage flow. The limit for the applied pressure is based on the exit hydraulic gradient. The analysis account for the changes in the soil plug permeability and different distances to the boundary conditions. The results

and the observations are described in Paper A.

The main part of the research is based on the physical models of buckets installed in sand. The test campaigns include the jacking installation tests and the suction installation tests. The varying conditions between different tests, apart from the installation methods, are: the different L/D ratio for the bucket model, the different distance to the bottom boundary of sand, the different soil relative density and the different geometry of the bucket skirt. The CPT-based method is applied on the laboratory data and the empirical coefficients k_p and k_f, and β-factors are derived with the fitting methods. The results and the observations are described in Papers B, C and D.

4.2 Numerical simulations of the seepage flow

The seepage flow characteristics are investigated in the commercial program PLAXIS 2D. The program is based on the finite element method and includes the built-in basic soil models. There is a consistent pattern in the sand behaviour and the closed form solutions are proposed for the normalized seepage length and for the pore pressure factor for different cases. The results of the seepage flow analysis are presented in paper A.

4.2.1 Modelling in PLAXIS 2D

An axisymmetric model is used for the simulations, with D equal to 4 m (a radius used in axisymmetry is $r = 2$ m). The round bucket geometry allows for a very simple model, which shortens the calculation time significantly. The installation process is divided into individual steps of given penetration depth with a steady-stage seepage calculation. The steps lie in a range of $0.1 \leq \frac{h}{D} \leq 2.0$. The penetration depth of the skirt is simulated by applying an impermeable interface to a line element. All calculation for the simulations are only limited to the ground-water flow. There is no loading and no movement of the skirt in the individual steps. The boundary conditions for the model and therefore prescribed in reference to the water flow only. The axisymmetric boundary is a closed boundary where the flow in any direction is prevented. The same condition is prescribed to the bottom boundary of the model. The free side boundary condition allows the water to flow in and out. The free soil surface has prescribed a specific flow condition, where the hydraulic head is set to H=20 m. The soil surface inside the bucket has the same flow condition, but the applied head is reduced in order to induce a flow in the soil. The change in head, ΔH, when multiplied by γ_w gives the value of the applied suction.

Three different cases are considered for this part of the research as seen in Fig. 4.2.

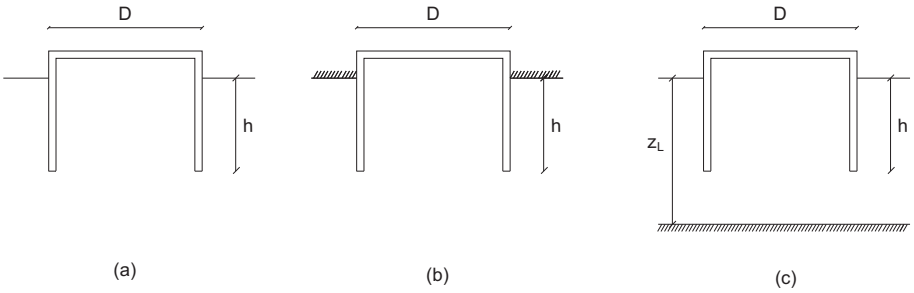

Fig. 4.2: Cases for the numerical analysis (Koteras et al., 2016)

Case (a) is a homogenous sand, case (b) consists of the impermeable layer above the sand and case (c) includes the impermeable layer below the sand, where z_L is referred to the distance from the soil surface to the impermeable layer. z_L varies in the interval $0.2 \leq \frac{h}{D} \leq 2.0$.

The domain boundaries should not influence the seepage flow results and therefore, a convergence analysis is performed. The excess pore pressure at the skirt tip is observed while increasing the domain size. If there are no considerable changes, the domain size is established. The result of the convergence analysis is a model with the bottom boundary set at 45 m below the soil surface, and the side boundary is situated at the distance of 10 D from the axisymmetry line. The bottom boundary does not account for case (c) where it is dictated by the z_L distance.

There are 2 different calculation phases used for the modeling. The first case is an initial phase where the pore pressure in the soil is calculated based on the water head defined for the project. The rest of the phases are the suction installation phases where the seepage flow around the skirt for different applied suction is obtained. This means that both the impermeable interface of each phase and the water head for the inside soil surface is activated for the calculation. The first suction installation phase consists of the interface of a length equal to 0.1 $\frac{h}{D}$. For each next phase the interface length increases by 0.1 $\frac{h}{D}$ until it reaches 2.0 $\frac{h}{D}$. For each suction phase the water head prescribed to the inside soil surface is decreasing in order to get an increasing trend for the applied suction value.

The soil model and the soil parameters for bearing behaviour are not influencing the results of the flow. The flow soil parameters are of the main importance in this type of calculations. A Van Genuchten model is assigned to the soil with a permeability coefficient for sand: $k_{x,y}$=7.128 m/day. x and y indicate that the parameter is the same for both directions of the 2D model. For the saturated soil zone that is the case for this research, the flow is modeled with the rules of Darcy's law.

Finally, in order to increase the precision of the desired results, the mesh of the numerical model is refined in the area of the soil plug and around the

skirt.

4.2.2 Analysis of the numerical results

The results extracted from the program are as follow:

- the exit flow velocity, v_{exit} from the stress point situated closest to the inside soil surface and the skirt,
- the pore pressure, u, at 5 different locations from the nodes at the inside and the outside interface.

The pore pressure extracted at the top of the inside interface is a direct value of the applied pressure, p. The pore pressure is also extracted at the tip, u_{tip}, just above the tip at the inside and at the outside interface, $u_{\text{tip,in}}$ and $u_{\text{tip,out}}$, and at the top of the outside interface, u_{out}. The excess pore pressure, Δu, is calculated by subtracting the hydrostatic pressure for given depth from the total results of the pore pressure.

The pore pressure factor, α, is derived as the ratio between Δu_{tip} and p, Eq.(2.6), for each $\frac{h}{D}$ calculation phase. The normalized seepage length is calculated based on the hydraulic gradients which are derived as follows:

$$i_{\text{exit}} = \frac{v_{\text{exit}}}{k}, \tag{4.1}$$

$$i_{\text{avg,in}} = \frac{p - \Delta u_{\text{tip}}}{h\gamma_w}, \tag{4.2}$$

$$i_{\text{avg,out}} = \frac{\Delta u_{\text{tip}} - \Delta u_{\text{out}}}{h\gamma_w}, \tag{4.3}$$

$$i_{\text{tip}} = \frac{\Delta u_{\text{tip,in}} - \Delta u_{\text{out,out}}}{2h_{\text{zone}}\gamma_w}. \tag{4.4}$$

h_{zone} is the distance between the node depth of the extracted pore pressure and the tip of the interface. The subsection 2.1.4 describes how to obtained the normalized seepage length, $\frac{s}{h}$, based on the hydraulic gradient. The normalized critical suction, $\frac{p_{\text{crit}}}{\gamma' D}$ is calculated with Eq. (2.25). The different soil cases resulted in the closed form solutions for α and $\frac{s}{h}$, which are presented in Paper A.

The development of the excess pore pressure at the skirt tip is influenced by the presence of the impermeable layer and increases the seepage effects, what results in a higher excess pore pressure at the tip. However, if the distance between the impermeable layer and the skirt tip is increasing, the influence becomes less significant. The results of simulations for all three cases are presented in Fig. 4.3.

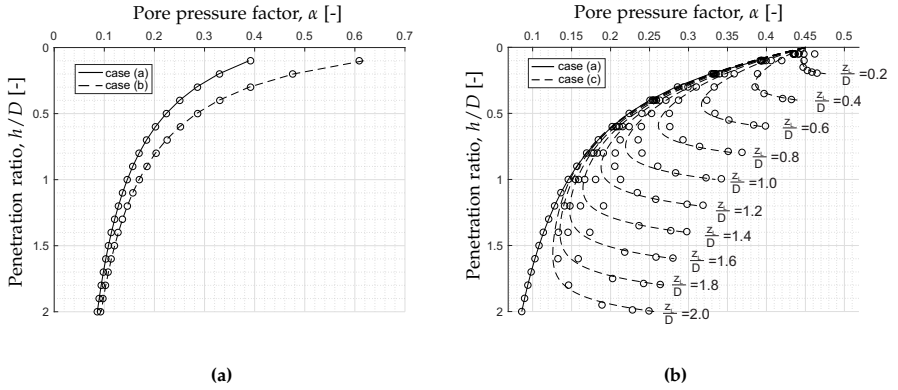

Fig. 4.3: The comparison of the pore pressure factor for different soil cases

Following expressions are proposed for each of the three cases:

$$\alpha_a = \frac{0.21}{\frac{h}{D} + 0.44} \tag{4.5}$$

$$\alpha_b = \frac{0.21}{\frac{h}{D} + 0.24} \tag{4.6}$$

$$\alpha_c = \alpha_a + a\frac{h}{D}\left(\left(\frac{h}{z_L}\right)^b + \frac{D}{z_L} - c\right) \tag{4.7}$$

where

$$a = 0.3\exp\left(-0.75\frac{z_L}{D}\right) - 0.35\exp\left(-4.4\frac{z_L}{D}\right) \tag{4.8}$$

$$b = 95\exp\left(-15\frac{z_L}{D}\right) + 4.8\exp\left(0.66\frac{z_L}{D}\right) \tag{4.9}$$

$$c = -\exp\left(-0.6\frac{z_L}{D}\right) + 7.7\exp\left(-8.3\frac{z_L}{D}\right) \tag{4.10}$$

The results for the seepage length in each of the three cases indicate that the values of the seepage length are the smallest at the skirt tip, then increases significantly for the average inside hydraulic gradient and slightly more for the exit hydraulic gradient. These three seepage length in case (a) decrease considerable in the first part of the penetration, up to $\frac{h}{D}$ = 1.0, and then become more stable. At the same time, the exit seepage length and the average inside seepage length become almost equal. Case (b) results are very similar to case (a), with the only difference at the beginning of the penetration, where the presence of the impermeable layer increases these values significantly. For case(c) the bottom impermeable boundary additionally increases the seepage length in its final penetration part in case of the exit gradient and the average inside gradient, but reduces the value in case of the tip gradient.

The seepage length for the outside average gradient is much higher comparing to the rest of the results. The seepage length increases proportionally with depth; however, the presence of the impermeable layer reduces the seepage length value in the close vicinity of that layer. The expressions for all seepage length derived from the numerical simulations are given in Paper A.

Figure 4.4 demonstrates how the impermeable layers are changing the critical suction pressure for the installation of the bucket foundation, which is based on the exit hydraulic gradient. Both case (b) and case (c) indicate that the presence of the impermeable layer is increasing the limit for the suction.

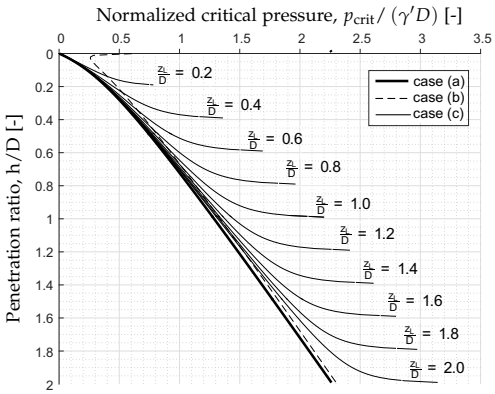

Fig. 4.4: Results of normalized critical suction for soil case (a), (b) and (c) (Koteras et al., 2016)

The results from PLAXIS 2D simulations directly show how the applied pressure influences the soil around the bucket skirt and the entire soil plug. If the time aspect is included, so the pore pressure is calculated with a transient flow, the visible difference in the behaviour of the seepage flow is observed for different permeability values. The seepage flow is limited by the time and cannot be fully developed, which is directly related to much less reduction in the soil penetration resistance, see Fig. 4.5.

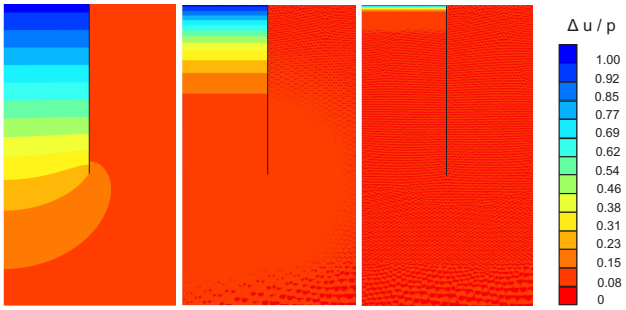

Fig. 4.5: Results of the ratio between excess pore pressure and the applied suction for soil with decreasing permeability in the transient flow analysis: on the example of sand, silt and clay

When considering the homogenous sand, where seepage is fully developed almost immediately, the reduction in the soil penetration resistance can be calculated using the CPT-based approach and applying the reduction factors to the individual parts of the resistance that are related to the critical pressure derived for different locations on the bucket skirt.

$$F_{\text{in}} = k_f \, \beta_{\text{in}} \, A_{\text{s,i}} \int q_c \, dz \tag{4.11}$$

$$Q_{\text{tip}} = k_p \, \beta_{\text{tip}} \, q_c(h) \, A_{\text{s,tip}} \tag{4.12}$$

$$F_{\text{out}} = k_f \, \beta_{\text{out}} \, A_{\text{s,o}} \int q_c \, dz \tag{4.13}$$

β-factors are derived as follows:

$$\beta_{\text{in}} = \left(1 - \frac{p}{p_{\text{crit,avg,in}}}\right) \tag{4.14}$$

$$\beta_{\text{tip}} = \left(1 - \frac{p}{p_{\text{crit,tip}}}\right) \tag{4.15}$$

$$\beta_{\text{out}} = \left(1 + \frac{p}{p_{\text{crit,avg,out}}}\right) \tag{4.16}$$

The bigger is the limit for the suction for the different hydraulic gradients to become critical, the less change in the soil penetration reduction takes place. The significantly higher seepage length for the outside average gradients show that there is much less increase in resistance, than the reduction in the inside skirt friction and in the tip resistance. The method requires a verification with the laboratory and the field tests of suction installation.

4.3 Physical modeling

Two laboratory set-ups have been used in the research for the installation tests: the set-up 'a' and the 'set-up 'b'. The set-up 'b' is the extended version of the former. The physical models and the detailed procedures for the installation tests are presented in Appendix E. The summary is also included in Paper B and in Paper C for the set-up 'a', and in Paper D for the set-up 'b'.

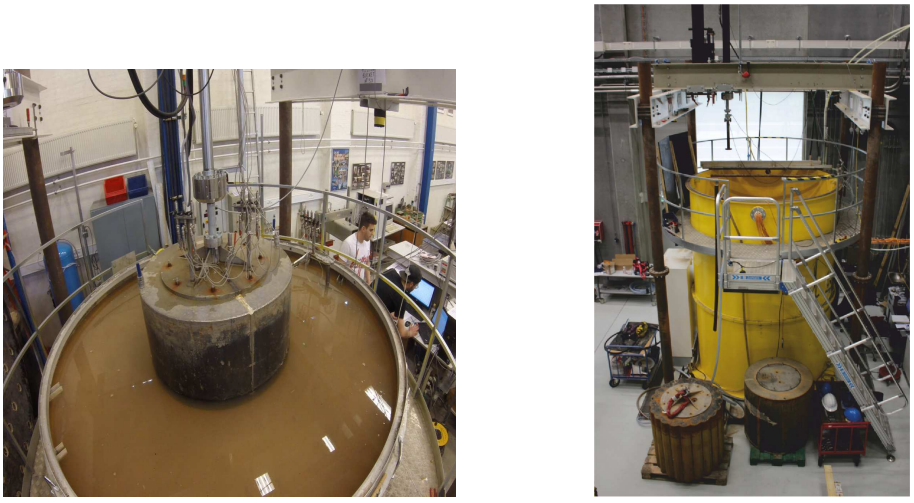

(a) (b)

Fig. 4.6: The set-up 'a' and the set-up 'b' for experimental installation tests

Two types of the installation tests are performed: the jacking installation, where the load on the bucket is applied through the hydraulic system, and the suction installation, where the suction pressure is applied under the bucket lid that is connected to a pumping system. Tests results are mainly used for the observation of the groundwater flow that occurs during the installation and its influence on the soil resistance reduction and the required suction. The elements included in the set-up 'a' are as following: (1) the soil tank; (2) the connection for the saturation system; (3) the ascension pipe for the control of applied gradient at the soil volume; (4) the bucket model; (5) the side boundary beam with pore pressure transducers; (6) the load cell; (7) the loading frame; (8) the hydraulic piston connected to the hydraulic pump; (9) the displacement transducer; (10) the vacuum pump; (11) the water container. These elements are presented in Fig. 4.7.

The model of L/D = 0.5 was used in the set-up 'a'; two models with a different skirt geometry and L/D = 1.0 are used in the set-up 'b', see Fig. 4.8. All three models consists of the skirt and the attached lid of 20 mm thick-

ness welded at the top of the skirt. Each model is equipped with 4 valves through which the suction can be applied, and through which CPTs can be performed after the installation is completed. The small steel channels of different lengths are attached to the skirt. Through the lid, they are connected to the pore pressure transducer, so the change in the pressure during the installation can be measured around the skirt. The locations for measurements are at $\sim 1/3$, $\sim 2/3$ and $\sim 3/3$ of the bucket skirt length and they are referred as PP1-PP7. For the model of L/D=0.5, there are only 6 locations; there is no measurements on the outside of the skirt tip. Figure 4.9 shows the dimensions and the locations of different elements on the bucket models.

Table 4.1 compares the different models in the geometry and dimensions. A_{skirt} and A_{tip} are the area of the entire skirt and the skirt tip respectively.

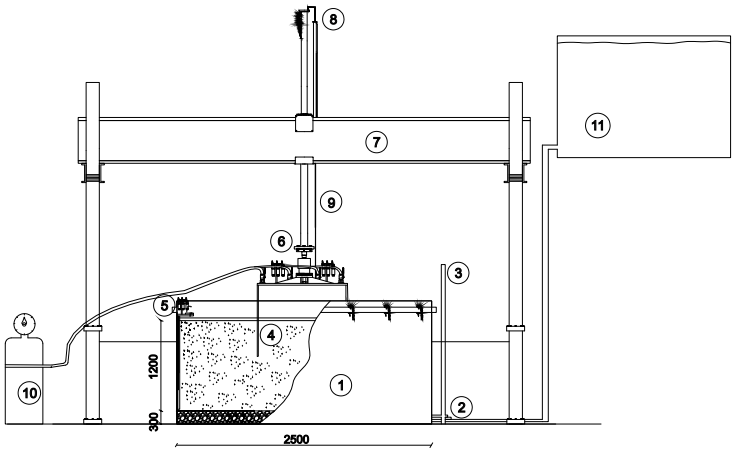

Fig. 4.7: The elements included in the laboratory set-up 'a' (Koteras and Ibsen, 2019)

Table 4.1: Geometry of the bucket foundation models

Type	L/D [-]	L [mm]	t [mm]	A_{skirt} [mm^2]	A_{tip} [mm^2]	t/D [-]	Mass [kg]
Round	0.5	500	3	$3.13{\cdot}10^6$	$9.40{\cdot}10^3$	$3{\cdot}10^{-3}$	201
Round	1.0	1000	3	$6.26{\cdot}10^6$	$9.40{\cdot}10^3$	$3{\cdot}10^{-3}$	214
Modular	$\sim$1.0	988	3	$8.23{\cdot}10^6$	$8.58{\cdot}10^3$	$\sim 1.7 \cdot 10^{-3}$	244

(a) (b) (c)

Fig. 4.8: Models of bucket foundation: (a) round bucket, L/D=0.5, (b) round bucket, L/D=1.0 and (c) modular bucket, L/D=1.0

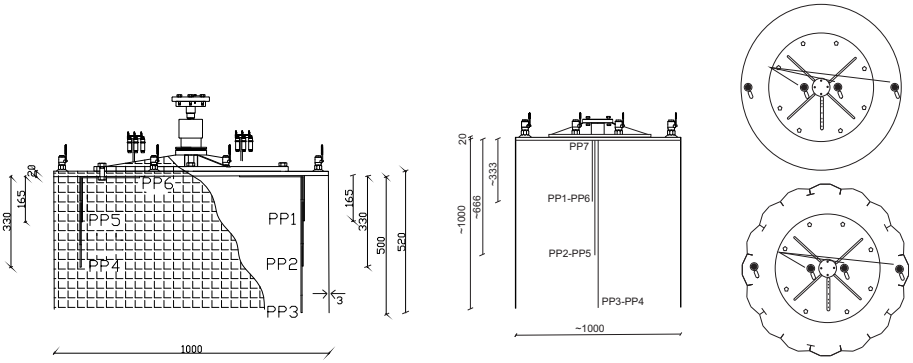

(a) (b)

Fig. 4.9: Dimensions and elements of (a) the round bucket model, L/D=0.5 (Koteras and Ibsen, 2019) and (b) the round and the modular bucket model, L/D=1.0

The soil container consists of the saturation system of perforated pipes placed at the bottom, covered by a gravel layer of 0.3m and a membrane. Next, sand of known properties is filled, see Table 4.2.

Table 4.2: Soil properties of Aalborg Sand no.1 (Borup and Hedegaard 1995)

Soil property	Value	Unit
Specific grain size, d_s	2.64	$[-]$
Maximum void ratio, $e_{\max}$	0.854	$[-]$
Minimum void ratio, $e_{\min}$	0.549	$[-]$
50%-quatile, d_{50}	0.14	[mm]
Uniformity coefficient, C_u	1.78	$[-]$

The set-up 'b' has been extended and improved what was dictated by the testing experience with the original set-up 'a'. The sand container have been increased significantly to the final height of 3.5 m. This allows for the installation tests where the bottom boundary is more distant, and for the installation of the bucket model that is submerged in the water. The first part of the tests were performed in 1.5 m of soil - low sand, and the second part of the tests were performed in 2.5 m of soil - high sand. This allows for the comparison between tests with different distance to the bottom boundary.

The new set-up is built-up in a new geotechnical laboratory of Aalborg University. The water container that supplies the set-up is situated much higher and allows for a higher hydraulic gradient to be achieved in the soil volume. The gradient is control by the improved water application system that measures the pressure of water entering the soil container. The laboratory system consists moreover of the vacuum system that can be used for the saturation of the pore pressure transducers. Another improvement is the change of the pump used for the suction installation. The vacuum pump used in the previous system was controlled manually while observing the recordings. The suction pump used in the set-up 'b' is controlled by setting the water extraction per minute, what is more precise. The water extracted is transported back to the container, so the system is water-closed. The same water level is kept during the installation process. Previously this was controlled manually by adding some water during the test. The biggest improvement is the changed location of the pore pressure transducers that measure the development of the excess pore pressure around the bucket skirt during the installation. They were previously located at the bucket lid, moving together with the bucket during the installation. As the bucket was not submerged, the changes in the pressures recorded in the locations around the bucket skirt were not only caused by the seepage flow, but also by the change in the hydrostatic pressure. The procedure for the separation of the excess pore pressure was difficult and the precision was slightly reduced. The pore pressure transducers in the set-up 'b' are situated at the top of the soil container and connected to the lid with long, flexible plastic tubes. The bucket is submerged prior the installation and the pore pressure transducers are saturated. The recording channels are zeroed down before the test starts. The records therefore are the direct measurements of the excess pore pressure caused by the seepage flow.

The boundary conditions are monitored much better in set-up 'b'. Previously, a rigid beam with the pore pressure transducers was inserted in the soil, close to the side boundary. The development of the excess pore pressure closed to the side boundary was possible to observed. The set-up 'b' consists of the built-in pore pressure transducers and the total pressure cells attached to the inside wall of the soil container and situated at the bottom of sand layer.

The main steps for the installation procedure in the lab are:

1. soil preparation: saturation, loosen up with the hydraulic gradient/ compact with the vibration, leveling;
2. CPT;
3. analysis of the soil parameters: uniform soil conditions are desired;
4. preparation of the bucket model: clean from previous installation, saturate pore pressure transducers in case of set-up 'a';
5. assembling the bucket model on the hydraulic piston;
6. filling the water to the soil container: around 10 cm in the set-up 'a', fully submerged skirt in the set-up 'b';
7. installation test;
8. pumping out the water to get the water level of around 10 cm above the soil surface;
9. visual observation of the soil;
10. CPT after installation;
11. uninstallation test/ removing the bucket.

The procedure for the installation test varies between the jacking and the suction test type. The jacking installation is a displacement controlled test with a speed of 1 m/h. The valves on the bucket lid must be opened during the installation, so no excess pore pressure is induced. The suction installation test is a load controlled test. It consists two phases: the self-weight installation test and the suction installation. The load is applied by the piston by carefully increasing the load until it reaches the value corresponding to the self-weight of the model. The load is kept constant for the rest of the installation process. The suction installation process starts with the valves on the lid being closed. The pump starts to apply the suction pressure. The installation proceeds and the suction pressure is controlled during the process. The excess pore pressure is built-up around the bucket skirt.

4.3.1 Reduction in soil penetration resistance

"The seepage flow plays a pivotal role in reducing the penetration resistance, allowing for full penetration despite the initial large soil resistance. "(Koteras and Ibsen, 2019) The laboratory results from the installation tests prove the beneficial aspects of the seepage flow on the suction installation process.

The CPT results of tests performed before the installation and after the installation allow for the analysis of the changes in the soil plug and the surrounding soil. The mean relative soil density is derived from each CPT test for the comparison, see appendix F. There is a significant decrease in the relative density of the soil plug after the suction installation. For tests performed on the bucket model with L/D=0.5, the average reduction is of 27.8%. These tests were performed in a dense sand conditions with the mean I_D before the installation varying between 88% to 91%. For the tests of the bucket model with L/D=1.0-low sand, the average reduction is of 36%, and these tests were performed in a slightly looser sand with the mean I_D before the installation varying between 72% to 76%. The tests performed in dense sand on the models with L/D=1.0-high sand show the average reduction of 38%. In general more reduction in soil penetration resistance is observed for tests on longer skirt bucket, as the phase of the suction installation is almost 2 times longer. The last mentioned tests includes the installation of the round and the modular bucket model. The comparison of the relative soil density before and after suction installation for the latter case indicated a slightly higher reduction. Figure 4.10 demonstrate how the relative density of dense sand is reduced on the example of tests performed on the L/D=0.5 model bucket and L/D=1.0-high sand model bucket for both the suction and the jacking installation.

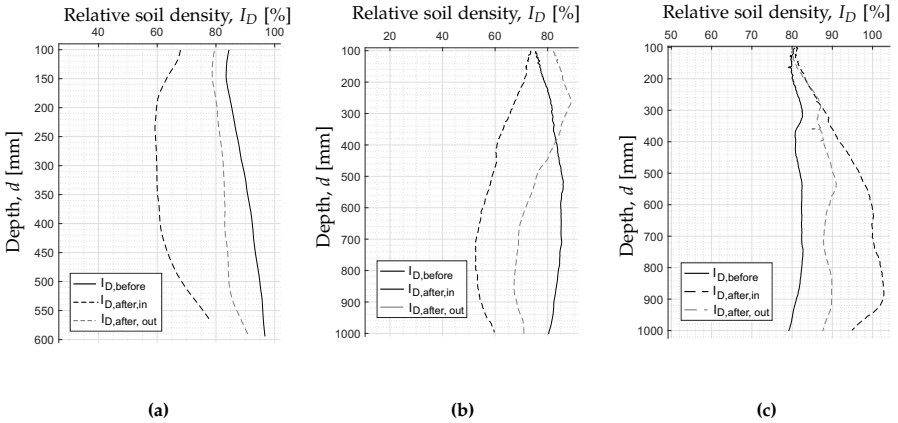

Fig. 4.10: The comparison of soil relative density before and after the installation: (a) test 1.9 (L/D=0.5, the suction installation), (b) test 3.14 (L/D=1.0, the suction installation) and (c) test 3.5 (L/D=1.0, the jacking installation)

The changes in the soil density are negligible for the suction installation in loose sand. For the medium dense sand with I_D of around 60%, there is a maximum of 20% in the reduction of the relative soil density.

When analyzing the CPT results for the jacking installation, the first observation is that in most of the tests the soil is slightly compacted after the

installation is completed. The shearing failure of the soil happens when the bucket skirt penetrates the soil resulting in the increased soil density. The tests were initial I_D was close to 90% indicates some small reduction in the density after the installation. For very compacted sand the dilation behavior is activated, resulting in a small reduction as an effect of the shear soil failure. The changes are rather small when compared to the changes resulting from the suction installation.

The CPTs results indeed indicate that the seepage flow reduces the strength of the soil. However, it is the direct comparison between the jacking tests and the suction tests in similar soil conditions that really captures the change in the soil penetration resistance as an effect of the seepage flow. There is much more reduction that was firstly indicated by the change in the CPT profiles, which means that the soil is able to regain its strength to some extend when the suction installation is completed.

As there is no seepage induced during the jacking installation and no reduction in the initial soil penetration resistance is expected, the ratio between the measured resistance during the suction installation and the measured resistance during the jacking installation, R_s/R_j, in similar soil conditions indicates how much the seepage flow is able to lower the required installation load. Figure 4.11 presents the ratio values for different tests.

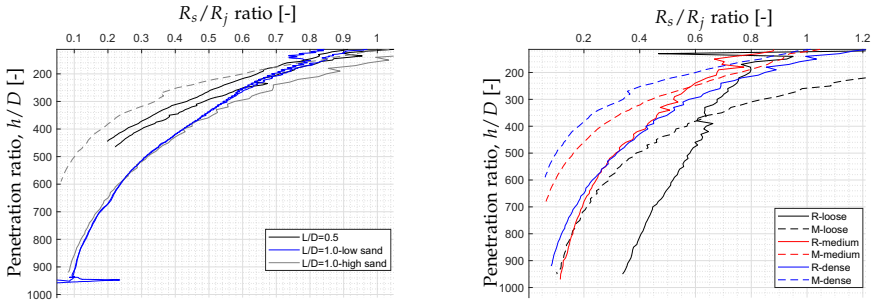

(a) **(b)**

Fig. 4.11: R_s/R_j ratio comparison for (a) dense sand but different L/D models and different z_L; and (b) for different soil densities and different skirt geometries (R - round, M - modular)

Tests used in fig. 4.11 are as follows: L/D=0.5 model presented with tests no. 1.2 and 1.9; L/D=0.5-low sand model presented with test no. 2.4 and 2.5; L/D=1.0-high sand model presented with tests no. 3.12, 3.24, 3.14 for the round bucket and test no. 3.19, 3.22, 3.23 for the modular bucket. First of all, there is no significant influence of the distance to the bottom boundary, z_L, at the resistance magnitude. A small difference is observed when compared the two different L/D ratios tests. Slightly more reduction takes place for L/D=0.5 for the same penetration depth; however, this is probably dictated

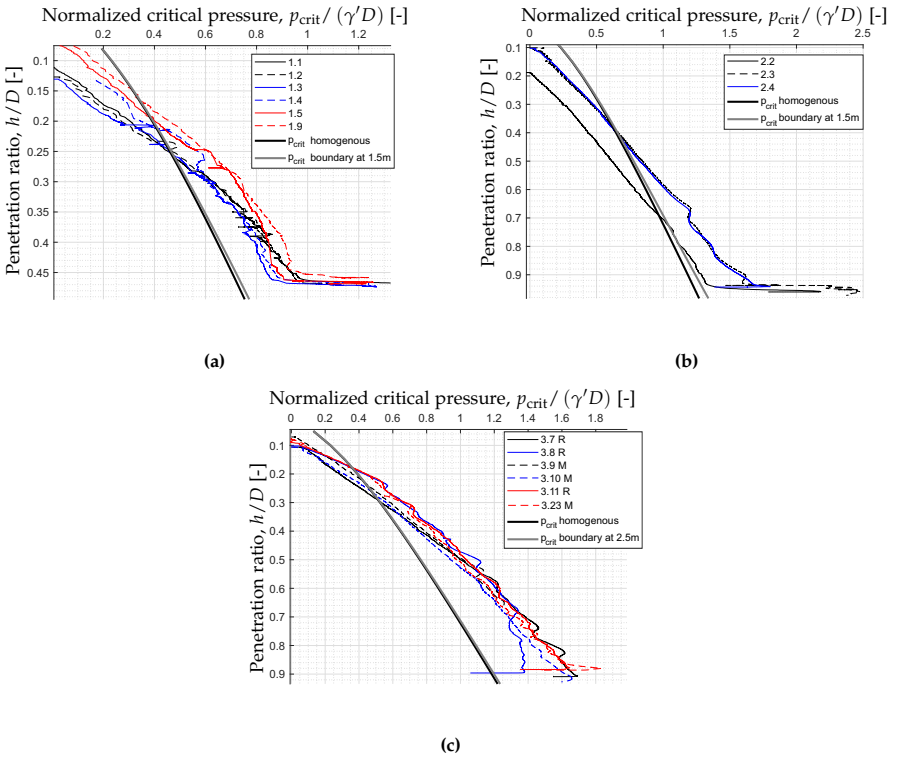

Fig. 4.12: Normalized applied pressure during suction installation with the critical values: (a) tests with L/D=0.5 model, (b) tests with L/D=1.0 model in low sand, (c) tests with L/D=1.0 model in high sand (R - round model, M - modular model)

by the fact that for the first test campaign where the L/D=0.5 model was used, the sand had a very high relative soil density and required a bit more suction for the final penetration, than the compared suction values at the same depth for the larger models.

The significant difference is seen when comparing two different skirt geometries for the similar soil conditions. Initially, the soil penetration resistance between the round bucket and the modular bucket varies a lot due to a considerable increase in the area of the penetrated skirt of modular bucket. The reduction is higher for the modular bucket for all different soil densities. The initial density of soil also influences the reduction factor. The higher the initial soil density is, the more significant is the reduction due to the seepage.

4.3.2 Applied suction during the installation

The applied suction during the bucket foundation installation is compared between different tests and presented in Fig. 4.12. The piping failure has

not been reported to any of the suction installations performed during the research. According to section 4.2 the critical pressure against the piping failure is dictated by the exit seepage length. The critical pressure calculated based on the expressions for the seepage length for homogenous sand and for sand with the impermeable layer at the bottom is plotted together with the results of the laboratory tests. The expressions are presented by Koteras et al. (2016), see Eqs. A.26 and A.30. In all of the tests, the limit has been exceeded.

The comparison is also made for the pore pressure factor development. The factor show the dependency on how the seepage flow evolves and what is the limit for the reduction in the soil penetration resistance. The pore pressure factor together with the numerical expressions derived by Koteras et al. (2016), see Eqs.A.20 and A.22, are presented in Fig. 4.13.

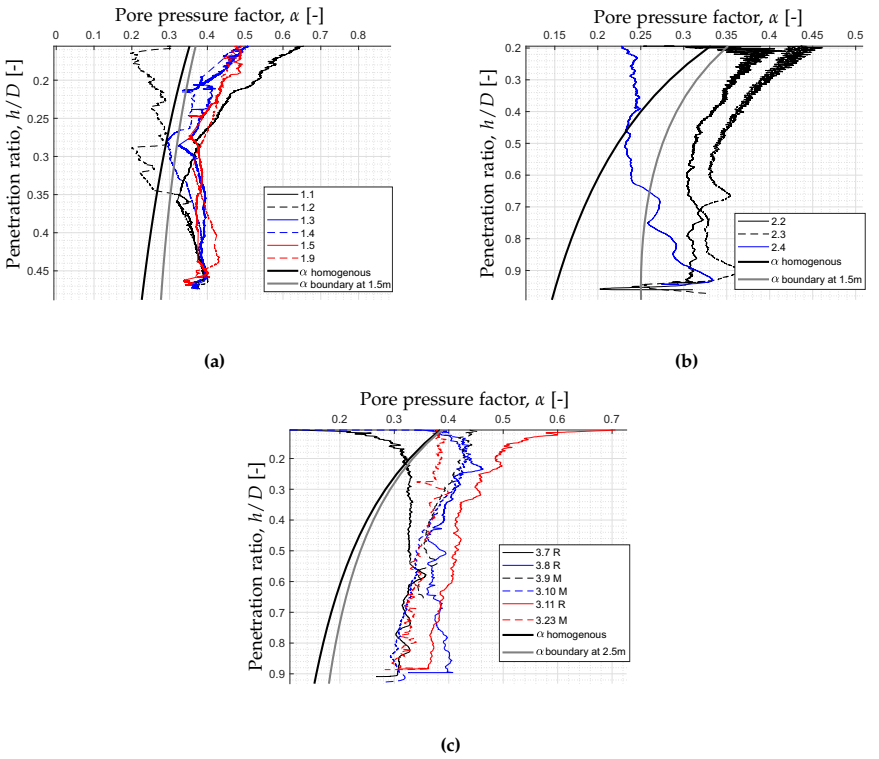

Fig. 4.13: Pore pressure factor, α, during suction installation with the numerical solutions: (a) L/D=0.5, (b) L/D=1.0-low sand, (c) L/D=1.0-high sand (R - round model, M - modular model)

The pore pressure factor decreases with the increasing depth. However, at some penetration depth the pore pressure factor becomes more constant. The depth is around h/D=0.3 for the case of the L/D=0.5 model and around h/D=0.5 for the case of the L/D=1.0 model. The results are not fitting well

with the solution proposed from the numerical simulations, even with the one that acocunts for the presence of the impermeable layer at the bottom.

4.3.3 Modular bucket model

The modular bucket model has been simultaneously tested with the round model at the high sand level in the improved set-up (b). The geometry of the modular bucket with a significantly increased skirt area and the additional stiffeners inside the bucket results in much higher initial soil penetration resistance during the jacking installation tests. At the maximum penetration depth for the modular bucket model, the soil resistance is around 3 times bigger in comparison with the jacking installation of the round model. The laboratory set-up limited the maximum jacking penetration of the modular bucket due to the load limits of the hydraulic piston. Interestingly, the total applied load required during suction installation is not so different between these two models. Figure 4.14 demonstrates the difference in the soil penetration resistance for the two different model types installed in loose, medium dense and dense sand. There is much bigger influence of the soil relative density on the jacking installation than on the suction installation. The much

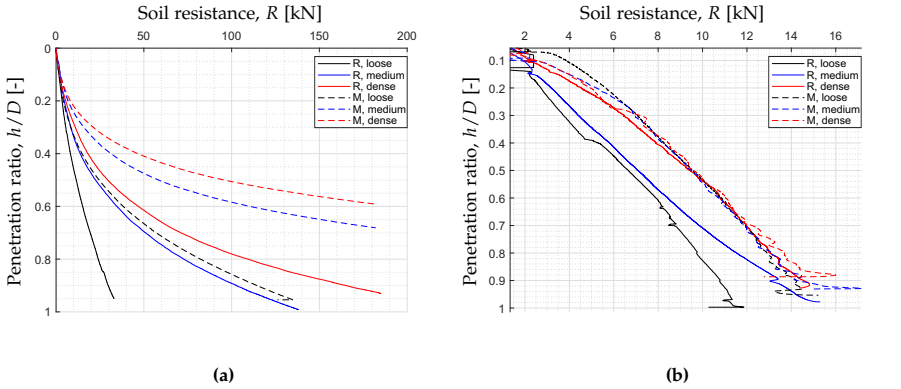

Fig. 4.14: The comparison of the soil penetration resistance for different soil densities: (a) jacking installations and (b) suction installations

higher jacking total load for the modular bucket compared to the round model is described as the effect of the shape factors that shall be included in the design of the initial soil penetration resistance. These shape factors add additional part of the resistance. Based on fig. 4.14, the increase in the modular bucket soil resistance is not only the results of the increased skirt, but there is an extra part resulting from the additional stress state, probably inside the soil plug, that need to be accounted for in the installation design. The shape factors for the modular bucket model are discussed in section 4.3.5. Figure 4.15 shows the dependency of the normalized applied suction and the

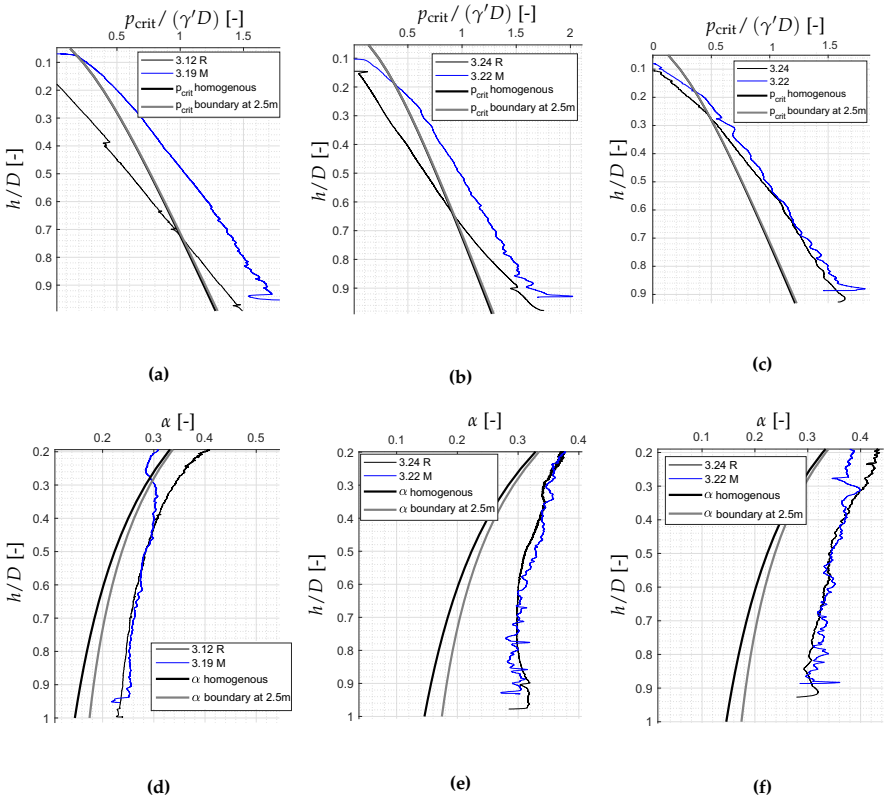

Fig. 4.15: The comparison of the normalized applied pressure and the pore pressure factor for high sand for tests with different soil density: loose(a,d), medium dense (b,e) and dense (c,f)

pore pressure factor on the soil density and the skirt geometry. As in the previous figure, the same numerical solutions for the critical suction and α factor from Paper A are shown.

The applied pressure is almost in the limit for the critical pressure for the loose sand where the round model is installed. The rest cases show that the limit is exceeded. The difference between the applied pressure for the round bucket and the applied pressure for the modular bucket decreases when the soil density increases. For the dense sand the difference is almost negligible. The pore pressure factor are again far from the numerical solutions regardless the soil density. The pore pressure factor does not vary much between the different skirt geometry in the same soil conditions. However, there is a dependency of the pore pressure factor on the soil density; an increase in the soil density, increases the pore pressure factor what is presented more directly in Fig. 4.16.

The increased skirt area of the modular bucket model is 30% more com-

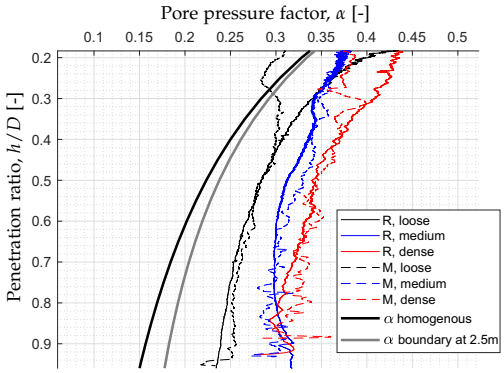

Fig. 4.16: Dependence of the pore pressure factor on the soil density

pared to the round model. The values of the applied pressure during the suction installation was expected to be larger in case of the modular model. However, it seems like the seepage flow is even more beneficial for the modular geometry case. If more suction is applied during the installation, the mechanism for the soil penetration resistance is the same for both the round and the modular model. For loose sand, where less suction is applied, this effect is less dominant.

4.3.4 Pore pressure development around the bucket skirt

The results of the excess pore pressure transducers around the skirt confirm that there is a seepage flow that is in a downward direction at the outside skirt, and in an upward direction for the inside skirt, as the water seeps from the higher water head to the smaller one in order to equalize the water pressure. Figure 4.17 presents the development of the excess pore pressure for L/D=0.5 model on the example of tests no. 1.5 and 1.9.

The results of the excess pore pressure are also collected from the numerical simulations for the model with the same boundary conditions. The boundary conditions are of a great importance, as the records of the excess pore pressure at the side boundaries during the suction installation tests indicate the development of the excess pore pressure, what could potentially affect the seepage flow around the skirt. The same boundary conditions are therefore used in the numerical simulations. Moreover, the permeability of the soil plug for the numerical model is adjusted to simulate the real behaviour according to the observations from the laboratory tests.

When the model with the same permeability for the entire soil is used, the excess pore pressure at the tip is highly underestimated, and also the rests of the pore pressure transducers are less comparable. Therefore, the area of the

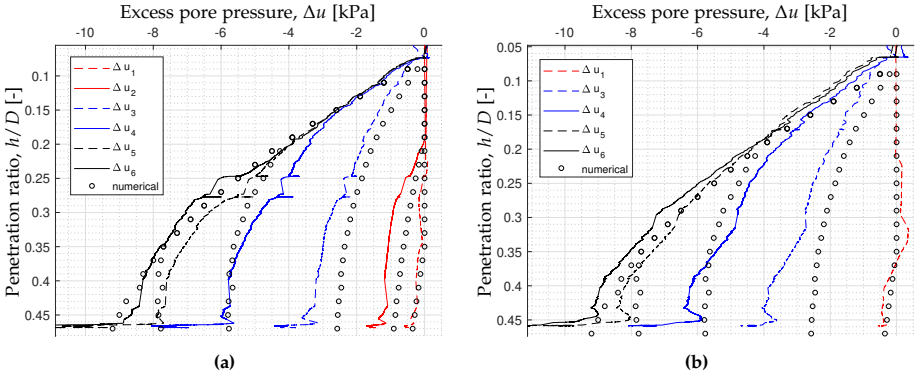

Fig. 4.17: The comparison of the excess pore pressure around the bucket skirt with numerical results for (a) test no. 1.5 and (b) test no. 1.9

soil plug in the numerical model is changed for its permeability value that corresponds to the CPTs results, where k_{fac} is set to 1.4 (see subsection 2.1.4 for the definition). These results are given in fig. 4.17. The results fits quite adequate except for the excess pore pressure at the tip, where the excess pore pressure is still underestimated, but less than in case of homogenous permeability.

The change in the soil permeability of the soil plug affects both the pore pressure factor and the critical suction against piping. New formulations are derived, however, they are only valid for this specific model conditions with the soil plug loosening to the prescribed magnitude. The change in the soil plug permeability increases the limit for the applied suction significantly. With the new formulations the applied suction in all tests is lower than the critical limit. Pore pressure factor formulation is giving slightly higher values, but it does still not capture the behavior of the seepage. The prediction is underestimating the values and it is giving a constant decrease over the depth, whereas the pore pressure factor become almost constant after reaching h/D=0.3 in the laboratory conditions. Figure 4.18 presents the new formulations together with the tests performed on the L/D=0.5m model, with $k_{\text{fac}} = 1.4$.

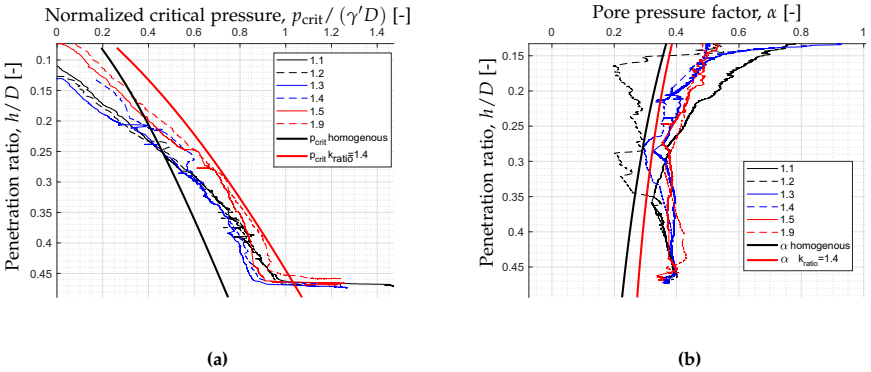

(a) **(b)**

Fig. 4.18: Laboratory results for L/D=0.5 tests in dense sand compared with the numerical formulations with an increased soil plug permeability: (a) the normalized applied pressure, (b) the pore pressure factor

The same comparison between the laboratory tests and the numerical results has been performed for the installation in high sand (L/D=1.0), with the round and the modular bucket model (tests no. 3.14 and 3.23 - both are in dense sand), see Fig. 4.19.

The simulations were performed for the numerical model with the uniform soil permeability and the model where the soil plug permeability is increased. The results of the numerical model with the uniform permeability indicate that the excess pore pressure is limited and underestimates the values at the tip when compared to the laboratory tests results. For the increased soil plug permeability, the first attempt assumed the soil plug loosening to its maximum (I_D=0), which resulted in k_{fac}=2.6. However, the correlation between the laboratory results and the simulation is not improved. This case shows that the excess pore pressure at the tip is significantly overestimated. Much better fit is obtained while allowing the dense sand for the loosening only up to its loose state of I_D=40%. This gives the permeability factor of 1.65. The results of both the round bucket and the modular bucket give the reasonable fit with the numerical data.

New formulations of the normalized seepage length and the pore pressure factor are derived for this specific conditions and plotted together with the results from suction installation in dense sand, see Fig. 4.20.

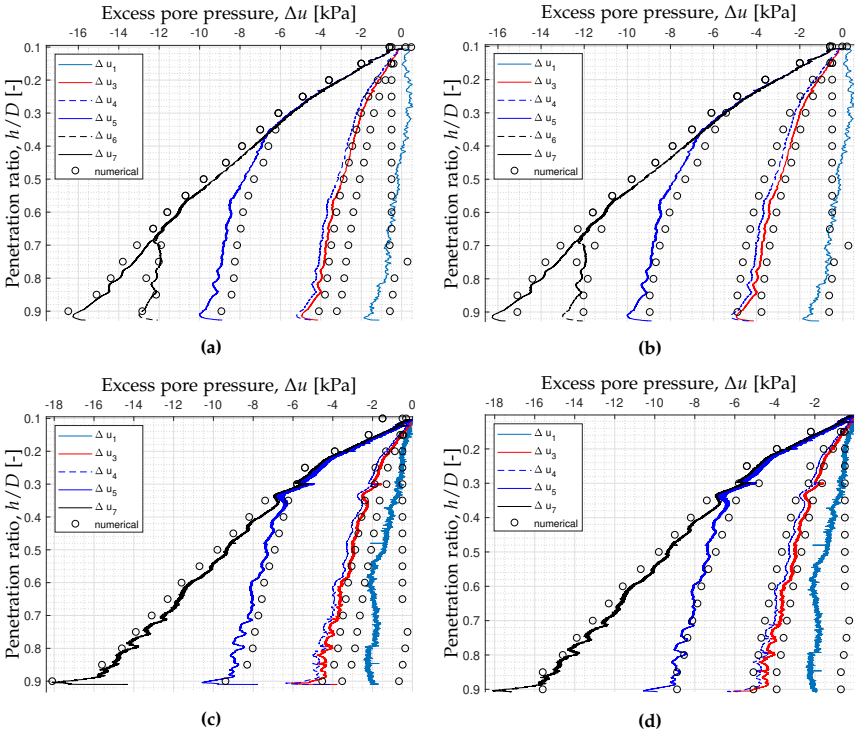

Fig. 4.19: The comparison of the excess pore pressure around the bucket skirt with numerical results: (a) R, k_{fac}=1, test no. 3.14, (b) R, k_{fac}=1.65, test no. 3.14, (c) M, k_{fac}=1, test no. 3.23, (d) M, k_{fac}=1.65, test no. 3.23

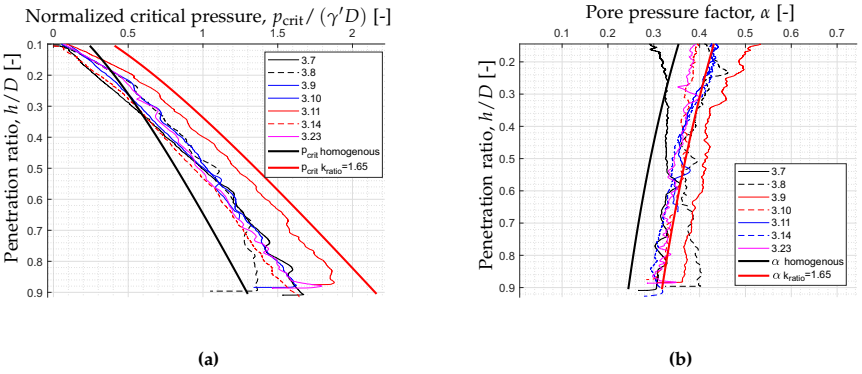

Fig. 4.20: Laboratory results for L/D=1.0 tests in dense sand compared with the numerical formulations with an increased soil plug permeability: (a) the normalized applied pressure, (b) the pore pressure factor

The applied pressure in any of the tests exceeds the critical value from the numerical model where the soil plug is loosened. The accurate fit is also

obtained for the pore pressure factor. However, the detailed observation of the numerical results lead to a decision that the excess pore pressure at the tip is not extracted directly from the tip, but as the last second value of the penetration depth on the inside skirt. This gives much better fit of excess pore pressure values (Fig. 4.19) and the pore pressure factor. As the skirt is represented in the numerical model as the line element with no assigned thickness, the tip experiences a lot of numerical instability during the calculations. It seems reasonable to choose the point that is situated less than 1 cm above, as this is only 1% of the entire skirt length.

4.3.5 CPT-based method application

The CPT-based method is used for the calculation of the soil penetration resistance, where the account is taken for the reduction due to the seepage flow. From the soil penetration resistance it is possible to establish how much suction is required for the installation, but the applied suction must be within the limits of the critical suction against the piping.

First step is to derive the empirical coefficients k_p and k_f that relates the cone resistance measured during the CPT to the skirt tip resistance and the skirt friction respectively. This is only applicable for the initial soil penetration resistance, where there is no contribution of the applied suction and the induced seepage flow. The initial soil penetration resistance is used in order to design the self-weight part of the installation, and also as a base for the calculations of the reduced resistance, see eqs. (4.11), (4.12) and (4.13).

The empirical coefficients are derived from the results of the jacking installation tests by the fitting and optimizing procedure. The first assumption is in the k_f value that is decided to be the same for the inside and for the outside skirt. This is, however, questionable. The research show that the soil plug that can develop inside the bucket during jacking installation causes an additional increase in the stress, especially for small scale testing equipment. For the model bucket with a diameter of 0.5 m, Lian et al. (2014a) reported that the stress pushing on the skirt are very different between the inside and the outside skirt. Chen et al. (2016) reported that for the bucket with 1.5 m diameter, the stress were similar for both sides of the skirt. The bucket used in the presented research has a diameter of 1 m and the increased stress inside the bucket could be a possibility. The second assumption is the constant values of both parameters, with no dependency on the depth. The assumption is acceptable as long as the soil conditions are uniform in a high extend. Finally, some suggestions have to be used and one of the two coefficient is chosen before fitting the other coefficient. The soil penetration resistance where only one of the coefficient is unknown is fitted to the total value of the applied

installation force over the penetration depth:

$$F_{\text{tot}} = k_f \beta_{\text{in}} A_{\text{s,i}} \int q_c \, dz + k_f \beta_{\text{out}} A_{\text{s,o}} \int q_c \, dz + k_p \beta_{\text{tip}} q_c(h) A_{\text{s,tip}} \tag{4.17}$$

The section presents the fit of the CPT-based method on the example of the jacking installation tests performed on the L/D=0.5 model. This is based on the procedure and the results presented in Paper C. From the different k_f coefficients chosen on the base of the previous research k_f=0.0023 gives the best fit for the results. The back-calculated k_p is in a range of 0.33-0.39, which is just slightly higher than the most probable value recommended by DNV (1992). The chosen value of k_f is also in the range given by DNV (1992).

The change in the single parts of the penetration resistance was proposed to be in relation to the critical suction limit for different locations around the skirt (Koteras et al., 2016). However, the laboratory results indicates that this solution is not likely. When using this approach, the tip resistance and the inside skirt friction are reduced to zero from the beginning of the installation and the increased outside skirt friction is still much less than the total applied load. Moreover, it is unlikely that there is no resistance from the skirt tip. The installation is a constant penetration process. Even though the gradient around the tip is very high, the surrounding soil constrained the tip in some extend. The changes in the surrounding soil outside the skirt for the very dense sand show a small reduction in density due to the dilative soil behavior, which is more dominant than the increase from the seepage. Therefore, the outside skirt friction is kept as the initial value, and is not increased due to the seepage. By observing the changes in the reduction of soil penetration resistance and comparing it to the ratio between the applied suction and the critical suction against piping, there is a visible proportion between these two, see Fig. 4.21(a).

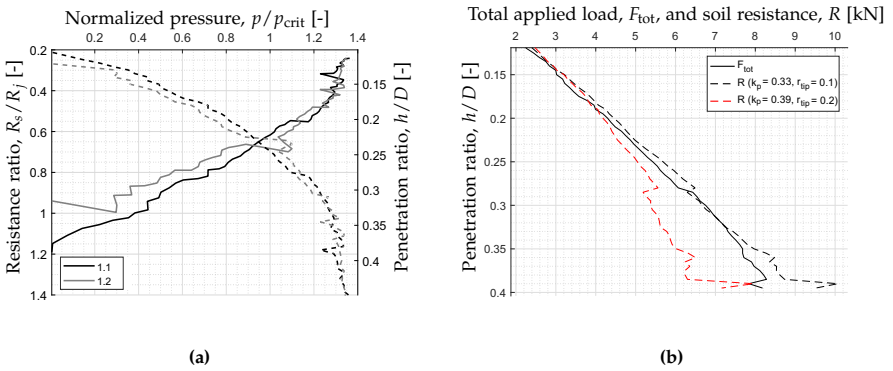

Fig. 4.21: (a) The resistance ratio R_s/R_j dependency on the pressure ratio p/p_{crit} (Koteras and Ibsen, 2019) and (b) the application of CPT-based method on tests 1.1 (Koteras and Ibsen, 2018)

The β factors for the tip resistance and the inside skirt friction is therefore designed in relation to the p/p_{crit} factor. The best fit with the laboratory data of suction installation for model L/D=0.5 has been established with the reduction factor β as the exponential function of the pressure ratio:

$$\beta_{in} = 1 - r_{in} \exp\left(\frac{p}{p_{crit}}\right) \quad \text{for } p \leq p_{crit} \tag{4.18}$$

$$\beta_{tip} = 1 - r_{tip} \exp\left(\frac{p}{p_{crit}}\right) \quad \text{for } p \leq p_{crit} \tag{4.19}$$

$$\beta_{out} = 1 \tag{4.20}$$

For $p \geq p_{crit}$ β-factor become 1. The critical pressure used in those equations is derived from the numerical model with k_{fac}=1.4 and the same boundary conditions as the laboratory soil container. r_{in} and r_{tip} are fitted for the maximum and the minimum value of k_p from the jacking installation tests by non-linear least squares fitting. These values are similar between the tests, with r_{in}=1, and the mean value of r_{tip} equal to 0.1 when k_p=0.33 is used and r_{tip} equal to 0.2 when k_p=0.39 is used. Figure 4.21(b) demonstrates the soil penetration resistance calculated with the CPT-based method together with the total applied load for test no. 1.1. This method is applied on the all 7 suction installation tests (tests no. 1.1-1.5 and 1.9) and results with the mean value of the coefficient of determination, R^2, equal to 0.88. Calculated reduced soil penetration resistance for all analyzed suction tests for L/D=0.5 model are in these minimum and maximum boundaries.

The design considerations are changed, when the tests from the extended version of the laboratory set-up are analyzed. The stresses measured at the boundary conditions indicate that the determination of k_p and k_f coefficients can not be based on the entire jacking penetration. There is a significant increase in the vertical stress measured at the bottom of the sand layer, centrally below the installed bucket, which suggests that only first 300 mm of the penetration should be used for the determination of the initial soil penetration resistance for all different soil conditions, see Fig. 4.22.

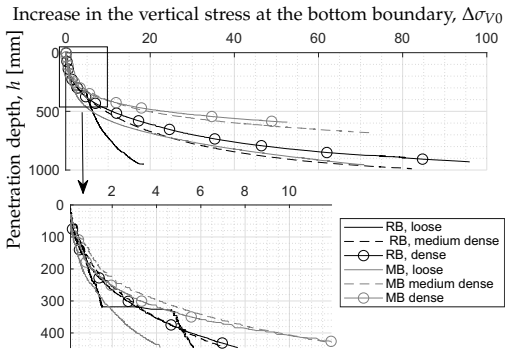

Fig. 4.22: The change in the vertical stress measured by the pressure cell below the bucket during jacking installation (data zoomed-in for the first 400mm in the lower figure)

The assumption for the same k_f coefficient for the inside and the outside skirt now is even more reasonable. Only 300 mm of the penetration limits the time for the soil plug development that would create the additional stress. For the further penetration, it is not of the main concern, as the induced seepage flow reduces the additional stress anyway.

The best fit for the initial soil penetration resistance for tests performed in dense sand is with k_f=0.001 and k_p=0.3, what corresponds to the most probable resistance according to DNV (1992). The fits in all tests for the 300 mm penetration give $R^2 > 0.98$. The values of the coefficients are slightly different from the chosen values for the L/D=0.5 model tests. The decrease in the soil density results in the increase of both coefficients: for medium dense sand the coefficients are k_f=0.002 and k_p=0.6, and for loose sand the coefficients are k_f=0.003 and k_p even up to 1.6.

The CPT-based method with the chosen coefficients k_p and k_f is finally applied on the model withL/D=1.0 and the round skirt geometry installed in dense sand, see fig. 4.23. The analysis showed, however, that the reduction in β-factors cannot be based on the exponential function of the (p/p_{crit}). Such configuration will lead to β-factors bigger than 1. Different configurations of the equation used for the calculations of the reduced soil penetration resistance have been studied, but the most reasonable fit has been obtained with the solution proposed by Senders and Randolph (2009), see Eq.(2.11), where β is equal to $(1 - p/p_{\text{crit}})$ for $p \leq p_{\text{crit}}$. The critical suction values against piping applied on this equation are derived from the numerical model of the same conditions as the laboratory tests, with homogenous sand, $p_{\text{crit,1}}$, and with increased value of permeability in the soil plug, $p_{\text{crit,2}}$.

Any of these two fits are very accurate, but they are close for describing the minimum and the maximum boundary. If the assumptions on the

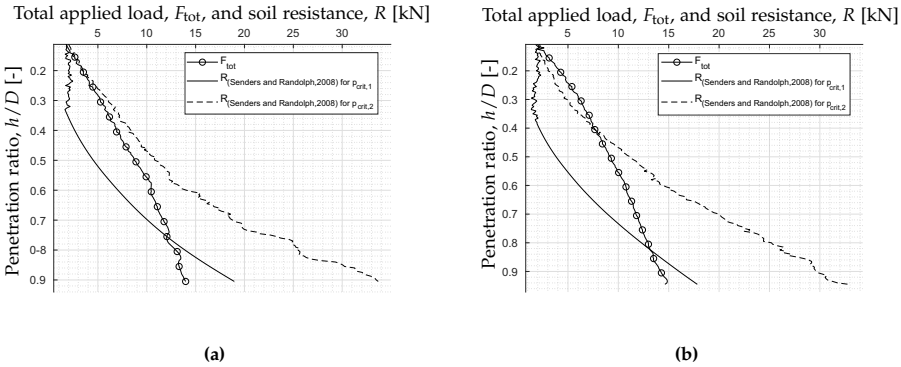

Fig. 4.23: The application of the CPT-based method on (a) test no. 3.7 and (b) test no. 3.14

reduced soil permeability is not taken into consideration, the total applied load is highly underestimated, and only reasonable in the very last stage of the penetration. With the assumption on the soil plug loosening, the applied load is highly overestimated. The difference between the applied load and the calculated reduced resistance is increasing with the penetration depth.

For the modular installation, the first step in the design method is to establish the shape factors for the initial soil penetration resistance. When using the same k_p and k_f coefficients for the CPT based method, the total applied load during the jacking installation is highly underestimated, even though the changed skirt and tip areas of the modular bucket are used. The analysis show that the best fit is obtained when the increase in the soil penetration resistance is related only to the increase in the inside skirt friction. A shape factor S_F is applied on the initial inside skirt friction. This is also confirmed with the observation from the laboratory tests. The modular bucket, after it is being removed from the soil, still has the plugged soil inside the skirt trapezoidal panels. Figure 4.24 presents the applied load during the jacking tests of modular bucket in different soil conditions for the first 300 mm of penetration. Figure also shows the solutions used for the round bucket with appropriate k_p and k_f values for different soil relative densities accounted for the changed bucket area. Finally, the solution including the shape factor is given.

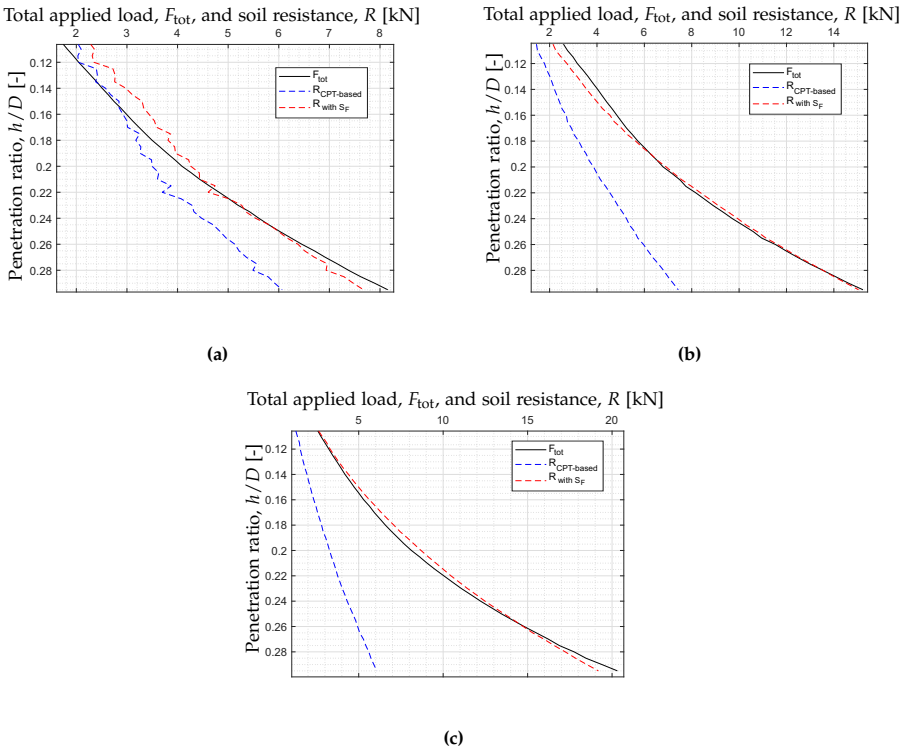

Fig. 4.24: The application of the CPT-based method on the jacking installation of modular bucket (a) loose sand, test no. 3.19 (b) medium-dense sand, test no. 3.21 and (c) dense sand, test no. 3.23

The fitted values of the shape factor for the inside skirt are given in Tab. 4.3. The soil penetration resistance that account for the shape factor in the inside skirt is as follows:

$$R_{withS_F} = F_{\text{out}} + F_{\text{in}} S_F + Q_{\text{tip}} \tag{4.21}$$

Table 4.3: S_F factors for different soil relative density fitted to the soil penetration CPT-based resistance with corresponding empirical coefficients

Soil conditions	k_p	k_f	S_F	R^2
Loose sand	1.6	0.003	3.20	0.955
Medium dense sand	0.6	0.003	5.65	0.995
Dense sand	0.2	0.001	13.75	0.993

The S_F factor increases significantly with the increasing soil density, so there is also a strong dependency between the extra plugged soil development inside the modular bucket and the level of the initial soil compaction.

For the jacking installation tests, thus for the self-weight penetration phase of the modular bucket installation, the shape factor plays an important role. However, as the results presented in subsection 4.3.2 indicate, the shape effects are almost insignificant during the suction installation. The more suction is applied, the more the shape effects of the modular bucket are reduced. From the comparison of the suction installation in dense sand it can be concluded that the changes between the required suction for the round bucket and the modular bucket are negligible. Therefore, the same β factors fit the installation data of the round model and the modular model. For confirmation, more tests with the modular bucket are required.

The CPT-based method for the suction installation has been mostly analyzed for dense sand conditions. More tests are required in order to make some reliable suggestions for medium dense and dense sand when it comes to the β-factors.

4.3.6 Soil plug heave development

Previous sections demonstrate that the soil plug loosening is a beneficial aspect of the suction installation for the bucket foundation. The seepage flow reduces the initial high soil penetration resistance and makes the installation feasible, even in very dense sand. However, the more loosening effect there is, the higher is the risk of the appearance of the soil plug heave. The soil that raises its level inside the bucket prevents from reaching the target penetration depth. The reduced penetrated skirt length could not satisfy the design for the in-place performance of the bucket foundation.

The observations and measurements from the laboratory tests indicate the soil plug heave development, even though the diameter of the bucket D=1 m is higher than the diameters used in the small-scale and centrifuge tests. For dense sand, the tests results of the CPT-s show that the void ratio of the soil plug is increasing considerable as an effect of the seepage flow. The increase in soil plug heave is due to the expansive behaviour of the soil.

For the tests performed in set-up (a) the average soil plug heave is equal to 10% of the total skirt length for the suction installation. There is also soil plug heave observations for the jacking installation tests with slightly smaller average value equal to 7%. These tests were performed in a very dense sand of $I_D \sim 90\%$.

From the tests performed in the set-up (b) but with a low sand level, the average soil plug heave is 5% for tests with I_D =71-76%.

The tests performed in dense sand with a high sand level give the average soil plug heave in dense sand of 9%. The heave is higher for the modular bucket tests, 12% in average. Not many tests have been performed, but for medium dense sand the heave is smaller 6% and 9% in average for the round and the modular bucket respectively. The two tests performed in loose sand

show that there is almost no plug heave for the round bucket and only 5% for the modular bucket.

For the jacking installation tests in the set-up (b), the soil plug heave is insignificant, sin 1.5% in case of the round bucket. The tests for the modular bucket were not completed due to the hydraulic piston limits on the maximum force. The only available result of the heave development is for loose sand conditions, 5% of the total skirt length.

Generally, previous research indicates the soil plug heave of the height around 10% for the suction installation, what is comparable with the results obtained from the laboratory tests in dense sand. Moreover, there is an influence of the soil plug heave development on the soil density, but this is corelated with the amount of applied suction pressure. The more suction is applied, the higher is the soil plug heave inside the bucket.

4.4 Further work

The research gives a lot of interesting results allowing for a wide analysis of the bucket foundation installation and the seepage flow development around the bucket skirt as an effect of the applied suction. The CPT-based method application for the soil penetration resistance during suction installation in dense sand is seen as a contribution to the design of the suction buckets installation. The method should still be tested and expanded in order to confirm the results presented in the thesis, but also to find a good correlation for the installations in different soil relative densities.

The seepage flow analysis should be expanded in the further research, to get even more precise results of the reduction in the soil penetration resistance. For now on, the seepage flow is analyzed for a steady-state seepage conditions. Based on the results of the excess pore pressures recorded during the installation in different soil conditions of the L/D=1.0 models, the hydraulic gradients on the inside skirt are calculated and presented in fig. 4.25.

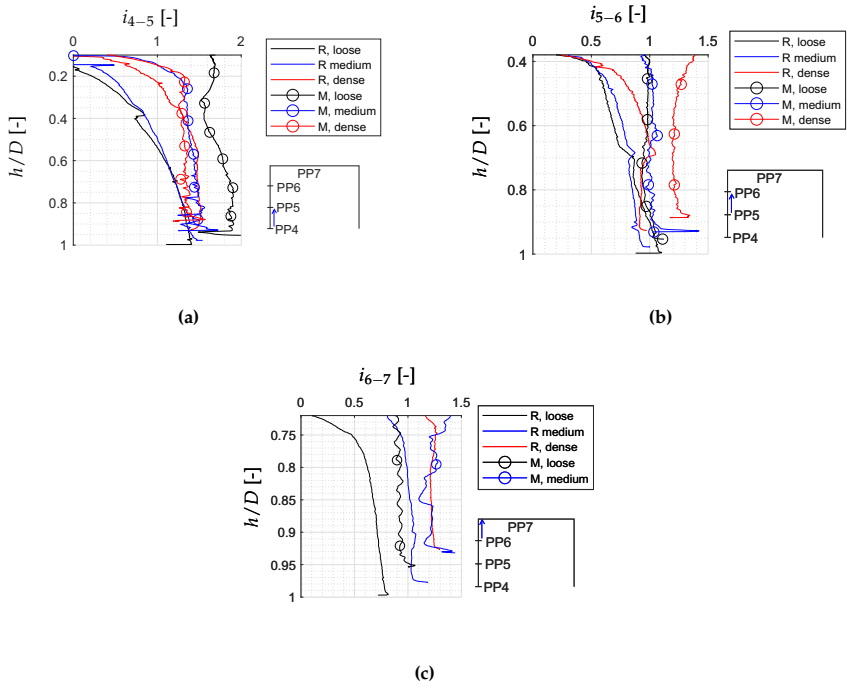

Fig. 4.25: The calculated hydraulic gradients between different locations at the inside skirt during the suction installation

The gradients are calculated for the different locations on the skirt, considering the differences in the excess pore pressure between the different measurement locations. Most of the results indicate that the critical gradient based on the analytical assumption for the steady-state seepage, $i_{\text{crit}} \sim 1$, is exceeded, even for the exit gradient (i_{6-7}) in medium dense and dense sand. There have been no piping failure during any of these installations what has been already mentioned. Interestingly, the values of the exit gradients increase with depth until reaching a value that becomes constant for further penetration. This value could be assessed as the critical value reached during the second stage of the suction installation as described by Senders and Randolph (2009). However, the value is bigger than the critical gradient for the steady-state seepage. Moreover, the total loosening of the inside skirt friction and the tip resistance is not giving a good fit with the results of the total applied load. The explanation could be seen in a different approach for the analysis of the seepage flow. Instead of the steady-stage seepage, it might be more adequate to analyze it with a transient flow problem coupled together with the continuous penetration of the skirt.

Chapter 5

Conclusions

The thesis has addressed many issues concerning the installation process of the suction bucket foundation, as the main motivation for the study assumed, namely the investigation of the cost-effective concept for the larger wind turbines. The concept of suction bucket foundation is recently a very popular research topic and the very first implementation of the mono bucket foundation in the wind energy market is just happening at the time of writing. The installation process is one of the foundation design aspects, where there is still a margin for the cost reduction. Moreover, a short-time experience with this solution makes the reliability of the concept slightly reduced.

The main part of the research is based on the scale laboratory tests at 1 g of the installation process for the suction bucket foundation. Two installation methods have been studied, the jacking installation, where the bucket is pushed into the soil by the hydraulic piston, and the suction installation, where the applied suction under the bucket lid is the main driving installation force. The laboratory set-up has been improved during the research study. The observations of the excess pore pressure and the boundary conditions are more precise and reliable. The height of the soil container increased, and the longer bucket skirt can be fully penetrated. The set-up with its improvements and two different sizes of the foundation model have allowed for analysis of the installation in dependency on the different skirt length to diameter ratio of the foundation, the different distance from the bucket tip to the bottom boundary of the set-up and the different soil relative density in which the bucket was installed. The final part of the laboratory tests included two models of similar dimensions but different skirt geometry: the round bucket model and the modular bucket model. The latter has a significantly thinner skirt with a trapezoidal shape, what increases its resistance against buckling during the installation, and reduces the total cost of the steel material for its production. The results of the laboratory tests are also sup-

ported by the outcome of the numerical simulations, where the seepage flow is analyzed.

The main advantage of the suction bucket foundation during its installation is the reduced soil penetration resistance effecting from the applied suction that induces the seepage flow around the bucket skirt. The seepage flow has been confirmed by the observations of the excess pore pressure recordings around the bucket skirt. The reduction in the soil penetration resistance is analyzed in two different ways. Firstly, it is analyzed based on the CPT results, performed before and after the installation test. The results indicate that there are changes in the soil density after the installation is completed. There is a significant change in the inside soil plug during the suction installation. The changes in the outside soil density are negligible. There are small changes in the soil density after the jacking installation tests. They are an effect of the localized failure due to the penetration, and are observed rather close to the skirt. Moreover, the reduction in soil penetration resistance is shown through the ratio between the direct measured soil resistance during the suction installation and during the jacking installation. Here, the soil resistance during the jacking installation is considered as the unreduced, initial resistance. The ratio indicates that the soil penetration resistance during the suction installation drops even up to 10% of its initial value for the modular bucket, and up to 30% for the round bucket. Such a high decrease is not observed from the CPT results, what means that the soil partially regains its strength after the seepage flow is terminated. The soil plug still has a lower strength than initially, and this should be accounted for in the in-place performance of the bucket foundation. Moreover, the research confirms the development of the soil plug heave of around 10% of the total skirt length, what also should be accounted for.

The reduction is dependent on the soil relative density, hence the amount of the applied suction during the installation. Less reduction takes place in looser sand deposit; however, the difference is not so significant. The dependency on the soil density is much distinct between the jacking installation tests. For the suction installation tests, the difference is visible especially for loose sand; however, in these tests the self-weight penetration was longer. When the tests reaches its final stage, the suction applied in all soil conditions are very similar, what can indicate that there is some critical void ratio towards which the soil goes during the suction installation, and that there is a limit to the reduction in the soil strength.

Another important goal for the research project is the optimization for the critical suction pressure that can be applied during the installation. The existing limits are often exceeded during the tests without any piping failure. The previous research has already indicated that the increase in the soil plug permeability leads to a higher limit for the critical suction. However, the formula requires the information on how much the soil-plug has loosen up,

and there are not many available data. The numerical study of the seepage flow gives the required information on the critical suction. The importance lies in the validation of the numerical data with the laboratory results so that the former are trustworthy, as the soil behavior under the seepage flow is still not fully understood. The comparison shows that the fit between the excess pore pressure developed around the bucket skirt is more precise when the numerical model account for the soil plug loosening. When homogenous soil is adopted in the numerical simulations, the excess pore pressures are highly underestimated. Based on the simulations where the soil plug permeability is increased, the derived critical suction gives the limit that is not exceeded in any of the laboratory tests. The numerical study additionally shows that the presence of the impermeable layer in a close location of the skirt tip, increases the development of the excess pore pressure at the skirt tip and also increases the suction limit.

The CPT based method for the soil penetration resistance during the suction installation in dense sand is derived with an acceptable fit with the laboratory data from the bucket model with L/D=0.5 ratio. The method is based on the empirical coefficients that relates the cone resistance from CPT to the initial soil penetration resistance, where the reduction due to the seepage is not included. The results of the jacking installation tests are used in order to validate these parameters. As for the dense sand, the coefficients are in a good correlation with the standards given by DNV (1992), they are increased significantly when the soil density is smaller. However, more tests are required for the evaluations of their range values. The initial soil penetration resistance is of a great importance for the self-weight penetration stage. In the suction phase, this initial penetration is reduced and the seepage effects are accounted for by applying β-factors to the skirt tip resistance and the inside skirt friction. As the results indicate, the soil friction on the outside skirt is left unchanged. β-factors are dependent on the ratio between the applied suction and the critical suction against piping. The critical suction pressure is therefore very important for the design, not only as the limit for the installation, but also because it affects the reduction in the soil penetration resistance. The increase in the soil-plug permeability increases the critical suction, but at the same time limits the maximum reduction of the soil resistance.

The same method applied on the longer bucket skirt, L/D=1.0, required some changes in the formulations of the β-factors, but they are still dependent on the ratio between the applied pressure and the critical limit value. The suggested application gives the lower and the upper boundary for the reduced penetration resistance, but the fit is not very precise. The improvement in the CPT-based method can lead to the reduction in the installation process; therefore, the research in this area is still highly recommended. This should also be extended to the installation examples in the different soil relative density.

Finally, the results of the installation of the modular bucket shows that the significant difference in the initial soil penetration resistance between the round and the modular bucket is negligible when the suction installation takes place. Almost the same suction is used for the installation of both models. Interestingly, the numerical results of the seepage analysis performed for the round bucket model, fit very well with the excess pore pressure recorded at the bucket skirt of the modular bucket. In addition, the excess pore pressure developed at the bucket skirt tip is similar in these two cases. The limits for the suction are therefore the same between the two different models and the CPT-based method derived for the round bucket seems to be applicable for the modular bucket as well. However, when analyzing the self-weight penetration stage, the shape factor should be applied on the inside skirt friction. The results show that there is an additional part of the resistance due to the changed geometry. The increase in the soil resistance captured by the shape factor is lost during the suction installation. Nevertheless, this is a completely new concept and still requires a lot of testing experience. Moreover, the scale testing experience must be supported by the full-scale installation tests. The scale could have a significant influence on the research outcome.

References

Allersma, H. G. B. (2003). Centrifugre research on suction piles: installation and bearing capacity. *Proceedings of BGA International Conference on Foundations*, pages 91–98.

Andersen, K. H., Jostad, H. P., and Dyvik, R. (2008). Penetration resistance of offshore skirted foundations and anchors in dense sand. *Journal of Geotechnical and Geoenvironmental Engineering*, 134(1):106–116.

API (2000). *Recommended practice for planning, designing and constructing fixed offshore platforms – Working stress design*. American Petroleum Institute: Recommended practice 2A-WSD, Washington, D.C., 21st edition edition.

Bilgili, M., Abdulkadir, Y., and Erdogan, S. (2011). Offshore wind power development in europe and its comparison with onshore couterpart. *Journal of Renewable and Sustainable Energy Reviews*, 15:905–915.

Birck, C. and Gormsen, C. (1999). Recent development in offshore foundation design. *Proceedings of European Wind Energy Conference and Exibition*, pages 365–368.

Bye, A., Erbrich, C., Rognlien, B., and Tjelta, T. I. (1995). Geotechnical design of bucket foundations. *Proceedings of the Offshore Technology Conference OTC*, 7793:869–883.

Byrne, B. W. and Houlsby, G. T. (1999). Drained behaviour of suction caisson foundations on very dense sand. *Proceedings of the Offshore Technology Conference*, OTC 10994:765–782.

Byrne, B. W. and Houlsby, G. T. (2003). Foundations for offshore wind turbines. *Philosophical Transactions of the Royal Society of London. Series A: Mathematical, Physical and Engineering Sciences*, 361(1813):2909–2930.

Carbon Trust (2019a). The offshore wind accelerator. https://www.carbontrust.com/offshore-wind/owa/. Accessed: 2019-10-07.

Carbon Trust (2019b). Suction installed caisson foundations for offshore wind: Design guidelines. the offshore wind accelerator. https://www.carbontrust.com/media/677454/owa-suction-caisson-design-guidelines-report.pdf.

Chen, F., Lian, J., Wang, H., Liu, F., Wang, H., and Zhao, Y. (2016). Large-scale experimental investigation of the installation of suction caissons in silt sand. *Journal of Applied Ocean Research*, 60:109–120.

Clausen, C. J. F. and Tjelta, T. I. (1996). Offshore platforms supported by bucket foundation. *Proceedings of* 15^{th} *Symposium on International Association for Bridge and Structural Engineering*, pages 819–829.

Cobra Group (2019). Kincardine offshore floating wind farm, scotland. http://www.grupocobra.com/en/proyecto/kincardine-offshore-floating-wind-farm/. Accessed: 2019-10-08.

Cotter, O. (2010). *The installation of suction caisson foundations for offshore renewable energy structures*. PhD Thesis, Oxford University.

Damgaard, M., Ibsen, L. B., Andersen, L. V., Andersen, P., and Andersen, J. K. F. (2013). Damping estimation of a prototype bucket foundation for offshore wind turbines identified by full scale testing. *Proceedings of* 5^{th} *International Operational Modal Analysis Conference*.

DNV (1992). *Foundations- Classification notes*. Det Norske Veritas, Oslo, Norway. February, 1992.

DNV (2014). *Design of Offshore Wind Turbine Structures. DNV-OS-J101*. Det Norske Veritas. May, 2014.

EEA (2019). Energy, the european environment agency. https://www.eea.europa.eu/themes/energy/intro#tab-news-and-articles. Accessed: 2019-10-01.

Erbrich, C. T. and Tjelta, T. I. (1999). Installation of bucket foundations and suction caissons in sand – geotechnical performance. *Proceedings of 31st Annual Offshore Technology Conference*, 1(OTC 10990):725–736.

European Commission (2017). Technology readiness level: Guidance principles for renewable energy technologies. annexes.

Feld, T. (2001). *Suction Buckets, a New Innovative Foundation Concept, applied to offshore Wind Turbines*. PhD Thesis, Aalborg University Geotechnical Engineering Group.

Foglia, A. (2015). *Bucket foundations under lateral cyclic loading*. PhD Thesis, Faculty of Engineering and Science, Aalborg University.

Guo, Z., Jeng, D., Guo, W., and He, R. (2016). Simplified approximation for seepage effect on penetration resistance of suction caissons in sand. *Journal of Ships and Offshore Structures*, 12(7):980–990.

Guttormsen, T. R., Eklund, T., and Såarrevik, P. (1997). Installation and retrieval of suction anchors. *Mooring & Anchoring*.

Harireche, O., Mehravar, M., and Alani, A. M. (2014). Soil conditions and bounds to suction during the installation of caisson foundations in sand. *Journal of Ocean Engineering*, 88:164–173.

Hogevorst, J. R. (1980). Field trials with large diameter suction piles. *Proceedings of the Offshore Technology Conference*, OTC 3817.

Houlsby, G. T. and Byrne, B. W. (2005). Design procedure for installation of suction caissons in sand. *Journal of Geotechnical Engineering*, 158(3):135–144.

Houlsby, G. T., Ibsen, L. B., and Byrne, B. W. (2005). Suction caissons for wind turbines. *Proceedings of the* 1^{st} *International Symposium on Frontiers in Offshore Geotechnics (ISFOG)*, 1:75–93.

Ibsen, L. B. (2008). Implementation of a new foundations concept for offshore wind farms. *Proceedings of Nordisk Geoteknikermøte Nr. 15: NGM 2008*, pages 19–33.

Ibsen, L. B. (2019). Mono-bucket for deutsche bucht, results of 18 years research, danish geotechnical society seminar. Accessed: 2019-10-23.

Ibsen, L. B. and Thilsted, C. L. (2010). Numerical study of piping limits for suction installation of offshore skirted foundations and anchors in layered sand. pages 421–426.

Iskander, M., El-Gharbawy, S., and Olson, R. (2002). Performance of suction caissons in sand and clay. *Canadian Geotechnical Journal*, 39:576–584.

Jaky, J. (1944). The coefficient of earth pressure at rest. *Journal of the Society of Hungarian Architects and Engineers*, pages 355–358.

Kanter, J. (2009). Largest offshore wind farm to go online. green. https://green.blogs.nytimes.com//2009/09/15/largest-offshore-wind-farm-to-go-online/. Accessed: 2019-10-02.

Kim, D., Choo, Y. W., Lee, J., Kim, D., Jee, S., Choi, J., Lee, M., and Park, Y. (2013). Numerical analysis of cluster and monopod suction bucket foundation. *Proceedings of the ASME 2013* 32^{nd} *International Conference on Ocean, Offshore and Arctic Engineering*.

Koteras, A. K. and Ibsen, L. B. (2018). Reduction in soil penetration resistance for suction-assisted installation of bucket foundation. *Proceedings of the* 9^{th} *International Conference on Physical Modeling in Geotechnics*.

Koteras, A. K. and Ibsen, L. B. (2019). Medium-scale laboratory model of mono-bucket foundation for installation tests in sand. *Canadian Geotechnical Journal*, 56(8):1142–1153.

Koteras, A. K., Ibsen, L. B., and Clausen, J. (2016). Seepage study for suction installation of bucket foundation in different soil combinations. *Proceedings of* 26^{th} *International Ocean and Polar Engineering Conference*, 2(25):697–704.

Lange, B., Aagaard, E., Andersen, P. E., Møller, A., Niklasson, S., and Wickman, A. (1999). Offshore wind farm bockstigen - installation and operation experience. *Proceedings of European Wind Energy Conference and Exhibition*, pages 300–303.

Larsen, K. A. (2008). *Static Behaviour of Bucket Foundations*. PhD Thesis, Department of Civil Engineering, Aalborg University.

Lehane, B. M., Schneider, J. A., and Xu, X. (2005). The uwa-05 method for prediction of axial capacity of driven piles in sand. In *Proceeding of International Symposium on Frontiers in Offshore Geotechnics (ISFOG)*, pages 19–21, Perth, Australia.

Lesny, K. (2011). *Foundations for Offshore Wind Turbines. Tools for Planning and Design*. Essen, Germany: VGE Verlag GmbH.

Lian, J., Chen, F., and Wang, H. (2014a). Laboratory tests on soil-skirt interaction and penetration resistance of suction caissons during installation in sand. *Journal of Ocean Engineering*, 84:1–13.

Lian, J., Ding, H., Zhang, P., and Yu, R. (2014b). Design of large-scale prestressing bucket foundation for offshore wind turbines. *Transactions of Tianjin University*, 18(2):79–84.

Madsen, S., Andersen, L. V., and Ibsen, L. B. (2012). Instability during installation of foundations for the offshore structures. *Nordic geotechnical meeting*.

Madsen, S. and Gerard, L. (2016). Buckling analysis for eudp offshore wind suction bucket on an industrial scale. *DCE Technical Memorandum*, 213.

Musial, W. and Butterfield, S. (2006). Energy from offshore wind. *Proceedings of Offshore Technology Conference*, OTC 18355.

Naturstyrelsen (2014). Havmøllepark horns rev 3. naturstyrelsen og energistyrelen.

Nielsen, S. A. (2016a). Innovations in foundations: The mono bucket. oceanology international and catch the next wave. Accessed: 2019-10-07.

Nielsen, S. D. (2016b). *Transient monotonic and cyclic load effects on mono bucket foundation*. PhD Thesis, Faculty of Engineering and Science, Aalborg University.

Nielsen, S. D., Ibsen, L. B., and Nielsen, B. N. (2017). Transiently loaded bucket foundations in saturated dense sand - demonstration of the boot effect. *Geotechnical Testing Journal*, 40(6):1101–1114.

NorthSEE (2014). Future energy industry trends. the north see region. https://northsearegion.eu/northsee/e-energy/future-energy-industry-trends/. Accessed: 2019-10-02.

offshoreWind (2015). First mono bucket foundation decommissioned at horns rev 2. https://www.offshorewind.biz/2015/07/10/first-mono-bucket-foundation-decommissioned-at-horns-rev-2/. Accessed: 2015-10-07.

Ørsted (2019). https://orsted.com/en/Our-business/Offshore-wind/Our-offshore-wind-farms. Accessed: 2019-10-02.

Randolph, M. and Gourvenec, S. (2011). *Offshore Geotechnical Engineering*. Spoon Press.

Scott, R. S. (1963). *Principles of Soil Mechanics*. Addison-Wesley Publishing Company, Inc.

Senders, M. and Randolph, M. F. (2009). Cpt-based method for the installation of suction caissons in sand. *Journal of Geotechnical and Geoenvironmental Engineering*, 135(1):14–25.

Senpere, D. and Auvergne, G. A. (1982). Suction anchor piles - a proven alternative to driving or drilling. *In Proceedings of the Offshore Technology Conference OTC*, 4206.

SPT Offshore (2019). Self installing monopiles (sim) for platform extensions. https://www.sptoffshore.com/solutions/self-installing-monopiles-sim-for-platform-extensions/. Accessed: 2019-10-08.

Sturm, H. (2017). Design aspects of suction caissons for offshore wind turbine foundations. *Proceedings of TC 209 Workshop - 19th ICSMGE*.

Tjelta, T. (2014). Installation of suction caissons for offshore wind turbines, danish geotechnical society seminar. 1^{st} april, 2014.

Tjelta, T. I. (1995). Geotechnical expierience from the installation of the europipe jacket with bucket foundation. *Proceedings of the Offshore Technology Conference*, OTC(7795).

Tjelta, T. I. (2015). The suction foundation technology. *Frontiers in Offshore Geotechnics*, III:85–93.

Tjelta, T. I., Guttormsen, T. R., and Hermstad, J. (1986). Large scale penetration test at a deepwater site. *Proceedings of* 18^{th} *Offshore Technology Conference*, OTC(5103):201–211.

Tran, M. N. (2005). *Installation of suction caissons in dense sand and the influence of silt and cemented layers*. PhD Thesis, University of Sydney, Australia.

Tran, M. N. and Randolph, M. F. (2008). Variation of suction pressure during caisson installation in sand. *Geotechnique*, 58(1):1–11.

Tran, M. N., Randolph, M. F., and Airey, D. W. (2007). Installation of suction caissons in sand with silt layers. *Journal of Geotechnical and Geoenvironmental Engineering*, 58:1183–1191.

Universal Foundation (2019a). https://universal-foundation.com/. Accessed: 2019-10-07.

Universal Foundation (2019b). Case study: Trial installation - uk north sea. https://222821-www.web.tornado-node.net/trial-installation-uk-north-sea/. Accessed: 2019-10-07.

Vaitkunaite, E. (2016). *Physical Modelling of Bucket Foundations Subjected to Axial Loading*. PhD Thesis, Faculty of Engineering and Science, Aalborg University.

Vattenfall (2018). Vattenfall group. https://group.vattenfall.com/uk/what-we-do/our-projects/european-offshore-wind-deployment-centre. Accessed: 2019-10-02.

WindEurope (2019a). https://windeurope.org/about-us/new-identity/. Accessed: 2019-10-01.

WindEurope (2019b). Offshore wind in europe - key trends and statistics 2018.

WindEurope (2019c). Wind energy in europe in 2018 - trends and statistics.

Part II

Papers and Appendices

Appendix A

Seepage study for suction installation of bucket foundation in different soil combinations

Aleksandra Katarzyna Koteras
Lars Bo Ibsen
Johan Clausen

The paper has been published in
The Proceedings of the 26^{th} *International Offshore and Polar Engineering Conference (ISOPE)* Vol. 2, pp. 697–704, 2016.
(the final draft version included in the thesis)

The layout has been revised.

Abstract

Research has proven the bucket foundation to be a feasible and an attractive solution for offshore wind turbines. Its potential derives partly from the cost-effectiveness due to the suction-assisted installation. The suction applied under the bucket lid produces a downward driving force and additionally reduces the soil penetration resistance. This installation process is the most effective in soil with high coefficient of permeability where the flow of pore water is easily induced. However, the technology is still under development and some issues require further investigation and reliable solutions. A series of numerical simulations performed on the flow analysis around the bucket penetrating into sand are presented in this paper. The characteristics of seepage arising from applied suction are investigated. The cases included in the research cover a wide range of bucket dimensions and different boundaries. The flow of pore water is studied for homogenous sand, sand overlaid by impermeable layer and sand situated above impermeable layer. In all three cases the seepage analysis gives the required information on the critical suction pressure and on the distribution of excess pore pressure around the bucket skirt. The exceedance of critical suction might lead to installation failure due to formation of piping channels, which break the hydraulic seal between the skirt and soil. The excess pore pressure arising due to applied suction changes the effective stress, hence the penetration resistance of soil. Therefore, both matters are important for the design. The results show that the appearance of the impermeable layer above or below sand affects the excess pore pressure in this layer. Moreover, it has been found that the appearance of impermeable layer increases the allowable suction during installation. Both, the critical suction and the pore pressure factor, describing the excess pore pressure developed at the tip of bucket skirt, are presented as closed form solutions for all three cases.

KEY WORDS: Offshore wind turbines; Bucket Foundation; Excess pore pressure; Critical suction; Layered soil.

A.1 Introduction

The past few years have shown a significant contribution of the renewable energy in the total produced energy in Europe. The wind industry strongly expands to the sea sector where the wind turbines are starting to be installed in more challenging conditions. Those conditions refer to both soil profiles and water depths. Moreover, the requirements for wind turbines dimensions grow continuously, resulting in demand for larger foundations,which are feasible for offshore conditions. Among many concepts used nowadays for offshore wind turbines, the suction bucket is found to be a competitive solution.

A quicker and quiet installation along with an easy decommissioning process are named as some of advantages of the skirted foundations (Tjelta, 2015). The bucket foundation is a large-diameter skirted structure installed into the soil with suction assistance. The installation process indicates the cost reduction as no heavy driving equipment is required. This type of foundation has extensively been used as suction anchors in oil and gas offshore industry. Andersen et al. (2005) mentioned more than 485 successfully performing anchors, which were installed in many different locations with water depths reaching almost 2000 m. This success led to further development where the suction caissons were used as permanent foundations for platforms known as the Draupner "E" and the Sleipner "T" (Tjelta, 1995; Bye et al., 1995). However, the loading regime for oil and gas structures differs significantly from the loading conditions on the offshore wind turbines, (Houlsby et al., 2005), and the design methods are limited and not precise. They require a further development. Nevertheless, the bucket foundation is considered to be a feasible solution for offshore wind turbines, and the research work proves how effective this solution is (Ibsen, 2008; Tjelta, 2015).

The installation of suction caisson starts with a self-weight penetration where no suction is applied. The self-weight penetration depth must be sufficient in order to ensure a seal between the bucket skirt and the surrounding soil. Afterwards, suction under the bucket lid can be applied. Required suction for penetration must be possible to predict, so that a pump capacity can be chosen and an appropriate rate of pumping can be applied. The installation will proceed as long as the driving force, resulting from the pressure differential on the lid and from the self-weight of the bucket, is balancing the soil penetration resistance. However, the installation fails when the suction exceeds the critical level at which piping channels in the soil plug arise and the hydraulic seal is broken. The design must predict the required suction level that will not exceed its critical value. (Ibsen and Thilsted, 2010)

The suction that can be applied is also dictated by how much pressure difference is achievable. A majority of installed caissons for oil and gas platforms are found in relatively deep waters where significant head difference can be obtained at the bucket lid. Moreover, most of suction caissons are today installed in clay where the penetration resistance is considerable smaller than in dense sand. However, the research performed for installation of skirted structures in dense sand shows that the high penetration soil resistance is actually significantly reduced through the seepage flow, strictly speaking through downward hydraulic gradient inside the caisson and the gradient at the tip (Fig. A.1). Therefore, the installation in dense sand does not require a level of the suction that cannot be achieved, even in relatively shallow or intermediate water depths. (Erbrich and Tjelte, 1999)

The aim of the article is to analyze the seepage flow around the bucket skirt resulting from suction applied under the bucket lid. The characteristics

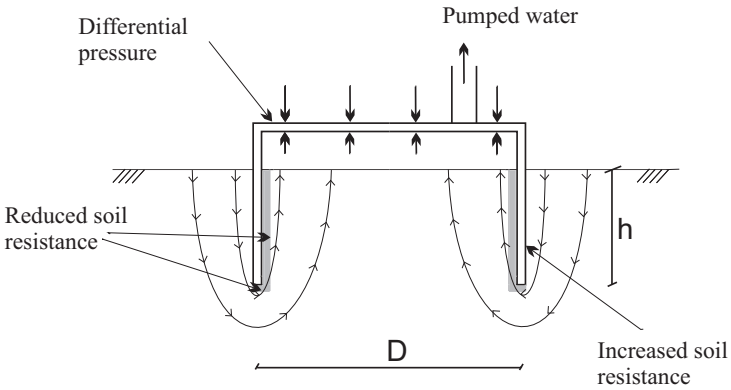

Fig. A.1: Seepage for suction installation of bucket

of seepage are investigated and described based on the results from numerical simulations performed in PLAXIS 2D. A consistent pattern of behavior is revealed and closed form solutions are proposed for the normalized seepage length and for the pore pressure factor for different soil combinations. Those solutions are used for predicting the reduction in soil resistance that results from the seepage flow.

A.2 State of art on the installation procedure for bucket foundation

The design guidance for the installation process of bucket foundation is often based on pile foundation standards. The classical approach presented by API (2000) for pile foundations axial bearing capacity is suggested to be used for soil resistance against penetration for skirted structures, like bucket foundations. The total soil resistance is based on assumed in situ effective stress and assumed soil parameters, such as tip resistance factor, N_q, coefficient of lateral earth pressure at rest, K_0, and pile-soil friction angle, δ. Another approach relates the penetration resistance of soil to the results of Cone Penetration Test, CPT, performed for soil investigation in given location, which is more direct in capturing real soil properties (DNV, 1992). The soil resistance consists of the part from skirt-soil friction on inside and outside, F_{in} and F_{out}, and the part from tip bearing, Q_{tip}, and it is related to the cone resistance, q_c, through empirical coefficients k_f and k_p respectively. $A_{\text{s,in}}$, $A_{\text{s,out}}$ and A_{tip}

are the areas of inside skirt, of outside skirt and of skirt tip respectively.

$$F_{\text{in}} = k_f \; A_{\text{s,in}} \int q_c \; dz \tag{A.1}$$

$$F_{\text{out}} = k_f \; A_{\text{s,out}} \int q_c \; dz \tag{A.2}$$

$$Q_{\text{tip}} = k_p \; q_c(h) \; A_{\text{tip}} \tag{A.3}$$

The reduction of soil resistance due to the seepage flow, which is not accounted for in API and DNV approaches, is being recently investigated. The method including the effects of flow, based on API-approach, is proposed by Houlsby and Byrne (2005). The seepage effects are included by exchanging the effective overburden pressure to its reduced or increased value due to the hydraulic downward or upward gradient. The gradients are calculated from excess pore pressure values with the assumption on linear distribution of excess pore pressure on the inside and outside of the caisson skirt. The excess pore pressure at the tip of the bucket skirt, Δu_{tip}, is related to the applied suction, p, through an α factor that is obtained from finite element analysis for different penetration depths.

$$\alpha = \frac{\Delta u_{\text{tip}}}{p} \tag{A.4}$$

A following solution fits the results of finite element analysis (Houlsby and Byrne, 2005).

$$\alpha = 0.45 - 0.36 \left(1 - \exp\left(\frac{h}{0.48D}\right)\right) \tag{A.5}$$

The average downward gradient is given by $\alpha p/(\gamma_w h)$ and the average upward gradient by $(1-\alpha)p/(\gamma_w h)$. The solution is valid only for homogeneous sand and penetration ratio, h/D, up to 0.8. The critical condition at which piping might occur is described through critical suction that can not be exceeded.

$$p_{\text{crit}} = \frac{\gamma' h}{1-\alpha} \tag{A.6}$$

Another method including the seepage effects is given by Senders and Randolph (2008), and it is based on CPT results, as proposed by DNV. They have proposed a method where the reduction in soil resistance is dependable on assumed value of critical pressure. The suction required for any penetration depth is based on equilibrium between the driving force and the resistance of soil. The bucket skirt penetrates as long as the driving forces exceed the resistance forces.

$$W + \frac{1}{4}\pi D_i^2 p = F_{\text{out}} + (F_{\text{in}} + Q_{\text{tip}}) \left(1 - \frac{p}{p_{\text{crit}}}\right) \tag{A.7}$$

W is the submerged self-weight of caisson and D_i is the inside caisson diameter. The critical hydraulic gradient appears first at the tip of the skirt, but the soil material present in surroundings fills up the piping channels. Therefore it is the exit hydraulic gradient, adjusted to the bucket wall, that controls the piping failure during installation. The hydraulic gradient is expressed as a ratio between the applied pressure and the seepage length, s, as following.

$$i = \frac{p}{\gamma_w s} \tag{A.8}$$

The critical hydraulic gradient, $i_{crit} = \gamma'/\gamma_w$, causes a piping failure and therefore, the critical pressure against piping is:

$$p_{crit} = s\gamma_w i_{crit} = s\gamma'. \tag{A.9}$$

Based on numerical simulations performed in PLAXIS and SEEP finite element programs, Senders and Randolph (2008) have proposed a solution for normalized seepage length.

$$\left(\frac{s}{h}\right)_{exit} = \pi - \arctan\left[5\left(\frac{h}{D}\right)^{0.85}\right]\left(2 - \frac{2}{\pi}\right) \tag{A.10}$$

The proposed method fits excellent with results from centrifuge model tests for installation of suction bucket, which were performed as a part of their research. Moreover, the comparison with the results from already mentioned cases of Draupner "E" and Sleipner "T" is also reasonable. A similar solution for normalized seepage length for exit hydraulic gradient has been obtained from numerical analysis performed in FLAC 3D, reported in (Ibsen and Thilsted, 2010).

$$\left(\frac{s}{h}\right)_{ref} = 2.86 - \arctan\left[4.1\left(\frac{h}{D}\right)^{0.8}\right]\left(\frac{\pi}{2.62}\right) \tag{A.11}$$

This solution was used for analyzing the results of field installation tests of suction caisson performed in the test site in Frederikshavn, Denmark (Ibsen, 2008). For the case where the soil profile indicates homogenous sand, the results are in a good fit with given solution. However, for cases where the presence of silt layers is reported, the applied suction exceeded the suction thresholds against piping without any noticeable failure. Therefore, the numerical study presented in (Ibsen and Thilsted, 2010) covers also a case of sand over a flow boundary where the distance between free surface and impermeable boundary is z_L. Following solution has been proposed by them.

$$\left(\frac{s}{h}\right) = \left(\frac{s}{h}\right)_{ref} + 0.1\left(\frac{D}{z_L}\right)\left(\frac{h}{z_L - h}\right)^{0.5} \tag{A.12}$$

The presence of impermeable layer changes the flow field and increases the suction threshold against piping. This is confirmed while comparing to field tests results, which supports the assumption, that it is indeed the exit gradient next to the caisson skirt that controls the piping failure.

The method presented in this article relates the changes in soil resistance through the values of critical pressure for each penetration depth. However, this research takes into consideration differences between the critical gradient for exit flow, the average critical gradient along the skirt and the critical gradient for the tip of the skirt. Moreover, the analysis consists of three cases with different soil profiles (Fig. A.2). In first case, case (a), the applied suction induces seepage flow in homogenous sand. The second case, case (b), includes impermeable soil layer above the sand in which seepage flow occurs. The third case, case (c), investigates the seepage flow in sand situated above impermeable soil layer.

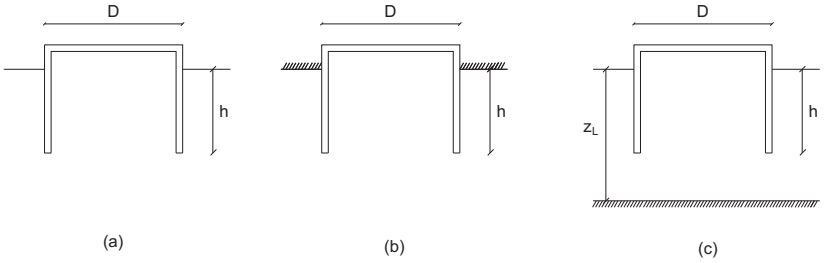

Fig. A.2: Cases with different soil profiles used in numerical simulations for seepage flow investigation

A.3 Model and assumptions

The seepage flow problem is solved numerically through simulations performed in PLAXIS 2D. An axisymmetric model is generated due to simple, circular geometry of bucket structure. Chosen diameter is $D = 4$m. The continuous process of installation is substituted with a series of discrete steady-state flow calculations for each analyzed penetration ratio, $0.1 \leq \frac{h}{D} \leq 2.0$, where an equilibrium between the driving forces and the soil penetration resistance is assumed. Such an approach was used by Tran and Randolph (2008), and it confirmed a good agreement with pressure records from centrifuge tests. The range of penetration depth is significantly wider comparing to recently performed researches, (Houlsby and Byrne, 2005), (Ibsen and Thilsted, 2010), in order to include larger foundations in the design method.

The model consists a surface with impermeable interfaces to simulate a bucket skirt. The flow around the bucket skirt should not be influenced by

the presence of domain boundaries. Therefore, boundaries are in an appropriate distance from the simulated skirt. The outer boundary is located in the distance of $10D$ and the bottom boundary in the distance of 45m. The suction under the bucket lid is simulated by applying appropriate groundwater flow boundary conditions. At the bottom and at the axisymmetric boundary, the groundwater flow boundary condition is set as closed. The behaviour of the outer boundary and the boundaries at free surface is chosen as a prescribed hydraulic head with an appropriate value of hydraulic head to be used. For the outer boundary and for the free surface outside the bucket a head of 20m above seabed is set, which is also a head value for the entire model. Inside the bucket, a decreased value of head is used, so that the seepage is developed around the bucket skirt. The soil used in simulations is an isotropic sandy soil with high coefficient of permeability, $k = 7.128$ m/day. Fig. A.3 shows the geometry and the size of domain used for the numerical simulations. For case (b) the groundwater flow boundary condition at the free surface outside the caisson is closed, and for case (c) the distance to the bottom boundary,z_L, varies in the range of $0.2 \leq \frac{z_L}{D} \leq 2.0$.

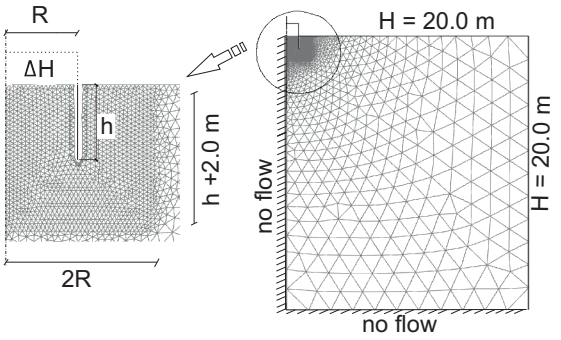

Fig. A.3: Geometry with finite element mesh and groundwater flow boundary conditions

The solution given later on in this paper cannot be applied for cases where the installation is performed with a high pumping rate. When penetration rate is high, more than 2 m/h, an engineering assessment is required to be sure if the seepage is given enough time to be fully-developed. Otherwise, the solution from this study is not valid. Moreover, the coefficient of permeability should be close to the one used in the numerical simulations, as the seepage calculations are sensitive to this parameter.

A.4 Calculation method

The simulation of bucket foundation installation in sand gives required information on excess pore pressure around the bucket skirt that result from

suction applied under the bucket lid. The results of excess pore pressure are of main interest for this study. Firstly, an empirical relation for the pore pressure factor, α, is to be found for all three soil cases Secondly, the results of pore pressure are required in order to derive a design method for predicting the soil penetration resistance where the effects of the seepage flow are included. The method is called AAU CPT-based method and it is based on DNV approach where, additionally, β factors are introduced for taking into account the changes in soil resistance due to flow.

$$F_{\text{in}} = k_f \; \beta_{\text{in}} \; A_{\text{s,in}} \int q_c \; dz \tag{A.13}$$

$$F_{\text{out}} = k_f \; \beta_{\text{out}} \; A_{\text{s,out}} \int q_c \; dz \tag{A.14}$$

$$Q_{\text{tip}} = k_p \; \beta_{\text{tip}} \; q_c(h) \; A_{\text{s,tip}} \tag{A.15}$$

The changes in soil resistance are a result of hydraulic gradient that appears in the soil. As mentioned before it is the exit hydraulic gradient that controls piping failure. However, first the critical gradient appears at the tip of skirt and then progresses up, along the bucket skirt. Therefore, the results of excess pore pressure are used for calculations of gradients at the tip of bucket skirt, i_{tip}, and the average gradients at the inside, $i_{\text{avg,in}}$, and outside skirt, $i_{\text{avg,out}}$. Those values are used in determining the seepage length values, eq. (**??**), and next the values of critical suction pressure, eq. (**??**). Finally, β factors are determine as following.

$$\beta_{\text{in}} = \left(1 - r \; \frac{p}{p_{\text{crit,avg,in}}}\right) \tag{A.16}$$

$$\beta_{\text{tip}} = \left(1 - r \; \frac{p}{p_{\text{crit,tip}}}\right) \tag{A.17}$$

$$\beta_{\text{out}} = \left(1 + r \; \frac{p}{p_{\text{crit,avg,out}}}\right) \tag{A.18}$$

Factor r is set to unity. It is presumed that the factor is increasing in less permeable soil or for installations performed with high rate of penetration, restricting the favorite effects of seepage.
The hydraulic gradient at the exit is calculated from the Darcy's law, extracting the flow velocity at the exit, v_{exit}.

$$i_{\text{exit}} = \frac{v_{\text{exit}}}{k} \tag{A.19}$$

The critical suction pressure determined from exit hydraulic gradient can not be exceeded, as this creates a risk of soil failure and prevents further installation. (Koteras and Ibsen, 2016) includes more detailed description of

the method and how the excess pore pressures are extracted from numerical model.

A.5 Results and discussion

The pore pressure factor for homogenous sand, soil case (a), is presented in Fig. A.4, together with the solution found in literature.

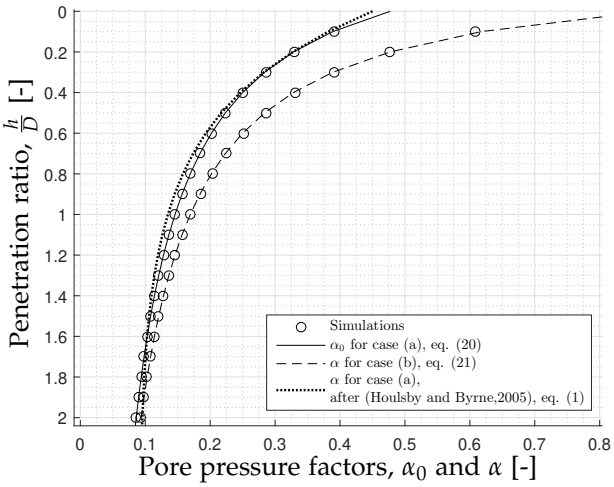

Fig. A.4: Results of α_0 for case (a) along with solution from (Houlsby and Byrne, 2005) and results of α for case (b)

The pore pressure factor for case of homogenous sand is called α_0 and the function fitted to the results is referred later on in other solutions for α. The main trend is a decrease in pore pressure factor for increasing penetration depth. It is concluded that the method and chosen model is valid, as the results of α_0 are closed to the proposed solution from (Houlsby and Byrne, 2005). Along with α_0 in Fig. A.4, there are also results of pore pressure factor, α, for soil case (b). After introducing different boundary conditions to simulate impermeable layer above sand, the change in pore pressure factor appears. There is a significant increase in α values for smaller penetration ratio due to changes in seepage flow. When the skirt of bucket is penetrated deeper into soil, the influence of impermeable layer at the top decays and the results difference between those two cases becomes smaller. Eq. (A.20) is chosen as a solution for α_0 for case (a), and eq. (A.21) is chosen as a solution

for α for case (b). Both solutions are presented in Fig. A.4.

$$\alpha_0 = \frac{0.21}{\frac{h}{D} + 0.44} \tag{A.20}$$

$$\alpha = \frac{0.21}{\frac{h}{D} + 0.24} \tag{A.21}$$

Fig. A.5 presents results of α for soil case with sand over impermeable layer, case (c). There is also a decrease in α values while the penetration depth increases. However, when the tip of skirt is approaching impermeable layer at the bottom, there is a sudden increase in α. This indicates that impermeable soil situated below sand influences the excess pore pressure around the skirt.

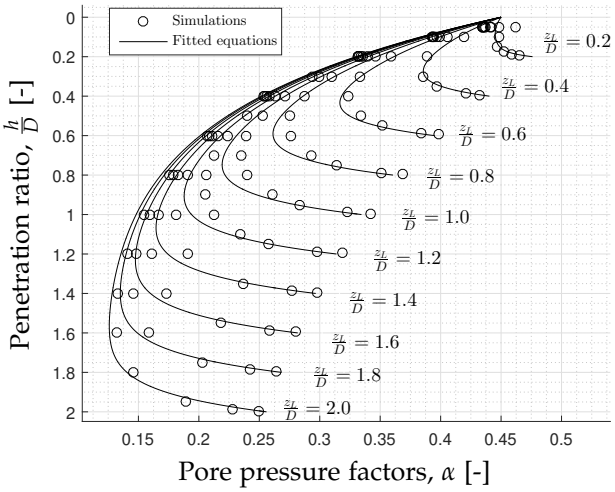

Fig. A.5: Results of α for different values of $\frac{z_L}{D}$, case (c)

The solution that is chosen to represent the pore pressure factor for case (c) is shown below.

$$\alpha = \alpha_0 + a\frac{h}{D}\left(\left(\frac{h}{z_L}\right)^b + \frac{D}{z_L} - c\right) \tag{A.22}$$

where

$$a\left(\frac{z_L}{D}\right) = 0.3\exp\left(-0.75\frac{z_L}{D}\right) - 0.35\exp\left(-4.4\frac{z_L}{D}\right) \tag{A.23}$$

$$b\left(\frac{z_L}{D}\right) = 95\exp\left(-15\frac{z_L}{D}\right) + 4.8\exp\left(0.66\frac{z_L}{D}\right) \tag{A.24}$$

$$c\left(\frac{z_L}{D}\right) = -\exp\left(-0.6\frac{z_L}{D}\right) + 7.7\exp\left(-8.3\frac{z_L}{D}\right) \tag{A.25}$$

Based on results of hydraulic gradients around the bucket skirt from numerical simulations, values of seepage length are calculated. Fig. A.6 presents the results and fitted functions for normalized seepage length for homogeneous sand, case (a), including values for exit, for average inside and for tip hydraulic gradients.

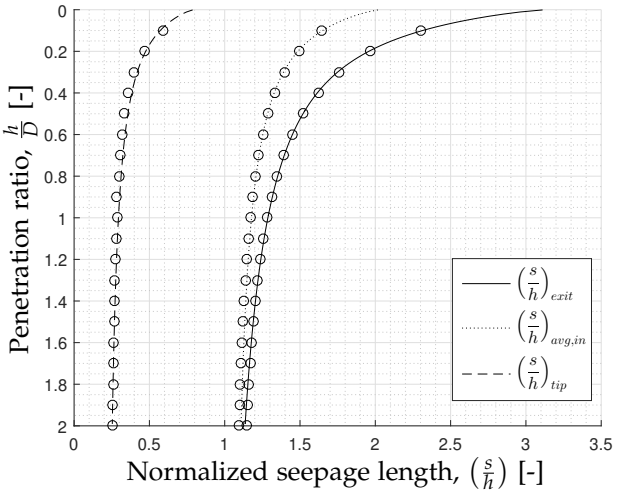

Fig. A.6: Results of $\left(\frac{s}{h}\right)$ for exit, average inside and tip hydraulic gradient for case (a)

Results confirm that the critical gradient will occur first around the skirt tip, as the seepage length values are the smallest for this area. When suction pressure increases, the critical hydraulic gradient progresses along the bucket skirt until it reaches the soil surface inside the bucket. When the critical pressure for exit seepage length is exceeded, a piping failure is expected, what prevents further installation. Following function represents the solution for seepage length for exit hydraulic gradient.

$$\left(\frac{s}{h}\right)_{\text{exit}} = \pi - \arctan\left[3.6\left(\frac{h}{D}\right)^{0.74}\right]\left(2 - \frac{1.8}{\pi}\right) \tag{A.26}$$

This solution has turned out to be a reference equation that is used later on in other solutions.

$$\left(\frac{s}{h}\right)_{\text{ref}} = \left(\frac{s}{h}\right)_{\text{exit}} \tag{A.27}$$

The results of normalized seepage lengths for soil profile with impermeable layer above sand, case (b), are presented in Fig. A.7. Again, the influence of impermeable layer at the top is observed where the change in seepage flow increases the values of seepage length for smaller penetration ratio. This influence becomes less and less significant for increasing $\frac{h}{D}$. For soil case (b),

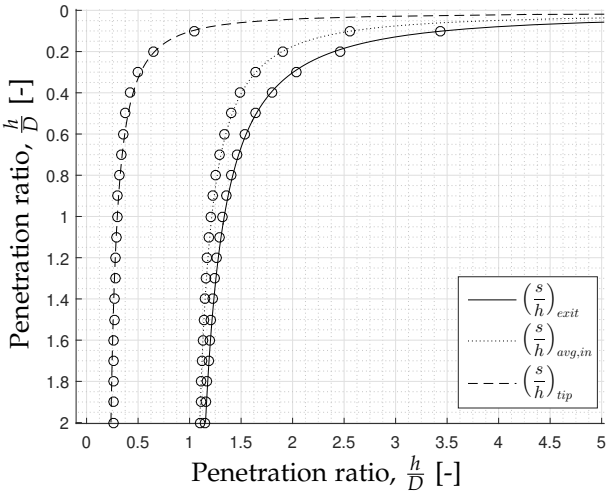

Fig. A.7: Results of $\left(\frac{s}{h}\right)$ for exit, average inside and tip hydraulic gradient for case (b)

results of normalized seepage length for exit hydraulic gradient are fitted to the following equation.

$$\left(\frac{s}{h}\right)_{\text{exit}} = \left(\frac{s}{h}\right)_{\text{ref}} + 0.05\left(\frac{h}{D}\right)^{-1.36} \tag{A.28}$$

Based on above graphs, a conclusion is made, that there is a dependency between all three presented seepage length functions. This is captured throughout a following relation, which is used as solutions for normalized seepage length for average inside hydraulic gradient and for tip gradient for case (a) and (b). Factors a and b are collected in Tab. A.1 and should be chosen based on soil case and location of hydraulic gradient.

$$\left(\frac{s}{h}\right) = a\left(\left(\frac{s}{h}\right)_{\text{exit}}\right) - b) + 1 \tag{A.29}$$

Table A.1: Chosen a and b factors for average inside and tip normalized seepage length for soil case (a) and (b)

		a	b
case (a)	$\left(\frac{s}{h}\right)_{\text{avg,in}}$	0.46	0.9
	$\left(\frac{s}{h}\right)_{\text{tip}}$	0.27	3.9
case (b)	$\left(\frac{s}{h}\right)_{\text{avg,in}}$	0.64	1
	$\left(\frac{s}{h}\right)_{\text{tip}}$	0.34	3.4

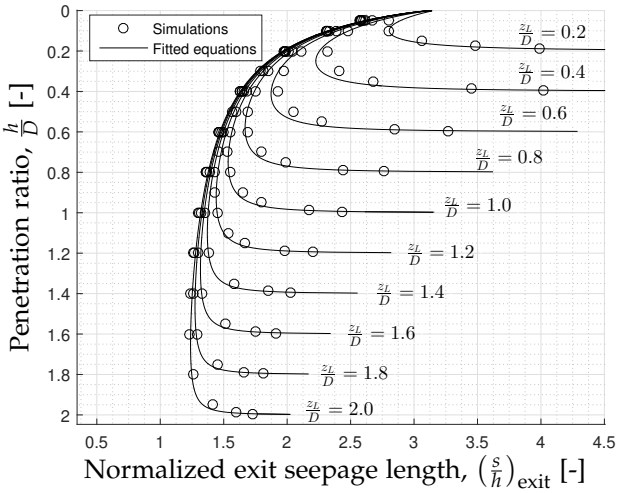

Fig. A.8: Results of $\left(\frac{s}{h}\right)$ for exit hydraulic gradient for case (c)

The last case to be presented here, case (c), includes impermeable layer below sand. Fig. A.8 presents the results of normalized seepage length for exit gradient for this case. For small penetration ratio, the trend is similar as it was for the two other soil cases with $\left(\frac{s}{h}\right)$ values decreasing for increasing penetration ratio. However, an influence of impermeable layer below sand is observed through a sudden increase in $\left(\frac{s}{h}\right)$ value while approaching this layer. Equation given below is the solution fitted to the numerical results:

$$\left(\frac{s}{h}\right)_{\text{exit}} = \left(\frac{s}{h}\right)_{\text{ref}} + a\left(\frac{D}{z_L}\right)\left(\frac{h}{z_L - h}\right)^{0.5}, \tag{A.30}$$

where

$$a = 0.14\exp\left(-0.4\frac{z_L}{D}\right) - 2019\exp\left(-55.4\frac{z_L}{D}\right). \tag{A.31}$$

For each condition where $\frac{z_L}{D}$ varies, normalized seepage length values for average inside and for tip gradient are calculated. Results from simulations with $\frac{z_L}{D} = 0.2$ and $\frac{z_L}{D} = 1.0$ are shown in Fig. A.9 and in Fig. A.10 respectively as an example. The results indicates that there is no significant difference for results of normalized seepage length for tip gradient in both cases. However, for results of normalized seepage length for average inside gradient, values are noticeable smaller for case of $\frac{z_L}{D} = 1.0$, what results in more reduction for soil resistance as β factor will be smaller. Analyzing the normalized seepage length results for exit hydraulic gradient, it can also be observed, that the values are smaller, when impermeable layer is situated further from skirt tip. Therefore, the closer the skirt tip to the impermeable layer is, the more suction

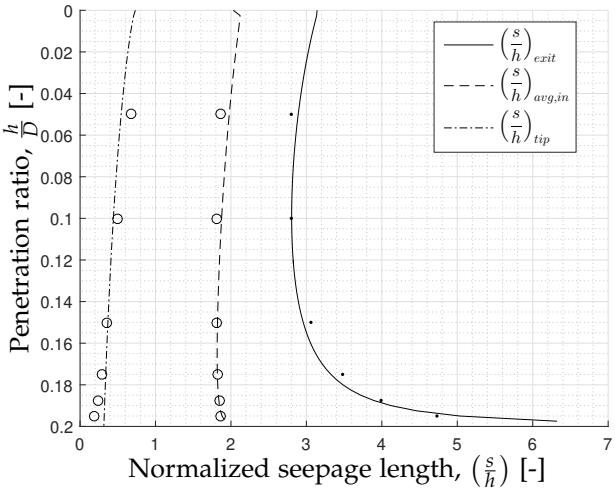

Fig. A.9: Results of $\left(\frac{s}{h}\right)$ for exit, average inside and tip hydraulic gradients for case (c) with $\frac{z_L}{D} = 0.2$

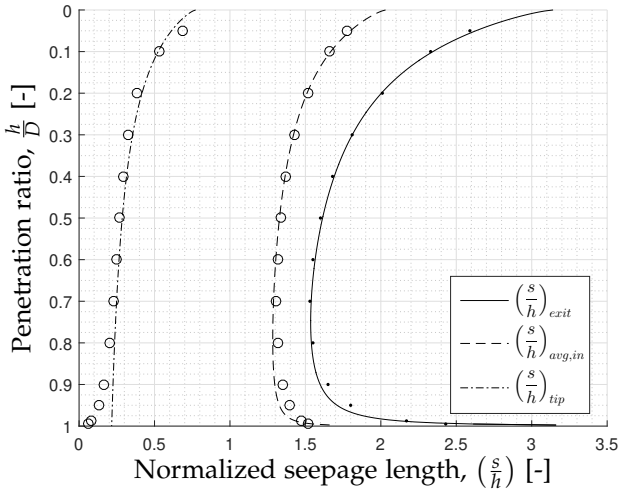

Fig. A.10: Results of $\left(\frac{s}{h}\right)$ for exit, average inside and tip hydraulic gradients for case (c) with $\frac{z_L}{D} = 1.0$

can be applied before soil failure. Nevertheless, the increase in values of seepage length for average inside gradient while approaching impermeable layer is less comparing to values of seepage length for exit gradient. This results in new curvature factor, factor b. The solution for normalized seepage

length for average inside gradient for case (c) is:

$$\left(\frac{s}{h}\right)_{\text{avg,in}} = 0.46\left(\left(\left(\frac{s}{h}\right)_{\text{ref}} + a\left(\frac{D}{z_L}\right)\left(\frac{h}{z_L - h}\right)^{b}\right) - 0.9\right) + 1, \tag{A.32}$$

where

$$b = 0.38\exp\left(0.1\frac{z_L}{D}\right) - 0.49\exp\left(-3.6\frac{z_L}{D}\right). \tag{A.33}$$

Factor a is the same as eq. (**??**). The solution for normalized seepage length for tip gradient is:

$$\left(\frac{s}{h}\right)_{\text{tip}} = a\left(\left(\frac{s}{h}\right)_{\text{ref}} - 3.9\right) + 1, \tag{A.34}$$

where

$$a = 0.3\left(\frac{z_L}{D}\right)^{-0.1}. \tag{A.35}$$

Nevertheless, chosen function does not account for a decrease in seepage length for tip gradient when approaching impermeable bottom layer. The value drops til zero when the impermeable layer is reached.

For average outside gradients the normalized seepage length results give the solution for case (a):

$$\left(\frac{s}{h}\right)_{\text{avg,out}} = 4.8\frac{h}{D} + 2.05 \tag{A.36}$$

case (b):

$$\left(\frac{s}{h}\right)_{\text{avg,out}} = \left(4.4\frac{h}{D} + 4.35\right) + 5.3\exp\left(-7.2\frac{h}{D}\right) \tag{A.37}$$

and case (c):

$$\left(\frac{s}{h}\right)_{\text{avg,out}} = 4.8\frac{h}{D} + 2.05 - a\left(\frac{h}{D}\right)\left(\left(\frac{h}{z_L}\right)^{b} + \left(\frac{D}{z_L}\right) - c\right), \tag{A.38}$$

where

$$a = 3.2\exp\left(0.03\frac{z_L}{D}\right) - 3.76\exp\left(-5.18\frac{z_L}{D}\right), \tag{A.39}$$

$$b = 1.74\exp\left(0.62\frac{z_L}{D}\right), \tag{A.40}$$

$$c = 6.46\exp\left(-5.23\frac{z_L}{D}\right) + 1.65\exp\left(-0.74\frac{z_L}{D}\right). \tag{A.41}$$

The chosen functions are in excellent correlation with results from numerical simulations, with coefficient of determination more that 0.98.

A.6 Critical suction pressure

Based on results of normalized seepage length, the normalized critical suction for bucket installation is obtained from the following equation. The allowable suction grows, when the seepage length results are increasing.

$$\frac{p_{\text{crit}}}{\gamma' D} = \left(\frac{s}{h}\right)_{\text{exit}} \left(\frac{h}{D}\right) \tag{A.42}$$

Fig. A.11 shows the results of normalized critical suction for homogenous sand along with proposed solution and the solutions found in (Senders and Randolph, 2009) and in (Ibsen and Thilsted, 2010). Even though, in previous proposed solution the range of penetration ratio was smaller, proposed solutions are really similar, what proves the validity of the model and method used in this research.

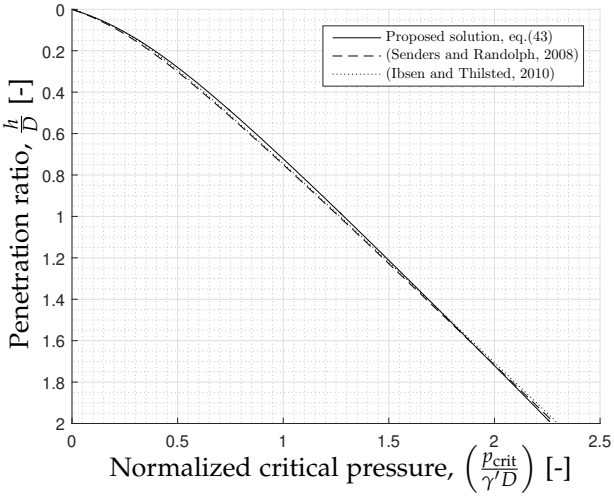

Fig. A.11: Results of normalized critical suction along with solutions given in (Senders and Randolph, 2009) and (Ibsen and Thilsted, 2010)

Results of normalized critical suction for all three soil cases used in this research are presented in Fig. A.12. Based on results, it can be concluded that the presence of impermeable layer results in increase of p_{crit}, as already mentioned in (Ibsen and Thilsted, 2010). On the other hand, the increase in critical pressure results in increase of β factors and, as a consequence, less reduction in soil resistance is expected.

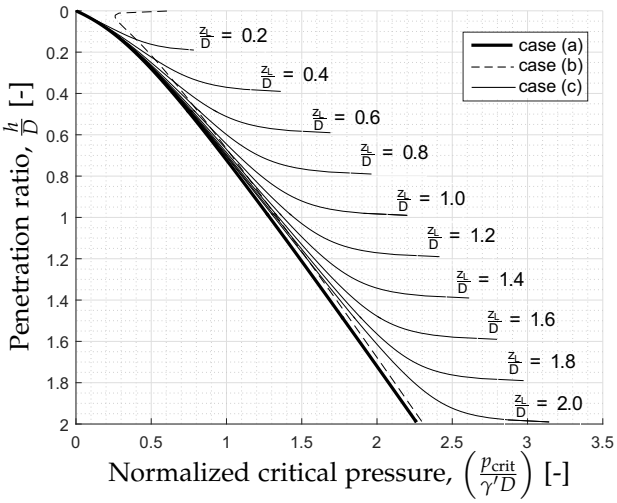

Fig. A.12: Results of normalized critical suction for soil case (a), (b) and (c)

A.7 Conclusions and recommendations

This paper proposes the method for calculation of soil resistance against the penetration during the installation of bucket foundation in sand. This method is based on CPT results and take into account the favorable effects of seepage flow through β factors. The results used for analysis come from numerical simulations where excess pore pressure around the bucket skirt was investigated for a wide range of penetration depth. Three soil cases considered in the research includes homogenous sand, sand overlaid by impermeable layer and sand situated above impermeable layer. Throughout the paper, solutions for pore pressure factor, α, and for normalized seepage length for hydraulic gradients at the exit, for the average gradient at the inside skirt and for the gradient at the tip of skirt are proposed. The results confirm, that the critical gradient appears first at the tip of skirt and then progress along the inside bucket skirt until it reaches free surface inside the bucket. At this very last step a soil failure due to piping channels is expected. What is more, the investigation shows, that the presence of impermeable layer in close vicinity of bucket skirt changes the characteristics of seepage flow around that skirt. The seepage length increases in such conditions, which results in increase of allowable suction that can be applied under the bucket lid. Conversely, the values of β factors are smaller comparing to the case with only homogenous sand and consequently, the reduction in soil resistance due to seepage flow is less significant.

Future work will be focus on investigation of values for seepage length

for soil with coefficients of permeability between the values characteristic for sand and clay, where the seepage flow is still expected, though more limited. Furthermore, different rates of penetration will be investigated to see what influence this has on the reduction in soil resistance. Another aim is to validate proposed solutions with tests results performed in small-scale and finally, in full-scale installation tests. The work presented here is considered to be an important step towards the development of full method for installation of suction bucket foundation to be used as design standards in future.

Acknowledgments

The work presented in this paper is funded by the EU7 as a part of the Project "Innwind - Innovative Wind Conversion Systems ($10-20$ MW) for Offshore Applications". The financial support is greatly appreciated.

References

Andersen, K.H., Jostad, H.P. & Dyvik, R. (2008). Penetration Resistance of Offshore Skirted foundations and Anchors in Dense Sand. Journal of Geotechnical and Geoenvironmental Enigneering 134, 106-116.

Byrne, B.W. & Houlsby, G.T. (2003). Foundations for Offshore Wind Turbines. Philosophical Transactions: Mathematical, Physical and Engineering Sciences 361, No. 1813, Mathematics, Physics and Engineering, 2909-2930.

Chen, F., Lian, J., Wang, H., Liu, F. & Zhao, Y. (2016). Large-scale experimental investigation of the installation of suction caissons in silt sand. Journal of Applied Ocean Research 60, 109–120.

DNV (1992). Foundations, classification notes No. 30.4, Det Norske Veritas, Hovik, Norway.

Erbrich, C.T. & Tjelta, T.I. (1999). Installation of bucket foundations and suction caissons in sand – Goetchnical performance. Proceedings of Offshore Technology Conference, OTC 10990, 31stEdition, 725-735.

Houlsby, G.T. & Byrne, B.W. (2005). Calculation procedures for installation of suction caissons in sand. Journal of Geotechnical Engineering 158, 135-144.

Houlsby, G.T., Ibsen, L.B. & Byrne, W.B. (2005). Suction caissons for wind turbines. In proceedings of Frontiers in Offshore Geotechnics: ISFOG, Perth, Australia, 75-93.

Houlsby, G.T., Kelly, R.B., Huxtable, J. & Byrne, B.W. (2006). Field trials of suction caissons in sand for offshore wind turbine foundations. Geotechnique

56, No. 1, 3-10.

Ibsen, L.B. & Brincker, R. (2004). Design of a New Foundation for Offshore Wind Turbines. In Proceedings of IMAX-22: A Conference on Structural Dynamics, Hyatt Regency Dearborn, Dearborn, Michigan, USA, 359-366.

Ibsen, L.B. & Bødker, L. (1994). Baskarp Sand No. 15. Data Report No. 9401, Geotechnical Engineering Group, Aalborg University, Aalborg, Denmark.

Ibsen, L.B., Hanson, M., Hjort, T. & Thaarup, M. (2009). MC-Parameter Calibration for Baskarp Sand No.15. DCE Technical Report 62, Department of Civil Engineering, Aalborg University, Aalborg, Denmark.

Koteras, A.K. (2017). Set-up and test procedure for suction installation and uninstallation of bucket foundation. DCE Technical Memorandum, No.63, Department of Civil Engineering, Aalborg University, Aalborg, Denmark.

Koteras, A.K. (2019). Suction and jacking installation of bucket foundation models: laboratory manual. DCE Technical Memorandum, No.74, Department of Civil Engineering, Aalborg University, Aalborg, Denmark.

Koteras, A.K. & Ibsen, L.B. (2018). Reduction in Soil Penetration Resistance for Suction-assisted Installation of Bucket Foundation in Sand. In proceedings of International Conference on Physical Modelling in Geotechnics: ICPMG, London, United Kingdom, 623-628.

Koteras, A.K. & Ibsen, L.B. (2019). Medium-scale laboratory model of mono-bucket foundation for installation tests in sand. Canadian Geotechnical Journal 56(8), 1142-1153.

Lehane, B.M., Schneider, J. & Xu, X. (2005). The UWA-05 method for prediction of axial capacity of driven piles in sand. In proceedings of International Symposium on Frontiers in Offshore Geotechnics: ISFOG, Perth, Australia, 19-21.

Lesny, K. (2011). Foundations for Offshore Wind Turbines – Tools for Planning and Design. Essen, Germany: VGE Verlag GmbH.

Lian, J., Chen, F. & Wang, H. (2014). Laboratory tests on soil-skirt interaction and penetration resistance of suction caissons during installation in sand. Journal of Ocean Engineering 84, 1–13.

Madsen, S., Andersen, L.V. & Ibsen, L.B. (2013). Numerical buckling analysis of large suction caissons wind turbines on deep water. Journal of Engineering Structures 57, 443-452.

Madsen, S. & Gerard, L. (2016). Buckling analysis for EUDP offshore wind suction bucket on an industrial scale. DCE Technical Memorandum, Vol. 213,

Department of Civil Engineering, Aalborg University, Aalborg, Denmark.

Randolph, M.F. & Gourvenec, S. (2011). Offshore geotechnical engineering, 1st Edition. New York: Spon Press.

Schneider, J.A. & Senders, M. (2010). Foundation design – a comparison of oil and gas platforms with offshore wind turbines. Journal of the Marine Technology Society 44(1), 32-51.

Senders, M. & Randolph, M.F. (2009). CPT-Based Method for the Installation of Suction Caissons in Sand. Journal of Geotechnical and Geoenvironmental Engineering, Vol. 135(1).

Sturm, H. (2017). Design Aspects of Suction Caissons for Offshore Wind Turbine Foundations. Proceedings of TC 209 Workshop, 19th ICSMGE, Seoul 20 September 2017.

Tran, M.N. & Randolph, M.F. (2008). Variation of suction pressure during caisson installation in sand. Geotechnique 58, No. 1, 1-11.

Vaitkunaite, E., Ibsen, L.B. & Nielsen, B. (2014). New medium-scale laboratory testing of bucket foundation capacity in sand. In Proceedings of the 24th International Offshore and Polar Engineering Conference, Busan, Korea, 514–520.

Appendix B

Medium-scale Laboratory Model of Mono-bucket Foundation for Installation Tests in Sand

Aleksandra Katarzyna Koteras
Lasr Bo Ibsen

The paper has been published in
Canadian Geotechnical Journal Vol. 56(8), pp. 1142–1153, 2019.
(the final draft version included in the thesis)

The layout has been revised.

Abstract

Design implications of suction installation of bucket foundations are still not well understood. During suction installation, applied suction under the bucket lid results in seepage flow through the surrounding sand. Seepage flow plays a pivotal role in reducing the penetration resistance, allowing for full penetration despite the initial large soil resistance. However, loosening of the inside soil plug might be problematic when the soil approaches its failure stage, due to soil piping or extensive soil heave inside the bucket foundation. To better understand the interaction between the soil and bucket skirt during suction installation, this paper describes the results of medium-scale tests of bucket foundation installation in sand, comparing jacking and suction installation. Experimental measurements of the pore pressure around the bucket skirt are compared to the numerical simulation results, to validate the finite-element model and to enable analysis of the soil behavior around the skirt.

KEY WORDS: Bucket foundation; Dense sand; Suction; Seepage; Soil resistance.

B.1 Introduction

Development of offshore wind energy has led to an increase in research aimed at reducing the total cost of wind turbines, particularly by developing cost-effective design solutions for the foundation. Suction bucket foundation technology, where the bucket lid is equipped with special valves for suction installation, offers advantages over jacking installation. Compared to jacking installation, the suction process is more environmentally friendly, cost-effective, and feasible, as it requires no heavy drilling equipment. Suction anchors have been extensively installed in various engineering devices and systems across different offshore sites. There are well-documented examples of skirted structures installed as foundations (Tjelta 1995; Andersen et al. 2008). For instance, a suction bucket foundation was used in the Frederikshavn, Denmark, for a wind turbine, which was the subject of a 5-year research project by Ibsen (2008) documenting its installation and operation.

The dense-sand seabed of the North Sea is the site of numerous offshore projects. Cohesionless soils have a higher penetration resistance than clay, and installation in these soils might be more problematic. Past research has shown that the application of suction not only creates the downward force required for installation, but also provides a large decrease in resistance for all permeable soils (Bye et al. 1995; Hogervorst 1980). Generation of seepage flow around the bucket skirt induces an upward hydraulic gradient within the inner soil and a downward gradient on the outside of the skirt, which

changes the effective soil stress and reduces the total soil penetration resistance (SPR). Studies have proposed different methods for calculating the soil resistance during the suction installation process for bucket foundations in sand (Erbrich and Tjelta 1999; Houlsby and Byrne 2005; Andersen et al. 2008; Senders and Randolph 2009). While consistently showing that the soil resistance varies depending on the value of the applied suction, these studies have not analyzed the interaction between the bucket skirt and the surrounding soil during seepage flow.

The suction installation process for a bucket foundation in sand consists of two parts: self-weight penetration and suction penetration. Self-weight penetration is necessary to create a sufficient seal between the bucket skirt and surrounding soil, without which suction application will not be effective. During the suction penetration stage, the required suction for a given penetration depth must be determined. Although the general principle for the relationship between suction and penetration depth is known, detailed design improvements for the installation can and should be made.

This paper presents a series of medium-scale tests for the bucket foundation installation using jacking and suction installation. Pore pressure (PP) around the bucket skirt and applied suction under the bucket lid are monitored during installation. Fig. B.1 shows the model used for installation tests. Measurements were used to confirm previous findings about the reduction in soil resistance and to investigate seepage flow around the bucket foundation. In addition, numerical simulations of suction installation tests were performed under the same conditions as the lab set-up. Comparing numerical and lab results allows analysis of the critical allowable suction for bucket foundation installation and better understanding of experimental results.

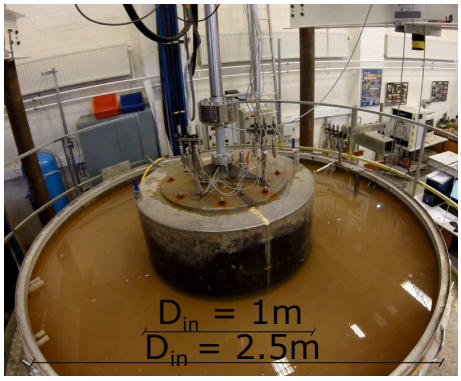

Fig. B.1: Bucket foundation model in test sand container with internal diameters D_{in}.

B.2 Soil Penetration Resistance of Skirt Structures

B.2.1 Calculation methods

Penetration resistance can be calculated based on either the ultimate bearing capacity theory or an empirical model that relates the results of the Cone Penetration Test (CPT) to SPR. In general, the total penetration resistance, R_{tot}, consists of the skirt tip resistance, Q_{tip}, and the inner and outer friction along the skirt, F_{inner} and F_{outer} respectively.

Equation (B.1) presents the classical approach based on the bearing capacity theory for the pile design (API 2014).

$$R_{\text{tot}} = A_{\text{tip}} \min\left[\sigma'_v(h) N_q, Q_{\text{lim}}\right] + (A_{\text{s,o}} + A_{\text{s,i}}) \min\left[K \tan\delta \int_0^h \sigma'_v(z)\, dz, f_{\text{lim}}\right] \tag{B.1}$$

where A_{tip}, $A_{\text{s,o}}$, and $A_{\text{s,i}}$ are the tip area, outside skirt area, and inside skirt area, respectively; σ'_v is the effective vertical soil stress; z is the depth below the soil surface; and h is the penetration depth. D_o and D_i are the outside and inside diameters of the bucket; and Q_{lim} and f_{lim} are the suggested limiting values for tip resistance and skirt friction, respectively.

Calculating total resistance with the classical approach presents difficulties for estimating the soil parameters, including the bearing capacity factor, N_q, coefficient of lateral earth pressure, K, and interface angle, δ. In this respect, the CPT-based approach is more straightforward (DNV 1992) because the measured cone resistance, q_c, can be linked to the skirt and the tip resistance of the foundation (eq.(B.2)). The CPT-based method is also more reliable than the classical approach because the CPT gives a record of the soil resistance with depth. Senders and Randolph (2009) and Chen et al. (2016) found that resistance calculated by the CPT-based approach fit the experimental data better than resistance calculated by the classical approach in eq.(B.1).

$$R_{\text{tot}} = A_{\text{tip}} q_c(h)\, k_p + (A_{\text{s,o}} + A_{\text{s,i}}) \int_0^h q_c(z)\, dz k_f \tag{B.2}$$

Empirical coefficients k_p and k_f relate the cone resistance to the skirt tip resistance and the friction along the skirt, respectively. A wide range of those parameters for sand are given by DNV (1992); however, many past studies on the penetration of skirted foundations have attempted to reduce this range (Lian et al. 2004; Lehance et al. 2005; and Andersen et al. 2008).

To enable detailed design of the suction installation process, effects of seepage must be included. The applied suction, p, and developed excess PP, u, around the bucket skirt change the resistance of sand. However, the complexity of the stress state during suction installation makes it difficult

to provide a good estimate of those changes. According to Houlsby and Byrne (2005), the stress state used to calculate SPR should be changed due to the hydraulic gradient, i, that develops in the surrounding soil. They assumed that a linear distribution of excess PP on the inside and outside of the skirt with depth. Therefore, the applied pressure and the development of excess PP at the tip provide sufficient information to estimate the stress level for each penetration depth. The PP factor, α, is the ratio of excess PP at the skirt tip to the applied suction. Based on numerical analyses, Houlsby and Byrne (2005) proposed a solution for the PP factor when the hydraulic conductivity, k, is uniform (eq.(B.3)) and the hydraulic conductivity of the inside plug is increased (eq.(B.4)). The ratio between the inside and outside hydraulic conductivity values, k_{in} and k_{out}, respectively, is termed k_{ratio}.

$$\alpha = 0.45 - 0.36\left[1 - exp\left(-\frac{h}{0.48D}\right)\right] \text{ for uniform } k \tag{B.3}$$

$$\alpha = \frac{\alpha_1 k_{\text{ratio}}}{(1-\alpha_1) + \alpha k_{\text{ratio}}} \text{ for increased } k_{\text{in}} \tag{B.4}$$

where D is the foundation diameter and α_1 is the PP factor for uniform k (eq.(B.3)).

The reduced soil resistance is calculated by replacing the effective soil unit weight, γ', with its reduced or increased value for the upward gradient on the inside skirt and for the downward gradient on the outside skirt, respectively $(\gamma' - [(1-\alpha)\, p/h]\,; \gamma' + (\alpha p/h))$. Comparison of the calculated resistance with the installation cases showed a good fit. However, certain variations of the key soil parameters were required to obtain a good fit.

Koteras et al. (2016) proposed another formulation that gives the best fit to the results of numerical analysis performed in PLAXIS 2D. Eq.(B.5) was found for the installation in sand of uniform hydraulic conductivity.

$$\alpha = \frac{0.21}{\frac{h}{D} + 0.44} \tag{B.5}$$

B.2.2 Critical pressure for suction installation

The design method for suction installation should consider limiting conditions, including the critical pressure, p_{crit}, that can be applied under the bucket lid during installation. As the hydraulic gradient develops inside the surrounding soil, the sand on the upward flow side loosens. The decrease in soil density can cause complete loosening of soil around the skirt, breaking the seal between the bucket skirt and soil. In this case, known as "piping", the installation process cannot proceed due to loss of the seal. The hydraulic gradient when the effective soil stress drops to zero is called the

critical gradient, $i_{\text{crit}} = \gamma'/\gamma_w$, where γ_w is the unit weight of water. The critical gradient is initially achieved around the skirt tip. As the localized pipes are constrained with surrounding soil, the critical gradient proceeds upward along the skirt, until it reaches the inner soil surface. The hydraulic gradient that controls piping is the exit gradient at the inner soil surface adjacent to the skirt (Senders and Randolph 2009). Critical pressure studies are normally performed with numerical simulations.

Erbrich and Tjelta (1999) proposed a solution for the critical suction number, S_N, reflecting the applied suction that causes the critical hydraulic gradient as a function of penetration ratio (h/D). The solution is based on numerically performed steady-state flow calculations. More recent studies relate the critical suction to a value of normalized seepage length at the exit, $(s/h)_{\text{exit}}$, where s is the exit seepage length. The seepage length at the exit is calculated based on the definition of hydraulic gradient that is equal to the change in hydraulic head, ΔH, divided by s. The value of exit hydraulic gradient, i_{exit}, can be determined from numerical simulation. The change in hydraulic head is equal to the applied suction divided by the water unit weight, and the exit seepage length is calculated from eq. (B.6).

$$s = \frac{\Delta H}{i_{\text{exit}}} = \frac{p}{i_{\text{exit}}\gamma_w} \tag{B.6}$$

Senders and Randolph (2009) performed numerical simulations of suction bucket installation in PLAXIS. To obtain normalized seepage length as a function of penetration ratio, PLAXIS results were analyzed with results by Erbrich and Tjelta (1999) and theoretical values for a sheet-pile wall (eq.(B.7)). Critical pressure for piping was calculated by combining equations for the critical gradient and seepage length (eq.(B.8)).

$$\left(\frac{s}{h}\right)_{\text{exit}} = \pi - \arctan\left[5\left(\frac{h}{D}\right)^{0.85}\right]\left(2 - \frac{2}{\pi}\right) \tag{B.7}$$

$$\frac{p_{\text{crit}}}{\gamma' D} = \left(\frac{h}{D}\right)\left(\frac{s}{h}\right) \tag{B.8}$$

Two assumptions were made: i) the inner friction along the skirt and the resistance at the skirt tip decrease linearly from their maximum values (no applied suction) to zero (critical suction); and ii) the outside friction along the skirt is unaffected (Senders and Randolph 2009). Reduced soil resistance, R_{reduced}, is calculated with eq.(B.9), which is valid for $p \leq p_{\text{crit}}$.

$$R_{\text{reduced}} = \left(Q_{\text{tip}} + F_{\text{inner}}\right)\left(1 - \frac{p}{p_{\text{crit}}}\right) + F_{\text{outer}} \tag{B.9}$$

The proposed method gives a good fit with results of suction installation tests performed in a centrifuge. However, compared to field tests of installation, the critical suction is exceeded with no failure occurrence.

Ibsen and Thilsted (2011) presented a similar solution for normalized seepage length based on simulations performed in FLAC (eq.(B.10)).

$$\left(\frac{s}{h}\right)_{\text{exit}} = 2.86 - \arctan\left[4.1\left(\frac{h}{D}\right)^{0.74}\right]\left(2 - \frac{1.8}{\pi}\right) \tag{B.10}$$

Koteras et al. (2016) conducted a similar study in PLAXIS 2D and obtained eq.(B.11) for the normalized seepage length of the exit hydraulic gradient. The CPT-based method was used to calculate soil resistance during the installation. However, changes in outside and inside friction on the skirt and the change in skirt tip resistance were based on normalized seepage lengths obtained for hydraulic gradients calculated on the inside skirt, outside skirt, and around the skirt tip, respectively. A comparison with laboratory or field tests has not yet been made.

$$\left(\frac{s}{h}\right)_{\text{exit}} = \pi - \arctan\left[3.6\left(\frac{h}{D}\right)^{0.74}\right]\left(2 - \frac{1.8}{\pi}\right) \tag{B.11}$$

Lian et al. (2014) and Chen et al. (2016) conducted laboratory tests of suction installation of bucket foundations in sand, using medium-scale (diameter: 0.5m, skirt length: 0.5m) and large-scale (diameter: 1.5m, skirt length: 0.5m) bucket models, respectively. Models were equipped with soil pressure gauges to record soil resistance inside and outside of the skirt. In both cases, suction measured during installation exceeded the critical value reported by Senders and Randolph (2009). Lian et al. (2014) proposed reduction coefficients for the inside friction on the skirt and for tip resistance (outside skirt friction was unaffected). When suction fell below the critical value, the reduction was linear between the maximum soil resistance and zero. When critical suction was exceeded without failure, the range for applied pressure increased by a factor of 1.5. For suction between p_{crit} and $1.5p_{\text{crit}}$, there was no resistance from the outside skirt or from the tip. Chen et al. (2016) concluded that the change in resistance was not linear and was different between the inner skirt friction and the tip resistance (outside skirt friction was not affected). They reported reduction ratios β_I (eq. (B.12)) and β_{tip} (eq. (B.13)), and proposed calculating the reduced SPR as shown in eq. (B.14).

$$\beta_I = 0.865\left(\frac{p}{p_{\text{crit}}}\right)^{1.03} \tag{B.12}$$

$$\beta_{\text{tip}} = 0.707\left(\frac{p}{p_{\text{crit}}}\right)^{1.86} \tag{B.13}$$

$$R_{\text{reduced}} = Q_{\text{tip}}\left(1 - \beta_{\text{tip}}\right) + F_{\text{inner}}\left(1 - \beta_I\right) + F_{\text{outer}} \tag{B.14}$$

In summary, either the bearing capacity or CPT-based approach can be used to calculate SPR during bucket foundation installation, but the calculation

must account for effects of suction-induced seepage. The above-mentioned methods lack accuracy, as they assume linear changes of soil resistance with penetration depth. Only Chen et al. (2016) proposed that those changes are nonlinear. To analyze changes in soil stress during suction installation, medium- or large-scale tests are required to investigate the interaction between the soil and bucket skirt. As the development of excess PP around the bucket skirt plays a key role in the suction installation process, it is important to record excess PP during tests. The present study focuses on these aspects.

B.2.3 Loosening of soil plug

In suction installation, seepage induced within the soil reduces the inside soil resistance. This reduction in soil resistance might alter the soil hydraulic conductivity inside the bucket. Houlsby and Byrne (2005) obtained reasonable fits of calculated SPR with field tests when applying α for increased k_{in}. Comparing the reduction in soil resistance with centrifuge results presented by Tran and Randolph (2008), a much better fit was obtained with $k_{\text{ratio}} = 1.5$. Harireche et al. (2014) showed results of the numerical analysis for pressure gradient development inside the soil related to the change in soil resistance. Comparison with centrifuge test results presented by Tran and Randolph (2008) showed that k_{ratio} should be > 1 and should increase with increasing penetration depth. Further investigation is needed to understand how the change in soil hydraulic conductivity inside the bucket should be included in the design calculation.

The test procedure presented in this paper includes CPTs performed before and after installation of the bucket foundation. Tested positions are both inside and outside the bucket, to capture changes in relative soil density due to suction installation and gradients in soil hydraulics as they appear. Then, possible changes in soil hydraulic conductivity can be assessed from the results of relative soil density.

B.3 Lab Model and Test Procedure

B.3.1 Set-up and bucket foundation model

The main aim of the lab tests reported herein is to analyze the soil-skirt interaction during installation of the bucket foundation model. The set-up is shown in Fig. B.2. Vaitkunaite et al. (2014) first introduced this facility for testing the capacity of the bucket foundation in sand. After adjustments, the same set-up is used for testing installation of the bucket foundation by jacking and suction installation approaches. The soil container (internal diameter: 2.5m, height: 1.52m) is equipped with a drainage system, consisting of pipes

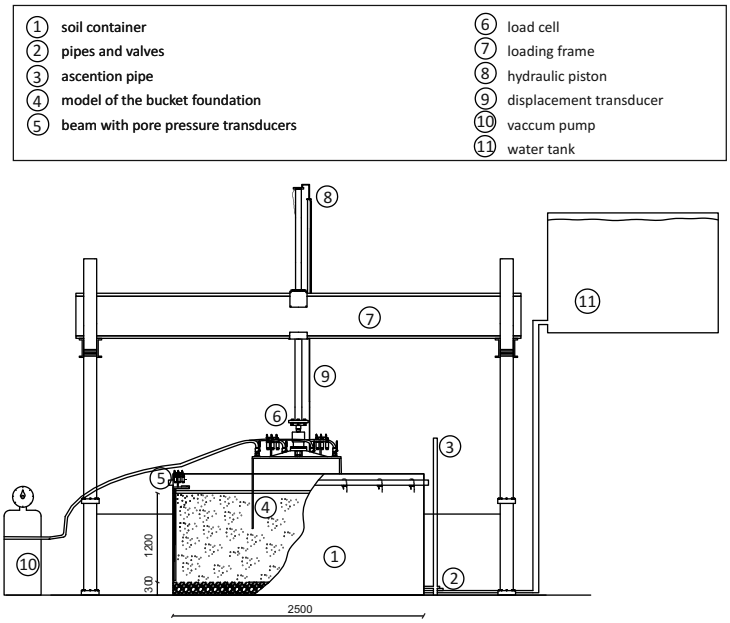

Fig. B.2: Laboratory set-up (dimensions in mm).

that are equally distributed over the bottom, a 300mm layer of highly permeable gravel, a geotextile sheet for preventing downward movement of sand particles, and a 1.20m layer of sand (Aalborg University Sand No. 1).

A medium-scale model of the bucket foundation is used (Fig. B.3), corresponding to a prototype size in 1:10 scale. The internal diameter, D_{in}, is 1m, skirt length, d, is 0.5m, and skirt thickness, t, is 3 mm. The self-weight of the model, including the connection flange to the loading system, is 201 kg. The bucket model is equipped with 4 valves on the lid, which are connected to the vacuum system during the suction procedure. Six PP transducers are attached to the inside and outside of the bucket skirt and under the bucket lid, for continuous analysis of seepage flow around the skirt during installation. PP is measured through open-ended pipes attached to the skirt. Open ends are positioned at locations PP1-PP3 on the outside skirt, PP4-PP6 on the inside skirt, and under the bucket lid. A displacement transducer is attached to the top of the bucket model, to measure bucket displacement during tests. A beam with PP transducers is installed close to the edge of the soil container to measure PP at the boundary.

B.3.2 Soil material

The chosen soil material is Aalborg University Sand No.1, which mainly contains quartz. The sand is graded; the largest grains are round, and the small

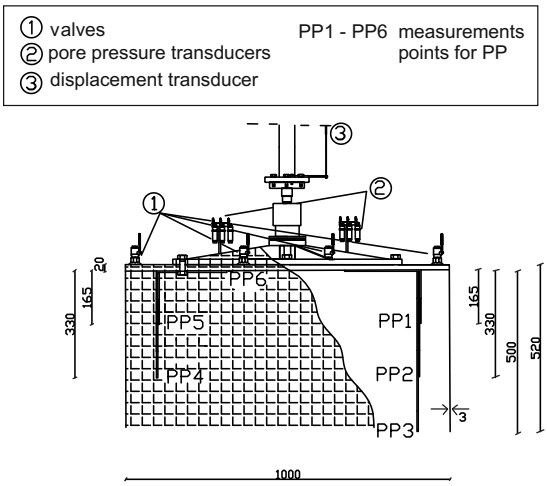

Fig. B.3: Model of bucket foundation (dimensions in mm).

grains are sharp-edged. Sand properties were measured directly by Ibsen and Brødker (1994) and are as follows: maximum void ratio, $e_{\max}$ = 0.854; minimum void ratio, $e_{\min}$ = 0.549; 50%-quantile, d_{50} = 0.14mm; uniformity coefficient, C_u = 1.78; and specific grain density, d_s = 2.64 g/cm^3. CPT results can be used to derive important soil parameters (Ibsen et al. 2009), including relative soil density, I_D; triaxial friction angle, φ_{tr}; triaxial dilation angle, ψ_{tr}; in situ void ratio, e_{insitu}; and effective soil unit weight, γ'. Ranges of values from all performed tests are included in Table B.1.

Table B.1: Range of values for soil parameters from CPTs for all installation tests.

Soil parameters	Range of values
Relative soil density [%]	88 - 91
Triaxial friction angle [°]	54 - 55
Triaxial dilation angle [°]	20 - 21
In situ void ratio [-]	0.63 - 0.65
Effective soil unit weight [kN/m^3]	9.7 - 9.9

Falling head tests were used to assess soil hydraulic conductivity k for different relative densities of material (Sjelmo 2012). For dense sand of ∼90% of relative soil density (average density for all tests in this paper), test results indicated $k \sim 7 \cdot 10^{-5}$ m/s.

B.3.3 Test procedure

Sand was saturated during the preparation procedure and the installation test through the drainage system. Before each test, sand was prepared to a dense, uniform condition. Relative density across tests ranged 88% to 91%.

An upward hydraulic gradient of 0.9 was applied by controlling the gradient through valves and an ascension pipe connected to the bottom of the sand container. Next, sand was vibrated to the desired density as follows. A wooden template with evenly located holes was set on the sand container. Then, a rod vibrator was slowly pushed into the sand through every second hole of the template, followed by the remaining holes on the way back, with the vibrator being slowly pulled each time.

To capture changes in soil resistance, sand conditions were analyzed through the CPT before and immediately after each installation test. A laboratory CPT device developed at Aalborg University was used. The device has a 15mm diameter cone with a cone angle of 30° and was calibrated at the laboratory before use. CPTs were performed at 4 positions before bucket installation (2 inside, 2 outside) and 8 positions after bucket installation (4 inside, 4 outside); see Fig. B.4. CPTs inside the bucket were performed through holes in valves on the bucket model. CPTs after bucket installation were performed within 5 min after the installation process was completed. Differences in relative soil density before and after installation indicated whether density changed due to the installation process.

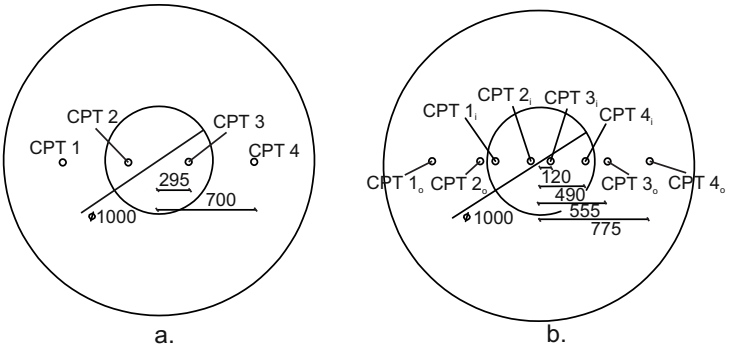

Fig. B.4: Positions used for CPTs performed before (a) and after (b) installation (dimensions in mm).

During jacking installation, a hydraulic piston was used to apply the required jacking force. A hydraulic motor worked as a displacement control with a displacement rate of ∼0.13 mm/s. Valves on the bucket lid were open during installation; thus, no excess PP inside the bucket was expected.

The suction installation process was divided into two steps: self-weight installation and suction application. Self-weight installation was performed by switching the hydraulic motor to work as a force control and applying a force corresponding to the self-weight of the bucket model. The achieved penetration depth provided an appropriate hydraulic seal between the soil and the bucket skirt for further suction application (minimum 50mm). Suction was applied through the vacuum system by connecting the valves on the

bucket lid with the vacuum pump. Pressure on the vacuum tank was manually increasing slightly until penetration occurred. Because the vacuum pump extracted water during installation, the water level had to be maintained by continuously refilling the water. Tilting of the bucket model was negligible. During installation, readings were recorded from the displacement, PP, and force transducers. All sensors were connected to signal transducer boxes, and recordings were transmitted through signal amplifiers (Spider8 and GC Plus) to the Catman program on the computer. Koteras (2017) described the model and test procedure in more detail.

An overview of all tests can be found in Table B.2. In the suction installation tests (Tests 1-3), a constant force of 2kN was applied along with the bucket self-weight of 2kN, for a total self-weight of 4kN. This force was added to the force from applied suction throughout the entire penetration depth. In the pure suction installation tests (Tests 4, 5, and 9), the self-weight was 2kN. The hydraulic motor worked as a force-controlled motor. Different self-weight penetration depths were obtained and its effect on the results is assessed later on in this paper. In the jacking installation tests (Tests 7, 9, and 10), there were 2 values of maximum penetration (Table B.2). The first value corresponded to the maximum force recorded when the bucket lid contacted the soil. As the sand continued to be pushed and the particles re-arranged to be more equally distributed under the bucket lid, the force increased significantly and penetration proceeded, resulting in the second maximum penetration value.

Table B.2: Overview of test campaign.

Test	Driving force for installation	Maximum installation force, F_{max} (kN)	Required suction for h=450mm, p_{req} (kPa)	Self-weight penetration, $h_{self\text{-}weight}$ (mm)	Maximum penetration, h_{max} (mm)
1	Suction + Force	11.6	9.18	125	462; 470
2	Suction + Force	11.6	9.21	127	468; 468
3	Suction + Force	11.1	8.23	130	468; 471
4	Suction	8.9	8.53	78	460; 474
5	Suction	9.0	8.67	73	462; 466
6	Force	57.7	-	-	483; 487
7	Force	59.1	-	-	483; 488
8	Force	58.0	-	-	477; 482
9	Suction	9.7	9.52	66	447; 458
10	Force	53.1	-	-	472; 479

B.4 Development of Hydraulic Gradients

B.4.1 Numerical formulation of seepage flow

Seepage in sand was formulated with a numerical model. Seepage flow around the bucket skirt during installation was simulated in the commercial program PLAXIS 2D. An axisymmetric model was generated, in which the bucket skirt was simulated as a rigid line segment with an impermeable interface. The line segment had a length equal to the designed penetration depth, h, and was situated 0.5m from the center axis (same distance as the radius r of the bucket model). The center axis, bottom and side boundaries were modelled as closed flow boundaries. Total dimensions of the model were the same as those of the sand container used in the lab set-up. A sketch of the mesh numerical model is shown in Fig. B.5. Simulations were performed for a penetration ratio (h/D) between 0.1 and 0.5, with an interval of 0.02.

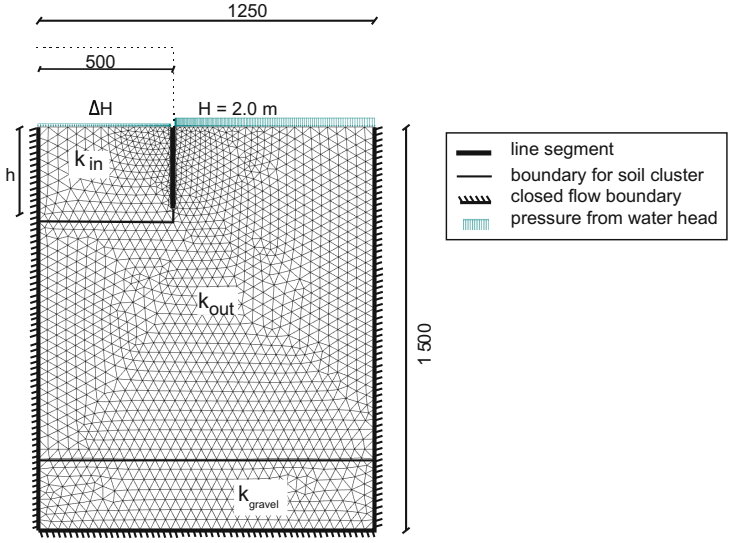

Fig. B.5: Mesh numerical model with boundary conditions (dimensions in mm).

Although the installation process is continuous, it is presented here as a series of discrete steps, with equilibrium between the soil resistance and the driving force being assumed in each step. Seepage flow was calculated as steady-state groundwater flow because the seepage is approximately stationary. Using the same approach, Tran and Randolph (2008) obtained good agreement of their numerical simulations with pressure results from centrifuge tests when installing the bucket foundation. Flow around the skirt was simulated by applying the flow boundary condition on the inner soil surface with an appropriate hydraulic head, H. A hydraulic head on the outer

soil surface of 2m was used. This number can be arbitrary, but must be sufficient to initiate the suction installation process. The head difference was directly related to the value of the applied suction. Here, the same model assumptions were applied as were used in Koteras et al. (2016), except that the distances to the boundaries were different. Suction values for each step of the numerical simulations were based on mean values from lab tests 5 and 9. In these tests, the self-weight penetrations of the bucket were the shortest (and, hence, the skirt penetration distances due to suction were the longest) among all tests.

The soil hydraulic conductivity k is relevant for flow calculations. Sjelmo (2012) performed falling head tests for Aalborg University Sand No.1 of different relative soil densities, I_D, reporting $k = 0.7 \cdot 10^{-4}$ m/s for $I_D = 90.8\%$ and $k = 1 \cdot 10^{-4}$ m/s for $I_D = 60.5\%$. These values are similar to the average I_D before suction installation (∼90%) and the inside I_D after suction installation (∼60%), respectively, in the present study and, therefore, were chosen to represent the lab test conditions for numerical analysis. A value of $k = 1$ m/s was used for gravel below the sand.

B.5 Test Results

B.5.1 Reduction in SPR

Results of CPTs were investigated and relative soil density was derived based on past CPT calibration (Ibsen et al., 2009). Fig. B.6 compares relative soil density results for suction and jacking installations from CPTs performed before and immediately after installation, for soil inside and outside the bucket.

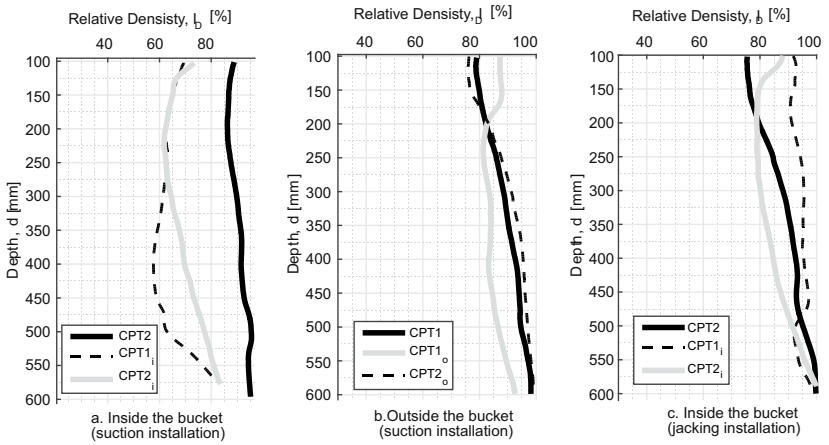

Fig. B.6: Relative soil densities before and after installation for (a, b) Test 5 and (c) Test 6. See Fig. B.4 for locations of CPTs.

Relative density of the soil plug significantly decreased with use of suction installation due to increased seepage, whereas changes in relative soil density on the outside of the bucket were insignificant. Jacking installation did not significantly change the relative soil density in the soil plug or in the soil outside the bucket. For all suction installation tests, the relative soil density showed a similar trend to Test 5. For all jacking installation tests, the CPT results were comparable to results of Test 6 (no change in relative soil density).

Table B.3: Results of relative soil density, I_D, and effective soil unit weight, γ'.

	Before installation		After installation			
			Inside the bucket		Outside the bucket	
Test	$I_{D,mean}$ (%)	γ'_{mean} (kN/m^3)	$I_{D,mean}$ (%)	$\Delta I_{D,mean}$ (%)	$I_{D,mean}$ (%)	$\Delta I_{D,mean}$ (%)
1	88	9.7	63	28.3	75	15
2	91	9.9	66	27.7	76	16.7
3	89	9.8	64	27.8	86	3.3
4	91	9.9	66	27.2	82	9.7
5	90	9.9	67	26.2	85	5.8
6	89	9.8	87	2.2	85	4.1
7	89	9.8	85	3.8	83	6.6
8	91	9.9	86	5.6	83	8.2
9	90	9.9	65	29.4	83	8.2
10	90	9.8	86	4.4	84	6.6

Table B.3 presents the mean relative soil density values, $I_{D,mean}$, for each test before and after installation, for soil inside the soil plug and outside the bucket, and the percentage change between results before and after installation, $(\Delta I_{D,mean})$. Calculations of mean values excluded the top 100mm of sand because of fluctuations resulting from the presence of the sand surface. Relative soil density results obtained before installation were compared with the results of the two closest CPT locations (see Fig. B.4). Mean values of the two comparisons inside and the two comparisons outside the bucket are also given in Table B.3. There was a significant, nearly 30% decrease in relative soil density inside the soil plug after suction installation, but minimal changes in the soil inner plug after jacking installation (<6%). For the outside soil, the changes were much less significant after suction or jacking installation. Only values from Tests 1 and 2 showed significant changes ($\sim$15%); however, in both tests, only two locations (CPT1$_o$ and CPT2$_o$) were analyzed (signals for locations CPT3$_o$ and CPT4$_o$ were not recorded). As only changes on one side of the bucket were investigated, these results are not very reliable.

A reduction in relative soil density is directly related to a reduction in SPR. As sand loosens, it shows less resistance to skirt penetration into the soil. This feature is beneficial for installation but might lead to failure or heave development. Reduced soil resistance was visible from the CPT tests and also from comparisons of the force required for jacking or suction installation. In

the 4 jacking installation tests, results of applied force vs. penetration depth were similar. This finding was expected because the same soil conditions were achieved before each of those tests (Fig. B.7a). The mean maximum force from all jacking installation tests was 57kN. The maximum value was the point where the displacement curve flattened, corresponding to the position where the bucket lid came in contact with the sand.

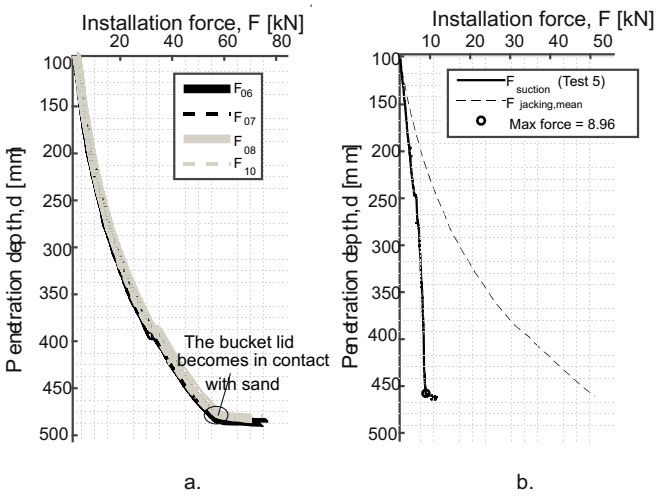

Fig. B.7: Results of jacking installation (a) and of suction (Test 5) vs. jacking installation (b).

Next, the average force reduction for suction installation, ΔF_{avg}, was calculated. Average force values from all 4 jacking installation tests were found for all recorded penetration depths, $F_{jacking,mean}$. These values were compared to the force used during each suction installation for each recorded penetration depth, $F_{suction}$.

ΔF_{avg} was determined as the mean change in force for all recorded penetration depths between 100mm and the maximum penetration depth. For each suction installation test, force included components resulting from the suction and from the self-weight of the bucket. The difference in bucket self-weights between Tests 1-3 (4kN) and all other tests (2kN) allowed investigation of the influence of different lengths of self-weight penetration on the final results. For Tests 1, 2, and 3, the ΔF_{avg} values were 43%, 45%, and 46%, respectively. For Tests 4, 5, and 9 (pure suction tests), reduction levels were slightly higher (ΔF_{avg} = 57%, 54%, and 50%, respectively). For these tests, suction was applied later, when self-weight penetration was longer, meaning that the reduction in force (and, thus, SPR) was induced on a shorter penetration length. As an example, the average reduction in force for Test 5 is shown in Fig. B.7b. Application of suction reduced the force on the entire penetration depth in each test by 40-60%. Compared to the mean maximum force

from all 4 jacking installation tests (57kN), the maximum force required by suction installation (Table B.2) was reduced 80-84%. The reduction in force can only be explained by the reduction of SPR. These results can be compared with past studies that identified the reduction factor for SPR by analyzing results of applied force. Allersma et al. (2003) found a reduction factor of 8 using centrifuge installation tests. Lian et al. (2004) found a reduction of 78-94% when comparing suction with jacking installation on a 1G set-up with a small-scale model. These results are comparable with the findings described above.

B.5.2 Soil heave development

Sand loosening is beneficial for installation because it reduces SPR, but it also causes the appearance of sand heave inside the bucket. Previous experimental studies in dense sand showed that soil heave development is highly probable during the suction installation process (Allersma et al. 2003; Tran et al. 2005). Heave development might be problematic for bucket performance as it can reduce the total stiffness of the foundation, therefore, should be considered during design. Table B.4 shows the heave height during all tests. Suction installation resulted slightly larger heaves than did jacking installation.

Table B.4: Change in void ratio and corresponding height of inside heave.

Test	Height of heave plug, h_{heave} (mm) ($\pm$ 5)	Void ratio before, e_{before}	Void ratio after, e_{after}	Ratio of heave height to skirt length, r_{heave} (%)
1	45	0.65	0.87	9.0
2	47	0.63	0.84	9.4
3	44	0.65	0.86	8.8
4	42	0.63	0.84	8.4
5	49	0.63	0.84	9.8
6	38	0.64	0.66	7.6
7	40	0.65	0.67	8.0
8	33	0.630	0.673	6.6
9	57	0.632	0.860	11.4
10	36	0.637	0.671	7.2

Soil movement towards the bucket cavity during sand installation is dictated by volume expansion, which results from the change in void ratio (Table B.4). An increase in void ratio inside the plug results in a larger void volume. With a constant volume of solid material, the increase in total volume results in increased heave development. Additionally, soil displaced by the bucket skirt is pushed inside or outside of the bucket. However, flow generated during suction installation pushes the soil inside according to the direction of flow. The heave height, r_{heave}, as a percentage of the total skirt length ranged 8-11% for suction installation and 7-8% for jacking installation. Tran

et al. (2005) found 6-8% of the embedded length as the heave development for suction installation tests. Observing similar results, Allersma et al. (2003) found that the amount of soil heave depended on the wall thickness, giving an increase of 5-10% of the embedded skirt length. The present paper did not test the influence of wall thickness on heave, although the results of heave development are comparable to those found in cited literature. The average amount of heave development for suction installation tests was ≈10%. The difference between jacking and suction installation is expected to be even more significant for full-scale tests.

B.5.3 Skirt-soil interaction due to seepage

Application of suction results in seepage flow around the bucket skirt. The total PP of water was recorded directly from lab tests. To determine the excess PP, hydrostatic pressure was subtracted from the total water pressure value. To observe the variation of PP during jacking installation both recorded PP, p_{measured} and calculated excess PP, u, are shown in Fig. B.8 (results of Test 6). As excess PP did not develop during jacking installation, seepage flow

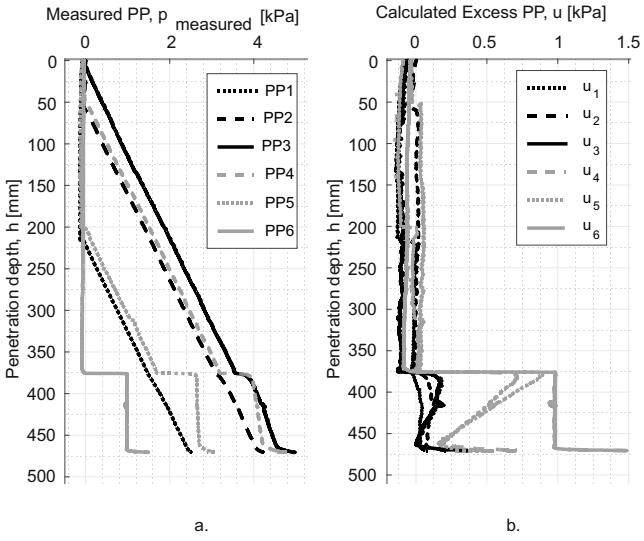

Fig. B.8: Measured PP (a) and calculated excess PP (b) during jacking installation for Test 6.

was not induced and, thus, there were no significant changes in SPR. For all jacking installation tests, a 1kPa change was observed during the last stage of installation, which was related to the height of the open valves on the bucket lid. As the bucket lid came in the contact with water, the water column inside the valves raised to the valve height, resulting in observed excess PP change.

To observe the variation of PP during suction installation both p_{measured} and u are shown in Fig. B.9 (results of Test 5). PP6 corresponds to the suction

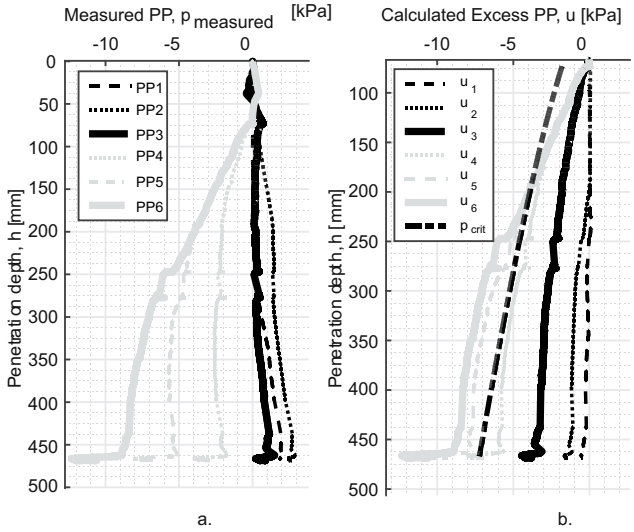

Fig. B.9: Measured PP (a) and calculated excess PP (b) during suction installation for Test 5.

pressure under the bucket lid (so u_6 is an exact value of applied pressure p). All other transducers showed a total pressure that included both hydrostatic pressure and excess PP. There was a significant amount of excess PP on the inside of the skirt (PP4 and PP5). The measured pressure was already negative, even though the hydrostatic pressure had not yet been deducted (Fig. B.9a). On the outside skirt, the excess PP was much smaller (PP1-PP2) and approached zero after the hydrostatic value was subtracted from the measured pressure. Hydrostatic pressure depends directly on the depth under the water table; thus, the highest value was reached in location PP3, followed by PP2, and the lowest value was at PP1. Excess PP was highest at location PP3, followed by PP2, and was nearly absent at PP1. As the excess PP was negative pressure, the highest total water pressure was obtained at PP2, followed by PP1; the total water pressure was nearly zero at PP3. Approaching the skirt tip from the outside soil surface and the inside plug of the bucket, there was an increase in generated excess PP. The excess PP results showed that there was an upward flow on the inside bucket wall, and that SPR was reduced due to the reduction in effective stress. Downward flow on the outside skirt was limited to locations close to the skirt tip, as there was almost no excess PP at PP1. Seepage flow was limited; thus, the changes in excess PP at the outside skirt were less significant than changes at the inside skirt. These findings suggest that it is reasonable to assume a constant SPR on the

outside skirt and a reduction in the inside soil plug. Interestingly, during all installation processes, the applied suction exceeded the theoretical value of critical suction given by Koteras et al. (2016) (see eqs.(B.8) and (B.11)), but no piping failure occurred.

Exceedance of critical suction pressure is shown in Fig. B.9b. It is assumed that piping forms around the skirt tip and proceeds above the inside soil surface. When piping reaches the soil surface, the hydraulic seal between the soil and skirt breaks, failure occurs, and no further installation is possible. In this study, no lab test failed. A discussion of the exceedance of critical pressure is presented later in the paper.

Next, the force required for suction installation was normalized to the average jacking force, $F_{\text{jacking,mean}}$. This normalized force was compared to the applied suction (normalized to the critical theoretical value of suction; eqs.(B.8) and (B.11)) and the penetration ratio for Tests 1 and 2. As shown in Fig. B.10, the reduction in the force required for suction installation (and, thus, in SPR) depended on the amount of applied suction. Soil resistance was reduced due to the seepage flow induced by the applied suction under the bucket lid. The reduction in soil resistance increased in proportion to the amount of applied pressure.

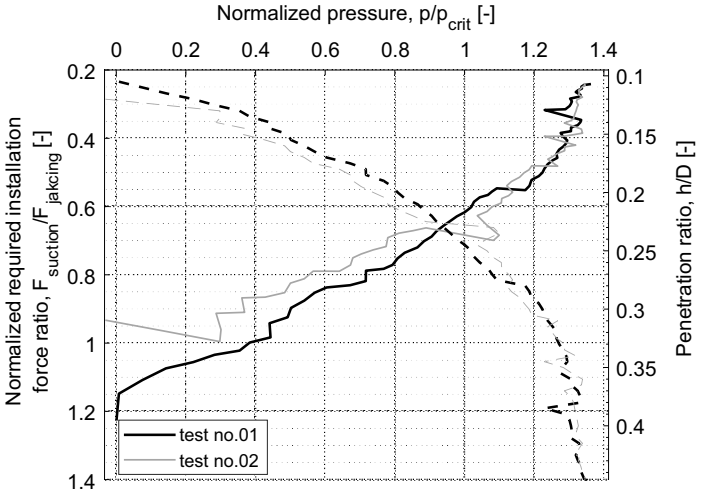

Fig. B.10: Required installation force ratio between suction and jacking installations. Solid line refers right y-axis; dotted line refers to left y-axis.

When the normalized pressure was 1 or more, the normalized suction installation force dropped more significantly. This drop occurred at a penetration ratio of around 0.25-0.3. Suction was kept more constant for the rest of the penetration, while the normalized suction installation force continued

to decrease. This finding suggests that suction was kept close to the critical level; however, the critical value was not exceeded, as none of the suction installation tests failed. A reduction factor >1 at the beginning of the installation should be ignored because the suction force included both the force arising from applied suction and the self-weight of the bucket.

Finally, the exit hydraulic gradient during suction installation was calculated from the excess PP results, based on results of suction applied at PP6 and excess PP at PP5 (closest location on the inside skirt). The change in excess PP between PP5 and PP6 was divided by the distance between those points (165mm), which was divided by γ_w. Figure B.11 presents results of the calculated exit gradient for all suction installation tests (Fig. B.11a) and the normalized critical pressure calculated from these exit gradient results (Fig. B.11b). Critical pressure was calculated, as explained before, by multiplying exit seepage length (eq.(B.6)) by the effective soil unit weight. The results in Fig. B.11 explain why there was no piping during suction installation, even though the theoretical critical suction was exceeded. The values of the exit hydraulic gradient ($\leq\sim$0.5) were much less than the critical gradient ($\sim$1.0). The critical pressure allowance based on exit critical gradients from experimental data was clearly larger than the limit suggested by numerical calculations. The normalized critical suction pressure calculated from experimental data was at least twice as large as the normalized numerical critical pressure.

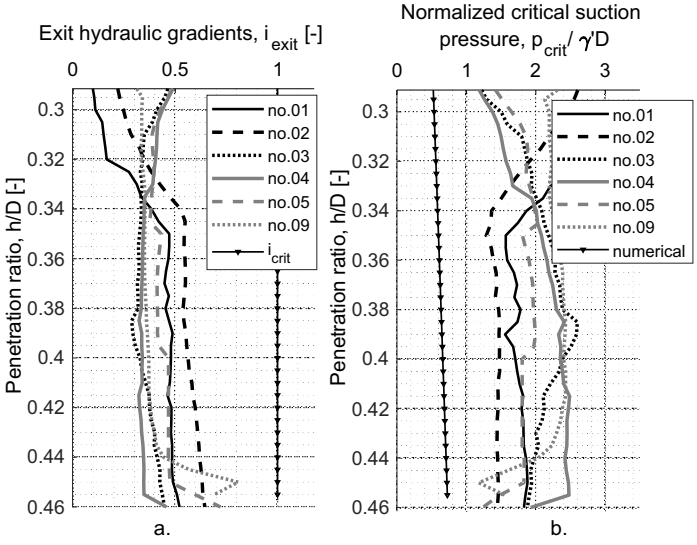

Fig. B.11: (a) Exit hydraulic gradients for suction installation tests and (b) normalized critical suction pressure based on those gradients' numerical solution (eq.(B.6)).

B.5.4 Boundary effects

The accuracy of scaled lab tests often depends on the boundary conditions of the set up. The seabed is unlimited, whereas the set-up boundaries were situated near the testing area. During each installation test, a beam with PP transducers was inserted into soil at the closest possible distance to the wall of soil container (see Fig. B.2). Positions of PP transducers on the beam are indicated in Fig. B.12a. Transducers were zeroed before the start of each test, such that direct measurements indicated the excess PP values. Figure B.12b shows the development of excess PP on the beam during Test 5 (suction installation). The excess PP is plotted versus the penetration depth of the bucket. Significant development of negative PP was observed, which increased as the installation progressed. The same trend was observed with all suction installation tests, whereas PP changes at the boundary were negligible for jacking installation tests.

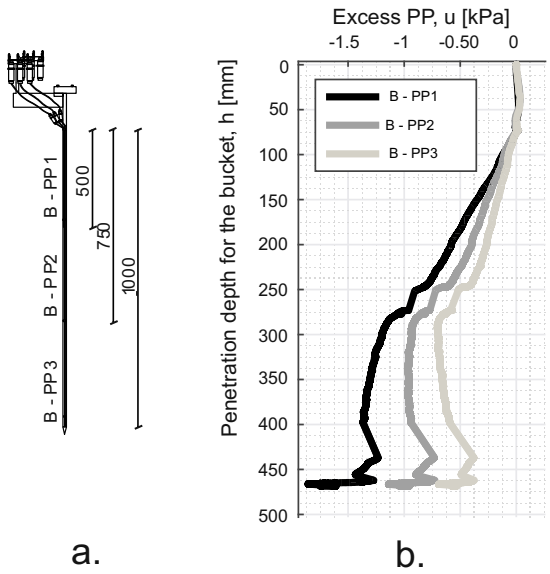

Fig. B.12: (a) Beam with PP transducer and (b)results of excess PP at beam during suction installation.

Seepage flow at the boundaries might influence seepage flow around the bucket skirt. The numerical model should have the same boundary conditions as the lab model, so that the comparison can be reasonable. The change in the model might therefore influence the normalized exit seepage from simulations and thus, theoretical critical suction

B.6 Comparison of Excess PP and Applied Suction Results

Next, the numerical model was adjusted to simulate the lab conditions. The numerical model included appropriate boundary conditions and increased hydraulic conductivity for the inner plug. Results of numerical simulations were compared to mean values of excess PP from Tests 5 and 9. Numerical simulations of suction installation tests provided results of total PP experienced by the soil. Excess PP values were calculated by subtracting the hydrostatic pressure from total PP. Fig. B.13 presents the development of excess PP due to the applied suction from both lab tests and numerical simulations, with excess PP results normalized by ($\gamma' D$).

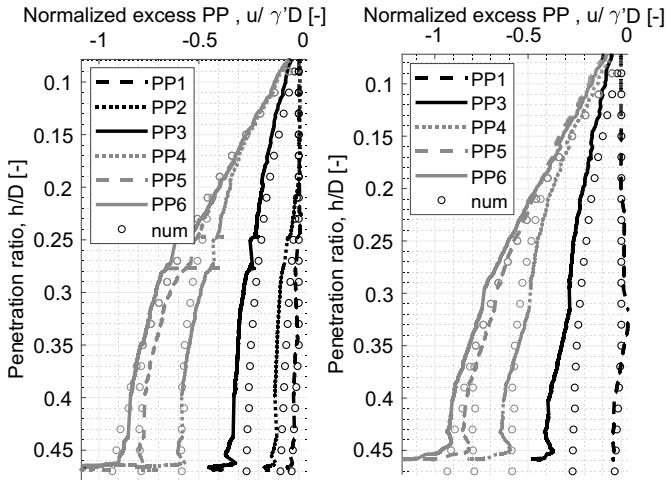

Fig. B.13: Comparison between numerical and lab results of PP change at skirt; (a) Test 5 and (b) Test 9.

Results of excess PP from medium-scale tests and numerical simulations were comparable, which confirmed that the numerical models can reasonably simulate installation data. The trend for the development of excess PP (and, thus, seepage flow) around the skirt was the same for both numerical and lab results (accuracy of pressure transducers used in lab tests was $\pm$0.2kPa). Results were the most diverse at the skirt tip, where the difference in excess PP between the numerical model and lab tests was $\sim$1kPa. Excess PP values measured during the lab tests were higher than values calculated numerically. Numerical simulations assumed a steady flow condition. Suction installation of a bucket foundation is generally assumed to be stationary, but seepage flow

around the bucket tip does not have time to develop fully because the tip is constantly penetrating into the soil. Therefore, the flow behavior around the tip might be unsteady, which can explain why the numerical results of excess PP differed from measured results at the tip.

A new formulation for PP factor (ratio of excess PP at the skirt tip to the applied suction) was derived based on data extracted from numerical simulations by curve fitting (eq.(B.15)).

$$\alpha = 0.47 - 0.25\left[1 - \exp\left(-\frac{h}{0.32D}\right)\right] \tag{B.15}$$

As the boundary conditions and hydraulic conductivity for the inner plug ($k_{out}/k_{in} \sim 1.4$) were different, this new formulation differed slightly from the one given in Koteras et al. (2016), resulting in greater excess PP at the skirt tip, a difference that increased with increasing penetration depth. Figure B.14 presents the new formulation of the PP factor as a function of penetration ratio (h/D) compared to the previous expression from Koteras et al. (2016), together with experimentally measured values from all suction installation tests.

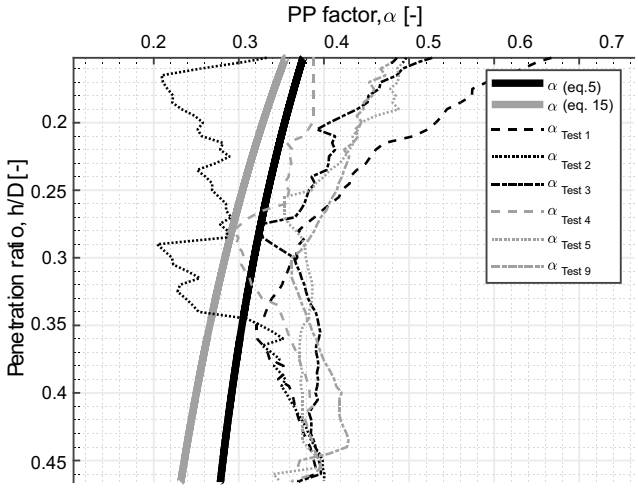

Fig. B.14: Comparison between numerical and lab tests of pressure factor at the tip.

The numerical expression underestimated excess PP measured around the tip. Interestingly, the trend for the PP factor is different from the trends in the literature. All studies presented in the "Calculation methods"subsection assumed a constant increase in excess PP with penetration; in contrast, the lab results here clearly stabilized to a constant value at around h/D = 0.3.

However, as the data here were limited to h/D<0.5, this trend should be investigated for higher penetration ratios. The change in bucket self-weight did not affect the PP factor, with results of tests using a self-weight of 4kN or 2kN being comparable.

Although the critical suction limits given in the previous literature were exceeded in the lab tests, piping failure was not observed. The critical condition for stationary flow arises when the critical gradient is developed ($i = i_{crit}$). It is important to consider γ', as a higher value will allow for more suction before the critical gradient is reached. Nevertheless, CPT results indicated that the sand loosened during installation, leading to a small drop in effective soil unit weight. However, plug loosening changes the void ratio and, thus, the hydraulic conductivity of soil. Seepage flow becomes less limited, and the hydraulic gradient drops due to the loss in hydraulic head.

A new formulation for critical suction pressure was derived based on the numerical results, using appropriate boundary conditions and increased plug hydraulic conductivity. The value of the exit flow velocity, v_{exit}, was determined from the model results. Using Darcy's law, the gradient was calculated as the ratio between the flow velocity and hydraulic conductivity. The critical pressure for the exit hydraulic gradient was calculated. The expression for normalized critical pressure was derived by curve fitting (eq.(B.16)). Figure B.15 presents results of the numerical simulations with eq.(B.16) and eq.(B.17) (using k_{ratio} = 1.4). Houlsby and Byrne (2005) developed eq.(B.17) as a solution for critical suction pressure, accounting for the increase in inner plug hydraulic conductivity (α in eq.(B.3)).

$$\frac{p_{crit}}{\gamma' D} = 1.32 \left(\frac{h}{D}\right)^{0.44} \tag{B.16}$$

$$\frac{p_{crit}}{\gamma' D} = \left(\frac{h}{D}\right) \left(1 + \frac{\alpha k_{ratio}}{1-\alpha}\right) \tag{B.17}$$

As shown in Fig. B.15, the new formulation fit the lab data better, as the critical pressure was not exceeded for any suction installation test. Hydraulic conductivity increased inside the soil plug and, therefore, more suction could be applied without piping. The same trend could very likely be applied in full-scale tests, although this possibility requires confirmation. Equation (B.17) by Houlsby and Byrne (2005) did not give a good approximation for critical suction, even with k_{ratio} = 1.4, as the theoretical critical pressure was significantly exceeded by lab data. The ratio of 1.4 is similar to the average kin/kout ratio of 1.5 (range: 1–2) reported by Tran et al. (2005), who used centrifuge tests during bucket foundation installation and showed that relative soil density drops and sand loosens with increasing penetration.

Finally, calculation of the exit hydraulic gradient from the lab tests (Fig. B.11) indicated that the normalized critical pressure can be approximately 2

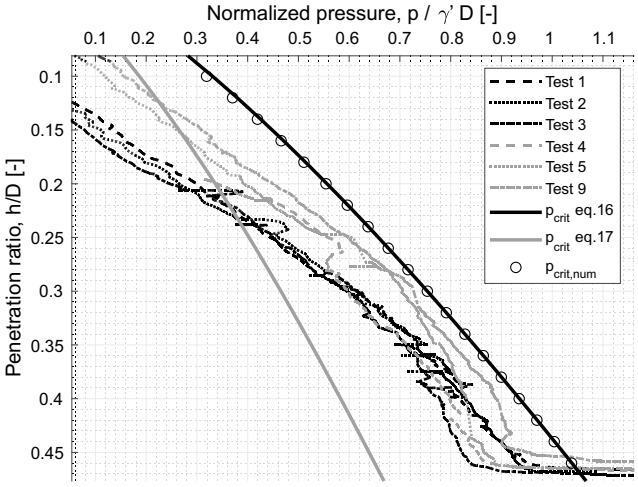

Fig. B.15: Normalized suction pressure results from installation tests with normalized critical suction based on numerical simulations.

times larger than the limit given by numerical simulations and can be larger than the limit given by the new numerical expression (eq.(B.16)). These results must be confirmed by additional tests with longer penetration depths and by full-scale models. Nevertheless, such an increase in the critical suction limit would allow for the installation of large-diameter bucket foundations, which would markedly reduce costs for offshore foundations.

B.7 Conclusions

Soil-skirt interactions during suction and jacking installations of a bucket foundation were analyzed by performing 10 medium-scale tests in dense sand. Soil resistance was significantly lower during suction than during jacking installation; this reduced soil resistance was confirmed by measurements of soil conditions before and after each installation through CPTs. Calculated relative soil density was decreased for soil inside the plug, but soil changes outside the bucket were negligible. These results confirmed the proposed assumptions for the calculation of SPR during suction installation. Whereas the inside friction and tip resistance were reduced by the applied suction, the possible increase on the outside friction can be neglected.

Excess PP values measured around the bucket skirt during suction installation confirmed the appearance of seepage flow that generally reduced SPR. Analysis of gradient development during installation was helpful in the as-

sessment of the redistribution of effective stresses and, thus, changes in SPR. Experimental and numerical results were comparable, thus validating the finite-element model and its assumptions. These findings allow for better understanding of the critical suction limits and piping. Sand loosening within the inside plug results in an increase of hydraulic conductivity. Increased hydraulic conductivity increases this limit for pressure, which is beneficial for suction installation, allowing deeper penetration and the installation of larger buckets. Finally, soil heave developed in dense sand in all suction installation tests, with a heave height of ≈10% of the total skirt length. The inside soil heave must be included in the design, as it can decrease the total stiffness of the foundation.

Acknowledgements

This research was funded by "EUDP Project"and by EU7 as a part of the Project "INNWIND - Innovative Wind Conversion Systems (10-20 MW) for Offshore Applications". The support is greatly appreciated.

REFERENCES

Allersma, H.G., Plenevaux, F., and Wintgens, J. 2003. Centrifuge research on suction piles: installation and bearing capacity. In Proceedings of BGA International Conference on Foundations: Innovations, observations, design and practice, Dunndee, UK, pp. 91-98.

Andersen, K. H., Jostad, H. P., and Dyvik, R. 2008. Penetration Resistance of Offshore Skirted Foundations and Anchors in Dense Sand. Journal of Geotechnical and Geoenvironmental Engineering, 134(1): 106-116.

API. 2014. Recommended practice for planning, designing and constructing fixed offshore platforms – Working stress design. American Petroleum Institute: Recommended practise 2A-WSD, Washington, D.C., 22nd Edition.

Bye, A., Erbrich, C.T., Rognlier, B., and Tjelta, T.I. 1995. Geotechnical design of bucket foundations. In Proceedings of 27th Annual Offshore Technical Conference, Houston, Texas, OTC 7793: 869-883.

Chen, F., Lian, J., Wang, H., Liu, F., Wang, H., and Zhao, Y. 2016. Large-scale experimental investigation of the installation of suction caissons in silt sand. Journal of Applied Ocean Research, 60: 109-120.

DNV. 1992. Foundations, classification notes No. 30.4. Det Norske Veritas, Høvik, Norway, 134th Edition. Erbrich, C., and Tjelta, T. 1999. Installation of bucket foundations and suction caissons in sand – Geotechnical perfor-

mance. In Proceedings of 31st Annual Offshore Technical Conference, Houston, Texas, OTC 10990(1): 725-736.

Harireche, O., Mehravar, M., and Alani, A. 2014. Soil condition and bounds to suction during the installation of caisson foundations in sand. Journal of Ocean Enineering, 88: 164-173.

Hogervorst, J.R. 1980. Field trials with large diameter suction piles. . In Proceedings of 12th Annual Offshore Technical Conference, Houston, Texas, OTC 3817: 217-22.

Houlsby, G. T., and Byrne, B. W. 2005. Design procedure for installation of suction caissons in sand. Journal of Geotechnical Engineering, 158(3): 135-144.

Ibsen, L. B. 2008. Implementation of a new foundations concept for offshore wind farms. In Proceedings of Nordisk Geoteknikermøte Nr. 15: NGM 2008, Sandefjord, Norway, pp. 19-33.

Ibsen, L.B., and Brødker, L. 1994. Baskarp Sand no. 15: data report 9301. Data Report 9401. Aalborg University, Aalborg.

Ibsen, L. B., and Thilsted, C. 2011. Numerical Study of Piping Limits for Suction Installation of Offshore Skirted Foundations and Anchors in Layered Sand. In Proceedings of International Symposium on Frontiers in Offshore Geotechnics (ISFOG), Perth, Australia, pp. 421-426.

Ibsen, L. B., Hanson, M., Hjort, T., and Thaarup, M. 2009. MC-Parameter Calibration of Baskarp Sand No. 15. DCE Technical Report, No. 62, Aalborg University, Denmark.

Koteras, A. K. 2017. Set-up and Test Procedure for Suction Installation and Uninstallation of Bucket Foundation. DCE Technical Memorandum, No. 63, Aalborg University, Denmark.

Koteras, A. K., Ibsen, L. B., and Clausen, J. 2016. Seepage Study for Suction Installation of Bucket Foundation in Different Soil Combinations. In Proceedings of 26th International Ocean and Polar Engineering Conference, Rhodos, Greece, 26 June-2 July, pp. 697-704.

Lehane, B., Schneider, J., and Xu, X. 2005. The UWA-05 method for prediction of axial capacity of driven piles in sand. In Proceedings of International Symposium on Frontiers in Offshore Geotechnics (ISFOG), Perth, Australia, pp. 19-21.

Lian, J., Chen, F., and Wang, H. 2004. Laboratory tests on soil-skirt interaction and penetration resistance of suction caissons during installation in sand. Journal of Ocean Engineering, 84: 1-13.

Senders, M., and Randolph, M. F. 2009. CPT-based method for the installation of suction caissons in sand. Journal of Geotechnical and Geoenviron-

mental Engineering, 135(1): 14-25.

Sjelmo, A. 2012. Soil-Structure Interaction in Cohesionless Soils during Monotonic Loading. Student thesis: Master thesis, Aalborg University, Denmark.

Appendix C

Reduction in Soil Penetration Resistance for Suction-assisted Installation of Bucket Foundation in Sand

Aleksandra Katarzyna Koteras
Lars Bo Ibsen

The paper has been published in
Proceedings of the 9th International Conference on Physical Modelling in Geotechnics (ICPMG) Vol. 1, CRS Press/Balkema pp. 623–628, 2018.
(the final draft version included in the thesis)

The layout has been revised.

Abstract

Bucket foundation is recently consider as a cost-effective solution for offshore wind turbines. However, the concept requires still a better understanding and a full design method that can be approved by standards. 1G laboratory tests for the installation of medium-scale bucket foundation have been performed in the laboratory of Aalborg University, Denmark. The main purpose of those tests is to investigate the interaction between the soil and the bucket skirt during the jacking and the suction installation process. The most often proposed method for the penetration resistance during installation of bucket foundation is a CPT-based method. The calculation requires information about empirical coefficients k_p and k_f, relating the skirt tip resistance and the skirt friction to the cone resistance measured during Cone Penetration Test, CPT. What is more, the suction-assisted installation in permeable soil adds additional parameters into the design resulting from the induced seepage flow around the bucket skirt. β-parameters introduced into the design describe a reduction in soil penetration resistance due to this flow. As an effect of tests results analysis, empirical coefficients and β-parameters are proposed. The use of those values leads to a reasonable fit between the applied force and the calculated soil resistance based on CPT, therefore, brings closer to the full design method for the suction installation of bucket foundation.

C.1 INTRODUCTION AND BACKGROUND

C.1.1 Motivation

The growth in the offshore wind energy market results in a large demand for more innovative and cost-effective solutions. As the foundation constitutes 20-30% of the total wind turbine budget, the cost-cuts found in the design of these sub-structures seems to be a way to go. Such a solution can be seen in the suction mono-bucket that has been proven to be feasible for challenging offshore conditions in oil and gas industry (Hogervorst 1980),(Tjelta 1995), (Bye et al. 1995). It is seen as a considerable cheap solution due to a simplicity in the geometry and a suction-assisted installation, which moves aside the requirements for heavy and expensive drilling equipment. Throughout the past few years the suction foundations have been successfully used also in the wind energy industry (Ibsen 2008).

C.1.2 Concept of suction bucket foundation

A bucket foundation is a skirted structure that consists of a skirt penetrated into the soil, closed with a lid element. The installation in frictional soils is

Fig. C.1: Laboratory installation test of a bucket model

accomplished in two stages. The first part is a self-weight penetration and the second part is achieved by pumping out the water from the cavity under the bucket lid. The first part is performed in order to ensure an appropriate hydraulic seal between the bucket skirt and the soil. The seal is required in order to achieve a suction pressure under the bucket lid. The second part of the installation is called a suction installation. For cohesive soil the available pump capacity is sufficient, as the penetration resistance is considerable low. Nevertheless, the installation is also possible for sandy soils. The initially high resistance is significantly reduced by the suction process. As an effect of applied suction under the bucket lid, a seepage flow is induced around the bucket skirt. This results in the inevitable gradients in the soil surrounding the skirt. The expectation for the flow is that it progress upward for the inside soil plug and downward in the soil outside of the skirt. The upward hydraulic gradient decreases the soil penetration resistance, whereas the downward gradient might give some increase. The significant decrease of resistance takes place also under the skirt tip due to a sudden change of the gradients. Studies confirm that a total penetration resistance of sand is substantially reduced and the increase of the resistance on the outside wall can be neglected (Lian et al. 2004),(Chen et al. 2016).

C.1.3 Effort of presented work

The knowledge about the suction installation of bucket foundation based on the recent research is still insufficient. There are no reliable standards that include all aspects of the installation. Therefore, a campaign of 10 laboratory tests for installation of medium-scale model of bucket foundation is conducted. A jacking installation tests and a suction installation tests are

performed in order to derive coefficients and factors required for the design. A laboratory set-up during the jacking installation test is presented in Figure C.1.

C.2 METHODOLOGY

C.2.1 1-g modeling

Installation tests at 1-g have been performed in the laboratory of Aalborg University, Denmark. There are two groups of tests performed in dense sand. First group includes the jacking installed bucket (test no. 06, 07, 08 and 10) and in the second group, the bucket model is installed with the assistance of suction (test no. 01, 02, 03, 04, 05 and 09). Two different installation manners are conducted to prove the significant reduction in the soil resistance due to the seepage flow. What is more, from the jacking installation tests, the empirical coefficients k_p and k_f can be derived. Suggested values of those coefficients are next used when analyzing the suction installation tests. From those tests the β-factors can be found. All parameters can be introduced into the design method for the soil penetration resistance of suction-assisted installation of bucket foundation.

Following subsections describe shortly the model and the procedure. More detailed report about the installation tests is given by Koteras (2017).

C.2.1.1 Bucket foundation model

The dimensions of bucket foundation and attached elements are presented in Figure C.2. The skirt thickness is 3 mm. This model is in scale 1 : 10 of a prototype size. The model is made of steel and the self-weight is equal to 201 kg. The bucket lid is equipped with 4 intake valves (1), 6 pressure transducers (2) and 1 displacement transducer (3). Measurements of pore pressure are taken from 6 different localizations on the skirt (PP1-PP6).

C.2.1.2 Soil preparation

A sand box of a 2.5m diameter and a height of 1.7m is equipped with a drainage system for a saturation. The sand box is filled with gravel til the height of 0.3m, and next with sand til the height of 1.5m. The properties of the sand are given in Table E.1. Before each of the tests the soil is fully saturated and prepared for a dense, uniform condition with a mean value of a relative density, I_D, equal 89.73 (the standard deviation: $\sigma = 1,02$). The preparation includes: first, a loosening of soil by application of a hydraulic gradient and next, a mechanical vibration. The sand condition is analyzed by cone penetration test, CPT. A cone of the device has a 15mm diameter and it

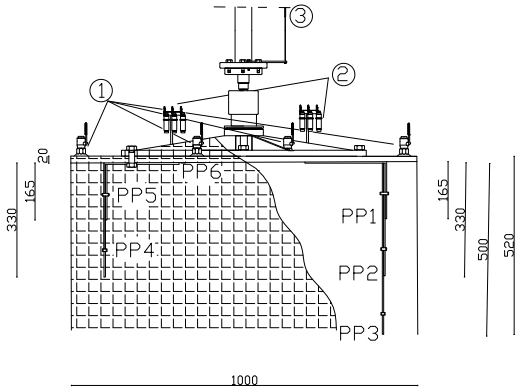

Fig. C.2: Model of bucket foundation

is with a 30° inclination. This test is performed before each installation and straight after each installation. The comparison allow for assessing whether the soil penetration resistance is reduced due to the installation manner.

Table C.1: Soil properties

$e_{\max}$	$e_{\min}$	d_{50}	C_u	d_s
[−]	[−]	[−]	mm	g/cm^3
0.854	0.549	0.14	1.78	2.64

C.2.1.3 Test procedure

The jacking installation is executed with a hydraulic piston as a displacement controlled operation. Open valves at the bucket lid ensure that the excess pore pressure of soil inside the bucket is not accumulated. Therefore, the soil penetration resistance is assessed to be at its initial, unreduced value. The measurements of the penetration depth, h, and the installation load, F_{install}, are monitored during the installation. Additionally, the pore pressure of soil around the bucket skirt and under the bucket lid are measured.

The suction installation includes two stages as mentioned before. The self-weight installation is induced by the hydraulic piston working as a force controlled. The force of a magnitude equal to the self-weight of the model is applied. When the hydraulic seal is realized, the suction pressure is applied by a vacuum system through the valves attached to the bucket lid. The measurements of the penetration depth, the applied suction, u, and the pore pressure around the soil skirt are monitored during the installation.

Both installations are performed in saturated soil condition, with a water level situated around 10cm above the soil level.

C.2.2 CPT-based method

Fairly simple design based on CPT is described by DNV (1992), where a soil penetration resistance of thin skirt structures, R_{soil}, is proposed. Both, the tip resistance of the skirt, Q_{tip}, and the friction on the inside and outside wall, F_{in} and F_{out}, are related to the cone resistance, q_c, through the empirical coefficients k_p and k_f, see Equation (C.1). The range of parameters is proposed for Sand and Clay in North Sea conditions. The proposal is based on the in-situ testing supported by the laboratory results, see Table C.2. The method, even though it is often used, does not include the reduction in resistance due to applied suction and generated flow through the soil. A_{tip} is an area of the bucket skirt.

$$R_{\text{soil}} = F_{\text{in}} + F_{\text{out}} + Q_{\text{tip}} \tag{C.1}$$

where

$$F_{\text{in}} = \pi D_i k_f \int_0^h q_c(h)dh \tag{C.2}$$

$$F_{\text{out}} = \pi D_o k_f \int_0^h q_c(h)dh \tag{C.3}$$

$$Q_{\text{tip}} = A_{\text{tip}} k_p q_c(h) \tag{C.4}$$

Table C.2: Recommended values of k_p and k_f from DNV

Empirical coefficients	Lowest expected	Highest expected
k_p	0.3	0.6
k_f	0.001	0.003

Empirical coefficients relating the cone resistance to the soil penetration resistance have been studied by others as well. One example is given by Lehane et al. (2005). The solution proposed is for an open-ended pile and it emerged from the real installation data. The open-ended pile in its construction and installation method is similar to the bucket concept and therefore, this case is cited in the article. The solution is based on the difference between inside and outside diameter, D_i and D_o, of the foundation, see Equation (C.5). Value of C is estimated here as 0.021 and the interface friction angle, δ, lies around 30°. Given a typical bucket foundation with $\left(\frac{D_i}{D_o}\right) = 0.98$, the value

of k_f would be above the values proposed in (DNV 1992).

$$k_f = C\left[1 - \left(\frac{D_i}{D_o}\right)^{0.2}\right]^{0.3} \tan\delta \tag{C.5}$$

Later on Senders & Randolph (2009) proposed the solution for the soil penetration resistance of suction bucket foundation based on CPT. The approach is similar to the solution proposed by DNV (1992), but the method includes the reduction in resistance due to the applied suction and the induced seepage flow. The inside friction and the tip resistance is linearly reduced from its maximum value when suction is not applied yet, to zero when the suction reaches its critical value (the critical suction is explained in the following section). For the analysis of centrifuge tests, coefficient k_f is chosen to be based on (Lehane et al. 2005), however, the value of C is adjusted in order to give values of k_f in the range of DNV values. In the research of Senders & Randolph (2009), the value $C = 0.012$ is chosen. Coefficient k_p is chosen to be equal 0.2 to represents a very dense sand condition. A very good agreement between the calculated soil resistance and the measurements of the jacking installations are obtained. Andersen et al. (2008) have described the results of laboratory, prototype and field tests. For laboratory tests the bucket with $D = 0.557$m, $h = 0.32$m was penetrated into the soil situated in the tank of $D = 1.6$m. Conditions are closed to the test conditions described in this paper. The proposed values of k_f for laboratory tests was back-calculated to be 0.0053.

The results obtained in this research are analyzed with the CPT-based method, however, a different approach is used when including the effects of seepage flow. β-parameters are used instead of a linear change proposed by Senders & Randolph (2009), see following equations.

$$F_{\text{in}} = \beta_{\text{in}} \pi D_i k_f \int_0^h q_c(h)dh \tag{C.6}$$

$$F_{\text{out}} = \beta_{\text{out}} \pi D_o k_f \int_0^h q_c(h)dh \tag{C.7}$$

$$Q_{\text{tip}} = \beta_{\text{tip}} A_{\text{tip}} k_p q_c(h) \tag{C.8}$$

Proposal for β-factors is given later on in the article.

C.2.3 Importance of the numerical analysis

The failure of the installation can happen due to the excessive applied pressure under the bucket lid. The limit gives the pressure that creates a piping channels between the bucket skirt and the soil trapped inside. In such a state, the hydraulic seal is broken and the suction process cannot proceed. Therefore, the critical value should be taken into the design. What is more, the

value of critical pressure, u_{crit}, is also used for the calculations of the soil resistance against the installation. The suction initiates the loosening process for the soil and, thus, changes the resistance. As the suction pressure approaches the critical value, soil resistance drops from its maximum value to zero.

An approach based on this theory is presented by Houlsby & Byrne (2005) where the soil resistance is reduced according to the hydraulic gradients appearing in the soil. The gradients describe the changes in water pressure inside the soil, which is closely related to the applied pressure. Similarly, the same approach is given in (Senders & Randolph 2009) where the soil resistance drops linearly to zero while the applied pressure approaches its critical value.

The critical pressure against the piping is studies numerically (Erbrich & Tjelta 1999), (Senders & Randolph 2009), (Ibsen & Thilsted 2011), (Koteras et al. 2016). The most often proposed method is to relate the critical pressure to the seepage length, s, based on the definition of the critical gradient, see Equations (C.9) and (C.10). The exit hydraulic gradient, i_{exit} is obtained from the numerical simulations.

$$s = \frac{u}{i_{\text{exit}} \cdot \gamma_w} \tag{C.9}$$

$$u_{\text{crit}} = \left(\frac{h}{D}\right) \cdot \left(\frac{s}{h}\right) \cdot \gamma' \cdot D \tag{C.10}$$

Different proposition of $\left(\frac{s}{h}\right)$ can be found in the latest state of art, and all of the solutions are characterized with similar values for varying $\left(\frac{h}{D}\right)$. Interestingly, critical pressure calculated based on those values is exceeded in all of the tests in the campaign, and in none of them the installation failure was observed.

C.3 RESULTS AND DISCUSSION

C.3.1 Empirical coefficients from jacking installation

There are 4 jacking installation tests included in the analysis of the empirical coefficients. For each of those tests, the soil penetration resistance is calculated based on CPT results and then, it is related to the jacking installation force. The soil penetration resistance is calculated with Equation (C.1). It can only be solved when one from two of the empirical coefficients is chosen before the calculations. Value of k_f is assumed to be the same for both, the inside and the outside friction. Based on the previous research, the values of k_f are chosen. The values of k_p are derived by fitting the results of installation

to the results of soil resistance from the CPT. The chosen values of k_f are as following:

- $k_f = 0.004$ based on (Lehane et al. 2005),
- $k_f = 0.0023$ based on (Senders & Randolph 2009) and
- $k_f = 0.0053$ based on (Andersen et al. 2008).

The optimization is done for all 3 values of k_f in 4 jacking installation tests. The coefficient of determination, R^2, is found for each case. The choice is made based on this coefficient, see Table C.3. As seen in the table, the best fit is obtained with $k_f = 0.0023$. The obtained values of k_p are in the range proposed by DNV (1992) - 0.3 to 0.6 for installation in sand.

Table C.3: Chosen values of empirical coefficients k_f and k_p

Test no.	k_f	k_p	R^2
06	0.023	0.38	0.991
07	0.023	0.36	0.998
08	0.023	0.39	0.998
10	0.023	0.33	0.994

As an example, the results of installation load and calculated soil resistance based on CPT are presented in Figure C.3 for test no. 06. The figure presents resistance calculated with 3 different values of k_f.

C.3.2 Critical pressure against piping

The solution for the normalized seepage length, $\left(\frac{s}{h}\right)$, is based on the numerical analysis presented by Koteras et al. (2016). However, the dimensions in the numerical model are adjusted, because it was realized that there are some boundaries effects on the development of the seepage flow. The excess pore pressure at the boundary of sand box has been measured during the installation in each test. Results show considerable values of the excess pore pressure at the boundary. Therefore, the numerical model used for this paper is of the same characteristics as the laboratory model, what includes the correct diameter of the bucket model and also the boundary conditions. The results of the applied suction in each test were compared with the calculated critical pressure and it was found that the critical pressure is exceeded in each of the suction installation tests. Nevertheless, there were no piping problem observed, which suggests that the chosen solution for the seepage length is not appropriate.

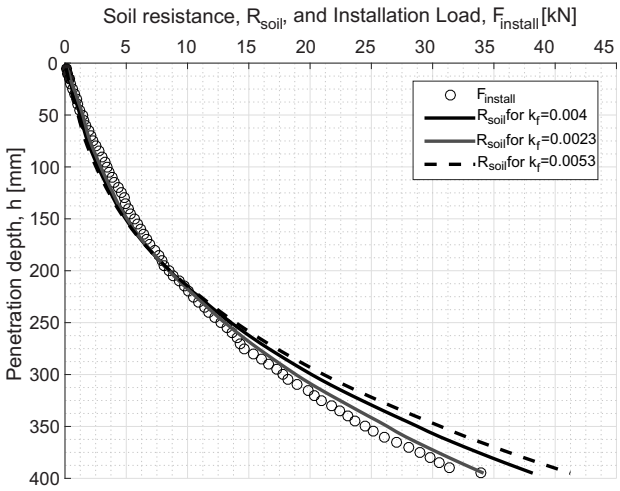

Fig. C.3: Soil resistance compared with installation load

Due to the observation of laboratory results the permeability of the soil inside the bucket has been increased. The results of CPT performed before and after the installation reveal the significant decrease in the relative soil density, I_D. As the soil becomes looser inside, the permeability of the soil increases. Appropriate values of the hydraulic conductivity, k, were applied for the inside and the outside soil elements of the numerical model before executing the simulations. Proposed solution for exit normalized seepage length from the numerical model that includes the increased value of k is given below.

$$\left(\frac{s}{h}\right)_{\text{exit}} = 1.25 \cdot \left(\pi - \arctan\left(2.5 \cdot \left(\frac{h}{D}\right)^{0.74}\right)\right)\left(2 - \frac{1.8}{\pi}\right) \tag{C.11}$$

With the proposed solution, the applied pressure in each test does not exceed the critical value, see Figure C.4

C.3.3 β-factors from the suction installation

The soil resistance for the suction installation is calculated by summing the inside and outside friction on the skirt and the tip resistance based on Equations (C.6), (C.7) and (C.8). The empirical coefficients are chosen based on the jacking installation tests as a value of 0.023 for k_f and a range of values between 0.33 to 0.39 for k_p. The proposed method includes different values

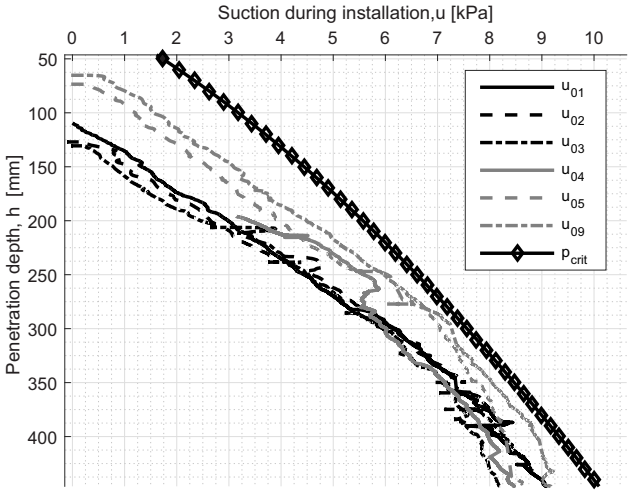

Fig. C.4: Applied pressure during suction installation tests

of β-factors for each separate part of the total soil resistance.

$$\beta_{\text{in}} = 1 - r_{\text{in}} \cdot \exp\left(\frac{u}{u_{\text{crit}}}\right) \tag{C.12}$$

$$\beta_{\text{tip}} = 1 - r_{\text{tip}} \cdot \exp\left(\frac{u}{u_{\text{crit}}}\right) \tag{C.13}$$

$$\beta_{\text{out}} = 1 \tag{C.14}$$

Unknowns r_{in} and r_{out} are found for the minimum and the maximum value of k_p coefficient by non-linear least squares fitting. They are found as constants, see Table C.4. The coefficients of determination given in table prove that the fitting process gave a fairly good estimation of the reduced soil penetration resistance for the bucket foundation. Moreover, the value of r_{tip} is closer to value 0.1 for $k_p = 0.33$, and closer to value 0.2 for $k_p = 0.39$. As an example, the installation load calculated from the applied suction and the reduced soil penetration resistance is presented in Figure C.5 for test no. 01.

C.4 SUMMARY AND FURTHER WORK

The suction bucket foundation has lately become a beneficial solution in the offshore wind market. However, a design method for the installation leaves a lot to be desired. First and foremost, there is still no reliable way of including the reduction in soil penetration resistance due to the applied suction. To

Table C.4: Proposed constants for β-factors and coefficient of determination, R^2

Test no.	for $k_p = 0.33$			for $k_p = 0.39$		
	r_{in}	r_{tip}	R^2	r_{in}	r_{tip}	R^2
01	1	0.11	0.97	1	0.16	0.95
02	1	0.14	0.85	1	0.19	0.74
03	1	0.15	0.78	1	0.19	0.72
04	1	0.15	0.89	1	0.19	0.90
05	1	0.1	0.88	1	0.14	0.89
09	1	0.09	0.86	1	0.13	0.88

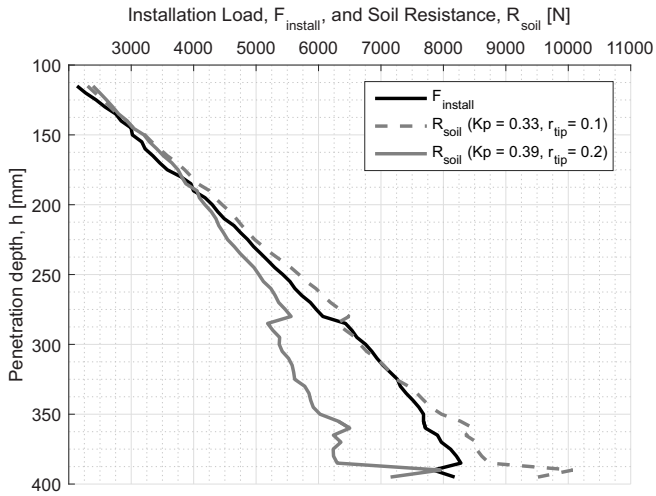

Fig. C.5: Soil resistance with proposed β-factors

improve the method, installation tests of bucket foundation have been performed at the laboratory facility on a medium scale model. The method used in the analysis is a CPT-based method, where a cone resistance is related to the soil penetration resistance by empirical coefficient. Even though, values of those coefficients can be found in literature, they vary between different sources. From the results of jacking installation, values of $k_f = 0.0023$ and $k_p = 0.33 - 0.39$ are proposed. From the results of suction installation, β-factors are proposed. β-factors cover the reduction of soil resistance due to the seepage flow, where the soil resistance is reduced as an exponential function of the ratio u/u_{crit}. Finally, calculated soil resistance is compared with the load applied during installation, and a reasonable fit is obtained.

Nevertheless, the tests results covers only medium scale testing. It is

strongly advised that the proposed method is used on a prototype models and on the full-scale foundation. Then, and only then, the method can be considered as reliable.

ACKNOWLEDGMENT

The research described in this paper is a part of a PhD Study funded by "EUDP Project" and by EU7 as a part of the "INNWIND - Innovative Wind Conversion Systems (19-20MW) for Offshore Applications" project. The support is greatly appreciated.

REFERENCES

Andersen, K.H., Jostad, H.P., & Dyvik, R. (2008). Penetration resistance of offshore skirted foundations and anchors in dense sand. *J. Geotech. and Geoenv. Eng. 134(1)*, 106–116.

Bye, A., C. Erbrich, B. Rognlien, & T. Tjelta (1995). Geotechnical design of bucket foundations.*In Proc., Offshore Technology Conference*, Houston, Texas. OTC 7793.

Chen, F., J. Lian, H. Wang, F. Liu, H. Wang, & Y. Zhao (2016). Large-scale experimental investigation of the installation of suction caissons in silt sand.*J. Applied Ocean Research 60*, 109–120.

DNV (1992). *Foundations, classification notes No. 30.4 (134 ed.)*. Hvik, Norway: Det Norske Veritas.

Erbrich, C. & T. Tjelta (1999). Installation of bucket foundations and suction caissons in sand geotechnical performance. *In Proc., 31st Annual Offshore Tech. Conf.*, Volume 1, Houston, Texas, pp. 725–736.

Hogevorst, J. (1980). Field trials with large diameter suction piles. *In Proc., Offshore Technology Conference*, Houston, Texas. OTC 3817.

Houlsby, G. & B. Byrne (2005). Design procedure for installation of suction caissons in sand. *In Proc., Institution of Civil Engineers*, Volume 158, pp. 135–144. Geotech. Eng.

Ibsen, L. (2008). Implementation of a new foundations concept for offshore wind farms.*In Proc., Nordisk Geoteknikermte Nr. 15: NGM 2008*, Sandefjord, Norway, pp. 19–33. Norsk Geoteknisk Forening.

Ibsen, L. & C. Thilsted (2011). Numerical study of piping limits for suction installation of offshore skirted foundations and anchors in layered sand.*In Proc., Int. Symp. on Frontiers in Offshore Geotechnics (ISFOG)*, Perth, Australia,

pp. 421–426.

Koteras, A., L. Ibsen, & J. Clausen (2016). Seepage study for suction installation of bucket foundation in different soil combinations.*In Proc., 26th Int. Ocean and Polar Eng. Conf.*, 26 June-2 July, Rhodos, Greece, pp. 697–704. Int. Society of Offshore and Polar Engineers.

Koteras, A. K. (2017). Set-up and test procedure for suction installation and uninstallation of bucket foundation. DCE technical report, Department of Civil Engineering, Aalborg Univ., Denmark.

Lehane, B., J. Schneider, & X. Xu (2005). The uwa-05 method for prediction of axial capacity of driven piles in sand.*In Proc., Int. Symp. on Frontiers in Offshore Geotechnics (ISFOG)*, Perth, Australia, pp. 19–21

Lian, J., F. Chen, & H. Wang (2004). Laboratory tests on soil skirt interaction and penetration resistance of suction caissons during installation in sand. *J. Ocean Eng. 84*, 1–13.

Senders, M. & M. Randolph (2009). Cpt-based method for the installation of suction caissons in sand.*J. Geotech. and Geoenv. Eng. 135(1)*, 14–25.

Tjelta, T. (1995). Geotechnical experience from the installation of the europipe jacket with bucket foundations.*In Proc., Offshore Technology Conference*, Houston, Texas. OTC 7795.

Appendix C.

Appendix D

Large scale installation testing of modular suction bucket

Aleksandra Katarzyna Koteras
Lasr Bo Ibsen

The paper is submitted to the journal *Géotechnique*.
(the manuscript sent for approval)

The layout has been revised.

Abstract

The paper show an investigation of the modular bucket foundation that has been developed as a new design concept for the large offshore wind turbines. This concept is more cost-effective than a regular round bucket and more resistant to the buckling failure during the installation. The paper results covers the jacking installation tests and the suction installation tests on the laboratory large-scale models, where the behavior of the round bucket is compared to the behavior of the modular bucket. The tests have been performed in varying sand relative densities. There is no significant difference in the applied pressure during suction installation in different sand conditions despite the huge difference visible in the jacking installation tests.

KEY WORDS: suction; soil-structure interaction; sands; model tests; seepage; offshore engineering.

Appendix D.

Appendix E

Manual for laboratory testing

The layout has been revised.

E.1 Objectives

The appendix describes laboratory rigs, bucket foundation models, all equipment used during tests and explains procedures for jacking installation, suction installation and uninstallation tests. The appendix is based on technical memorandums published as manuals for laboratory work (Koteras 2017; Koteras 2019). Bucket foundation is installed in permeable soil that is prepared for specific conditions prior each test. The set-up allows for soil condition modification when it comes to sol density. Soil conditions are tested by performing cone penetration tests, CPTs. The main purpose of this appendix is to make the reader familiar with test procedure and enable one for a reproduction of experiment in different experimental location. Tests evaluate dependency of installation process on the geometry of foundation, different ratio of foundation skirt length to the diameter, L/D, different distance to the boundary, z_L, and different soil relative density, I_D. Research covers 2 test campaigns:

1. Tests performed in a 'Large Yellow Tank', located at the Department of Civil Engineering in Aalborg University in its old location (set-up 'a'),
2. Tests performed in an improved 'Extended Large Yellow Tank', moved to a new location of the department in 2017 (set-up 'b').

E.2 Safety instruction

Anybody working in the laboratory must follow the safety instruction.

- Read specifications and manuals for a specific set-up or equipment before starting any kind of work.
- Working in the lab is only allowed in safety shoes.
- When using the crane the operator and everyone in neighborhood must wear a safety helmet.
- In case of any doubts or if a problem occurs, always ask the technicians for help.

Specific instruction when working with a large soil tank:

- Use helmet with all works at height.
- Use safety belts connected to the loading frame with all works at height.
- Use helmet, vibration gloves, earmuffs, knee protection (optional) when vibrating. The vibration of 1 hour followed by 1 hour break/other work.

E.3 Set-up

The set-up main parts are as followed: a soil container, a loading frame, a hydraulic system for load application, a suction pump and a working deck around the top of soil container. There is a water access and a vacuum access from laboratory system. Measuring system includes a displacement transducer, a load cell, piezometers (pore pressure transducers) and total pressure cells (only in set-up 'b'). Set-up 'a' can be found in Paper B (fig. B.2) and set-up 'b' is shown in fig. E.1.

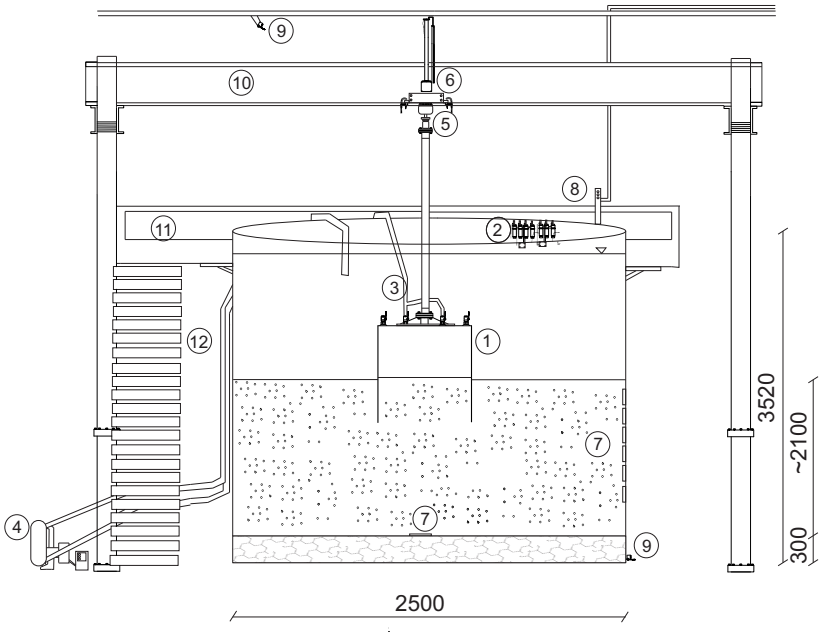

Fig. E.1: Set-up 'b': (1) Bucket model, (2) Pore pressure transducers, (3) Pipes for the suction application, (4) Suction pump, (5) Load cell on the loading piston, (6) Displacement transducer, (7) Stress sensors and pore pressure transducers, (8) Vacuum access point, (9) Water access points, (10) Loading frame, (11) Working platform around the soil container, (12) Access ladder (dimensions in mm) (Koteras 2019)

The steel soil container has been up-built in the set-up 'b'. Previously the height was 1.5m. Additional round cylinder of 2m height has been built up on the previous container, resulting in a total height of 3.5m. The container consists of a drainage system built from perforated pipes equally placed at the bottom, covered by the gravel layer and a geotextile membrane. Sand is filled on top of the gravel layer. Saturation of sand takes places through the

drainage system prior each test. The system has a water connection at the bottom of the container. For set-up 'b' water can access the soil container also from the top ((9) in fig. E.1). Water containers are situated higher than set-ups, so the appropriate hydraulic gradient can be achieved.

E.3.1 Soil properties

Table E.1: Soil properties of Aalborg Sand no.1 (Borup and Hedegaard 1995)

Soil property	Value	Unit
Specific grain size, d_s	2.64	$[-]$
Maximum void ratio, $e_{\max}$	0.854	$[-]$
Minimum void ratio, $e_{\min}$	0.549	$[-]$
50%-quatile, d_{50}	0.14	[mm]
Uniformity coefficient, C_u	1.78	$[-]$

E.3.2 Bucket foundation models

The bucket foundation model tested in set-up 'a' is a medium-scale model with skirt length to diameter ratio, L/D, equal to 0.5. Models tested in set-up 'b' are large-scale models with L/D ratio equal to 1. Outside diameter is 1m ($\sim$ 1 for modular bucket). The lid has a 20mm thickness and is equipped with 4 valves located at the center line. The skirt has 3mm thickness in round buckets and 1.7mm thickness in modular bucket. Each model is equipped with small channels situated at the inside and outside of skirt ending at a distance of 1/3, 2/3 and 3/3 of L. Channels are connected to the pressure transducers. One channel measures pore pressure directly below the lid which gives the records of applied suction. Pore pressure measurements points are referred as PP1-PP7. For the medium scale model there are only 6 measurements points (PP1-PP6) as there is only one channel at the end of the skirt from the inside.

The pore pressure transducers have been placed on the bucket lid in set-up 'a'. In the improved set-up, pore pressure transducers are moved to the top of soil container. Technical drawings of medium scale model (L/D=0.5) is shown in Paper B, fig. B.3, and the large scale models (L/D=1.0) in Paper D, fig. **??**. Figure E.2 shows all three models and fig. E.3 illustrates pore pressure measurement system for set-up 'b'

(a) (b) (c)

Fig. E.2: Models of bucket foundation: (a) round bucket, L/D=0.5, (b) round bucket, L/D=1.0 and (c) modular bucket, L/D=1.0

E.3.3 Hydraulic system

The model of bucket is connected to a hydraulic piston that can either be controlled by force or by displacement. A hydraulic pump is for a maximum pressure of 250bars and the pressure is regulated by the rate of force/displacement. The cylinder attached to the piston is also of 250bars maximum pressure, however, this cylinder is only displacement controlled. Including the safety factor, a value of around 180kN can be applied with the piston. Additional load cell is fixed to the cylinder in order to make a force controlled installation. The capacity of small load cell is only 20kN and must be removed for jacking installation tests. Appropriate control gains are set for two different types of tests (they should be adjusted before test campaign to give a smooth response of the piston during work).

E.3.4 Displacement transducer

The external displacement transducer is fixed to the loading frame (fixed with clamps in set-up 'a' and fixed permanently in set-up 'b'). It is connected to the top of the piston and measures its dislocation during test.

E.3.5 Suction application

A vacuum pump with manometer is used for suction application in test set-up 'a', see fig. E.4a. The pump is connected with small transparent pipes to the bucket lid through valves. The under pressure is controlled manually with a small valve on the pump. The vacuum pump is connected to the compressed air system in the laboratory. In set-up 'b' a LSM type suction pump is used, see fig. E.4b. Here, the applied suction is controlled with

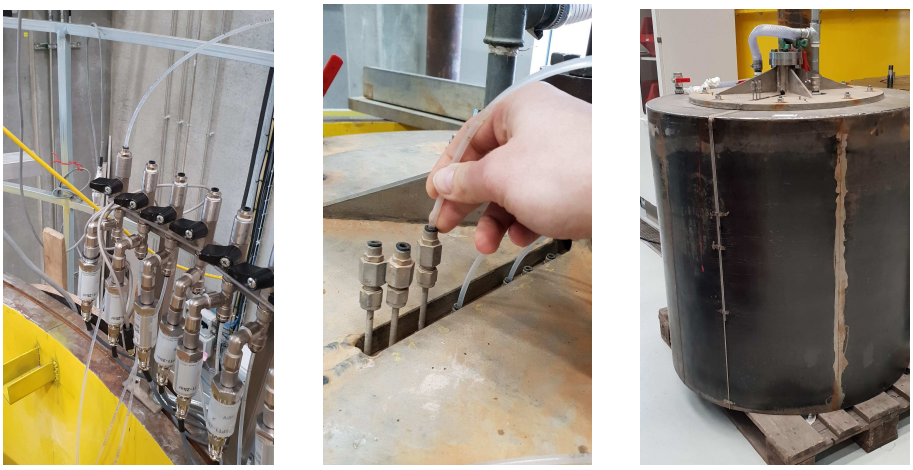

(a) (b) (c)

Fig. E.3: Pore pressure measurement system for set-up 'b': (a) connection on the soil tank, (b) connection on the bucket lid and (c) channels on the bucket skirt

water extraction per minute. The pump can work in both direction, pumping water in and out. Wider pipes with higher resistance to suction pressure are connected to the valves on the bucket lid.

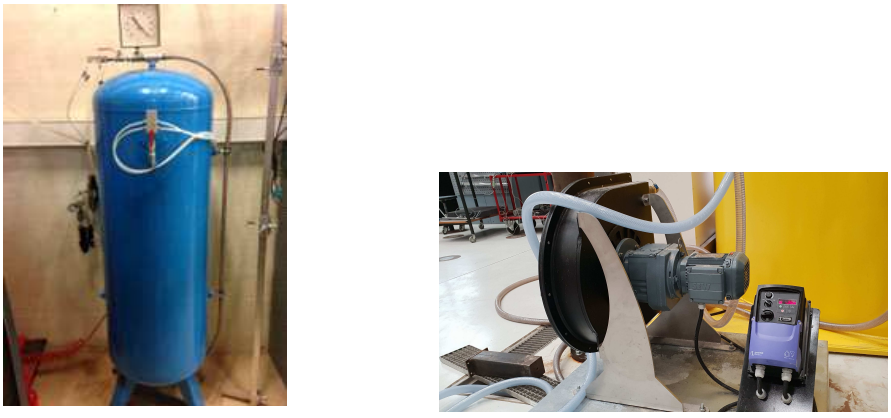

(a) (b)

Fig. E.4: Suction system: (a) vacuum pump from set-up 'a' and (b) suction pump from set-up 'b'

E.3.6 Piezometers and total pressure cells

The boundary conditions during installation tests are monitored. In set-up 'a' a special beam with piezometers is installed close to the side boundary.

Transducers on the beam are saturated before the beam is pushed into the soil. This means that the water is sucked from the bottom of small tubes until it reaches pore pressure transducers through small transparent plastic tubes. The beam is shown in Paper B (Fig. B.12). The reansducers connected to the beam measure the excess pore pressure during installation test at the side boundary. The beam is installed with hydraulic piston.

The procedure has been improved for set-up 'b'. Not only the height of soil container has been increased, but piezometers and pressure cells are fixed to the side boundary and placed at the bottom of sand layer, (7) in fig. E.1 and fig. **??** in Paper D. There are 8 piezometers and 8 total pressure cells in the soil container. Even though, the producer gives the sensitivity parameters of transducers and their initial set-ups, the calibration is recommended. Often the ranges must be adjusted for different conditions. The calibration procedure uses a reference transducer connected to a pressure mechanism. The calibrated transducer is connected to the system as well. While measuring equipment connected to the system shows a correct applied pressure, the measured pressure of calibrated transducer can be adjusted by setting a correct initial value and then corrected calibration factor.

E.3.7 CPT device

The CPT device is a mini model designed at Aalborg University. It has a cone diameter of 15mm and inclination of 30°. The length is adjusted to a given set-up, so the measurement range is a slightly bigger than L of bucket model. The resistance inside the cone is measured by 4 strain gauges coupled in a full-bridge. Cone penetration resistance, q_c, is related to the soil strength and stiffness parameters based on (Ibsen et al. 2009). Especially in set-up 'b' an appropriate piston extension is used to keep the cone of CPT close to the soil surface due to length limitation. The device is fixed to the bottom of the piston. The piston works as a displacement controlled with a rate of 5 mm/s CPT procedure is performed before and after each test in location given in fig. B.4 in Paper B. After installation, in case of set-up 'b', water is removed from the top of soil container until the level of water is approximately 5cm above the soil. This allows for CPT and also inspection of soil level inside and outside the bucket. A special side extension to CPT is used so even when the bucket is slightly rotated, CPT can still be performed through valves, see fig. E.5.

E.3.7.1 Calibration

Before each test campaign, CPT is calibrated. For a calibration, a special lathe device is used. The CPT is set in the device and a force is applied to the cone (there should be a small rubber block put on the cone for protection).

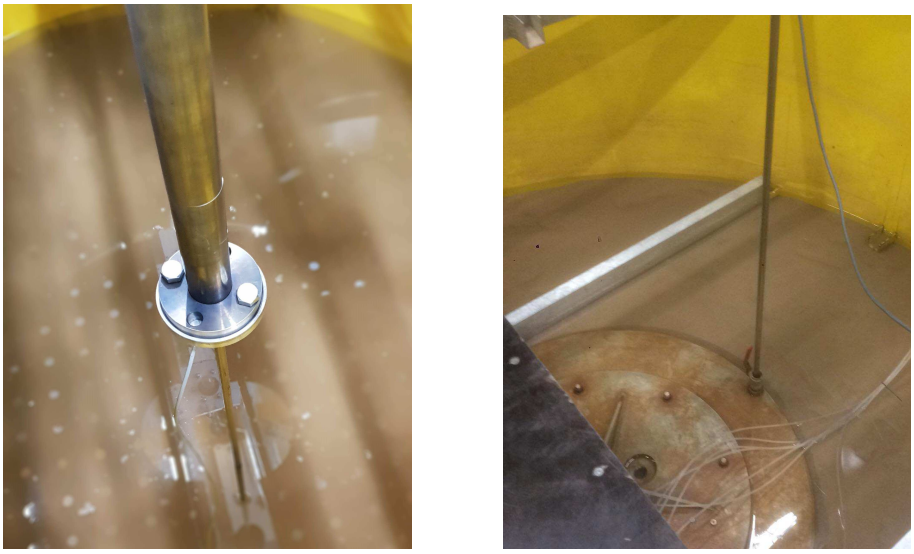

(a) (b)

Fig. E.5: (a) Performance of CPT before and (b) after installation

The transducers inside the cone are connected to a measurement device. Calibration factor are chosen based on the measurements, when the real applied load is known.

E.3.7.2 Soil parameters derived from CPT results

Formulas for derived parameters are described by (Ibsen et al. 2009) and are derived from results of traixial and cone penetration tests. Relative soil density, I_D [%] is estimated based on q_c [N], see eq.(E.1) .The effective vertical stress, σ'_v, are calculated for the effective soil unit weight, γ' from eq.(E.2). The insitu void ratio, $e_{\text{in situ}}$, is obtained in an iterative procedure with eq.(E.3) until both values of I_D are equal. An initial guess on $e_{\text{in situ}}$ is the minimum void ratio.

$$I_D = 5.14 \left(\frac{\sigma'_v}{q_c^{0.75}} \right)^{-0.42} \quad [\%] \tag{E.1}$$

$$\gamma' = \frac{d_s - 1}{1 + e_{\text{in situ}}} \gamma_w \quad \left[\text{kN/m}^3 \right] \tag{E.2}$$

$$I_D = \frac{e_{\max} - e_{\text{in situ}}}{e_{\max} - e_{\min}} \quad [\%] \tag{E.3}$$

Strength parameters are based on I_D and γ results. The expression for traixial friction angle, φ_{tr} [°], and dilation angle, ψ_{tr} [°] are given by eqs.(E.4)

and (E.5). The cohesion, c [kPa], and tangent friction angle, φ_t [°], are given by eqs.(E.6) and (E.7).

$$\varphi_{\text{tr}} = 0.152 I_D + 27.4 \sigma_3^{'-0.281} + 23.2 \ [^\circ] \tag{E.4}$$

$$\psi_{\text{tr}} = 0.195 I_D + 14.9 \sigma_3^{'-0.098} - 9.95 \ [^\circ] \tag{E.5}$$

$$c = 0.032 I_D + 3.52 \ [\text{kPa}] \tag{E.6}$$

$$\varphi_t = 0.11 I_D + 32.3 \ [^\circ] \tag{E.7}$$

Stiffness parameter is as the secant modulus at 50% strength and depends on the reference confining pressure, $\sigma_v^{'\text{ref}}$. m is the amount of stress dependency. For a reference pressure 100kPa the parameter m is found as 0.58.

$$E_{50} = E_{50}^{\text{ref}} \left(\frac{c cos(\varphi_t) + \sigma_v' sin(\varphi_t)}{c cos(\varphi_t) + \sigma_v^{'\text{ref}} sin(\varphi_t)} \right)^m \ [\text{kPa}] \tag{E.8}$$

$$E_{50}^{\text{ref}} = 0.6322 I_D^{2.507} + 10920 \ [\text{kPa}] \tag{E.9}$$

E.4 Soil preparation

Soil is prepared before each test to get a uniform condition with a desire soil relative density. First step is to apply the hydraulic gradient equal to 0.9 of its critical value, $0.9 i_{\text{crit}}$. The gradient looses sand to a certain degree and redistributes soil grains. This is important, as the previous test leaves a very non-uniform soil in the container. The gradient has been observed at the ascension pipe in set-up 'a', but the set-up 'b' has a connection of water system to the soil container equipped with a pressure measurement system. The appropriate pressure for a desire gradient can be set. Such a gradient is applied for around 10 minutes. If soil experience a critical hydraulic gradient, piping channels are induced on the soil volume what destroys the uniform soil conditions. The second step is the vibration procedure. A mechanical rod vibrator is used in the procedure. The wooden platform with holes is placed above the sand, see fig. E.6. The rod is inserted in every second hole (black spots), and on the way back in every second remaining hole (white spots). Vibration should follow a zig-zag route. First a dashed square is vibrated, then the entire area (dashed square is vibrated twice). Finally, the surface should be leveled, so that the recordings during installation tests are more precise.

To obtain loose sand again (in case of set-up 'b') a tube connected to a high water pressure is inserted in many positions on the entire volume. This induces many piping channels across the soil. Procedure is repeated until the soil is completely loose and there is no noticeable resistance from soil when inserting the tube. Loosening is performed almost on the entire depth,

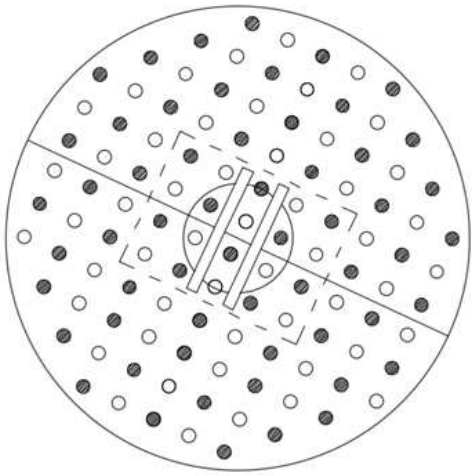

Fig. E.6: A plan for the vibration (Koteras 2017)

wheres vibration is performed only for around 1m depth (limitation of this method). CPT is performed in 4 locations, as described before. Measurements are as followed:

- time [s]
- displacement [mm]
- cone resistance [kN]

Installation test begins if soil conditions are satisfied.

E.5 Installation test

Water level in soil-container is raised by letting the water in from the top. Water coming from the bottom creates the upward hydraulic gradient inside the soil and reduces its strength. A steel plate is set on the soil surface where the water is entering to avoid washing away soil particles. The higher soil container allows for model foundation submersion prior installation test. In set-up 'a' the soil was cover by water to the height of around 10cm above soil surface. However, it is the soil-skirt interaction and water flow around it that is of the main importance for the installation tests, so the results are comparable. Nevertheless, the procedure of results extraction is much simpler in set-up 'b'. As the pore pressure transducers are located above, on the top of soil container, they do not move together with penetrating foundation. The reference point is not changing so the recordings from transducers give

a direct measure of excess pore pressure. In set-up 'b' the measured pore pressure is corrected together with a changing static pore pressure together with penetration depth of bucket.

Additionally, a new suction pump used in set-up 'b' is connected to two pipes: one is fixed at the lid for suction application, the other is fixed at the top of soil container in order to return the water extracted through the lid. This keeps the water level constant during installation. In set-up 'a' water was only sucked to the vacuum pump. The water was refilled from the top of soil container with additional hose, trying to keep the water level constant.

Pore pressure transducer connected to the bucket model are saturated before each test. All connection, from the bottom of steel tubes on the bucket through the plastic small tubes and up to the pore pressure transducer, must be filled with water. This ensure more stable measurement signals. In set-up 'a' the bucket model is submerged in additional water container for the process of saturation. For set-up 'b' the model is submerged before installation so it can be simply saturated with a use of the vacuum system just before installation starts.

The bucket is placed inside the soil container on a special built-up platform and connected to the piston. Next, platforms can be removed. The starting position of bucket should be slightly above soil surface, $\sim 1 - 2$cm. Soil container is filled with water.

Important! All cables are check before installation test if none of them is blocked. The measurements during installation test are as followed:

- time [s]
- applied load on the load cell [kN]
- displacement [mm]
- pore pressures around the skirt of bucket model and below the lid [kPa]
- pore pressures and total soil stress at the soil container [kPa]

After installation is completed, CPT are performed in 8 locations (4 inside the bucket through removable valves, and 4 outside the bucket). The water must be removed before CPT procedure down to the level of approximately 5-10cm above soil surface. Additionally, visual observations are performed.

E.5.1 Jacking installation test

Jacking installation is a displacement controlled test. The speed for penetration is 1m/hour. Maximum force applied on the piston is around 180kN (with included safety factor). Valves on the lid are open during installation test. All pore pressure transducers on the model are saturated before installation. Installation test is finished when there is no significant displacement

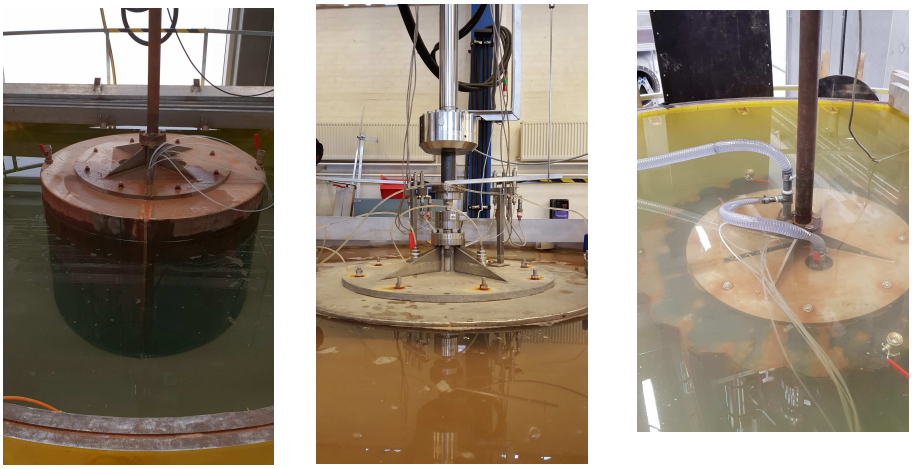

(a) (b) (c)

Fig. E.7: Installation tests: (a) jacking installation, (b) suction installation in set-up 'a' and (c) suction installation in set-up 'b'

with increasing force, or if the load maximum limit is reached. Figure E.7a shows jacking installation test where valves are open and only pore pressure transducers are connected to the channels on the model.

E.5.2 Suction installation test

Suction installation test is divided in two phases: the self-weight installation and the suction installation. Test is controlled by the load applied on the hydraulic piston, where the small load cell must be attached. The speed for penetration is 1m/hour. Suction pump is connected to the valve on the lid, see figs. E.3(b) and E.7(c). The water pumped out during suction installation in set-up 'b', comes back to the soil container with the pipe connected to the outlet of suction pump. All pore pressure transducers on the model are saturated before installation.

In first stage the bucket is hanged on the piston. The load measured by the load cell indicates the self-weight of the model. This load is slowly reduced to zero; hence, the bucket model penetrates into the soil for a depth that ensures the hydraulic seal between the skirt and the soil. When self-weight installation is finished, valves on the lid must be closed and the suction pump is turned on. Firstly, work of the pump induces a high resistance force on the hydraulic pump, where the tension load increases. The hydraulic system is adjusted manually, so that the applied force by the piston is close to the self-weight load only. The load causing further penetration is due to the applied suction. Both, load on the piston and the water extraction on the

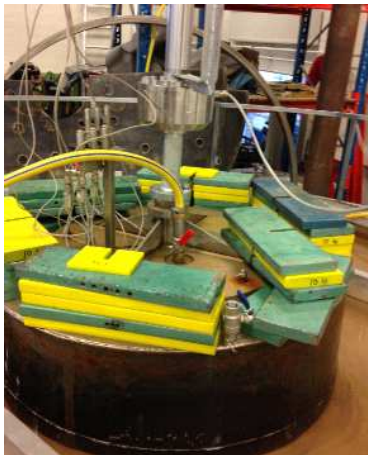

Fig. E.8: Uninstallation test with using overpressure (Koteras 2016)

suction pump is controlled manually to keep a constant rate of installation. Installation test is finished when there is no more significant extension with increasing applied pressure, or if the applied pressure drops significantly.

E.5.3 Uninstallation test

Uninstallation tests in set-up 'a' are performed by using an overpressure. The bucket is connected to the piston, but with a gap between the connection pieces, so that the piston can be controlled manually, when the bucket is pushed up by applied pressure. Tests have been performed on the model with and without extra loads on it. The extra load is simulating a higher self-weight of foundation. Pore pressures around the bucket skirt and the applied pressure under the lid are recorded during the test. Tests proves that decommissioning with applied pressure inside the bucket is a relatively simple process.

For set-up 'b' uninstallation tests were a displacement controlled with a speed of 1m/hour in order to investigate the friction on the bucket skirt separately from the tip resistance.

E.6 Data acquisition

All transducers used i set-up are converting the electrical signal into the engineering units like meters [m], niutons [N] and pascals [Pa]. The calibration factor is often given by the producer, but in some cases a separate calibration procedure is required, as mentioned before. The calibration factor are then specified in a software used for recording and storing the data. Initial settings

for the transducers are also required. The measurement system requires an input of 'zero value'. For the transducers inside the soil tank, zero-down procedure happens once, before any sand or water is added to the container. For the rest of transducers, signals are zeroed before initialization of each test.

References

Borup, M., and Hedegaard, J. 1995. Baskarp Sand No. 15: data report 9403. Data Report, Aalborg University: Geotechnical Engineering Group, Aalborg

Ibsen, L.B., Hanson, M., Hjort, T., and Thaarup, M. 2009. MC-Parameter Calibration for Baskarp Sand No.15. DCE Technical report 62, Aalborg University: Department of Civil Engineering, Aalborg.

Koteras, A. K. (2017). Set-up and Test Procedure for Suction Installation and Uninstallation of Bucket Foundation. Aalborg: Department of Civil Engineering, Aalborg University. DCE Technical Memorandum, No. 63

Koteras, A. K. (2019). Suction and jacking installation of bucket foundation models: laboratory manual. Aalborg: Department of Civil Engineering, Aalborg University. DCE Technical Memorandum, No. 74

Appendix E.

Appendix F

Laboratory tests results

The layout has been revised.

F.1 Overview of test results

The appendix contains laboratory test results of jacking and suction installation tests divided into two parts:

- Laboratory tests performed in a 'Large Yellow Box' in the geotechnical laboratory at Sohngaardsholmsvej 57, Aalborg - set-up 'a'
- Laboratory tests performed in an extended version of 'Large Yellow Box' in the geotechnical laboratory at Thomas Manns Vej 23, Aalborg - set-up 'b'

F.1.1 List of symbols

D	bucket diameter
L	bucket skirt length
I_D	relative soil density
F_{tot}	total applied load
p	applied suction
$h_{\text{plug-heave}}$	height of soil plug heave
q_c	cone resistance
d	depth
φ	friciton angle
ψ	dilation angle
e	void ratio
γ	soil unit weight
h	penetration depth
Δu	excess pore pressure at the skirt
Δu_{beam}	excess pore pressure at the side boundary
u_b	pore pressure at the boundary (set-up 'b')
$\sigma_{V,b}$	vertical stress at the sand bottom (set-up 'b')
$\sigma_{H,b}$	horizontal stress at the side boundary (set-up 'b')

F.1.2 Locations for measurements

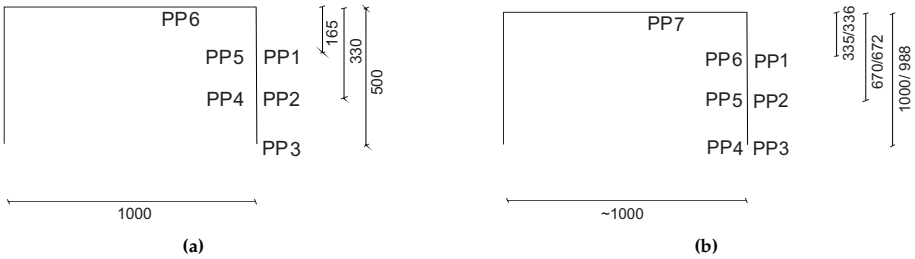

Fig. F.1: Positions for pore pressure measurements: (a) for set-up 'a' and (b) for set-up 'b' (measurements in mm)

F.1.3 Tests overview

Set-up 'a':

- 1.2 m sand over 0.3 m gravel in sand box of a diameter equal to 2.5 m;
- bucket dimensions L = 0.5 m, L/D = 0.5;
- round bucket model.

Set-up 'b' - low sand:

- 1.2 m sand over 0.3 m gravel in sand box of a diameter equal to bucket dimensions 2.5 m;
- L = 1.0 m, L/D = 1;
- round bucket model.

Set-up 'b' - high sand:

- 2.2 m sand over 0.3 m gravel in sand box of a diameter equal to bucket dimensions 2.5 m;
- L = 1.0 m, L/D = 1;
- round and modular bucket models.

The soil container for the set-up 'b' consists of the total pressure cells and pore pressure transducers set at the bottom of the sand layer and attached to the inside wall of the soil container. Distance between the sand bottom to the first measurement point is 233 mm, and then there is 383 mm between each next location. There are 7 locations on the soil container wall.

Table F.1: List of tests for set-up 'a'

Test no.	Type of installation	I_D [%]	F_{tot} for 450 mm [kN]	$h_{self\text{-}weight}$ [mm]	p for 450 mm [kPa]	$h_{plug\text{-}heave}$ [mm]
1.1	Suction + weight	87.83	12.13	89.8	10.49	45
1.2	Suction + weight	90.78	10.24	127	9.23	47
1.3	Suction + weight	90.01	9.91	130.6	8.20	44
1.4	Suction	91.13	10.28	78.8	8.43	42
1.5	Suction	90.31	10.56	73.5	8.54	49
1.6	Jacking	89.72	51.56	-	-	38
1.7	Jacking	89.44	50.76	-	-	40
1.8	Jacking	90.59	52.19	-	-	33
1.9	Suction	91.22	10.68	65.4	9.12	57
1.10	Jacking	89.74	51.45	-	-	36

Table F.2: List of tests for set-up 'b' - low sand

Test no.	Type of installation	I_D [%]	F_{tot} for 900 mm [kN]	$h_{self\text{-}weight}$ [mm]	p for 900 mm [kPa]	$h_{plug\text{-}heave}$ [mm]
2.1	Suction	36.62	11.37	148.4	11.98	7.1
2.2	Suction	71.57	11.81	188.0	12.63	39.5
2.3	Suction	76.18	14.46	100.9	15.83	62
2.4	Suction	74.47	14.11	102.6	15.43	59

Table F.3: List of tests for set-up 'b' - high sand

Test no.	Type of installation	Geometry	I_D [%]	F_{max} [kN]	$h_{self\text{-}weight}$ [mm]	p_{max} [kPa]	$h_{plug\text{-}heave}$ [mm]
3.1	Jacking	Round	55.81	120.71 106.31 (950mm)	-	-	17.8
3.2	Jacking	Round	34.37	28.03 24.52 (950mm)	-	-	13.6
3.3	Jacking	Round	64.90	137.89 120.87 (950mm)	-	-	8.7
3.4.	Jacking	Round	71.60	165.34 148.60 (950mm)	-	-	16
3.5.	Jacking	Round	81.48	185.23 F_{max} reached by the piston (h_{max}=930 mm	-	-	-
3.6.	Jacking	Round	83.70	186.47 F_{max} reached by the piston (h_{max}=898 mm	-	-	-
3.7.	Suction	Round	86.97	13.98 13.39 (950mm)	175.4	16.44 15.85 (950mm)	91.7
3.8.	Suction	Round	79.37	12.71	101.9	13.57	103.9
3.9.	Suction	Modular	82.44	14.74	78.0	16.14	115.9
3.10.	Suction	Modular	86.25	16.63	84.5	18.65	124.9
3.11.	Suction	Round	84.42	16.27	70.5	18.74	100.3
3.12.	Suction	Round	42.30	13.20 12.51 (950mm)	136.5	15.74 14.79 (950mm)	4.8
3.13.	Suction	Round	77.33	installation stopped on h=468 mm			
3.14.	Suction	Round	82.76	15.03 14.55 (900mm)	105.6	16.31 15.99 (900mm)	83.0
3.15.	Jacking	Modular	43.18	140.12	-	-	53.4
3.16	Jacking	Modular	42.25	134.82	-	-	45.86
3.17	Jacking	Modular	63.32	182.06 F_{max} reached by the piston (h_{max}=681.2 mm	-	-	-
3.18	Jacking	Modular	74.25	182.31 F_{max} reached by the piston (h_{max}=591.8 mm	-	-	-

Table F.4: Table F.3 cont.

Test no.	Type of installation	Geometry	I_D [%]	F_{max} [kN]	$h_{self\text{-}weight}$ [mm]	p_{max} [kPa]	$h_{plug\text{-}heave}$ [mm]
3.19	Suction	Modular	40.13	15.22 14.22 (900mm)	69.3	16.84 15.60 (900mm)	46.5
3.20	Jacking	Round	41.73	33.10	-	-	19.1
3.21	Suction	Modular	60.72	13.49	144.5	14.19	101.1
3.22	Suction	Modular	61.92	17.39 14.26 (900mm)	102.9	19.44 15.36 (900mm)	88.2
3.23	Suction	Modular	78.13	16.32 16.02 (900mm)	104.03	18.11 17.54 (900mm)	118.1
3.24	Suction	Round	57.99	15.33 14.23 (950mm)	145.3	16.77 15.40 (950mm)	62.6

F.2 Results from set-up (a)

Test 1.1

Type	h/D	Geometry
Suction	0.5	Round

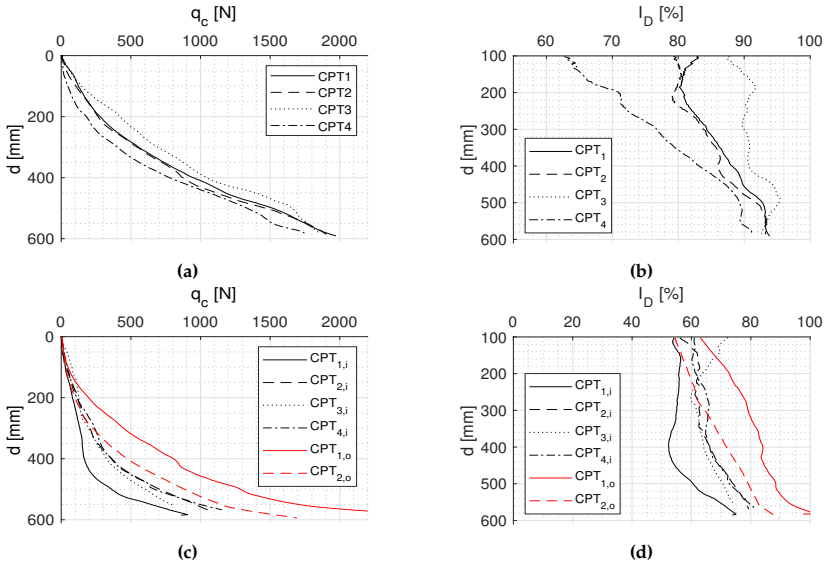

Fig. F.2: Results of CPT (a-b) before installation and (c-d) after installation

(a) Before installation

$I_{D,mean}$	87.83 %
φ_{mean}	41.96°
ψ_{mean}	19.88°
e_{mean}	0.653
γ_{mean}	9.73 kN/m^3

(b) After installation

$I_{D,mean,in}$	$I_{D,mean,out}$
63.93 %	74.69 %
$I_{D,mean,in(1,4)}$	$I_{D,mean,out(2)}$
61.99 %	67.32 %

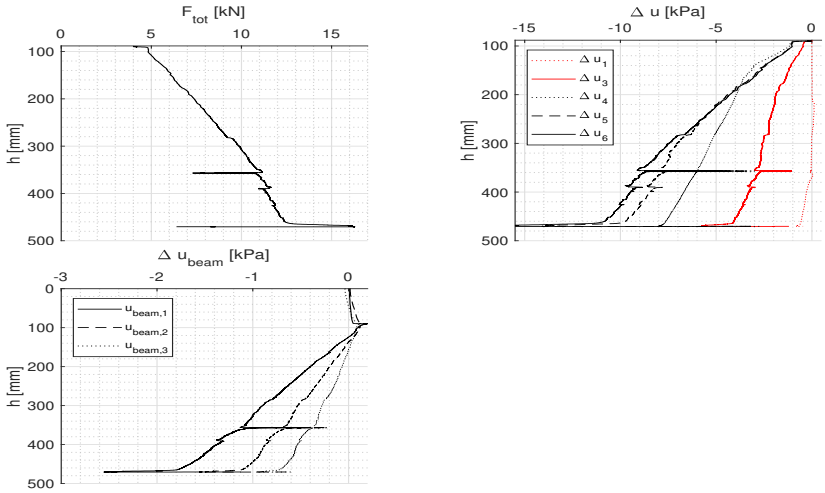

Fig. F.3: Results of installation test

Test 1.2

Type	h/D	Geometry
Suction	0.5	Round

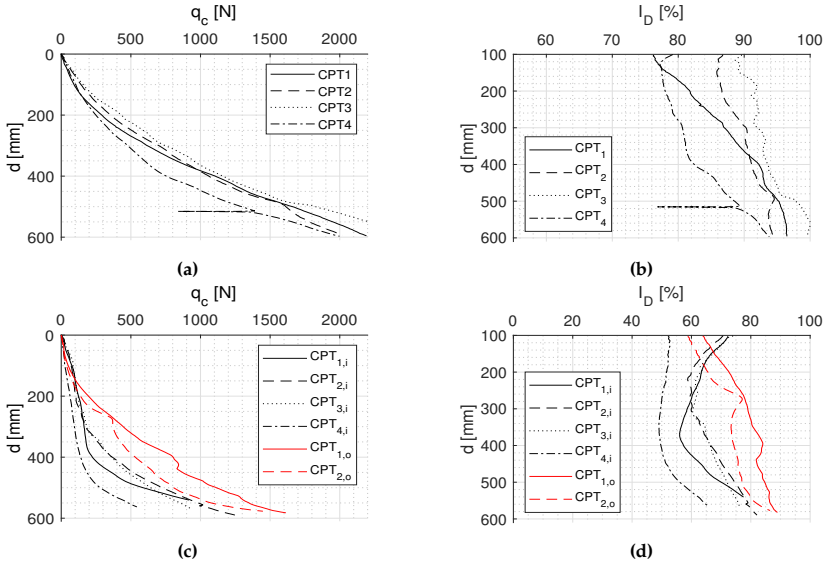

Fig. F.4: Results of CPT (a-b) before installation and (c-d) after installation

Table F.6: Soil parameters

(a) Before installation

$I_{D,mean}$	90.78 %
φ_{mean}	42.29°
ψ_{mean}	20.45°
e_{mean}	0.628
γ_{mean}	9.88 kN/m^3

(b) After installation

$I_{D,mean,in}$	$I_{D,mean,out}$
62.34 %	75.61 %
$I_{D,mean,in(1,4)}$	$I_{D,mean,out(2)}$
57.82 %	72.43 %

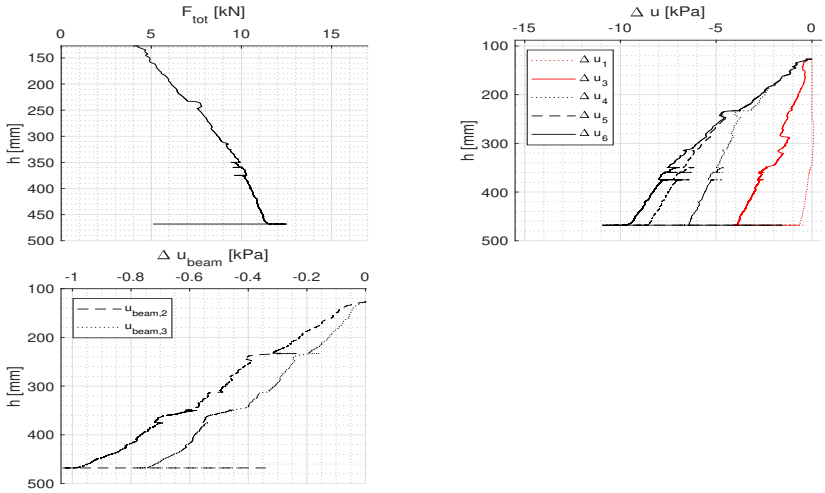

Fig. F.5: Results of installation test

Test 1.3

Type	h/D	Geometry
Suction	0.5	Round

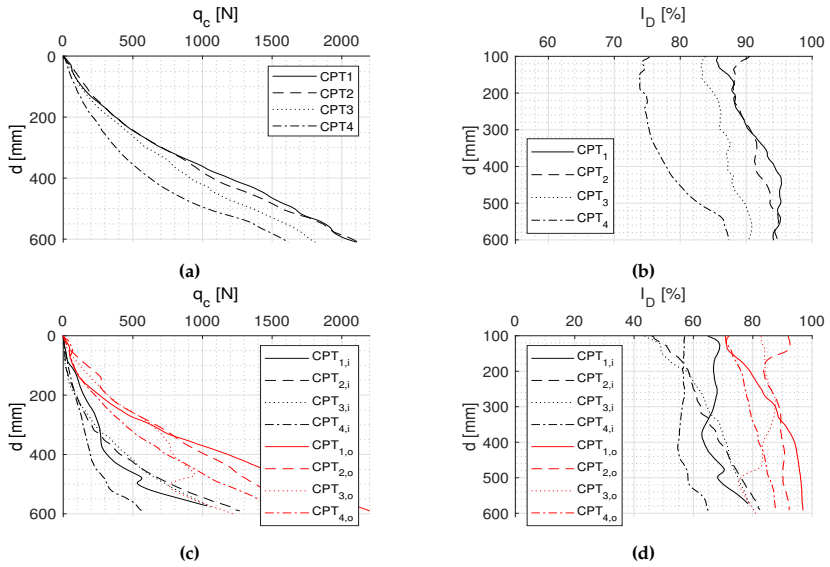

Fig. F.6: Results of CPT (a-b) before installation and (c-d) after installation

Table F.7: Soil parameters

(a) Before installation

$I_{D,mean}$	90.01 %
φ_{mean}	42.20°
ψ_{mean}	20.30°
e_{mean}	0.635
γ_{mean}	9.84 kN/m^3

(b) After installation

$I_{D,mean,in}$	$I_{D,mean,out}$
64.11 %	85.83 %
$I_{D,mean,in(1,4)}$	$I_{D,mean,out(2)}$
62.52 %	89.97 %

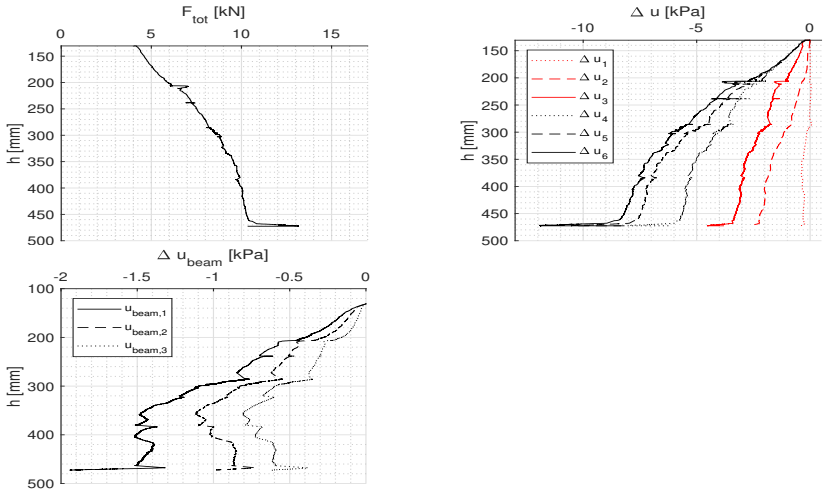

Fig. F.7: Results of installation test

Test 1.4

Type	h/D	Geometry
Suction	0.5	Round

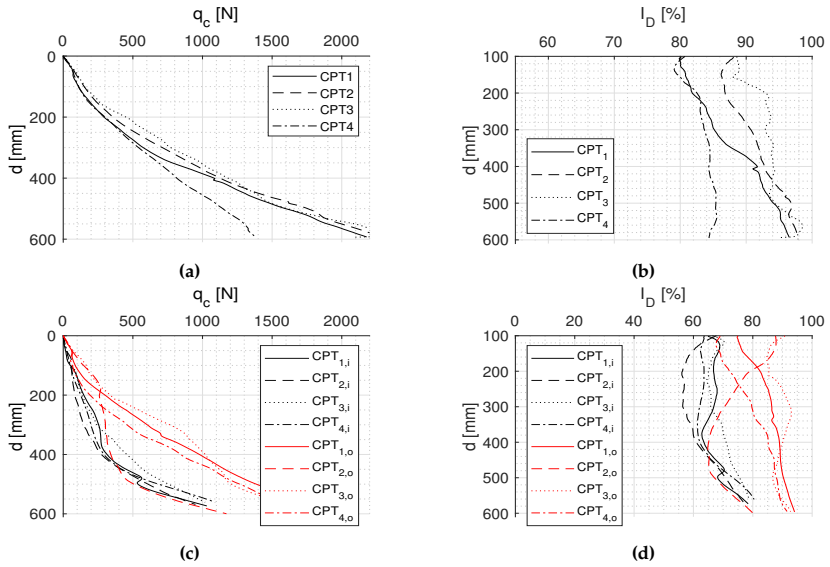

Fig. F.8: Results of CPT (a-b) before installation and (c-d) after installation

Table F.8: Soil parameters

(a) Before installation

$I_{D,mean}$	91.13 %
φ_{mean}	42.32°
ψ_{mean}	20.52°
e_{mean}	0.625
γ_{mean}	9.90 kN/m^3

(b) After installation

$I_{D,mean,in}$	$I_{D,mean,out}$
66.33 %	78.42%
$I_{D,mean,in(1,4)}$	$I_{D,mean,out(2,3)}$
66.59 %	79.76%

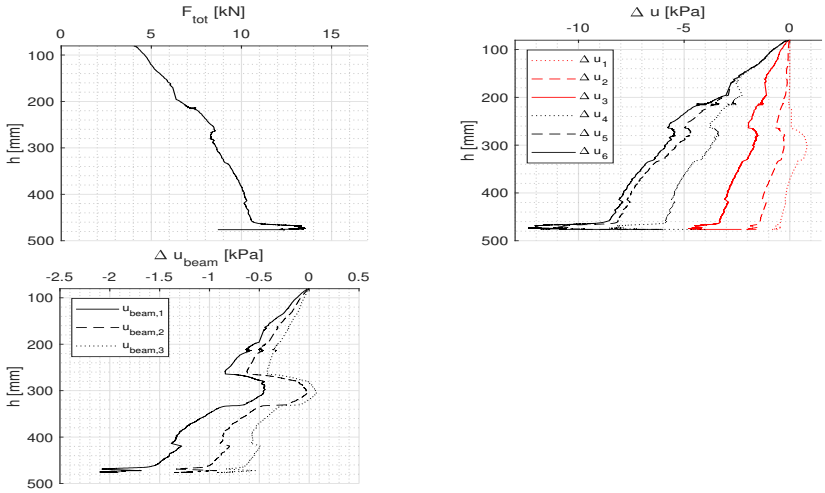

Fig. F.9: Results of installation test

Test 1.5

Type	h/D	Geometry
Suction	0.5	Round

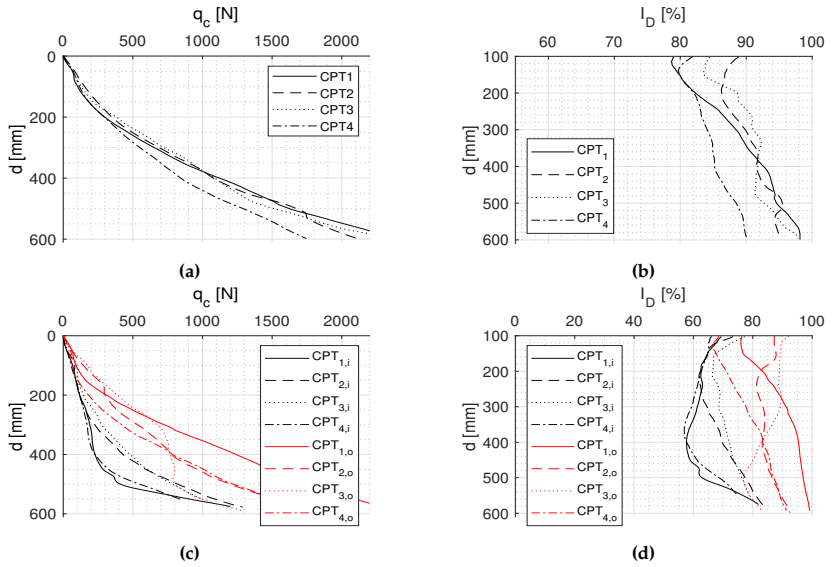

Fig. F.10: Results of CPT (a-b) before installation and (c-d) after installation

Table F.9: Soil parameters

(a) Before installation

$I_{D,mean}$	90.31 %
φ_{mean}	42.23°
ψ_{mean}	20.36°
e_{mean}	0.632
γ_{mean}	9.86 kN/m^3

(b) After installation

$I_{D,mean,in}$	$I_{D,mean,out}$
66.69%	85.05%
$I_{D,mean,in(1,4)}$	$I_{D,mean,out(2,3)}$
63.01%	87.94%

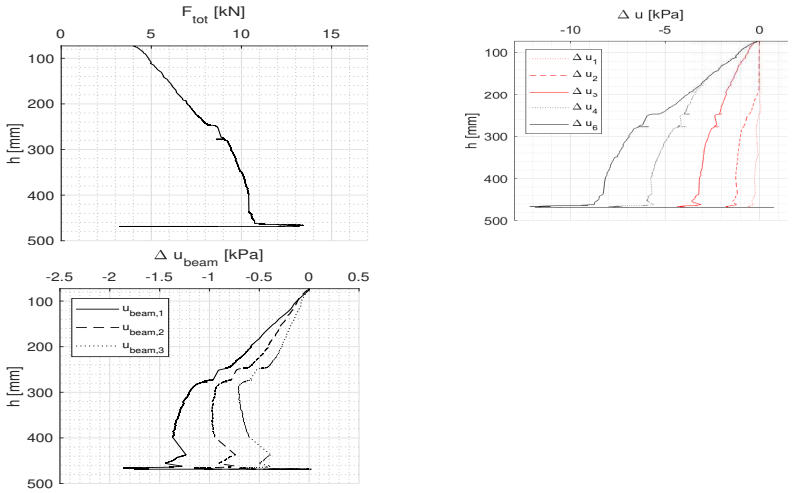

Fig. F.11: Results of installation test

Test 1.6

Type	h/D	Geometry
Jacking	0.5	Round

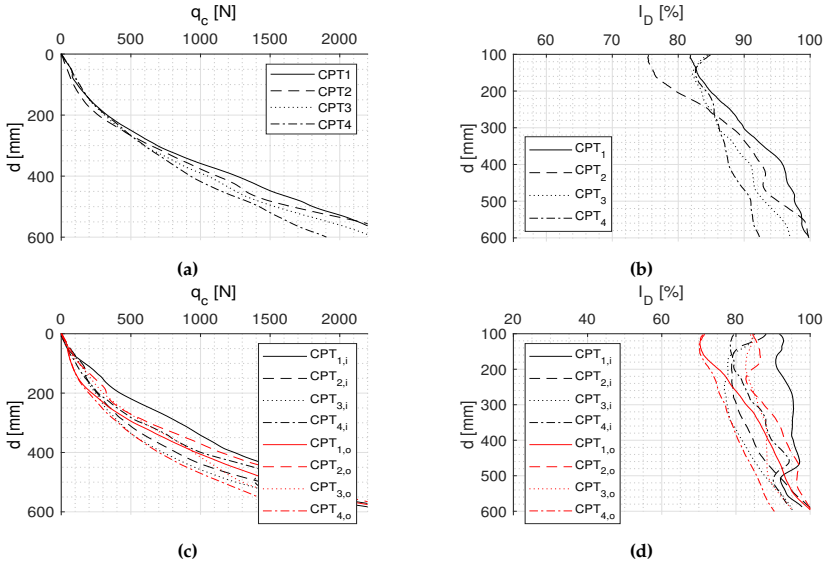

Fig. F.12: Results of CPT (a-b) before installation and (c-d) after installation

Table F.10: Soil parameters

(a) Before installation

$I_{D,mean}$	89.72 %
φ_{mean}	42.17°
ψ_{mean}	20.25°
e_{mean}	0.624
γ_{mean}	9.83 kN/m^3

(b) After installation

$I_{D,mean,in}$	$I_{D,mean,out}$
87.19 %	85.48 %
$I_{D,mean,in(1,4)}$	$I_{D,mean,out(2,3)}$
90.30 %	87.86%

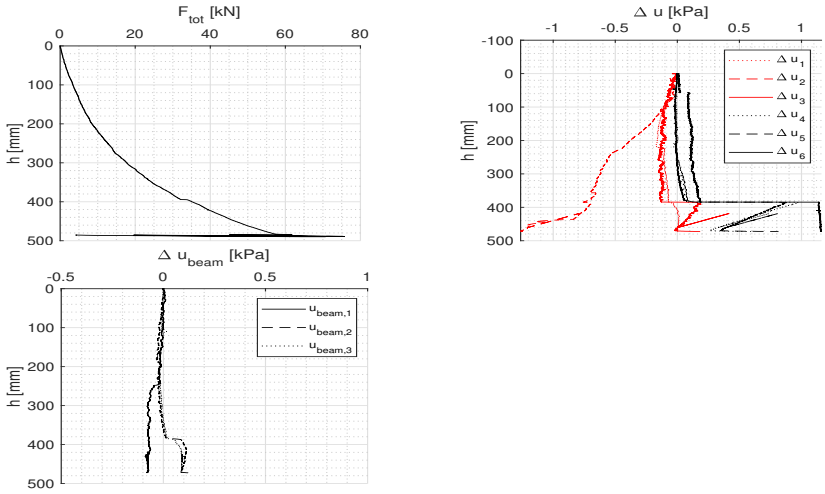

Fig. F.13: Results of installation test

Test 1.7

Type	h/D	Geometry
Jacking	0.5	Round

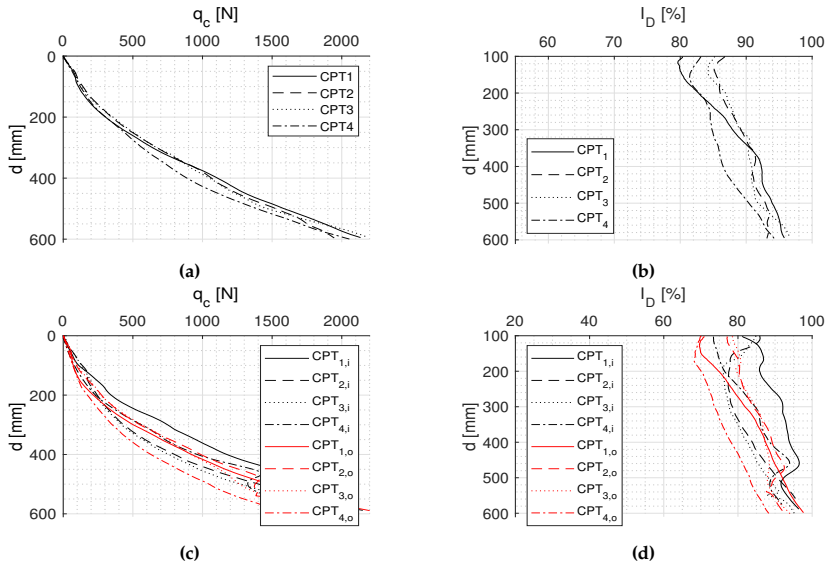

Fig. F.14: Results of CPT (a-b) before installation and (c-d) after installation

Table F.11: Soil parameters

(a) Before installation

$I_{D,mean}$	89.44 %
φ_{mean}	42.14°
ψ_{mean}	20.19°
e_{mean}	0.640
γ_{mean}	9.81 kN/m^3

(b) After installation

$I_{D,mean,in}$	$I_{D,mean,out}$
85.39 %	82.85%
$I_{D,mean,in(1,4)}$	$I_{D,mean,out(2,3)}$
87.75 %	84.70 %

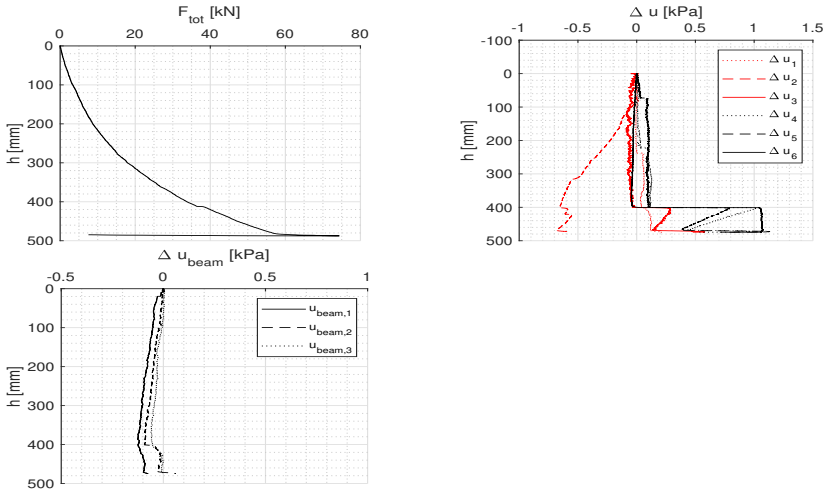

Fig. F.15: Results of installation test

Test 1.8

Type	h/D	Geometry
Jacking	0.5	Round

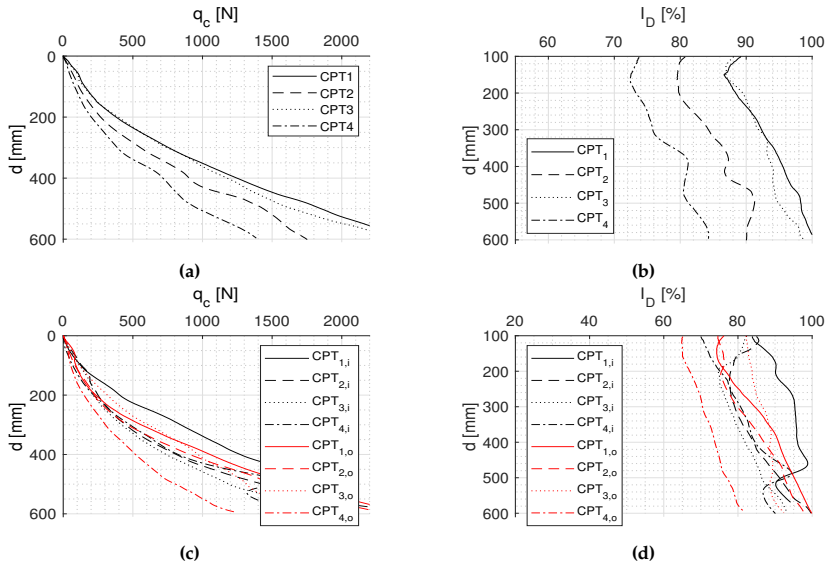

Fig. F.16: Results of CPT (a-b) before installation and (c-d) after installation

Table F.12: Soil parameters

(a) Before installation

$I_{D,mean}$	90.59 %
φ_{mean}	42.26°
ψ_{mean}	20.42°
e_{mean}	0.630
γ_{mean}	9.88 kN/m^3

(b) After installation

$I_{D,mean,in}$	$I_{D,mean,out}$
85.53 %	82.54%
$I_{D,mean,in(1,4)}$	$I_{D,mean,out(2,3)}$
87.70 %	85.57 %

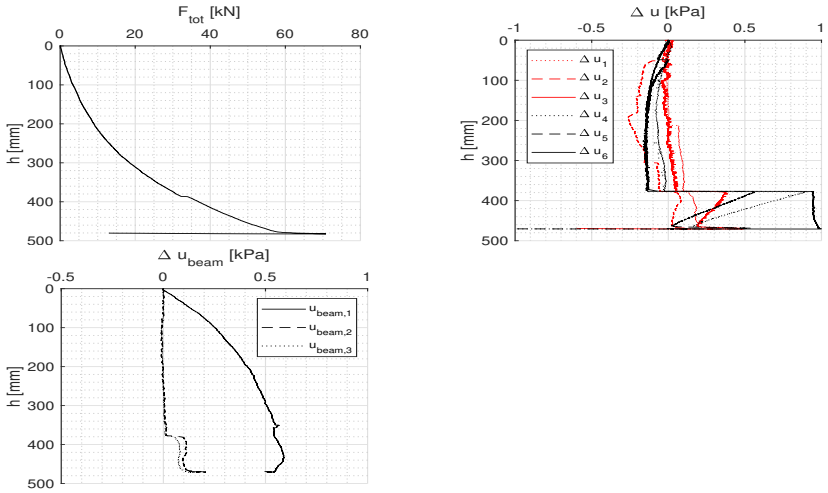

Fig. F.17: Results of installation test

Test 1.9

Type	h/D	Geometry
Suction	0.5	Round

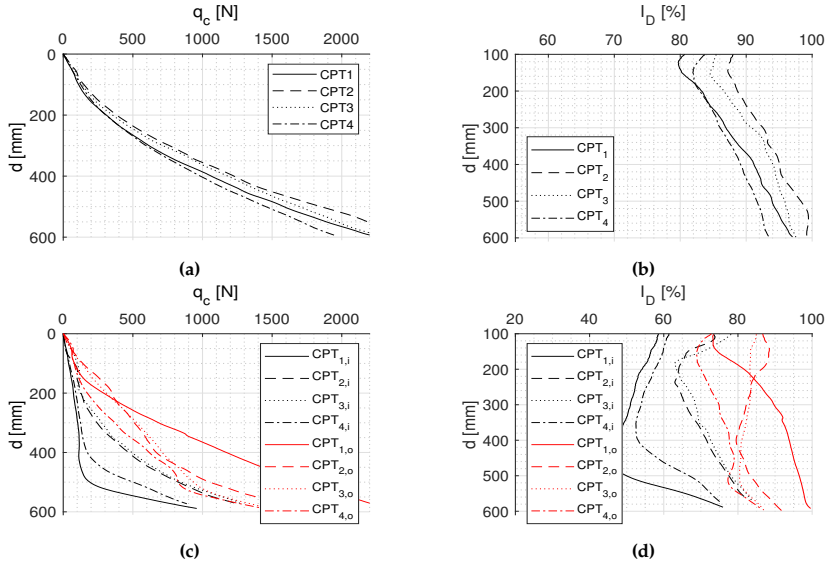

Fig. F.18: Results of CPT (a-b) before installation and (c-d) after installation

Table F.13: Soil parameters

(a) Before installation

$I_{D,mean}$	91.22 %
φ_{mean}	42.33°
ψ_{mean}	20.54°
e_{mean}	0.624
γ_{mean}	9.91 kN/m^3

(b) After installation

$I_{D,mean,in}$	$I_{D,mean,out}$
63.76 %	82.89 %
$I_{D,mean,in(1,4)}$	$I_{D,mean,out(2,3)}$
56.21 %	86.76%

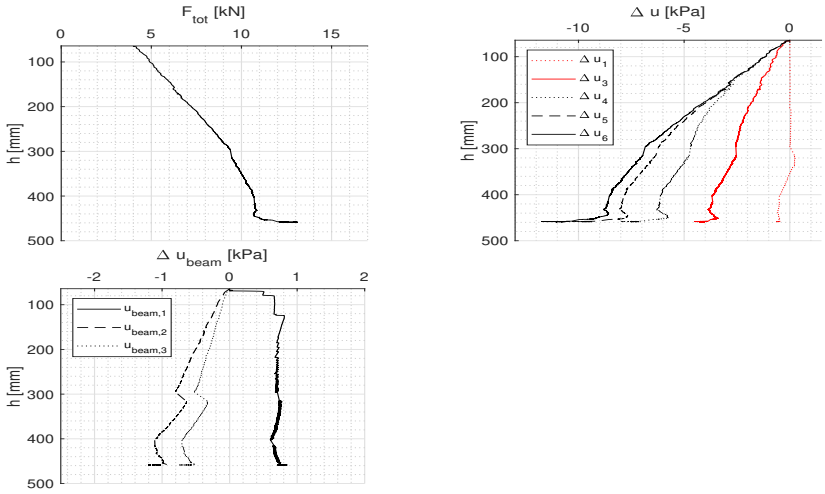

Fig. F.19: Results of installation test

Test 1.10

Type	h/D	Geometry
Jacking	0.5	Round

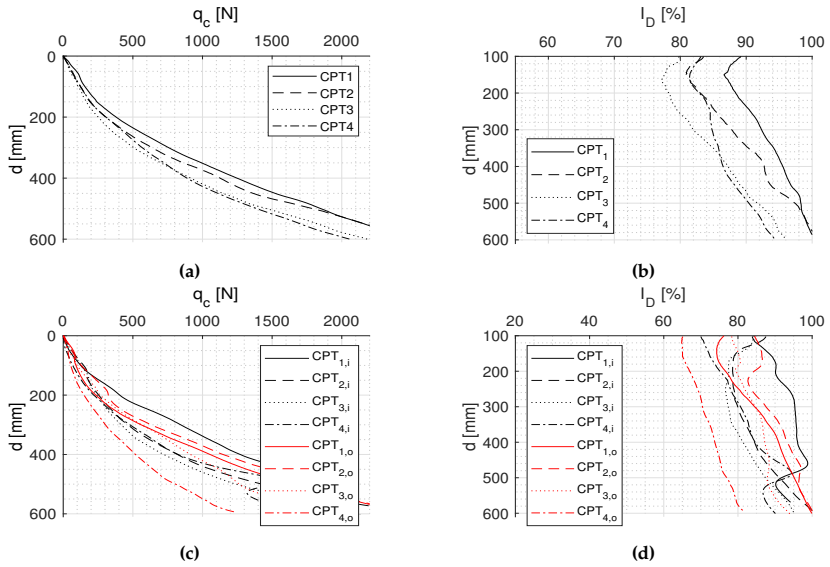

Fig. F.20: Results of CPT (a-b) before installation and (c-d) after installation

Table F.14: Soil parameters

(a) Before installation

$I_{D,mean}$	89.74 %
φ_{mean}	42.17°
ψ_{mean}	20.25°
e_{mean}	0.637
γ_{mean}	9.83 kN/m^3

(b) After installation

$I_{D,mean,in}$	$I_{D,mean,out}$
83.76 %	82.89 %
$I_{D,mean,in(1,4)}$	$I_{D,mean,out(2,3)}$
87.70 %	88.86%

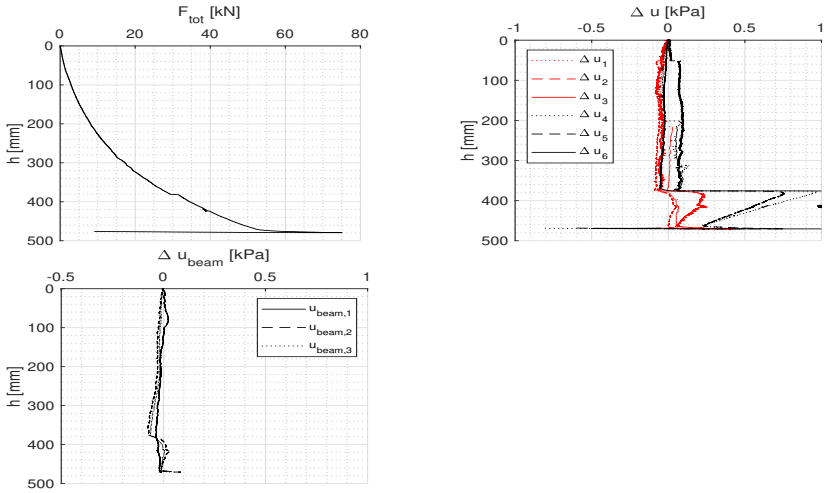

Fig. F.21: Results of installation test

F.3 Results from set-up (b) - low sand

Test 2.1

Type	h/D	Geometry
Suction	1.0	Round

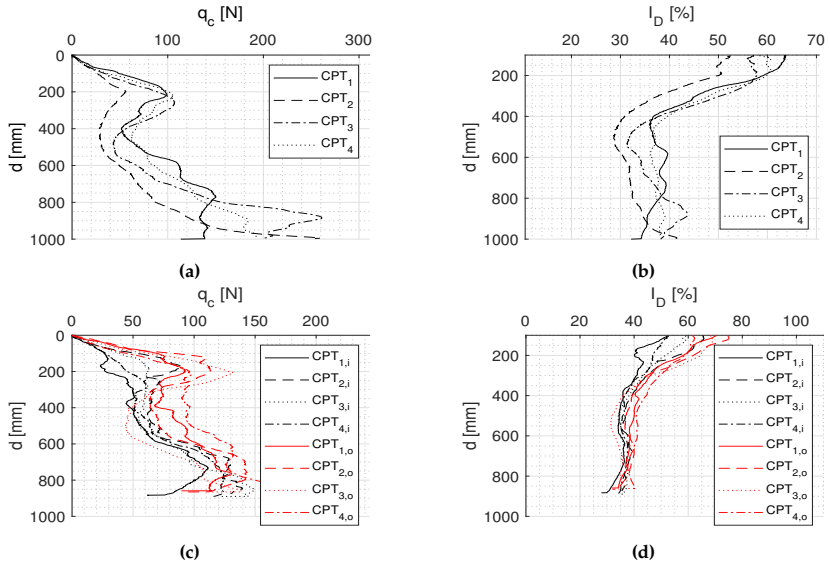

Fig. F.22: Results of CPT (a-b) before installation and (c-d) after installation

Table F.15: Soil parameters

(a) Before installation (300-1000mm)

$I_{D,mean}$	36.62 %
φ_{mean}	36.33°
ψ_{mean}	9.89°
e_{mean}	0.740
γ_{mean}	9.19 kN/m^3

(b) After installation (300-1000mm)

$I_{D,mean,in}$	$I_{D,mean,out}$
36.67 %	38.51 %
$I_{D,mean,in(1,4)}$	$I_{D,mean,out(2)}$
35.95 %	38.78 %

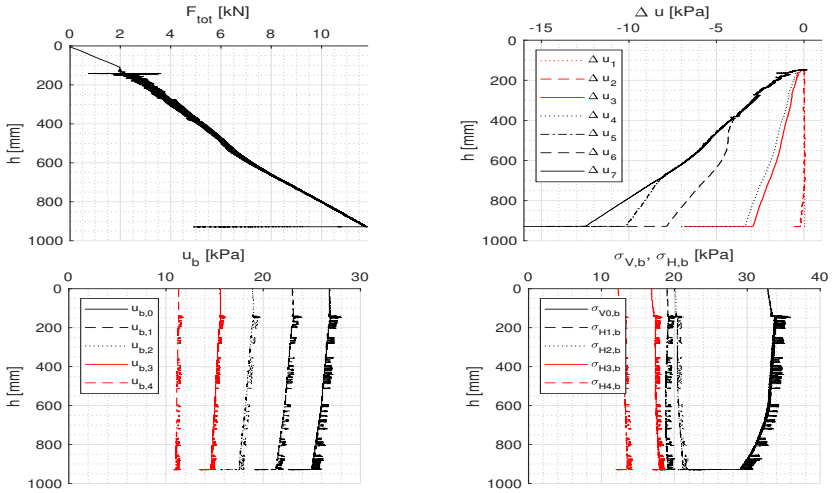

Fig. F.23: Results of installation test

Test 2.2

Type	h/D	Geometry
Suction	1.0	Round

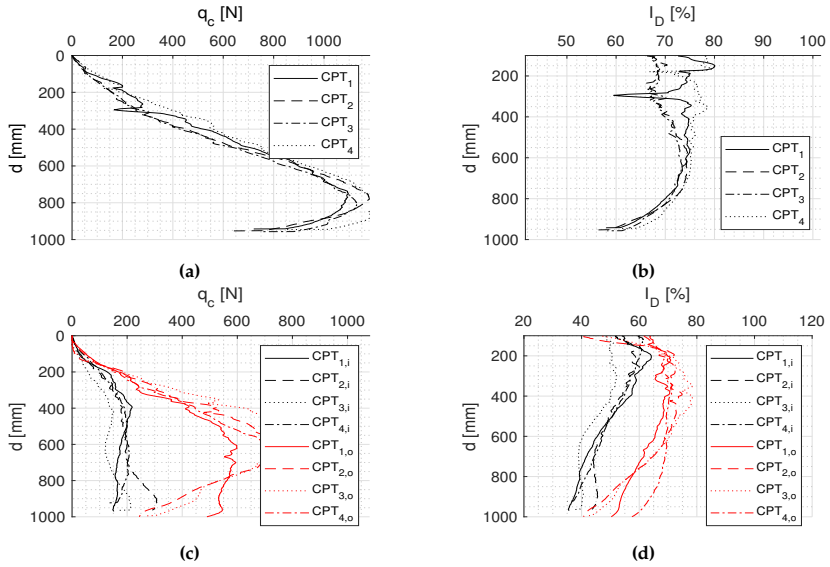

Fig. F.24: Results of CPT (a-b) before installation and (c-d) after installation

Table F.16: Soil parameters

(a) Before installation

$I_{D,mean}$	71.57 %
φ_{mean}	40.17°
ψ_{mean}	16.71°
e_{mean}	0.642
γ_{mean}	9.74 kN/m^3

(b) After installation

$I_{D,mean,in}$	$I_{D,mean,out}$
48.61 %	64.98 %
$I_{D,mean,in(1,4)}$	$I_{D,mean,out(2)}$
49.72 %	63.35 %

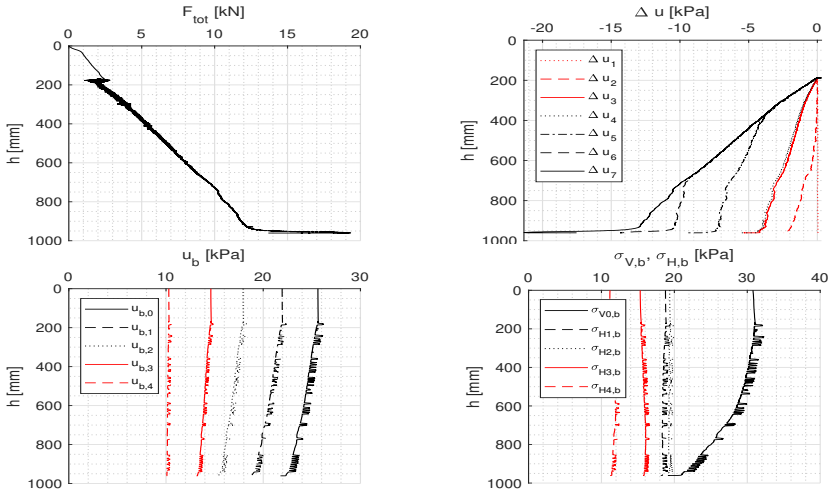

Fig. F.25: Results of installation test

Test 2.3

Type	h/D	Geometry
Suction	1.0	Round

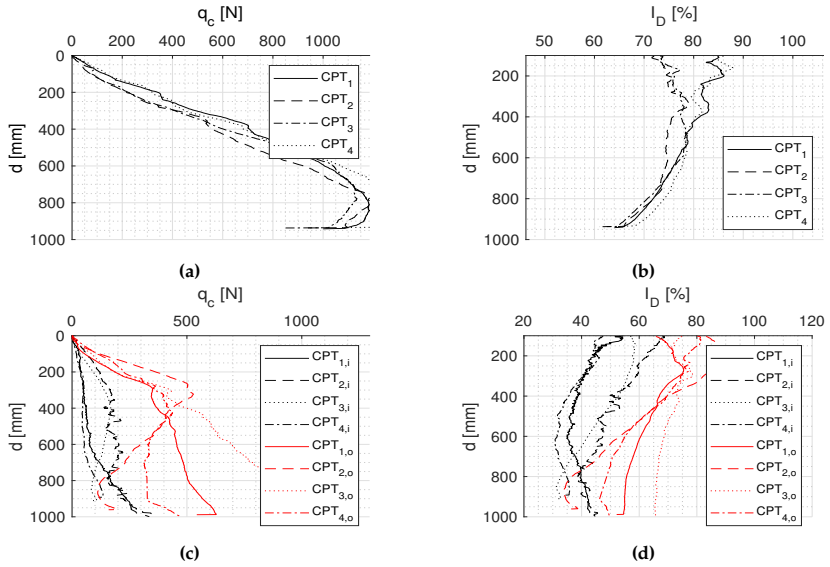

Fig. F.26: Results of CPT (a-b) before installation and (c-d) after installation

Table F.17: Soil parameters

(a) Before installation

$I_{D,mean}$	76.18 %
φ_{mean}	40.68°
ψ_{mean}	17.61°
e_{mean}	0.629
γ_{mean}	9.82 kN/m^3

(b) After installation

$I_{D,mean,in}$	$I_{D,mean,out}$
43.22 %	64.16 %
$I_{D,mean,in(1,4)}$	$I_{D,mean,out(2)}$
38.37 %	61.62 %

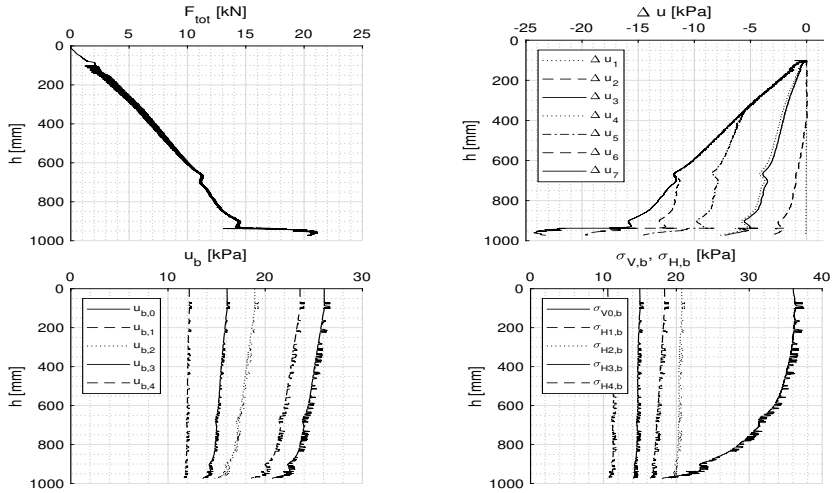

Fig. F.27: Results of installation test

Test 2.4

Type	h/D	Geometry
Suction	1.0	Round

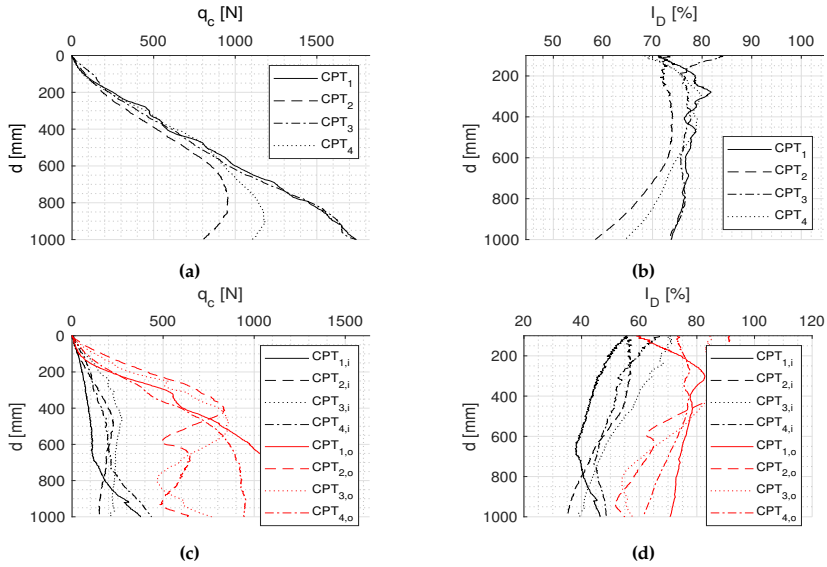

Fig. F.28: Results of CPT (a-b) before installation and (c-d) after installation

Table F.18: Soil parameters

(a) Before installation

$I_{D,mean}$	74.47 %
φ_{mean}	40.49°
ψ_{mean}	17.27°
e_{mean}	0.634
γ_{mean}	9.78 kN/m^3

(b) After installation

$I_{D,mean,in}$	$I_{D,mean,out}$
49.15 %	72.63 %
$I_{D,mean,in(1,4)}$	$I_{D,mean,out(2)}$
47.28 %	73.48 %

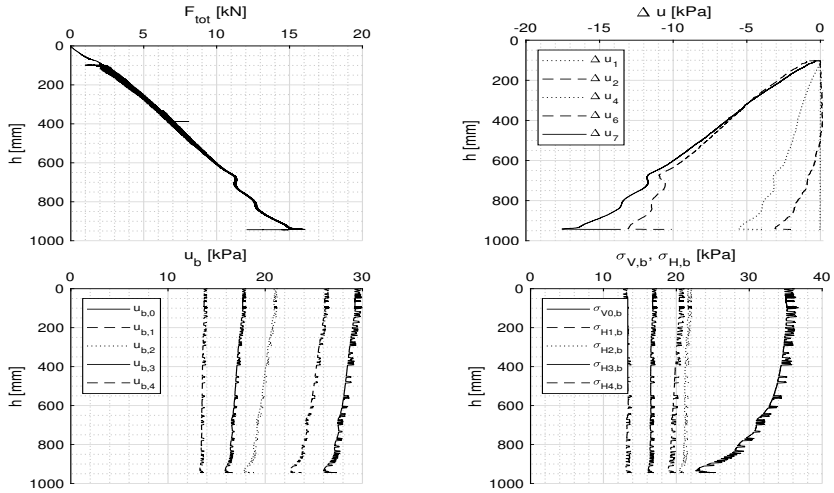

Fig. F.29: Results of installation test

F.4 Results from set-up (b) - high sand

Test 3.1

Type	h/D	Geometry
Jacking	1.0	Round

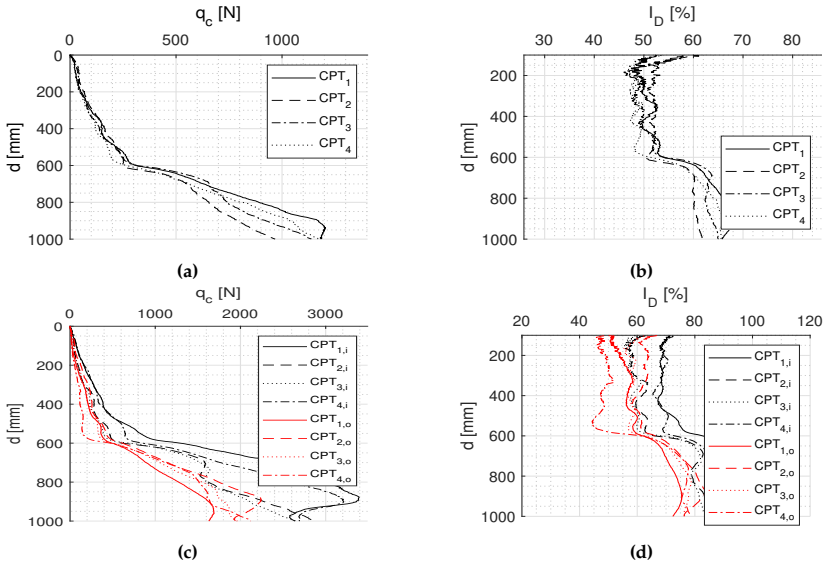

Fig. F.30: Results of CPT (a-b) before installation and (c-d) after installation

Table F.19: Soil parameters

(a) Before installation

$I_{D,mean}$	55.81 %
φ_{mean}	28.44°
ψ_{mean}	13.63°
e_{mean}	0.686
γ_{mean}	9.48 kN/m^3

(b) After installation

$I_{D,mean,in}$	$I_{D,mean,out}$
73.73 %	64.57 %
$I_{D,mean,in}(1,4)$	$I_{D,mean,out}(2,3)$
78.33 %	67.32 %

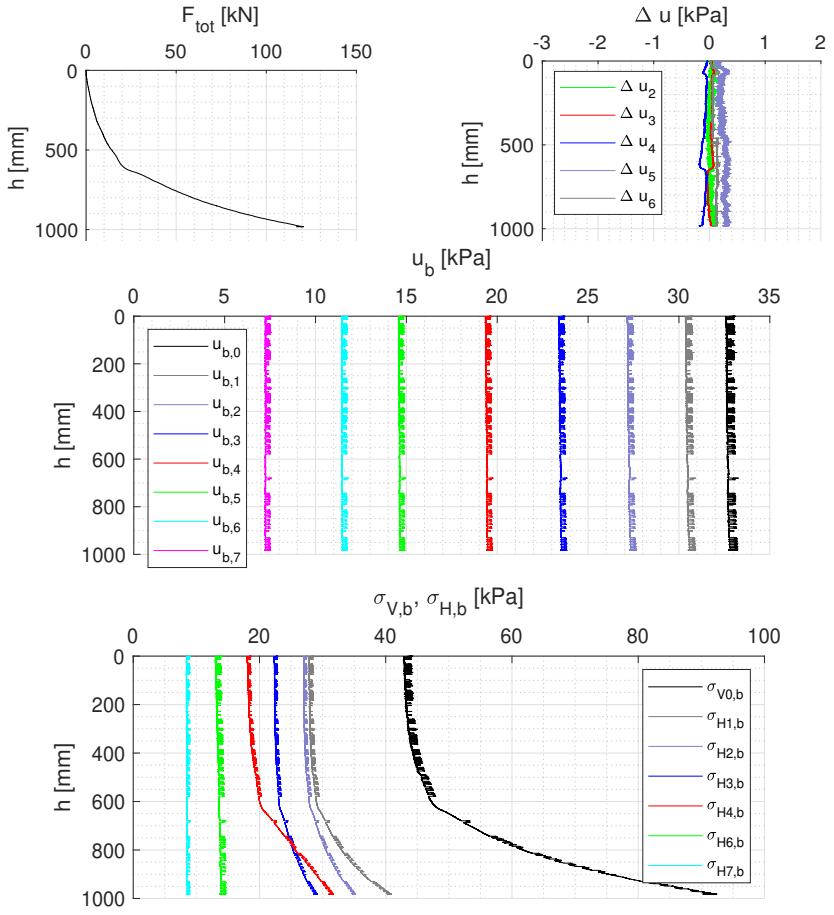

Fig. F.31: Results of installation test

Test 3.2

Type	h/D	Geometry
Jacking	1.0	Round

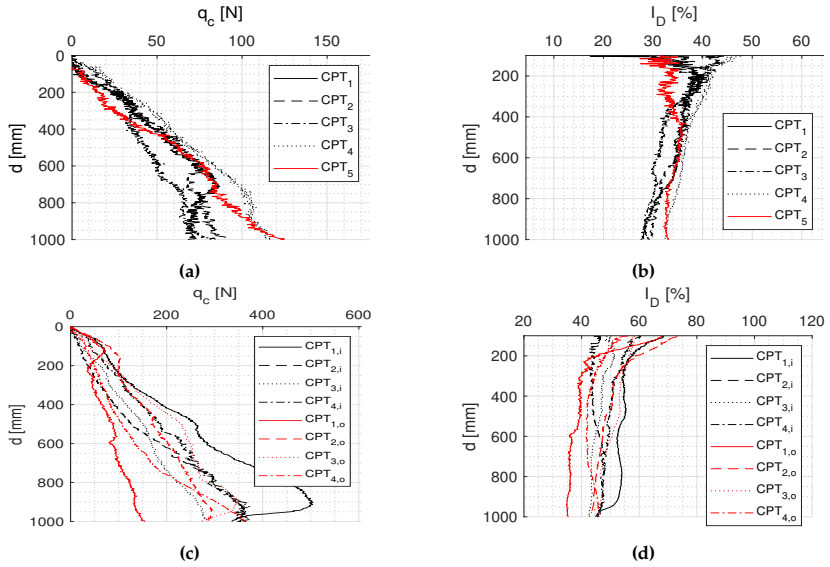

Fig. F.32: Results of CPT (a-b) before installation and (c-d) after installation

Table F.20: Soil parameters

(a) Before installation

$I_{D,mean}$	34.37 %
φ_{mean}	36.08°
ψ_{mean}	9.45°
e_{mean}	0.746
γ_{mean}	9.16 kN/m^3

(b) After installation

$I_{D,mean,in}$	$I_{D,mean,out}$
49.00 %	46.38 %
$I_{D,mean,in(1,4)}$	$I_{D,mean,out(2,3)}$
52.26 %	50.62 %

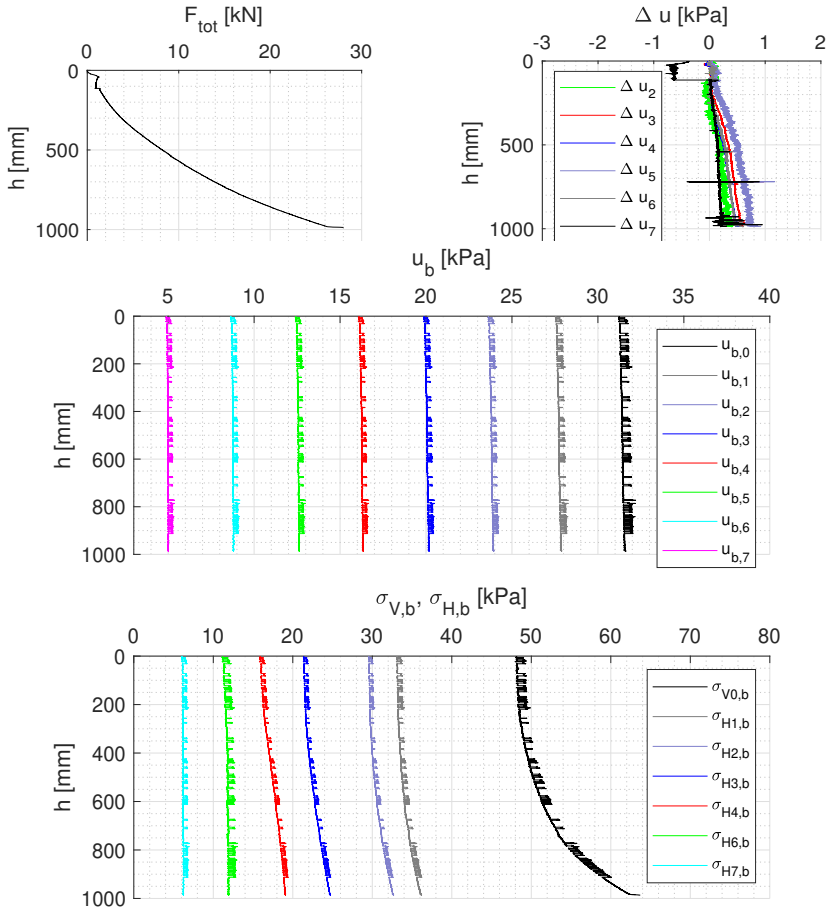

Fig. F.33: Results of installation test

Test 3.3

Type	h/D	Geometry
Jacking	1.0	Round

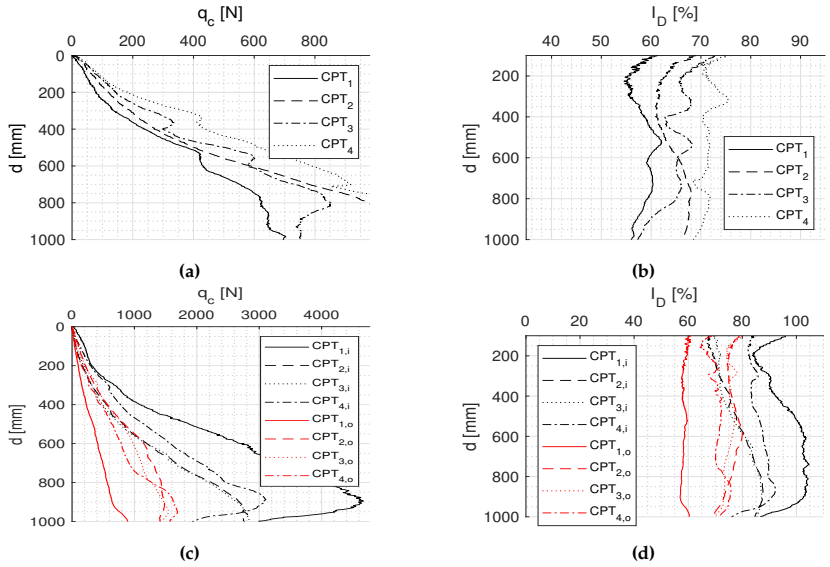

Fig. F.34: Results of CPT (a-b) before installation and (c-d) after installation

Table F.21: Soil parameters

(a) Before installation

$I_{D,mean}$	64.9 %
φ_{mean}	39.43°
ψ_{mean}	15.41°
e_{mean}	0.661
γ_{mean}	9.63 kN/m^3

(b) After installation

$I_{D,mean,in}$	$I_{D,mean,out}$
85.04 %	70.17 %
$I_{D,mean,in(1,4)}$	$I_{D,mean,out(2,3)}$
91.37 %	75.52 %

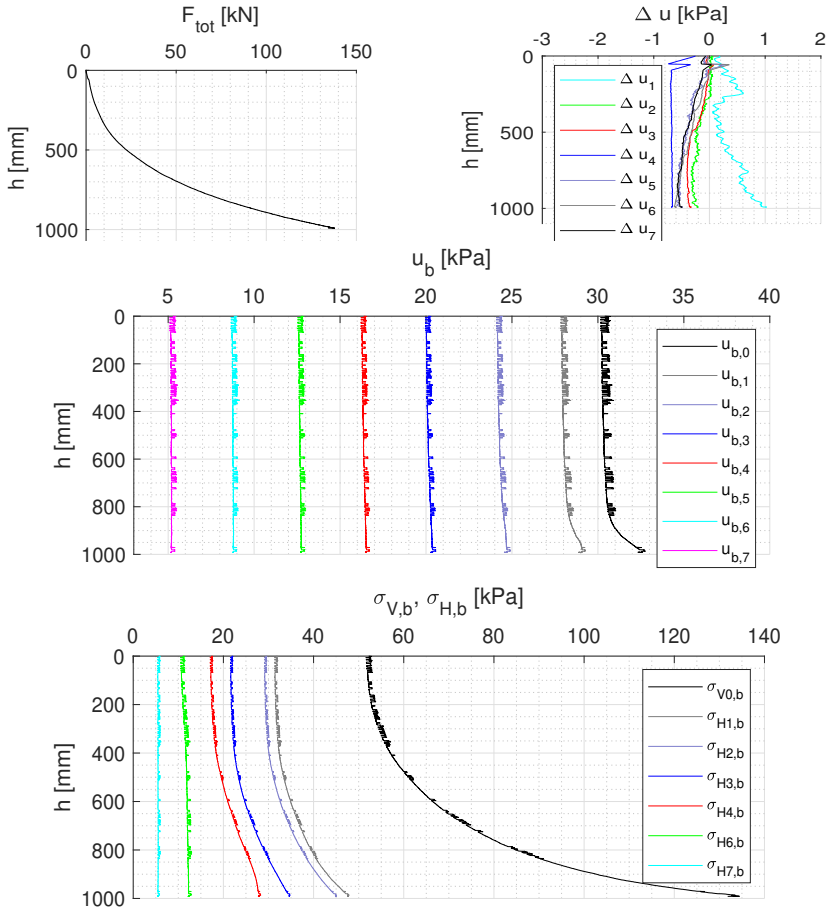

Fig. F.35: Results of installation test

Test 3.4

Type	h/D	Geometry
Jacking	1.0	Round

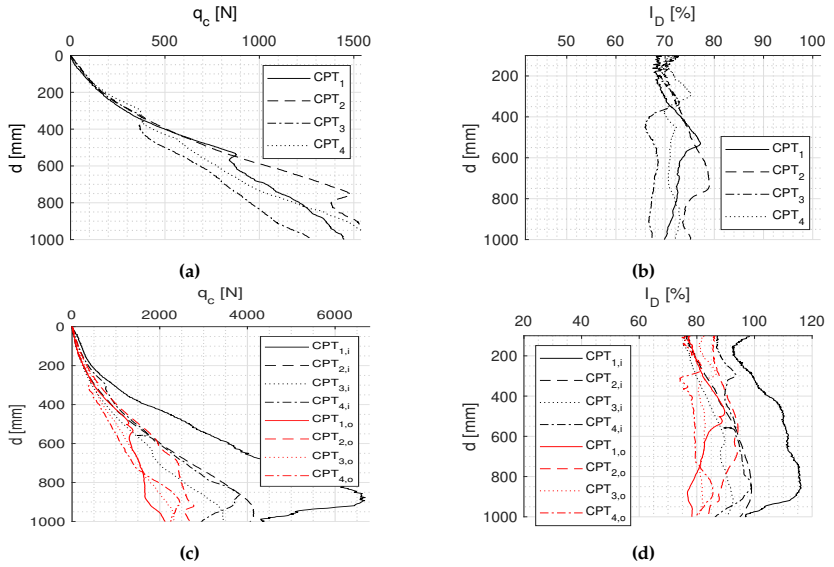

Fig. F.36: Results of CPT (a-b) before installation and (c-d) after installation

Table F.22: Soil parameters

(a) Before installation

$I_{D,mean}$	71.6 %
φ_{mean}	40.18°
ψ_{mean}	16.71°
e_{mean}	0.642
γ_{mean}	9.74 kN/m^3

(b) After installation

$I_{D,mean,in}$	$I_{D,mean,out}$
93.78 %	83.38 %
$I_{D,mean,in(1,4)}$	$I_{D,mean,out(2,3)}$
99.43 %	85.88 %

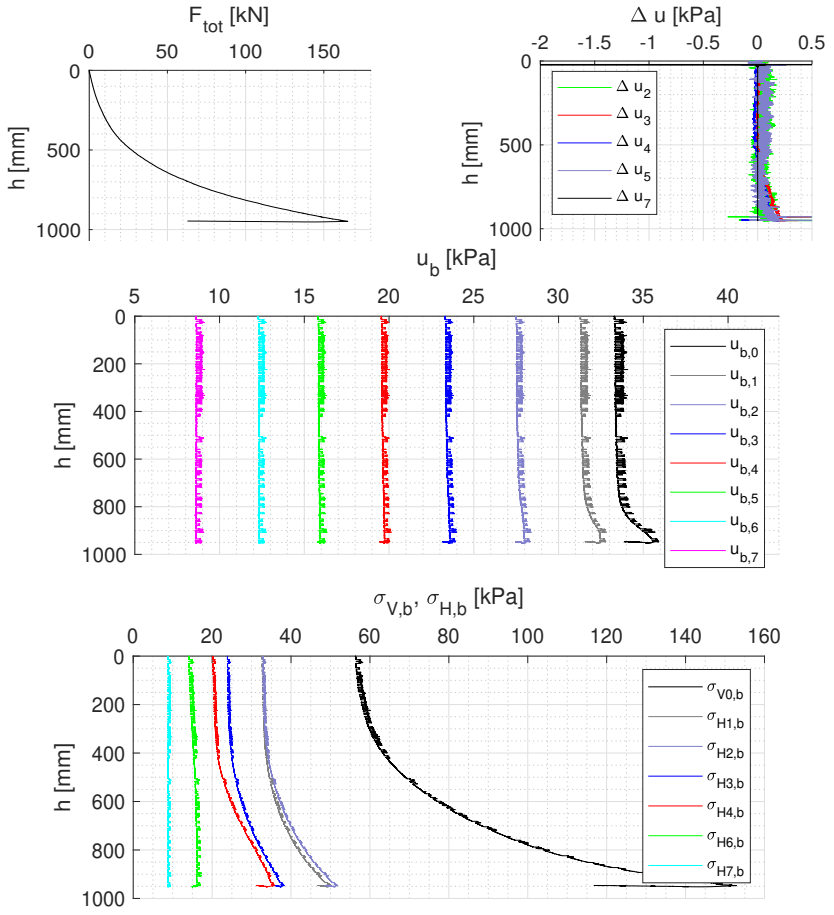

Fig. F.37: Results of installation test

Test 3.5

Type	h/D	Geometry
Jacking	1.0	Round

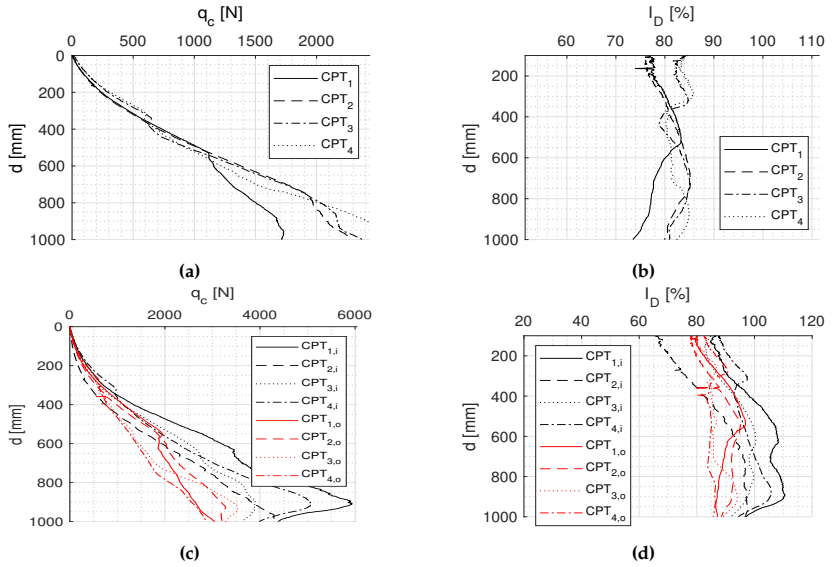

Fig. F.38: Results of CPT (a-b) before installation and (c-d) after installation

Table F.23: Soil parameters

(a) Before installation

$I_{D,mean}$	81.48 %
φ_{mean}	41.26°
ψ_{mean}	18.64°
e_{mean}	0.614
γ_{mean}	9.91 kN/m^3

(b) After installation

$I_{D,mean,in}$	$I_{D,mean,out}$
94.70 %	% 87.58
$I_{D,mean,in(1,4)}$	$I_{D,mean,out(2,3)}$
98.88 %	88.01 %

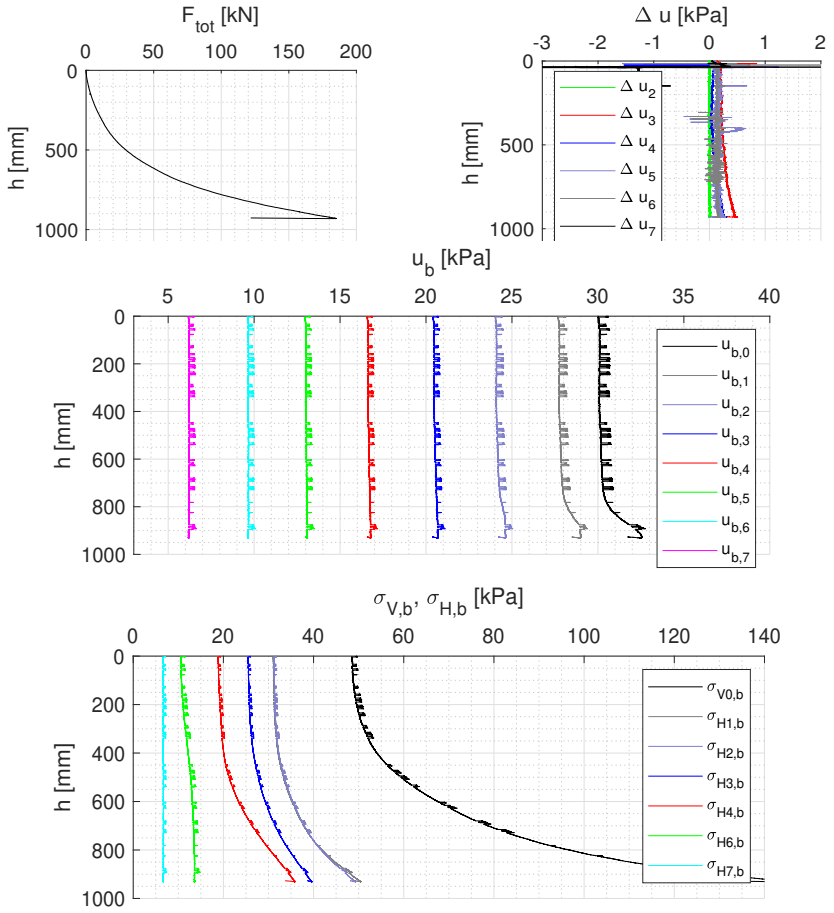

Fig. F.39: Results of installation test

Test 3.6

Type	h/D	Geometry
Jacking	1.0	Round

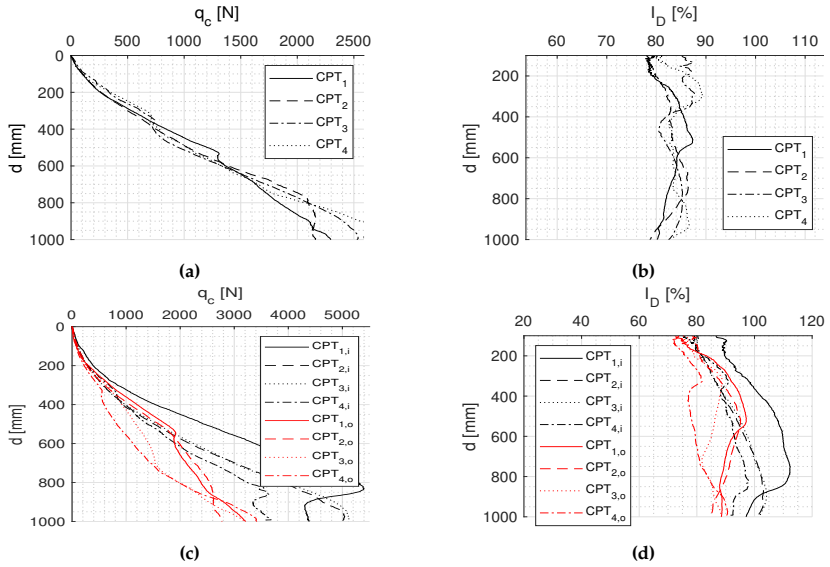

Fig. F.40: Results of CPT (a-b) before installation and (c-d) after installation

Table F.24: Soil parameters

(a) Before installation

$I_{D,mean}$	83.70 %
φ_{mean}	41.51°
ψ_{mean}	19.07°
e_{mean}	0.608
γ_{mean}	9.95 kN/m^3

(b) After installation

$I_{D,mean,in}$	$I_{D,mean,out}$
95.25 %	% 85.94
$I_{D,mean,in(1,4)}$	$I_{D,mean,out(2,3)}$
96.71 %	86.71 %

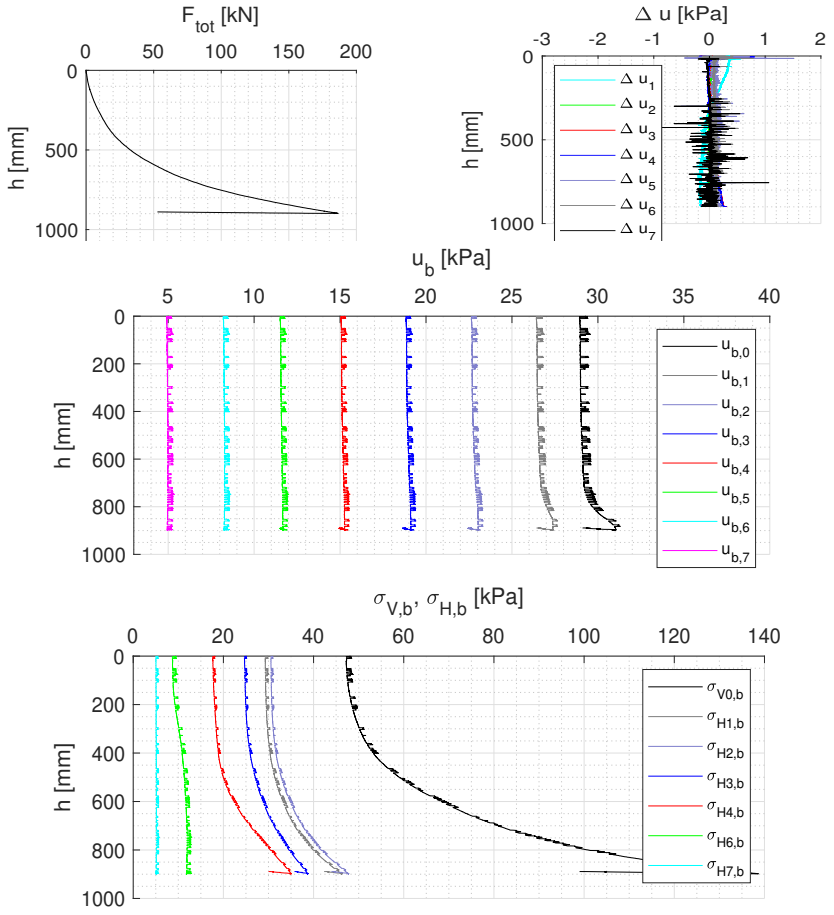

Fig. F.41: Results of installation test

Test 3.7

Type	h/D	Geometry
Suction	1.0	Round

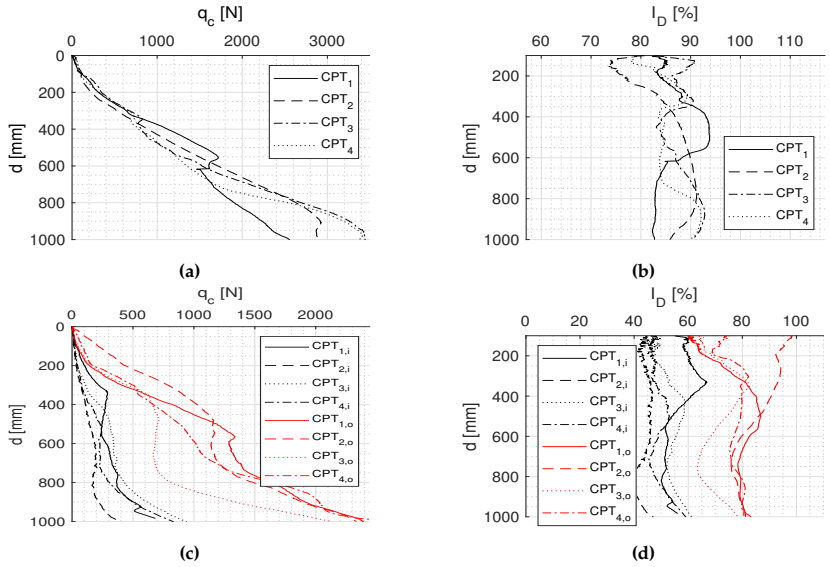

Fig. F.42: Results of CPT (a-b) before installation and (c-d) after installation

Table F.25: Soil parameters

(a) Before installation

$I_{D,mean}$	86.97 %
φ_{mean}	41.87°
ψ_{mean}	19.71°
e_{mean}	0.599
γ_{mean}	10.00 kN/m^3

(b) After installation

$I_{D,mean,in}$	$I_{D,mean,out}$
50.90 %	% 78.23
$I_{D,mean,in(1,4)}$	$I_{D,mean,out(2,3)}$
49.06 %	77.98 %

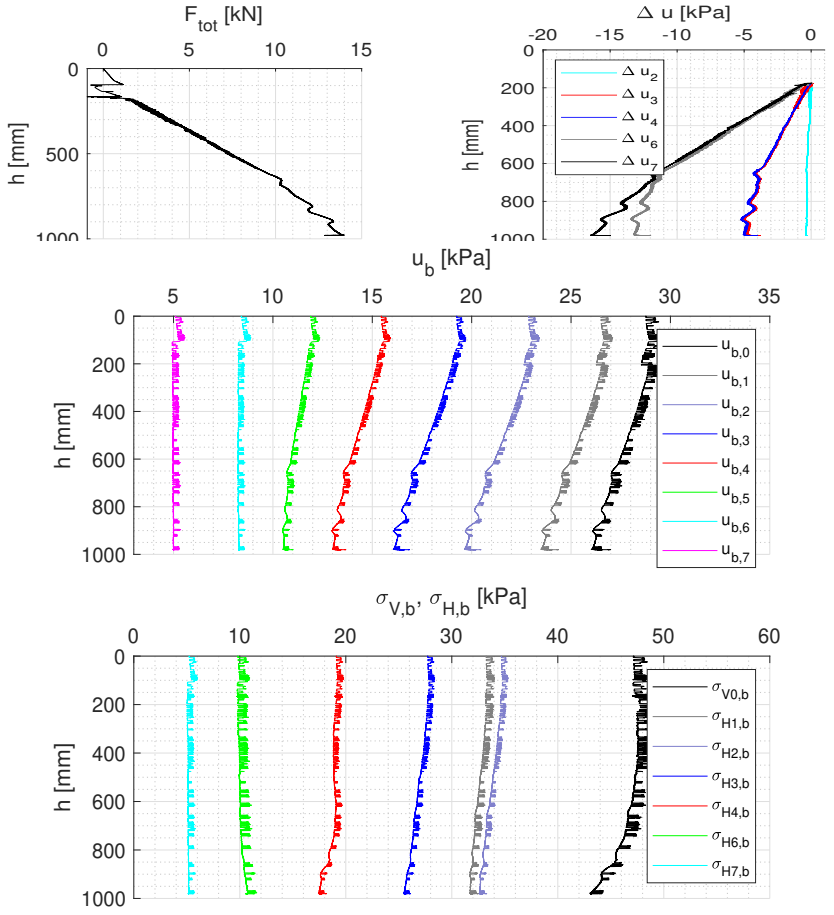

Fig. F.43: Results of installation test

Test 3.8

Type	h/D	Geometry
Suction	1.0	Round

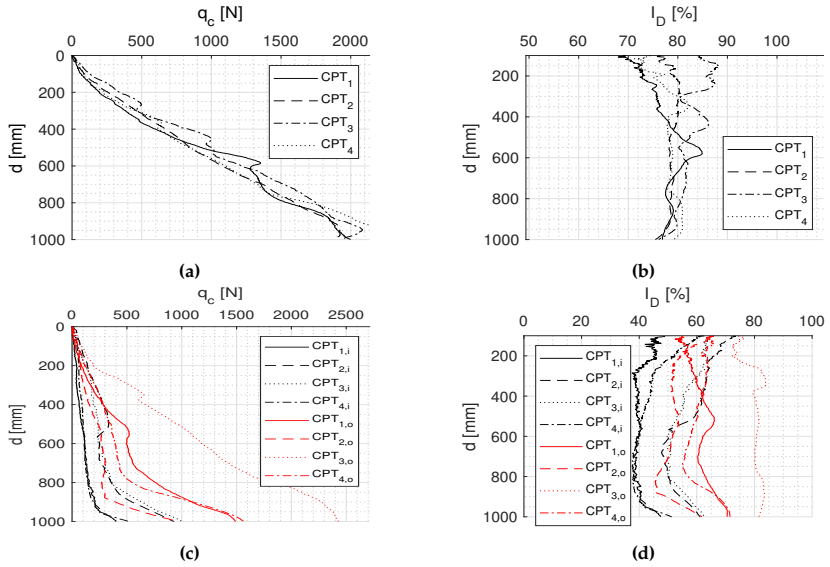

Fig. F.44: Results of CPT (a-b) before installation and (c-d) after installation

Table F.26: Soil parameters

(a) Before installation

$I_{D,mean}$	79.37 %
φ_{mean}	41.03°
ψ_{mean}	18.23°
e_{mean}	0.620
γ_{mean}	9.87 kN/m^3

(b) After installation

$I_{D,mean,in}$	$I_{D,mean,out}$
49.41 %	% 64.07
$I_{D,mean,in(1,4)}$	$I_{D,mean,out(2,3)}$
42.00 %	52.23/ 80.36 %

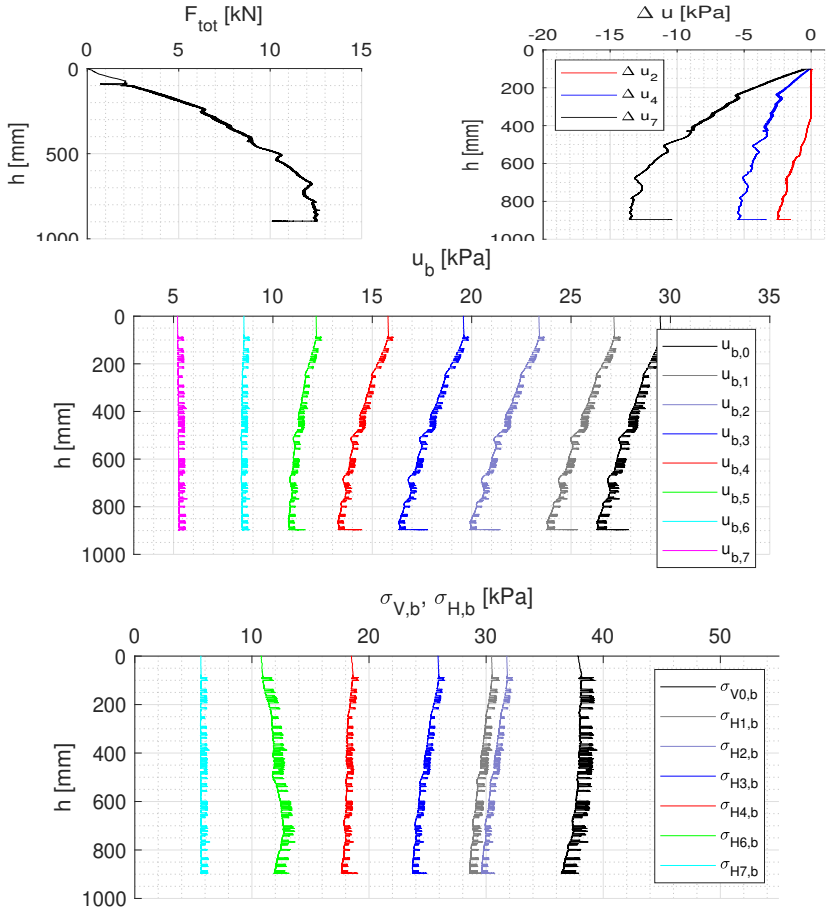

Fig. F.45: Results of installation test

Test 3.9

Type	h/D	Geometry
Suction	1.0	Modular

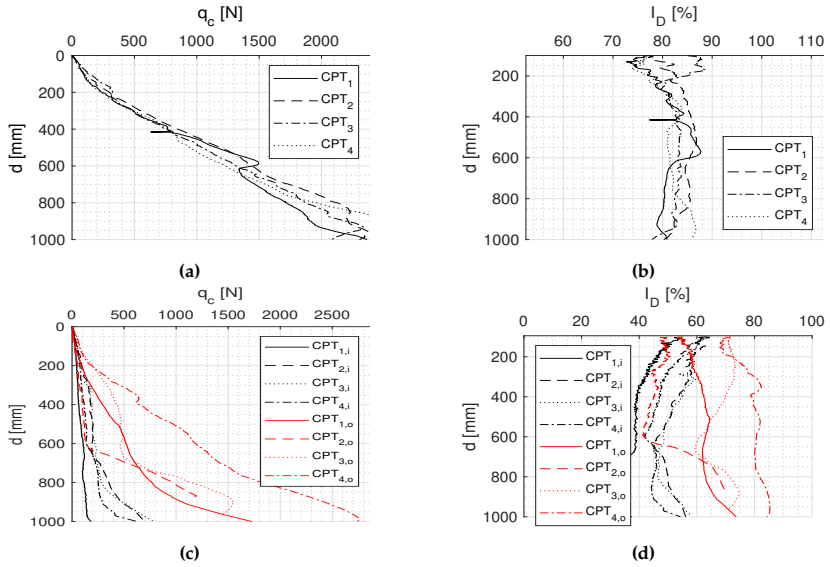

Fig. F.46: Results of CPT (a-b) before installation and (c-d) after installation

Table F.27: Soil parameters

(a) Before installation

$I_{D,mean}$	82.44 %
φ_{mean}	41.37°
ψ_{mean}	18.83°
e_{mean}	0.611
γ_{mean}	9.92 kN/m^3

(b) After installation

$I_{D,mean,in}$	$I_{D,mean,out}$
48.23 %	% 65.49
$I_{D,mean,in(1,4)}$	$I_{D,mean,out(2,3)}$
43.68 %	59.80 %

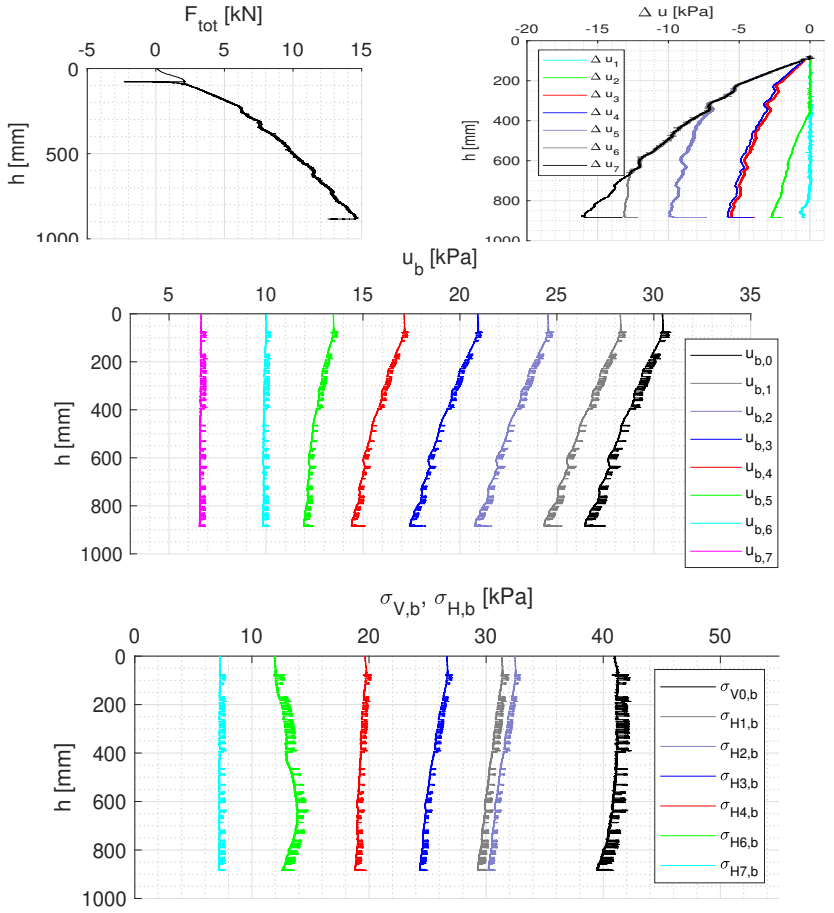

Fig. F.47: Results of installation test

Test 3.10

Type	h/D	Geometry
Suction	1.0	Modular

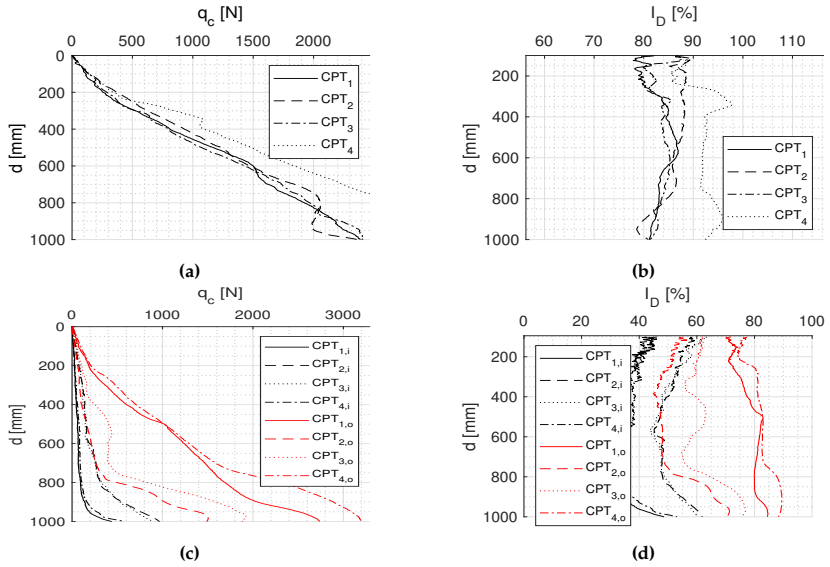

Fig. F.48: Results of CPT (a-b) before installation and (c-d) after installation

Table F.28: Soil parameters

(a) Before installation

$I_{D,mean}$	86.25 %
φ_{mean}	41.79°
ψ_{mean}	19.57°
e_{mean}	0.601
γ_{mean}	9.99 kN/m^3

(b) After installation

$I_{D,mean,in}$	$I_{D,mean,out}$
44.26 %	% 69.19
$I_{D,mean,in(1,4)}$	$I_{D,mean,out(2,3)}$
37.32 %	57.62 %

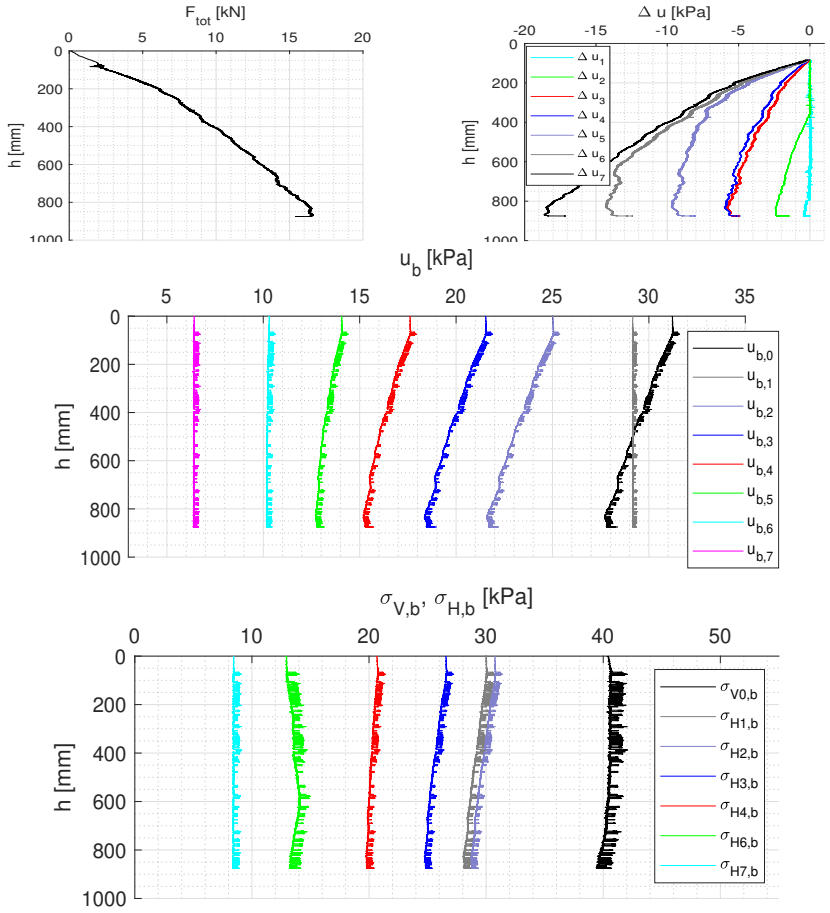

Fig. F.49: Results of installation test

Test 3.11

Type	h/D	Geometry
Suction	1.0	Round

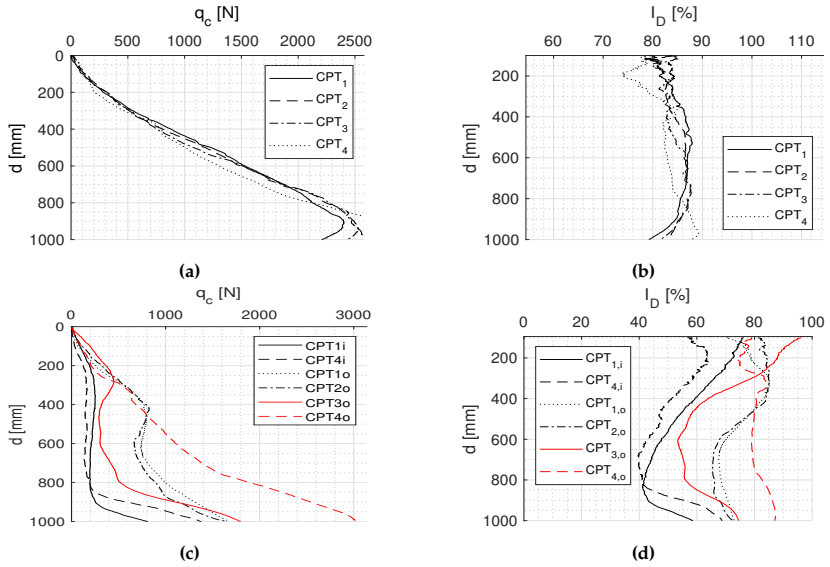

Fig. F.50: Results of CPT (a-b) before installation and (c-d) after installation

Table F.29: Soil parameters

(a) Before installation

$I_{D,mean}$	84.42 %
φ_{mean}	41.59°
ψ_{mean}	19.22°
e_{mean}	0.606
γ_{mean}	9.96 kN/m^3

(b) After installation

$I_{D,mean,in}$	$I_{D,mean,out}$
53.11%	% 74.42
$I_{D,mean,in(1,4)}$	$I_{D,mean,out(2,3)}$
53.11 %	70.96 %

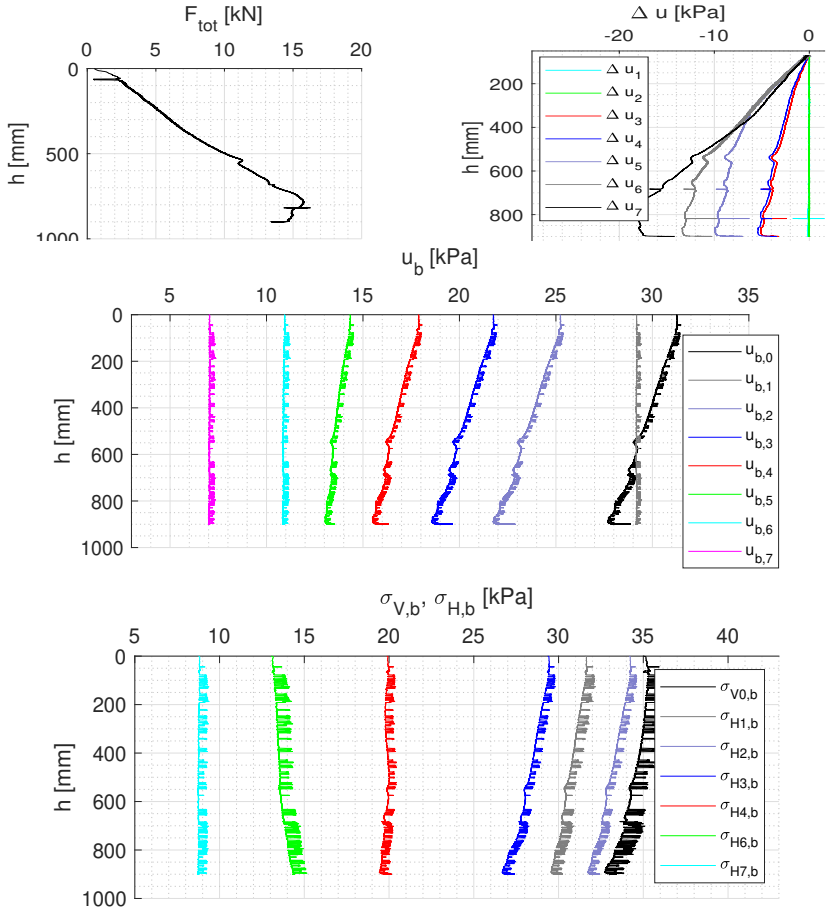

Fig. F.51: Results of installation test

Test 3.12

Type	h/D	Geometry
Suction	1.0	Round

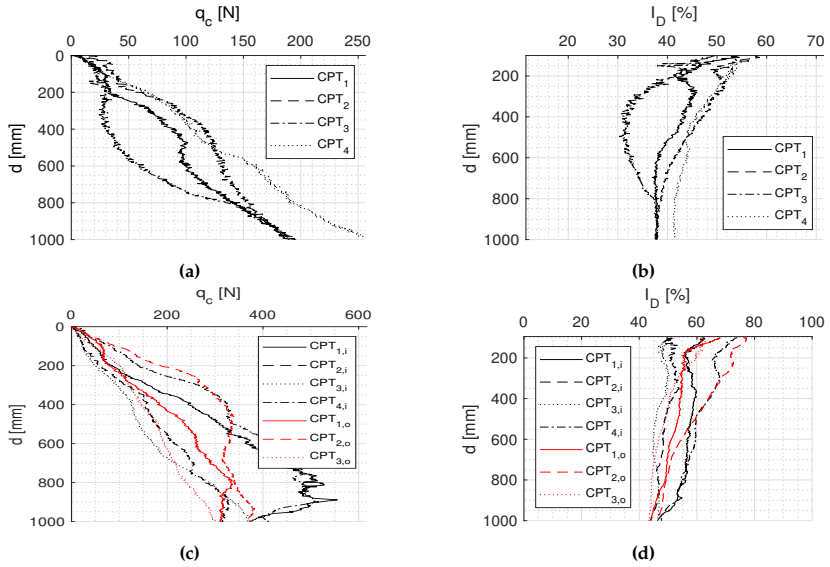

Fig. F.52: Results of CPT (a-b) before installation and (c-d) after installation

Table F.30: Soil parameters

(a) Before installation

$I_{D,mean}$	42.30 %
φ_{mean}	36.95°
ψ_{mean}	11.00°
e_{mean}	0.724
γ_{mean}	9.27 kN/m^3

(b) After installation

$I_{D,mean,in}$	$I_{D,mean,out}$
53.15 %	53.46%
$I_{D,mean,in(1,4)}$	$I_{D,mean,out(2,3)}$
58.23 %	54.17 %

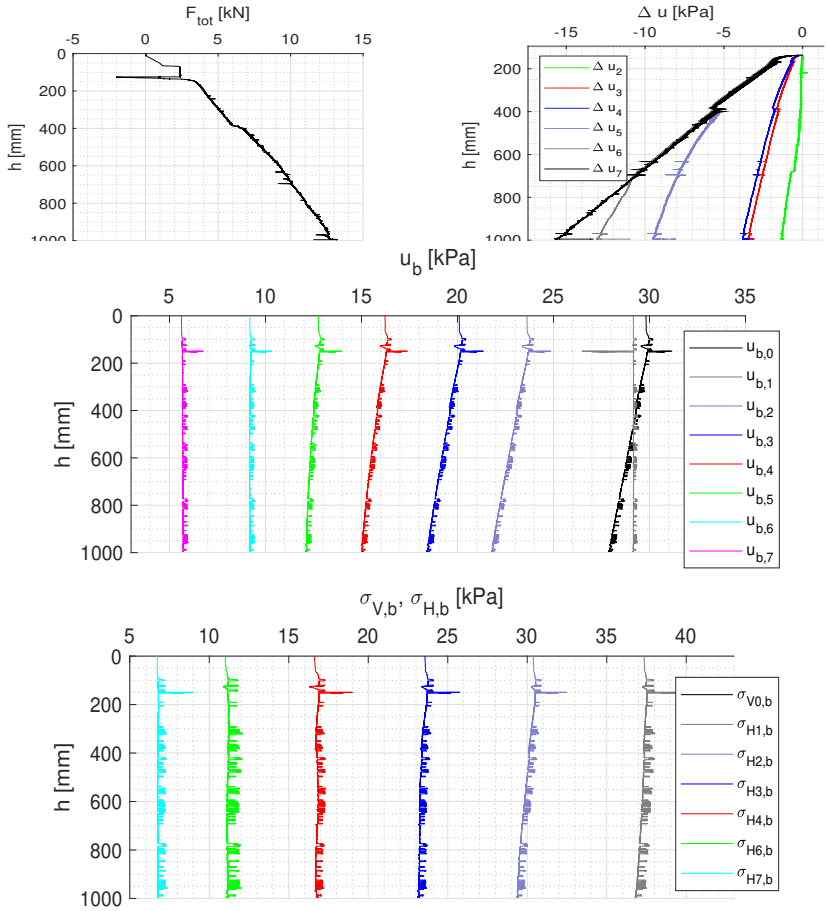

Fig. F.53: Results of installation test

Test 3.13

Type	h/D	Geometry
Suction	1.0	Round

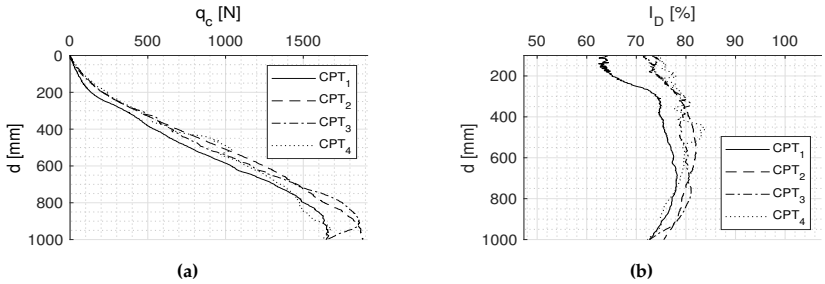

Fig. F.54: Results of CPT before installation

Table F.31: Soil parameters

$I_{D,mean}$	77.33 %
φ_{mean}	40.81°
ψ_{mean}	17.83°
e_{mean}	0.626
γ_{mean}	9.84 kN/m^3

Table F.32

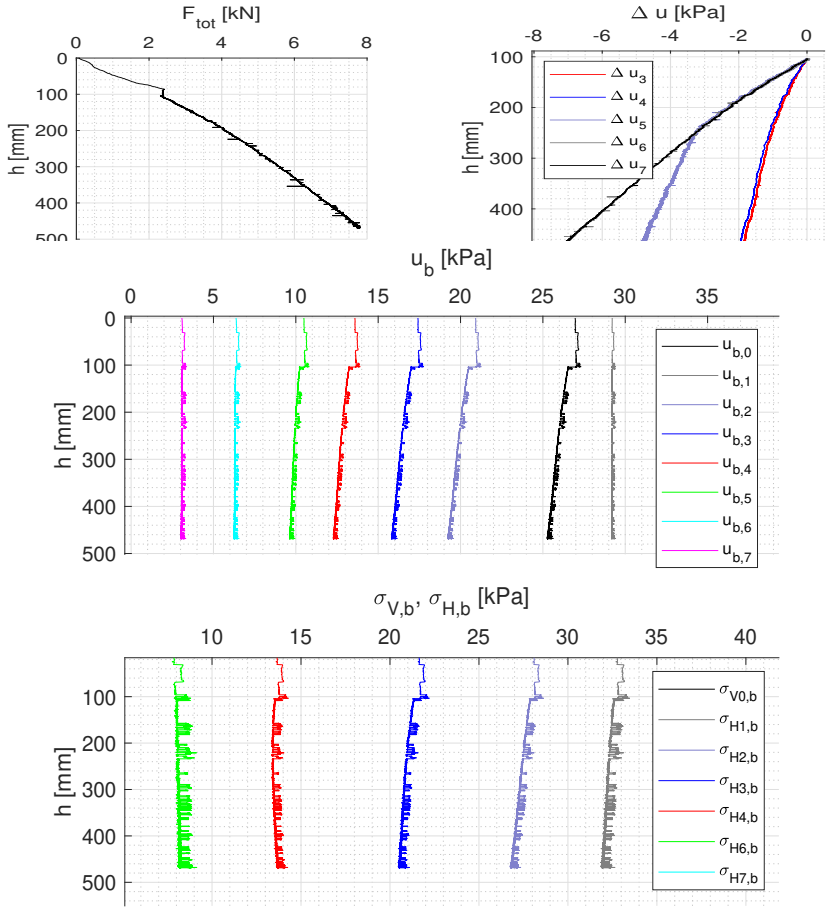

Fig. F.55: Results of installation test

Test 3.14

Type	h/D	Geometry
Suction	1.0	Round

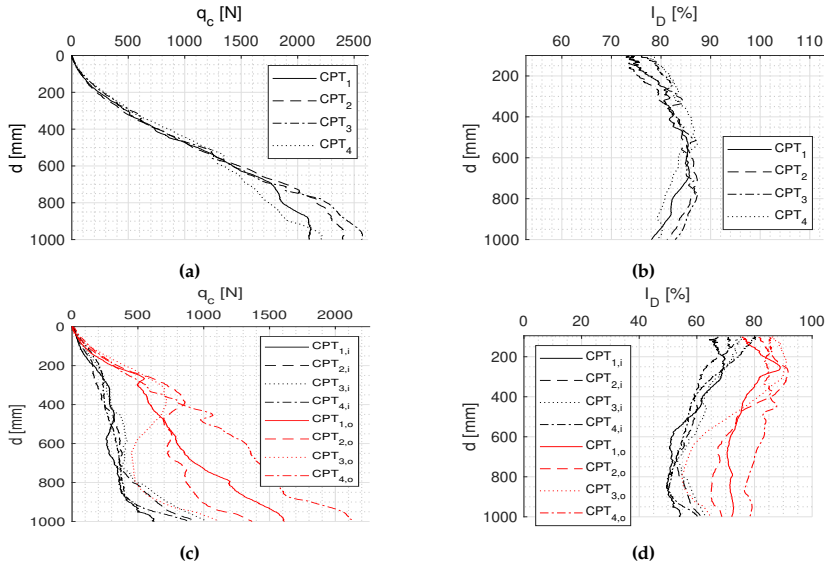

Fig. F.56: Results of CPT (a-b) before installation and (c-d) after installation

Table F.33: Soil parameters

(a) Before installation

$I_{D,mean}$	82.76 %
φ_{mean}	41.40°
ψ_{mean}	18.89°
e_{mean}	0.611
γ_{mean}	9.93 kN/m^3

(b) After installation

$I_{D,mean,in}$	$I_{D,mean,out}$
59.80 %	76.15 %
$I_{D,mean,in(1,4)}$	$I_{D,mean,out(2,3)}$
58.73 %	73.38 %

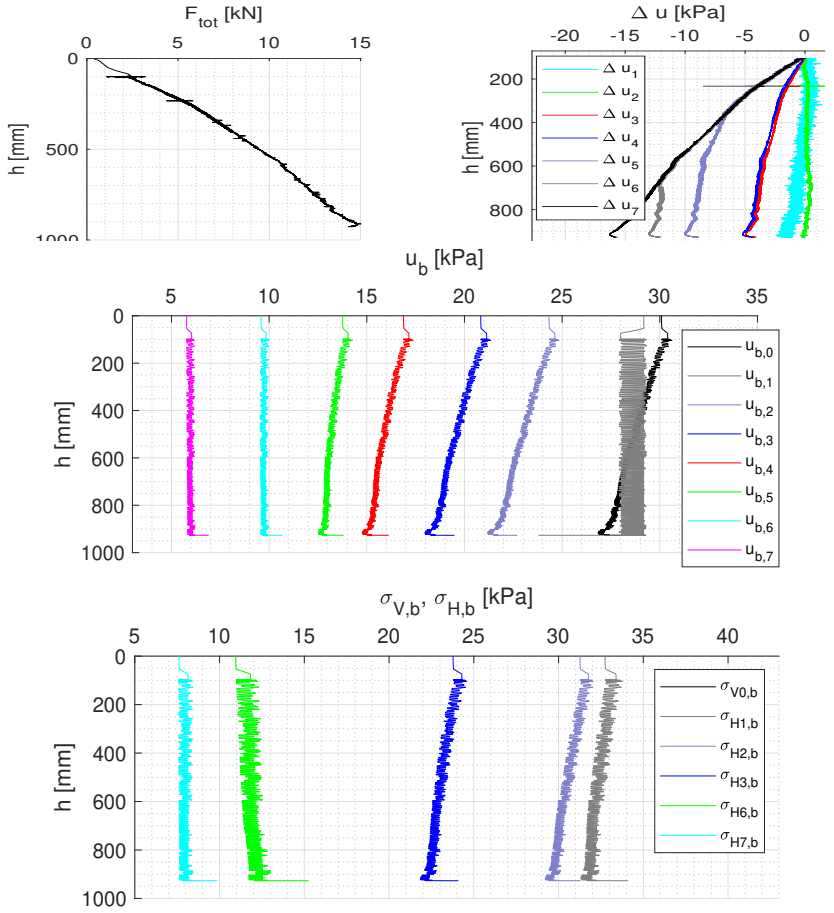

Fig. F.57: Results of installation test

Test 3.15

Type	h/D	Geometry
Jacking	1.0	Modular

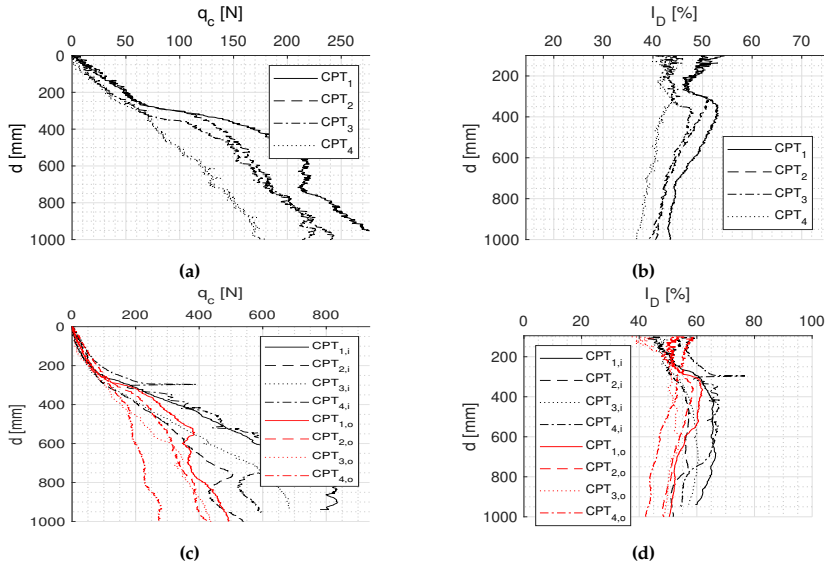

Fig. F.58: Results of CPT (a-b) before installation and (c-d) after installation

Table F.34: Soil parameters

(a) Before installation

$I_{D,mean}$	43.18 %
φ_{mean}	37.05°
ψ_{mean}	11.17°
e_{mean}	0.722
γ_{mean}	9.29 kN/m^3

(b) After installation

$I_{D,mean,in}$	$I_{D,mean,out}$
58.27 %	% 51.82
$I_{D,mean,in(1,4)}$	$I_{D,mean,out(2,3)}$
61.39 %	52.09 %

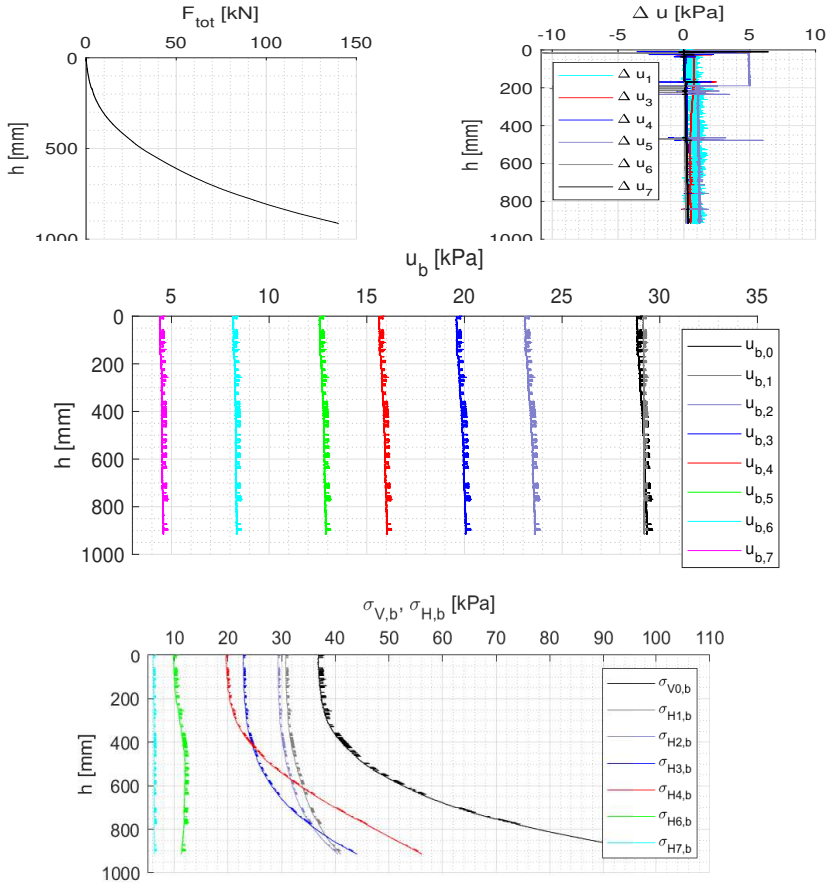

Fig. F.59: Results of installation test

Test 3.16

Type	h/D	Geometry
Jacking	1.0	Modular

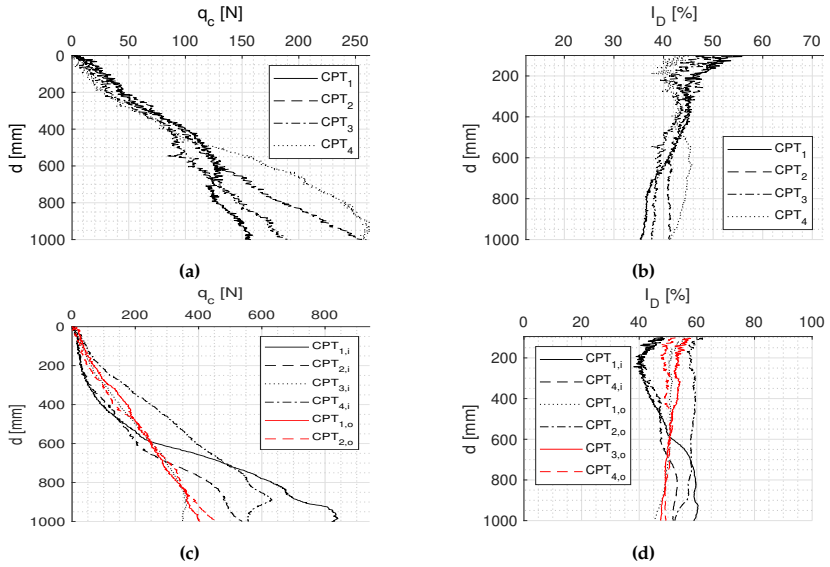

Fig. F.60: Results of CPT (a-b) before installation and (c-d) after installation

Table F.35: Soil parameters

(a) Before installation

$I_{D,mean}$	42.25 %
φ_{mean}	36.95°
ψ_{mean}	10.99°
e_{mean}	0.724
γ_{mean}	9.27 kN/m^3

(b) After installation

$I_{D,mean,in}$	$I_{D,mean,out}$
49.12 %	% 50.32
$I_{D,mean,in(1,4)}$	$I_{D,mean,out(2,3)}$
49.12 %	51.05 %

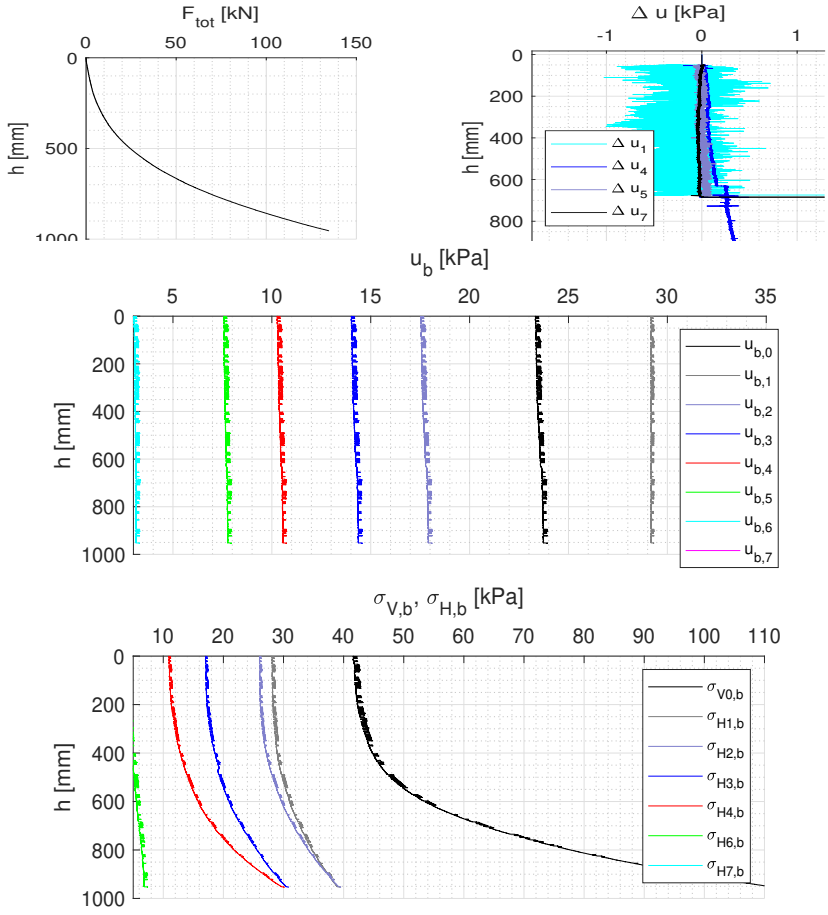

Fig. F.61: Results of installation test

Test 3.17

Type	h/D	Geometry
Jacking	1.0	Modular

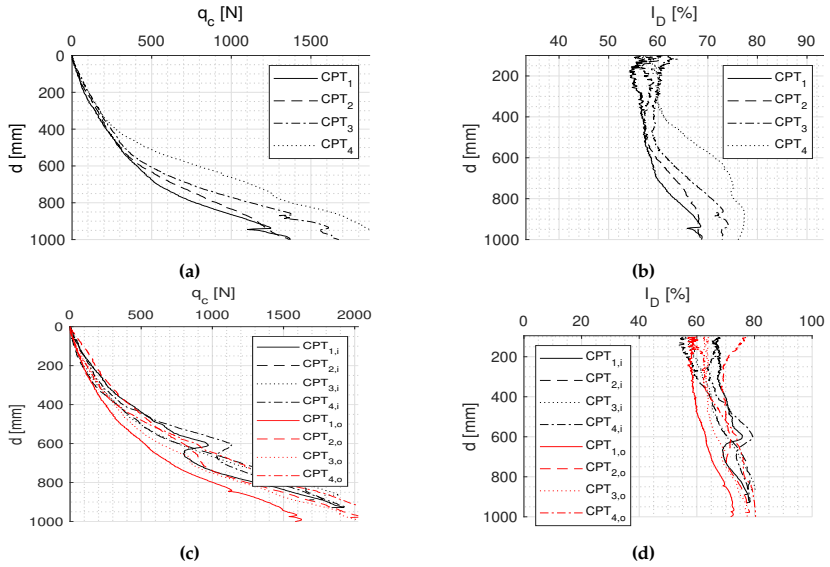

Fig. F.62: Results of CPT (a-b) before installation and (c-d) after installation

Table F.36: Soil parameters

(a) Before installation

$I_{D,mean}$	63.32 %
φ_{mean}	39.27°
ψ_{mean}	15.10°
e_{mean}	0.665
γ_{mean}	9.60 kN/m^3

(b) After installation

$I_{D,mean,in}$	$I_{D,mean,out}$
69.45 %	% 68.33
$I_{D,mean,in(1,4)}$	$I_{D,mean,out(2,3)}$
71.37 %	69.81 %

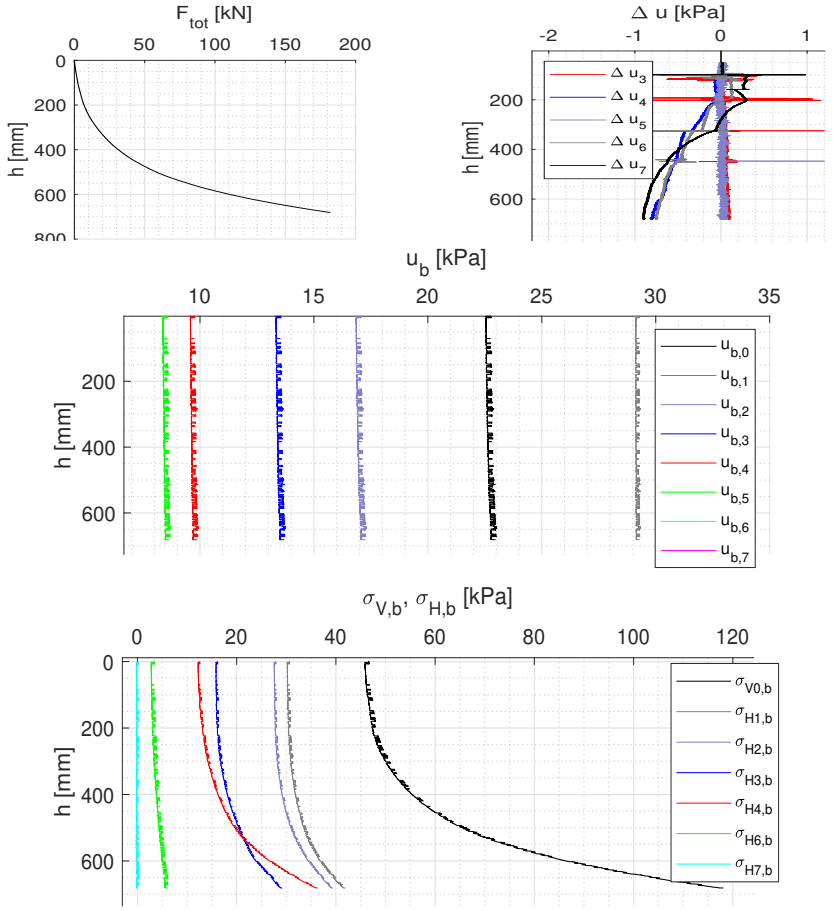

Fig. F.63: Results of installation test

Test 3.18

Type	h/D	Geometry
Jacking	1.0	Modular

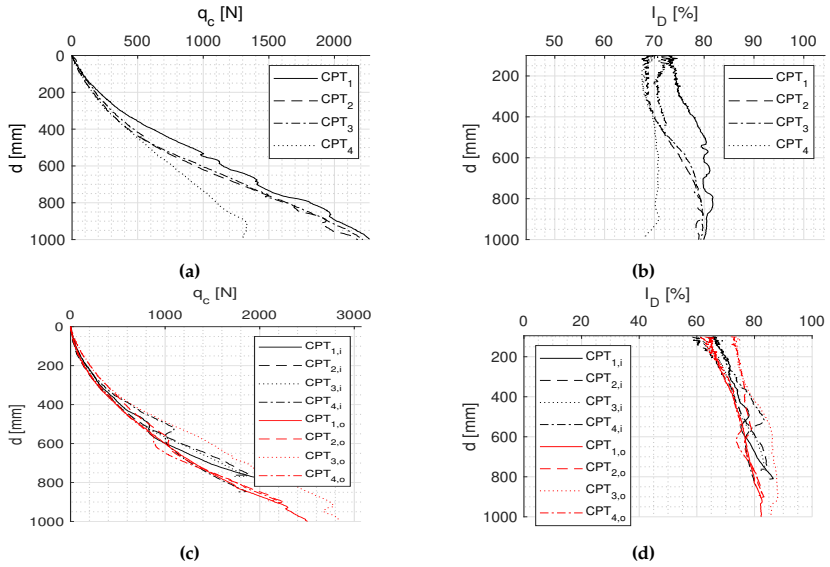

Fig. F.64: Results of CPT (a-b) before installation and (c-d) after installation

Table F.37: Soil parameters

(a) Before installation

$I_{D,mean}$	74.25 %
φ_{mean}	40.47°
ψ_{mean}	17.23°
e_{mean}	0.634
γ_{mean}	9.78 kN/m^3

(b) After installation

$I_{D,mean,in}$	$I_{D,mean,out}$
74.91 %	% 76.97
$I_{D,mean,in(1,4)}$	$I_{D,mean,out(2,3)}$
75.81 %	79.80 %

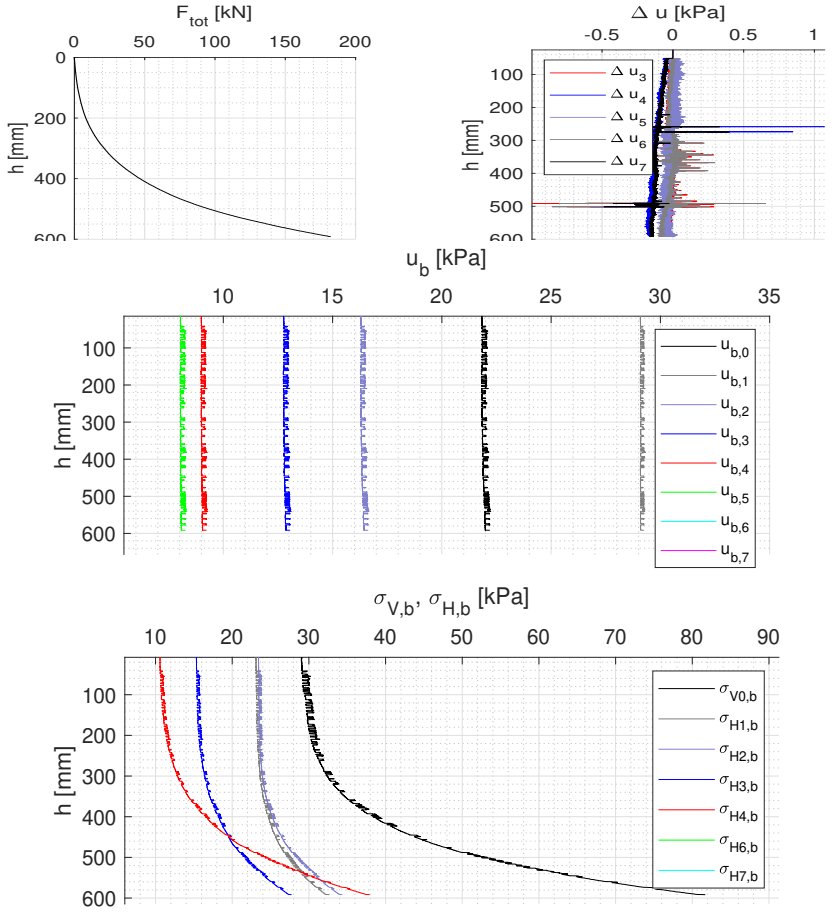

Fig. F.65: Results of installation test

Test 3.19

Type	h/D	Geometry
Suction	1.0	Modular

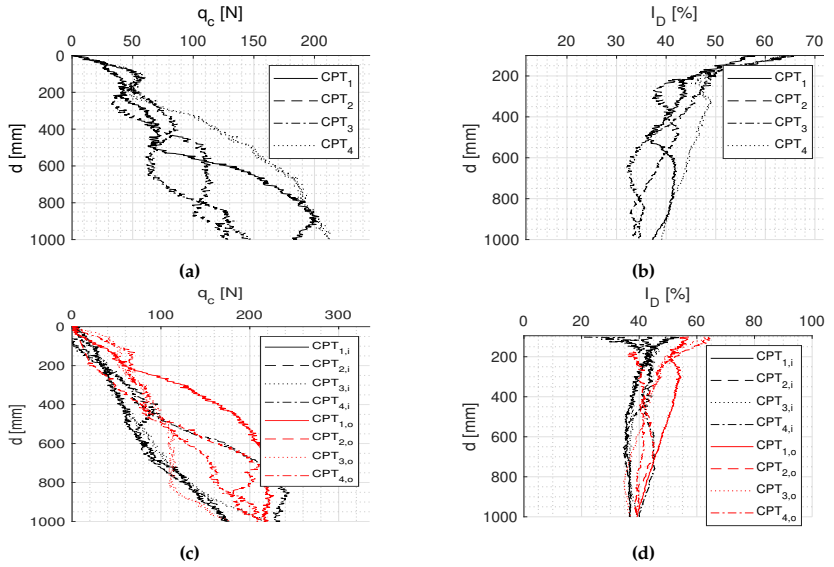

Fig. F.66: Results of CPT (a-b) before installation and (c-d) after installation

Table F.38: Soil parameters

(a) Before installation

$I_{D,mean}$	41.73 %
φ_{mean}	36.89°
ψ_{mean}	10.89°
e_{mean}	0.726
γ_{mean}	9.27 kN/m^3

(b) After installation

$I_{D,mean,in}$	$I_{D,mean,out}$
39.75 %	43.84 %
$I_{D,mean,in(1,4)}$	$I_{D,mean,out(2,3)}$
40.41 %	41.73 %

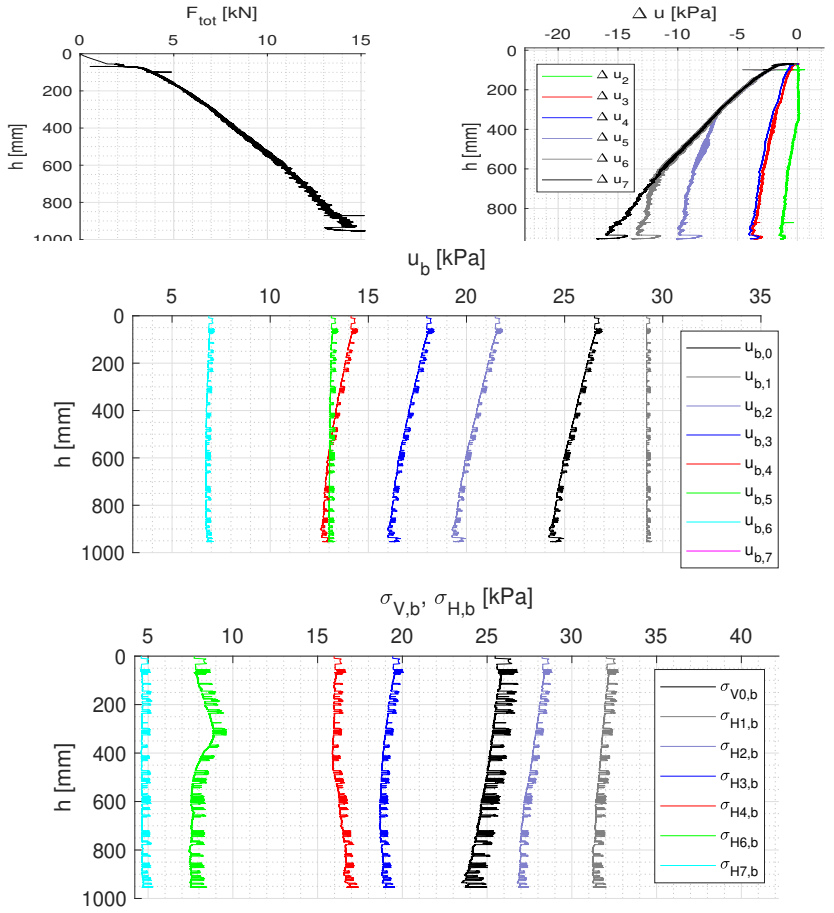

Fig. F.67: Results of installation test

Test 3.20

Type	h/D	Geometry
Jacking	1.0	Round

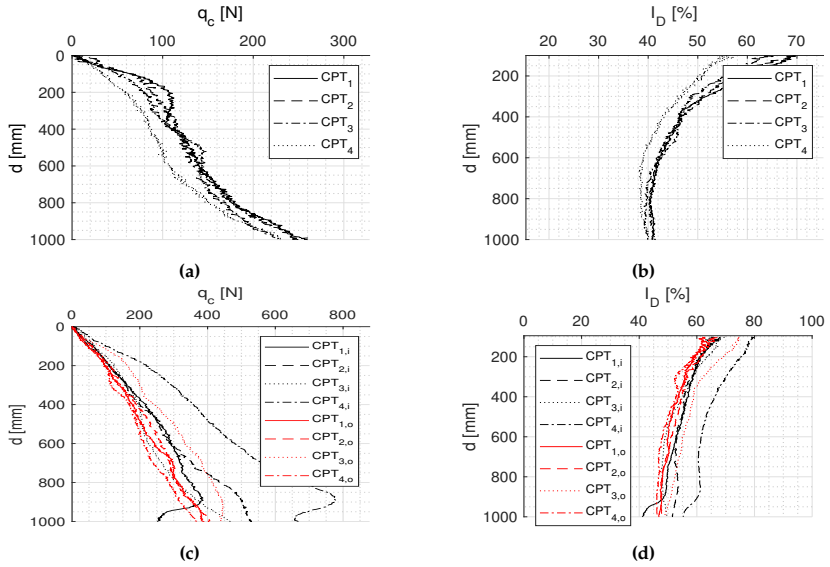

Fig. F.68: Results of CPT (a-b) before installation and (c-d) after installation

Table F.39: Soil parameters

(a) Before installation

$I_{D,mean}$	41.34 %
φ_{mean}	36.85°
ψ_{mean}	6.85°
e_{mean}	0.727
γ_{mean}	9.26 kN/m^3

(b) After installation

$I_{D,mean,in}$	$I_{D,mean,out}$
53.72 %	50.31 %
$I_{D,mean,in(1,4)}$	$I_{D,mean,out(2,3)}$
56.03 %	51.97 %

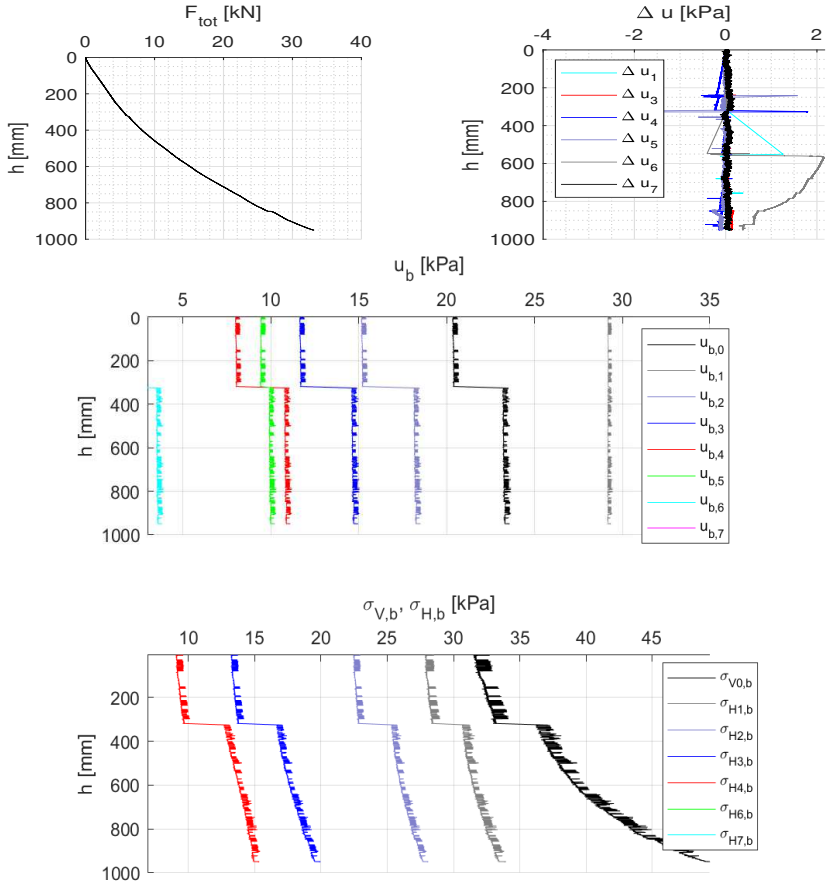

Fig. F.69: Results of installation test

Test 3.21

Type	h/D	Geometry
Suction	1.0	Modular

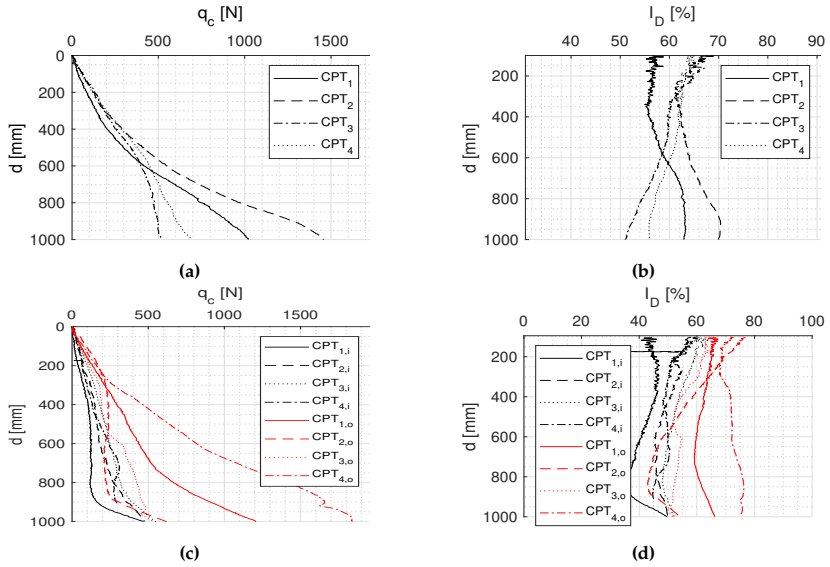

Fig. F.70: Results of CPT (a-b) before installation and (c-d) after installation

Table F.40: Soil parameters

(a) Before installation

$I_{D,mean}$	60.72 %
φ_{mean}	38.98°
ψ_{mean}	14.59°
e_{mean}	0.672
γ_{mean}	9.56 kN/m^3

(b) After installation

$I_{D,mean,in}$	$I_{D,mean,out}$
48.57 %	61.19 %
$I_{D,mean,in(1,4)}$	$I_{D,mean,out(2,3)}$
46.01 %	55.01 %

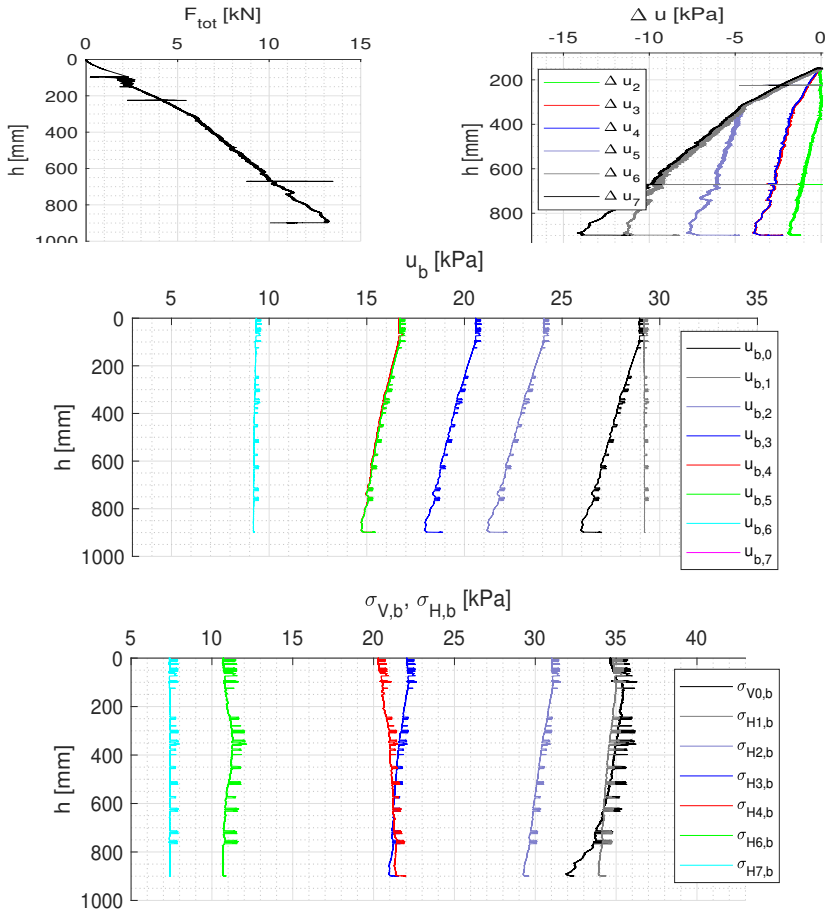

Fig. F.71: Results of installation test

Test 3.22

Type	h/D	Geometry
Suction	1.0	Modular

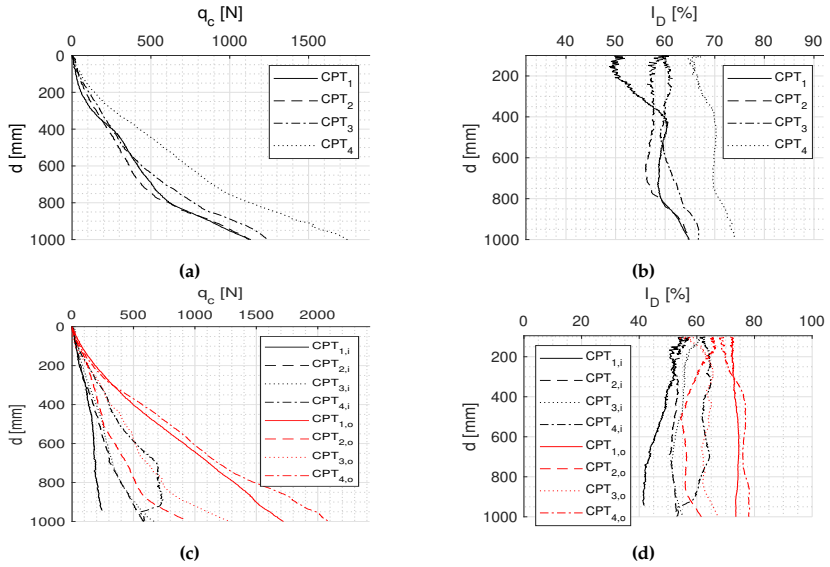

Fig. F.72: Results of CPT (a-b) before installation and (c-d) after installation

Table F.41: Soil parameters

(a) Before installation

$I_{D,mean}$	61.92 %
φ_{mean}	39.11°
ψ_{mean}	14.83°
e_{mean}	0.669
γ_{mean}	9.58 kN/m^3

(b) After installation

$I_{D,mean,in}$	$I_{D,mean,out}$
51.29 %	67.6 %
$I_{D,mean,in(1)}$	$I_{D,mean,out(2,3)}$
47.11 %	60.83 %

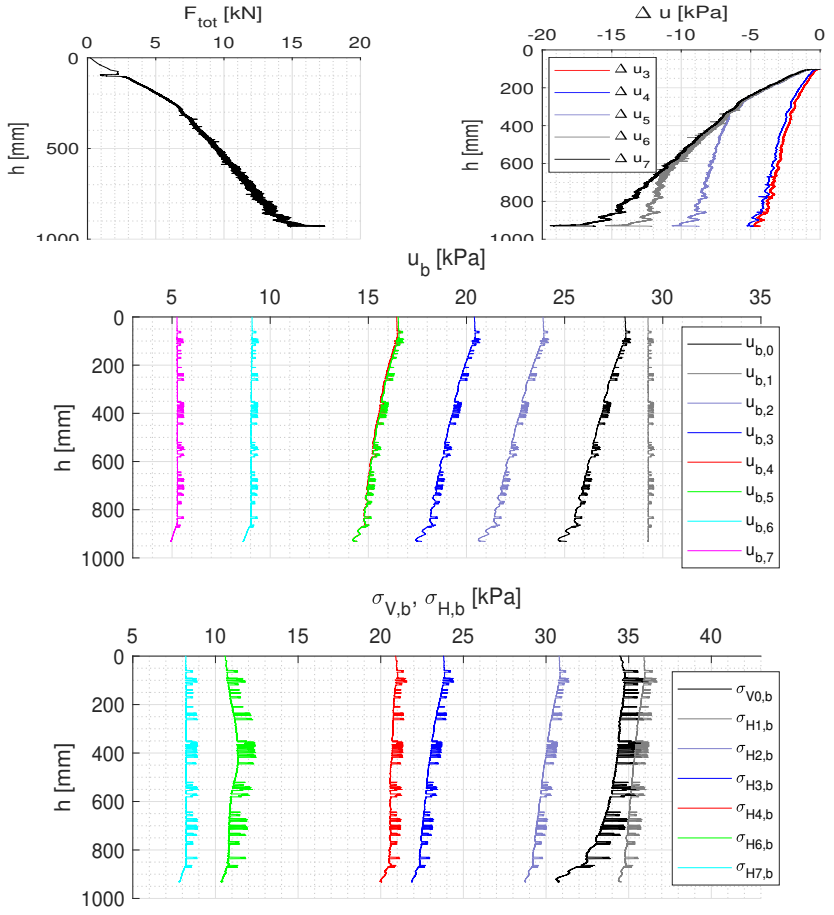

Fig. F.73: Results of installation test

Test 3.23

Type	h/D	Geometry
Suction	1.0	Modular

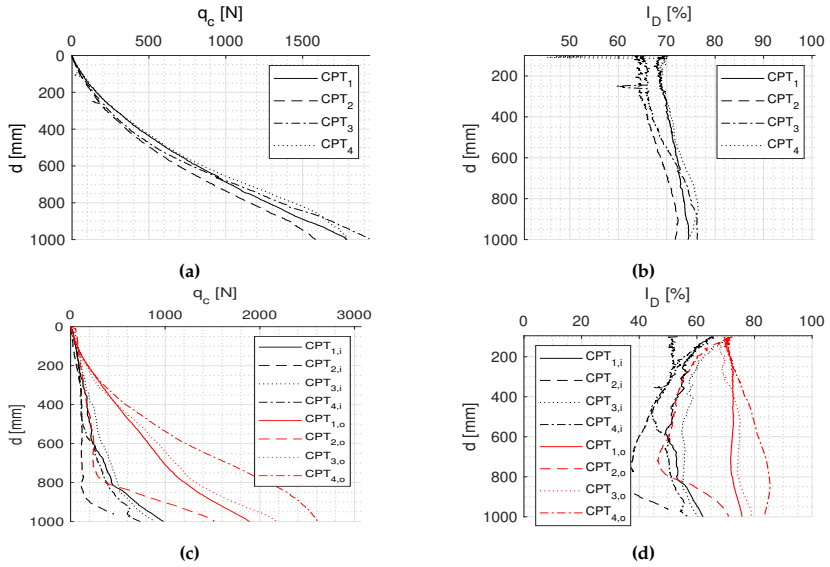

Fig. F.74: Results of CPT (a-b) before installation and (c-d) after installation

Table F.42: Soil parameters

(a) Before installation

$I_{D,mean}$	78.13 %
φ_{mean}	40.89°
ψ_{mean}	17.99°
e_{mean}	0.624
γ_{mean}	9.85 kN/m^3

(b) After installation

$I_{D,mean,in}$	$I_{D,mean,out}$
52.11 %	70.32%
$I_{D,mean,in(1,4)}$	$I_{D,mean,out(2,3)}$
49.53 %	64.73 %

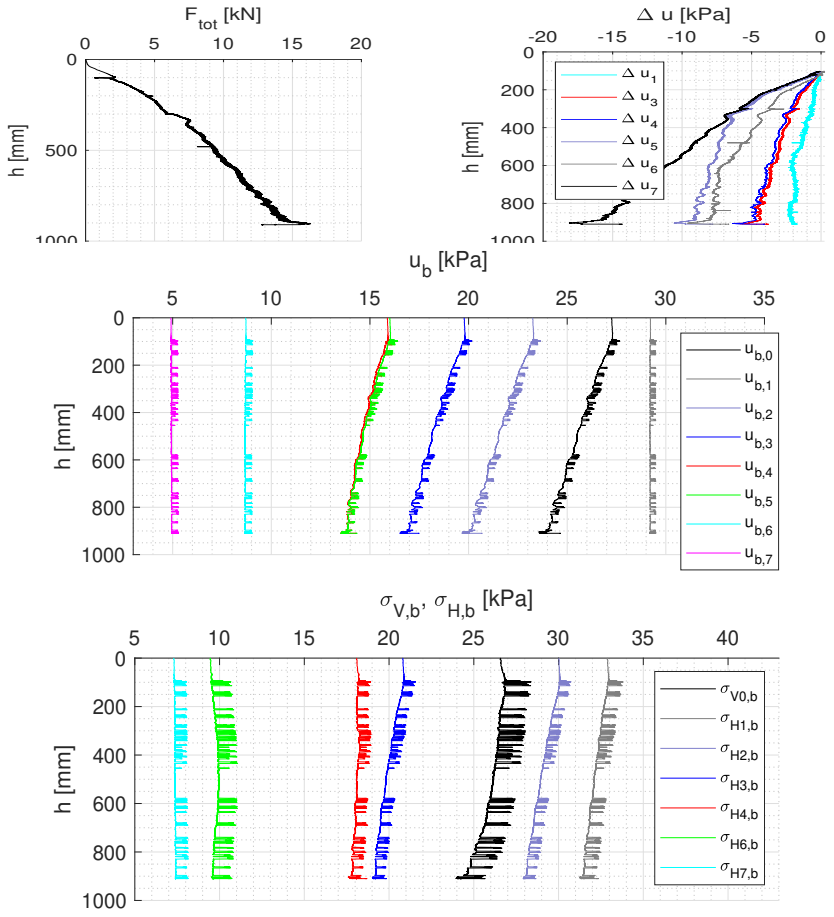

Fig. F.75: Results of installation test

Test 3.24

Type	h/D	Geometry
Suction	1.0	Round

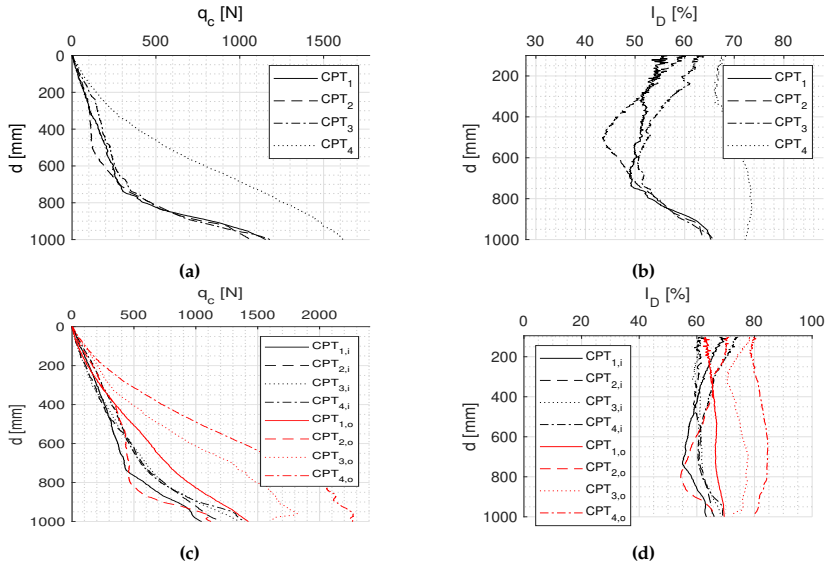

Fig. F.76: Results of CPT (a-b) before installation and (c-d) after installation

Table F.43: Soil parameters

(a) Before installation

$I_{D,mean}$	57.99 %
φ_{mean}	38.67°
ψ_{mean}	14.06°
e_{mean}	0.680
γ_{mean}	9.52 kN/m^3

(b) After installation

$I_{D,mean,in}$	$I_{D,mean,out}$
62.14%	71.48%
$I_{D,mean,in(1,4)}$	$I_{D,mean,out(2,3)}$
62.67%	64.38%

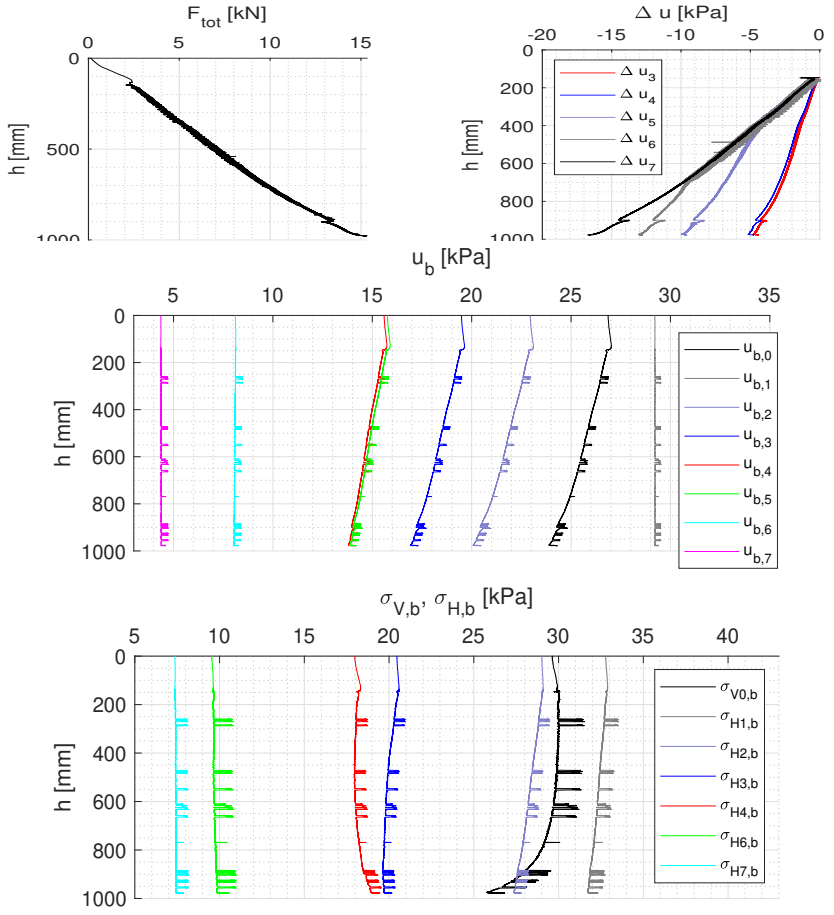

Fig. F.77: Results of installation test

SUMMARY

The production of renewable energy on the global scale experiences a large growth due to the well-known reasons. Offshore wind power is one of the most promising sources with a high development range. The costs of offshore energy are being rapidly reduced; however, there is still much to be improved. Lowering the costs of offshore wind farms is not only the key to lower energy prices, but primarily is the great contribution to the climate goals for the future.

The installation of foundations is often named as one of the main issues that influences the total costs of the offshore energy. The majority of offshore wind turbines are supported by monopile foundations. However, the demand for increasing size of offshore wind turbines is the reason why a better solution is desired. Therefore, more and more effort is put on the development of a suction bucket foundation that seems to be more cost-effective and environmentally friendly due to the suction installation manner. The concept is commonly used in the oil and gas industry, but as loading conditions for offshore wind turbines are very different, a further research and new design methods are required. The concept is already proven to be feasible, but the suction installation process is still not fully understood and can be optimized.

This thesis focuses on the bucket installation by analyzing the soil-structure response during the suction and the jacking installation. Medium-scale tests of the installation have been performed at Aalborg University laboratory in fine grained sand. The tests prove that the suction installation can be performed and easily controlled even in very dense sand. The suction applied during the installation can be much higher that the proposed suction limits and no failure is observed. Moreover, the tests results indicate a huge difference between the soil resistance against two different installations, as the seepage flow, induced by the applied suction, reduces the soil stresses inside the bucket and below the skirt tip. The cone penetration tests performed before and after each test confirm that the soil trapped inside the bucket is significantly loosened up.

The thesis covers also the numerical analysis of seepage around the skirt for different boundary conditions and with applied changes in the soil permeability of the inside soil plug due to the mentioned loosening. The numerical part is a basis for the analysis of the critical suction which is later on evaluated by laboratory tests results.

Finally, the thesis includes results of the test campaign where two different bucket models are used and compared. An increase in bucket foundation diameter requires an increase in skirt thickness at the same time. Otherwise, too thin structure will lead to a buckling failure during the installation. Obviously, the total cost of steel material increases significantly. However, a modular bucket with the internal stiffeners used for tests has a much lower skirt thickness. The changed shape gives much higher buckling resistance and savings in material costs at the same time. Jacking tests show that the soil resistance for the modular bucket is significantly higher than for the round bucket with a similar diameter, but the suction installation tests show that the reduced soil resistance is almost the same in both cases. These results are very promising, showing that large-diameter mono-buckets with modular shape can be feasible for suction installation.

ISSN (online): 2446-1636
ISBN (online): 978-87-7210-536-9 AALBORG UNIVERSITETSFORLAG